
**Distributed Hydrologic Modeling of the Upper Roanoke River
Watershed using GIS and NEXRAD**

Brian C. McCormick

Thesis submitted to the faculty of
Virginia Polytechnic Institute and State University
in partial fulfillment of the requirements for the degree of

Master of Science

in

Civil Engineering

Dr. Randel L. Dymond
Dr. Conrad D. Heatwole
Dr. David F. Kibler

March 27, 2003
Blacksburg, VA, USA

Keywords: Distributed Hydrologic Modeling, GIS, NEXRAD, radar.

Distributed Hydrologic Modeling of the Upper Roanoke River Watershed using GIS and NEXRAD

Brian C. McCormick

ABSTRACT

Precipitation and surface runoff producing mechanisms are inherently spatially variable. Many hydrologic runoff models do not account for this spatial variability and instead use “lumped” or spatially averaged parameters. Lumped model parameters often must be developed empirically or through optimization rather than be calculated from field measurements or existing data. Recent advances in geographic information systems (GIS) remote sensing (RS), radar measurement of precipitation, and desktop computing have made it easier for the hydrologist to account for the spatial variability of the hydrologic cycle using distributed models, theoretically improving hydrologic model accuracy.

Grid based distributed models assume homogeneity of model parameters within each grid cell, raising the question of optimum grid scale to adequately and efficiently model the process in question. For a grid or raster based hydrologic model, as grid cell size decreases, modeling accuracy typically increases, but data and computational requirements increase as well. There is great interest in determining the optimal grid resolution for hydrologic models as well as the sensitivity of hydrologic model outputs to grid resolution.

This research involves the application of a grid based hydrologic runoff model to the Upper Roanoke River watershed (1480km²) to investigate the effects of precipitation resolution and grid cell size on modeled peak flow, time to peak and runoff volume. The gridded NRCS curve number (CN) rainfall excess determination and ModClark runoff transformation of HEC-HMS is used in this modeling study. Model results are evaluated against observed streamflow at seven USGS stream gage locations throughout the watershed.

Runoff model inputs and parameters are developed from public domain digital datasets using commonly available GIS tools and public domain modeling software. Watersheds and stream networks are delineated from a USGS DEM using GIS tools. Topographic parameters describing these watersheds and stream channel networks are also derived from the GIS. A gridded representation of the NRCS CN is calculated from the soil survey geographic database of the NRCS and national land cover dataset of the USGS. Spatially distributed precipitation depths derived from WSR-88D next generation radar (NEXRAD) products are used as precipitation inputs. Archives of NEXRAD Stage III data are decoded, spatially and temporally registered, and verified against archived IFLOWS rain gage data. Stage III data are systematically degraded to coarser resolutions to examine model sensitivity to gridded rainfall resolution.

The effects of precipitation resolution and grid cell size on model outputs are examined. The performance of the grid based distributed model is compared to a similarly specified and parameterized lumped watershed model. The applicability of public domain digital datasets to hydrologic modeling is also investigated.

The HEC-HMS gridded SCS CN rainfall excess calculation and ModClark runoff transformation, as applied to the Upper Roanoke watershed and for the storm events chosen in this study, does not exhibit significant sensitivity to precipitation resolution, grid scale, or spatial distribution of parameters and inputs. Expected trends in peak flow, time to peak and overall runoff volume are observed with changes in precipitation resolution, however the changes in these outputs are small compared with their magnitudes and compared to the discrepancies between modeled and observed values. Significant sensitivity of runoff volume and consequently peak flow, to CN choices and antecedent moisture condition (AMC) was observed. The changes in model outputs between the distributed and lumped versions of the model were also small compared to the magnitudes of model outputs.

Acknowledgements

As I approach the end of my graduate studies at Virginia Tech, it is time to pause and look back on where the trail has led and thank those who have helped me along the way. I am reminded of approaching a summit in the high country after days of climbing. I'm thrilled to finally arrive, yet realize it is now time to reorient myself towards other goals. Indeed, our time on the windswept summits of life is ephemeral. From the summit though, I have a good view of my route up and a deep appreciation to all those who have helped me out along the journey. To all my family, friends, and mentors, I cannot thank you enough for your guidance and support. All humor aside, my time at Virginia Tech has been the best seven years of my life.

I'd like to thank my family: Mom, Dad, David, and Greg, for providing the support and gentle encouragement not to give up when the trail grew rough. To all my friends who have traveled with me or are still alongside: Melissa, Ed, Rodger, Jake and all the others, thanks for reminding me what the journey is really about.

Thanks to everyone in the Virginia Tech Civil Engineering GIS program for keeping the work days interesting. Ed Chamberlayne, thanks for the cap and gown and congratulations on your hillshade award. Paul Bartholomew, thanks for the chocolate chip cookie recipe. Craig Moore and Tim Bayse, my fellow CEE Measurements collaborators, thanks for everything. Milko Maykowskyj, thanks for demystifying UNIX. Thanks also to the fourteen jars of crunchy peanut butter that have provided the sustenance necessary for the hours of research and writing over the past year.

Dr. David Kibler, thanks for encouraging me to pursue graduate study (pointing out the trailhead so to speak) as well as the mentorship you have provided. Steve Keighton and Mike Gillen at the National Weather Service Blacksburg Forecast Office, thanks for the advice and the datasets. Roger White at the USGS, thanks for the streamflow data.

I ended up putting many miles on my bike in the past year performing unofficial "handlebar" surveys of the Upper Roanoke Watershed. Interestingly, riding was my most effective time to reflect and make insights about my research. It was on a trip over John's Creek mountain last July that I figured out how to separate grid scale and grid resolution. More importantly though, this time in the saddle helped me realize that a watershed is much more than simply a series of gridded hydrologic attributes.

Mountaineering, and life, aren't only about bagging peaks. Robert Pirsig sums it up best with "It is the sides of the mountain which sustain life, and not the top." And from the peak on which I am currently standing, I can see many other mountainsides on which I plan to travel.

The trail goes on forever...

Brian McCormick
Blacksburg, VA

Table of Contents

1.0 Introduction	1-1
1.1 Statement of Problem	1-2
1.2 Research Objectives	1-3
2.0 Literature Review and Background Information	2-1
<u>2.1 Historical Uses of GIS in Hydrology</u>	2-1
2.1.1 Watershed and Stream Channel Delineation from Elevation Models	2-2
2.1.2 Calculation of Model Parameters	2-4
2.1.3 Preparation of Hydrologic Model inputs	2-4
2.1.4 Hydraulic Modeling of River Channels and Floodplains	2-5
<u>2.2 Radar Measurement of Precipitation</u>	2-5
2.2.1 Determination of Rainfall Intensity from Reflectivity	2-6
2.2.2 Uncertainties in Radar Measurement of Precipitation	2-7
2.2.3 Calibration of Radar by Ground based Gages and Mosaicing	2-8
2.2.4 NWS NEXRAD Processing	2-8
<u>2.3 Modeling Definitions and Classifications</u>	2-9
<u>2.4 Review of Applicable, Available Distributed Runoff Models</u>	2-11
2.4.1 CASC2D	2-11
2.4.2 Hydrotel	2-11
2.4.3 MIKE-SHE	2-11
2.4.4 HEC-HMS	2-12
<u>2.5 Scale and resolution issues in distributed watershed modeling</u>	2-12
2.5.1 Effects of Radar Rainfall Resolution	2-13
2.5.2 Conditions Governing the Dominance of Spatial or Temporal Variability	2-14
<u>2.6 Case Studies Utilizing Radar and GIS in Hydrology</u>	2-14
2.6.1 Hydrologic Model of the Buffalo Bayou Using GIS	2-14
2.6.2 Runoff Simulation using Radar Rainfall Data	2-15
2.6.3 Application of ModClark to the Salt River Basin, MO	2-15
2.6.4 Resolution Considerations in Using Radar Rainfall Data for Flood Forecasting	2-15
<u>2.7 The Natural Resources Conservation Service Curve Number Method</u>	2-16
2.7.1 History of the SCS CN Method	2-16
2.7.2 Summary of SCS CN Method Runoff Equations	2-17
2.7.3 The Curve Number as Quantification of Soil and Land Use Characteristics	2-18
2.7.3.1 Hydrologic Soil Group (HSG)	2-18
2.7.3.2 Land Use and Landcover (LULC)	2-19
2.7.4 CN Variability with Antecedent Moisture Condition	2-19
2.7.5 Limitations of the SCS CN Method for Modeling Historical Events	2-21
3.0 Methodology: GIS and Modeling Techniques	3-1
<u>3.1 HEC-HMS Model Architecture and Required Inputs</u>	3-4
3.1.1 HEC-HMS Basin Model	3-4
3.1.2 HEC-HMS Meteorologic Model	3-5
3.1.3 HEC-HMS Control Specifications and Model Runs	3-5
3.1.4 Gridded and Lumped SCS CN Rainfall Excess Calculation	3-5
3.1.5 ModClark / Clark UH surface runoff transformation	3-6
3.1.6 Spatial and Temporal Resolution Limitations and Requirements	3-8
<u>3.2 Discussion of Digital Datasets Used in Modeling Study</u>	3-8
3.2.1 Surface Soil Characterization	3-8
3.2.2 Land Use and Land Cover	3-12
3.2.3 Elevation Data	3-15
3.2.4 NEXRAD Rainfall Data	3-16
3.2.5 IFLOWS Rainfall Data	3-20
3.2.6 USGS Streamflow Data	3-23

<u>3.3 Software and Programs Utilized</u>	3-25
3.3.1 GIS Software: ARC/INFO, GRID, ArcView	3-25
3.3.2 Programs to Decode NEXRAD Stage III Archives	3-26
3.3.3 GIS Based Model Preprocessor: HEC-GeoHMS	3-27
3.3.4 Modeling Software: HEC-HMS	3-27
<u>3.4 Map Projections and Coordinate Systems Used</u>	3-27
3.4.1 Hydrologic Rainfall Analysis Project (HRAP)	3-27
3.4.2 Standard Hydrologic Grid (SHG)	3-28
3.4.3 Geographic Coordinates (Latitude and Longitude)	3-29
<u>3.5 Study Area: The Upper Roanoke River Watershed, VA</u>	3-29
<u>3.6 Data Processing and Preparation of Model Inputs</u>	3-33
3.6.1 Creation of Gridded SCS CN Estimate	3-33
3.6.2 HEC-GeoHMS Processing	3-40
3.6.2.1 <i>Watershed and Stream Channel Delineation</i>	3-42
3.6.2.2 <i>HEC-HMS Basin File and Map File Creation</i>	3-48
3.6.2.3 <i>HEC-HMS Grid Cell Parameter File Creation</i>	3-49
3.6.3 Processing of archived NEXRAD Stage III Data	3-53
3.6.4 Comparison of Radar to Gage Precipitation	3-58
3.6.5 Intercomparison of Varied Precipitation Resolutions	3-59
3.6.6 Creation of streamflow database from USGS records (DSSTS)	3-59
<u>3.7 Basin Model Parameterization</u>	3-59
3.7.1 Subwatershed Baseflow Calculation	3-59
3.7.2 Subwatershed Parameterization: t_c , R, AMC	3-61
3.7.2.1 Antecedent Moisture Condition (AMC)	3-61
3.7.2.2 Time of Concentration (t_c)	3-61
3.7.2.3 Clark's Reservoir Coefficient (R)	3-61
3.7.3 Channel Network Parameterization: k, x	3-62
<u>3.8 Development of Similarly Parameterized, Spatially Lumped Model</u>	3-63
3.8.1 Lumped SCS CN Rainfall Excess Calculation	3-64
3.8.2 Clark Unit Hydrograph Surface Runoff Transformation	3-64
3.8.3 Spatially Averaged Precipitation Inputs	3-65
<u>3.9 Data Collection and Analysis Plans</u>	3-66
3.9.1 Sensitivity to rainfall resolution and Grid Scale	3-66
3.9.2 Sensitivity to CN and AMC	3-67
3.9.3 Comparison of Lumped and Distributed Runoff Models	3-67
4.0 Model Results	4-1
<u>4.1 Correlation of NEXRAD and IFLOWS Precipitation Data</u>	4-1
<u>4.2 Comparison of Precipitation Resolutions</u>	4-7
4.2.1 Storm Total Statistics for 1km to 10km Precipitation Resolution at 1km Cell Size	4-7
4.2.2 Visualization of Varied Precipitation Resolutions	4-9
4.2.3 Storm Total Statistics for 400m to 10k Precipitation Resolution and Cell Size	4-11
<u>4.3 Model Results at Base (4km) Precipitation Resolution</u>	4-11
4.3.1 Evaluation of October 1997 Storm Event	4-12
4.3.2 Evaluation of March 1998 Storm Event	4-13
4.3.3 Evaluation of April 1998 Storm Event	4-13
4.4 Model sensitivity to CN / AMC	4-14
<u>4.5 Effects of Precipitation Resolution on Model Results</u>	4-20
4.5.1 Effects of Precipitation Resolution on Runoff Volume	4-21
4.5.2 Effects of Precipitation Resolution on the Runoff to Rainfall Ratio	4-22
4.5.3 Effects of Precipitation Resolution on Hydrographs, Peak Flow, and Time to Peak	4-34
<u>4.6 Effects of Physical Parameter Resolution on Model Results</u>	4-37
<u>4.7 Comparison of Lumped and Distributed Model Results</u>	4-41
4.7.1 Effects of Spatial Lumping on Runoff Volume	4-41
4.7.2 Effects of Spatial Lumping on Hydrographs, Peak Flows, Times to Peak	4-44

5.0 Discussion and Conclusions	5-1
<u>5.1 Achievement of Objectives</u>	5-1
<u>5.2 Use of NEXRAD Stage III products in Hydrologic Modeling</u>	5-2
<u>5.3 Effects of Precipitation Resolution on Model Results</u>	5-4
<u>5.4 Effects of Physical Parameter and Computational Cell Size on Model Results</u>	5-4
<u>5.5 Effects of Spatial Distribution on Model Results</u>	5-5
<u>5.6 Evaluation of HEC-GeoHMS Processing Capabilities</u>	5-5
<u>5.7 Evaluation of HEC-HMS Gridded SCS CN, ModClark Model</u>	5-6
<u>5.8 Future Research</u>	5-6
5.8.1 Investigation of Spatial Variability in Precipitation Events	5-7
5.8.2 Investigation of Spatial Variability in Watershed Characteristics	5-7
5.8.3 Improvements in Model Specification and Parameterization	5-7
Appendices	
<u>A: References</u>	A-1
<u>B: Glossary</u>	B-1
<u>C: Sample ARC/INFO Projection (*.prj) Files</u>	C-1
<u>D: CN creation with ARC/INFO GRID</u>	D-1
CN Grid *.aml script	D-1
CN Tables from TR-55 (SCS, 1986)	D-5
<u>E: Radar Data Processing Utilities</u>	E-1
Summary of Radar Processing Steps	E-1
xmrgbatch.sh shell script	E-5
xmrgtoasc.c C program	E-6
XMRG file format	E-11
ASCII grid file format	E-13
hrap2shg.aml Arc Macro Language Script	E-15
hrap2shg.prj ARC/INFO Projection File	E-18
shg2dss.bat DOS batch file	E-20
grid2point.aml Arc Macro Language Script	E-21
<u>F: Grid Resampling Techniques (ESRI, 2002)</u>	F-1
Nearest Neighbor Reassignment	F-1
Bilinear Interpolation	F-2
<u>G: Sample HMS model input files</u>	G-1
Distributed Model Basin file	G-1
Control Specifications	G-12
Meteorologic Models	G-13
Grid cell parameter file	G-14
Lumped model basin file	G-16
<u>H: HEC-HMS Model Results</u>	H-1
October 1997, Varied Precipitation Resolution	H-1
March 1998, Varied Precipitation Resolution	H-8
April 1998, Varied Precipitation Resolution	H-15
March 1998, Varied Physical Parameter and Precipitation Resolution	H-22
<u>I: Precipitation Hyetographs</u>	I-1
<u>J: VITA</u>	J-1

List of Tables

2.1	Hydrologic Model Classifications	2-10
3.1	NLCD Classifications and Descriptions	3-12
3.2	Storm total precipitation summary statistics for Upper Roanoke Watershed	3-17
3.3	Table 3.3: Rain gage locations and names for the Upper Roanoke Watershed	3-21
3.4	Table 3.4: USGS Stream Gage locations for the Upper Roanoke River Watershed	3-23
3.5	Summary of datasets used.	3-25
3.6	Curve Numbers for SSURGO and NLCD attributes	3-35
3.7	Eight point pour flow directions	3-43
3.8	Subwatershed Baseflow for Upper Roanoke River Subwatersheds	3-60
3.9	Model Parameters for Upper Roanoke River Subwatersheds	3-63
3.10	Model Parameters for Upper Roanoke River Channel Segments	3-63
4.1	Regression results on gage and radar data	4-3
4.2	Storm Total Precipitation for Radar – Gage Pairs, October 1997	4-4
4.3	Storm Total Precipitation for Radar – Gage Pairs, March 1998	4-5
4.4	Storm Total Precipitation for Radar – Gage Pairs, April 1998	4-6
4.5	Storm total summary statistics for October 1997 Event	4-7
4.6	Storm total summary statistics for March 1998 Event	4-8
4.7	Storm total summary statistics for April 1998 Event	4-8
4.8	Percent Changes in Storm Total Precipitation Volume with Changes in Resolution	4-9
4.9	Storm Total Summary Statistics for Bilinearly Interpolated Precipitation Data	4-11
4.10	Hydrograph characteristics at watershed outlet, October 1997 event	4-18
4.11	Hydrograph characteristics at watershed outlet, March 1998 event	4-19
4.12	Hydrograph characteristics at watershed outlet, April 1998 event	4-19
4.13	Effects of Precipitation resolution on Runoff Volume	4-21
4.14	Subwatershed Runoff Volumes for Varied Physical Parameter Resolution	4-38
4.15	Gage Runoff Volumes for Varied Physical Parameter Resolution	4-38

List of Figures

2.1	Sample storm total Precipitation for 9/27/02 showing beam blockage by Poor Mountain	2-7
2.2	Variation of SCS CN with AMC	2-20
3.1	Grid Cell Size versus Grid Resolution	3-2
3.2	GIS Processing Flowchart	3-3
3.3	Hydrologic Soil Group Classification for Upper Roanoke Watershed from SSURGO	3-10
3.4	Hydrologic Soil Group Classification Carvins Cove Reservoir Area from SSURGO	3-11
3.5	National Land Cover Dataset for Upper Roanoke River Watershed	3-14
3.6	National Land Cover Dataset for Area surrounding Carvins Cove Reservoir	3-15
3.7	Digital Elevation Model for Upper Roanoke River Watershed, VA from USGS	3-16
3.8	Storm total precipitation for the October 1997 storm event	3-18
3.9	Storm total precipitation for the March 1998 storm event	3-19
3.10	Storm total precipitation for the April 1998 storm event	3-20
3.11	IFLOWS rain gage locations in and around the Upper Roanoke River Watershed	3-22
3.12	IFLOWS rain gage locations and storm total precipitation depths for March 1998	3-23
3.13	USGS Stream Gage Locations in Upper Roanoke River Watershed, VA	3-24
3.14	Location of Upper Roanoke River Watershed in Virginia	3-31
3.15	Location of Upper Roanoke Watershed in Southwest Virginia	3-32
3.16	USGS Digital Line Graph Data for Upper Roanoke River Watershed	3-33
3.17	Flowchart for Curve Number Processing	3-36
3.18	Gridded SCS CN, AMC II, for Upper Roanoke River Watershed	3-37
3.19	Gridded SCS CN, AMC II, for Carvins Cove Reservoir	3-38
3.20	Gridded CN, AMC I, for Upper Roanoke River Watershed	3-39
3.21	Gridded CN, AMC III, for Upper Roanoke River Watershed	3-40
3.22	HEC-GeoHMS Processing	3-41
3.23	Sinks in Upper Roanoke River Watershed DEM	3-42
3.24	Eight point pour flow directions	3-43
3.25	Flow Directions for Upper Roanoke River Watershed	3-44
3.26	Flow Accumulation for Upper Roanoke River Watershed	3-45
3.27	Stream Network for Upper Roanoke River Watershed	3-46
3.28	Raster Stream Network for Area Near Ellet, VA on North Form of Roanoke River	3-47
3.29	Subwatershed Delineation for Upper Roanoke River Watershed	3-48
3.30	Subwatershed Discretization and Connectivity for Upper Roanoke River Watershed	3-49
3.31	Gridded Representation of Upper Roanoke River Watershed, 1 kilometer grid resolution	3-50
3.32	Gridded Representation of Upper Roanoke River Watershed, 500 meter grid resolution	3-51
3.33	Gridded Representation of Upper Roanoke River Watershed, 4 kilometer grid resolution	3-52
3.34	Gridded CN for area near Roanoke VA, 1km cell size	3-53
3.35	Gridded Precipitation Data Processing	3-54
3.36	Upscaling and Downscaling of NEXRAD data for March 19 th , 1998, 0200 UTC	3-58
3.37	Subwatershed Average Precipitation for March 19 th , 1998, 0200UTC	3-65
4.1	Comparison of NEXRAD and IFLOWS Data at Masons Cove IFLOWS gage (LID 1111)	4-2
4.2	Comparison of NEXRAD and IFLOWS Data at Peters Creek IFLOWS gage (LID 1112)	4-3
4.3	Rendering of Gridded Precipitation Depth for March 19 th , 1998 0200UTC 4km (base) Resolution.	4-9
4.4	Rendering of Gridded Precipitation Depth for March 19 th , 1998 0200UTC 1km (smoothed) Resolution.	4-10
4.5	Rendering of Gridded Precipitation Depth for March 19 th , 1998 0200UTC 10km (degraded) Resolution.	4-10
4.6	Measured and Modeled Hydrographs at Walnut Street Gage, October 1997	4-12
4.7	Measured and Modeled Hydrographs at Niagara Gage, March 1998	4-13
4.8	Observed and Modeled Hydrographs at Niagara Gage, April 1998	4-14

4.9	Hydrographs at the Walnut Street Gage under varied AMC, October 1997	4-15
4.10	Hydrographs at the Walnut Street Gage under varied AMC, March 1998	4-16
4.11	Hydrographs at the Niagara Gage under varied AMC, March 1998	4-16
4.12	Hydrographs at the Walnut Street Gage under varied AMC, April 1998	4-17
4.13	Hydrographs at the Niagara Gage under varied AMC, April 1998	4-18
4.14	Storm Total Precipitation Depths at Varied Precipitation Resolutions	4-22
4.15	Mean Storm Total Precipitation, October 1997	4-23
4.16	Mean Storm Total Precipitation, March 1998	4-23
4.17	Mean Storm Total Precipitation, April 1998	4-24
4.18	Runoff to Rainfall Ratio at varied Precipitation Resolutions	4-25
4.19	Runoff to Rainfall Ratio, October 1997	4-26
4.20	Runoff to Rainfall Ratio, March 1998	4-26
4.21	Runoff to Rainfall Ratio, April 1998	4-27
4.22	Observed and Modeled Runoff Volume, Shawsville, VA	4-28
4.23	Observed and Modeled Runoff Volume, Lafayette, VA	4-29
4.24	Observed and Modeled Runoff Volume, Glenvar, VA	4-29
4.25	Observed and Modeled Runoff Volume, Walnut Street Gage	4-30
4.26	Observed and Modeled Runoff Volume, Niagara, VA	4-30
4.27	Observed and Modeled Runoff Volume, Confluence of Back Creek and Roanoke River	4-31
4.28	Observed and Modeled Runoff Volume at Walnut Street Gage, October 1997	4-32
4.29	Observed and Modeled Runoff Volume at Niagara Gage, March 1998	4-33
4.30	Observed and Modeled Runoff Volume at Niagara Gage, April 1998	4-33
4.31	Hydrographs at the Walnut Street Gage, October 1997	4-34
4.32	Hydrographs at the Niagara Gage, March 1998	4-35
4.33	Hydrographs Peaks at the Niagara Gage, March 1998	4-36
4.34	Hydrographs at the Niagara Gage, April 1998	4-36
4.35	Subwatershed Runoff Volumes For Varied Physical Parameter and Precipitation Resolution	4-39
4.36	Runoff Volumes at Stream Gage Points For Varied Physical Parameter and Precipitation Resolution	4-39
4.37	Runoff Volumes For Varied Physical Parameter and Precipitation Resolution, Ironto Subbasin	4-40
4.38	Subwatershed Runoff Volumes For Varied Physical Parameter and Precipitation Resolution, Confluence of Back Creek and Upper Roanoke River	4-40
4.39	Runoff Volumes from Lumped and Distributed Models	4-42
4.40	Runoff Volumes from Lumped and Distributed Models, October 1997	4-42
4.41	Runoff Volumes from Lumped and Distributed Models, March 1998	4-43
4.42	Runoff Volumes from Lumped and Distributed Models, April 1998	4-43
4.43	Hydrographs at Walnut Street Gage, October 1997	4-44
4.44	Hydrographs at Niagara Gage, March 1998	4-45
4.45	Hydrograph peaks at Niagara Gage, March 1998	4-45
4.46	Hydrographs at Niagara Gage, April 1998	4-46
5.1	Unused Cells in Bilinear Interpolation	5-3

List of Equations

2.1	Radar Measured Losses vs. Reflectivity	2-6
2.2	Relation of Reflectivity and Rainfall Rate	2-6
2.3	SCS Runoff Equation	2-17
2.4	SCS Initial Abstraction Equation	2-17
2.5	SCS Runoff Equation	2-17
2.6	Relation between Potential Maximum Retention and CN	2-17
3.1	Continuity Equation	3-6
3.2	Storage Outflow Relation for Linear Reservoir (Clarks UH)	3-6
3.3	Finite Difference Approximation for Outflow (Clarks UH)	3-6
3.4	Routing Coefficient Ca (Clarks UH)	3-6
3.5	Routing Coefficient Cb (Clarks UH)	3-6
3.6	Average Outflow (Clarks UH)	3-7
3.7	Cell Travel Time (ModClark)	3-7
3.8	Clarks definition of the Reservoir Coefficient	3-62
3.9	HEC definition of the reservoir coefficient	3-62

1.0 Introduction

Models are used by hydrologists to generate synthetic datasets when actual data is unavailable. For example: historical streamflow records may not be long enough in duration, an estimate may be needed of the effects of urbanization on surface runoff, or a flood forecast may be needed to warn downstream communities of impending danger. In surface water hydrology, mathematical models are often used to estimate outputs, such as streamflow, given known inputs, such as precipitation. Computer models are implemented when the equations inherent in a mathematical model become too numerous or complex to be solved by hand.

Precipitation and surface runoff generation mechanisms are inherently spatially variable. Historically, most hydrologic runoff models are spatially lumped, meaning that model parameters are spatially averaged across a watershed. These model parameters often must be developed empirically or through optimization. It is believed that model accuracy could be improved by accounting for the spatial variability of precipitation and runoff producing mechanisms. Unfortunately, the data and computing requirements of spatially distributed hydrologic models have historically been formidable. Advances in geographic information systems (GIS), remote sensing (RS), radar measurement of precipitation, and desktop computing have made it easier for the hydrologist to implement and use distributed models.

Distributed runoff models have large appetites for spatially distributed data. Mathematically, these models are computationally more intensive requiring greater computing capabilities and longer run times. GIS and RS provide the hydrologist with many relevant data sets characterizing soil type, elevation, land use and land cover, and precipitation. With careful application of GIS tools and the aforementioned data sets, the hydrologist can define many of the parameters and create many of the inputs required to run a distributed hydrologic model.

Spatial variability in soil characteristics, topography, land use and land cover, and precipitation all lead to spatial variability in surface runoff production. Available digital datasets and GIS tools enable the hydrologist to account for the spatial variability of these critical physical characteristics. Measurement of precipitation by weather radar, especially when coupled with ground based gage networks, provides an accurate measure of the spatial distribution and magnitude of precipitation across a watershed.

Grid based distributed models assume homogeneity of model parameters within each grid cell. For a grid or raster based hydrologic model, as grid cell size decreases, modeling accuracy should increase, but data and computational requirements will increase as well. Therefore, there is great interest in determining the optimal grid resolution to adequately and efficiently model hydrologic processes. The modeler should also be aware of model output sensitivity to the grid resolution of model inputs.

Accurate distributed modeling requires that essential spatial variability of all pertinent hydrologic parameters is represented. The most important input to a surface runoff

model is precipitation data. The measurement of precipitation by weather radar provides a critical data source to accurately describe the location and spatial distribution of precipitation. The National Weather Service (NWS) Weather Service radar, 1988 Doppler (WSR-88D) next generation radar (NEXRAD) system provides accurate estimates of spatially varied precipitation depths. NEXRAD stage III data are used as the precipitation inputs in this modeling study.

The Upper Roanoke watershed is 1480km² (571mi²) above the confluence of Back Creek and the Roanoke River. Terrain and landcover are highly varied from the forested slopes of the Jefferson National Forest to the urbanized areas of downtown Roanoke. Elevation and orographic effects cause spatial variability of precipitation intensity. The spatial variability in hydrologic characteristics as well as the flooding history of the Upper Roanoke River make the Upper Roanoke Watershed an ideal one for research on scale issues in distributed hydrologic modeling.

The ModClark model of the Hydrologic Modeling System of the Hydrologic Engineering Center (HEC-HMS) of the US Army Corps of Engineers (USACE) was used to model the Upper Roanoke River Watershed. The HEC-HMS ModClark model splits a watershed into a series of square grid cells. Precipitation and rainfall excess are computed individually at the grid cell level. Rainfall excess for each cell is lagged and routed through a linear reservoir to the watershed outlet where the cell runoff hydrographs are summed to produce the watershed hydrograph. Each grid cell has individual precipitation inputs and runoff producing parameters.

Publicly available digital data from the Natural Resources Conservation Service (NRCS), United States Geological Survey (USGS), and National Weather Service (NWS) were used to calculate model parameters and generate model inputs.

Modeled hydrographs are generated at varied grid resolutions and compared with each other and observed hydrographs for multiple storm events to evaluate model performance. Hydrograph shapes, peak flowrates, times to peak, and runoff volumes, are compared for model runs at varied grid scales.

1.1 Statement of Problem

Hydrologic modeling and river flow forecasting can potentially be improved by accounting for spatial variability of precipitation and runoff producing characteristics. Available digital datasets, GIS tools and advances in desktop computing provide the capabilities for distributed modeling. To efficiently use spatially distributed data, issues related to scales of data must be understood. As grid cell sizes become smaller, data transmission, data storage and computational requirements increase. As grid cell sizes become larger, rainfall and surface runoff are located less precisely with respect to basin boundaries, or areas of locally intense rainfall or surface runoff production may be aggregated into their surroundings. Data resolution must be fine enough so that the essential spatial variability is captured. To effectively and efficiently implement a grid

based hydrologic model, it is necessary to choose an appropriate grid scale and understand the effects of grid scale and data resolution on model results.

1.2 Research Objectives

The overall objective of this research is to investigate the effects of spatially distributed precipitation resolution and grid scale on a grid based distributed hydrologic runoff model of the Upper Roanoke River Watershed, VA. Specific objectives necessary to meet this goal are to:

- Implement a distributed hydrologic runoff model using existing GIS datasets and tools.
- Utilize gridded precipitation estimates derived from NWS-88D NEXRAD stage III data as inputs to the distributed runoff model.
- Quantify the effects of precipitation resolution and physical parameter grid scale on a distributed hydrologic runoff model.
- Compare the performance of a distributed hydrologic runoff model to a similarly specified and parameterized lumped model.

The remainder of this document describes the steps taken to address these research objectives and the results. Chapter 2 provides a review of the literature, historical use of weather radar and GIS in hydrology, and fundamental definitions and concepts. Chapter 3 describes the datasets used, GIS processing techniques and modeling techniques used to achieve the above objectives. Chapter 4 describes the results of the modeling study. Chapter 5 interprets the model results, makes recommendations concerning grid based distributed hydrologic modeling, and describes future areas of research in distributed hydrologic modeling with GIS.

2.0 Literature Review and Background Information

Chapter 2 provides a review of the literature, documents historical use of GIS and weather radar in hydrology, and develops fundamental definitions and concepts.

2.1 Historical use of GIS in Hydrology

Precipitation and surface runoff generation are inherently spatially variable. Spatial variability in soil characteristics, topography, land use and land cover, and precipitation all lead to spatial variability in surface runoff generation. Tools and data that allow the hydrologist to account for and quantify the spatial variability and magnitude of these hydrologic characteristics are available from geographic information systems (GIS), remote sensing (RS), and weather radar such as Weather Service Radar 1988 Doppler (WSR-88D) Next Generation Radar (NEXRAD). In fact, “considering the spatial character of parameters and precipitation controlling hydrologic processes, it is not surprising that GIS have become an integral part of hydrologic studies (Vieux, 2001).” Unfortunately, though these GIS tools have been available, the available technology is only recently becoming more widely used for water resources work. Maidment and Djokic (2000) cite the following reasons for this delay in implementation:

- Suitable data has been lacking.
- The expense of GIS technology has limited its use to larger organizations, while most of the services in the field are in the domain of small consulting companies.
- The engineering community has not been educated enough in GIS, while the GIS community has not been educated enough in engineering fields, making cross-discipline communication and implementation difficult.

Recent development of digital datasets, advances in GIS software and the lower cost of required hardware, and standardized data processing procedures are making GIS more accessible and useful to hydrologists and engineers.

Maidment (1991) identified four major applications of GIS to hydrology:

1. hydrologic assessment,
2. hydrologic parameter determination,
3. hydrologic model setup using GIS, and
4. hydrologic modeling within GIS.

For assessment, hydrologic factors pertaining to a situation are mapped within a GIS. Parameter determination uses analyses of terrain, land use and land cover, and other data layers to calculate hydrologically relevant parameter values. Hydrologic modeling within GIS is typically limited to steady state processes due to the time static nature of GIS. GIS systems are excellent for dealing with spatially varied data. When it comes to temporally – varied data, most GIS systems do not have extensive capabilities (DeBarry, et al., 1999). Many studies therefore have coupled GIS with existing hydrologic models to exploit the spatial strengths and graphical display capabilities of GIS and the dynamic modeling capabilities of hydrologic models. GIS are useful for parameter estimation, preparation of hydrologic model inputs, and display and analysis of hydrologic model outputs, especially when the spatial distribution of these items is being considered.

GIS have historically been used in hydrology and hydraulics for watershed and stream channel delineation, calculation of topographic parameters, preparation of hydrologic and hydraulic model inputs and display of model outputs. The GIS algorithms and techniques used to accomplish the above tasks are discussed in the following sections.

2.1.1 Watershed and Stream Channel Delineation from Elevation Models

Accurate delineation of watershed boundaries, calculation of watershed areas and the determination of stream channel locations are critical tasks for the hydrologist. These attributes can be calculated from field surveys, orthophotos and contour maps, however these processes can be time consuming. A more expedient and repeatable approach consists of deriving the necessary information from readily available digital elevation models (DEMs) (DeBarry, et al., 1999). Automated delineation of watershed boundaries and channel networks from DEMs is incorporated into many commonly available GIS packages and requires minimal GIS experience to implement.

Elevation models in GIS are either raster based, as is the case with USGS DEMs, or vector based as in the case of a triangulated irregular network, TIN. TINs typically allow more efficient use of data storage space as the nodes defining a TIN are only placed where necessary to define critical topographic points. A raster DEM conversely employs a regularly spaced series of points, leading to redundant or superfluous data in areas with less topographic relief. Watershed and stream channel delineation from raster DEMs is typically more computationally efficient and is more often used. Raster DEMs, such as the USGS DEMs or National Elevation Dataset (NED) are the most widely available source of digital elevation data (DeBarry, et al., 1999) and will be the focus of the following discussion.

The delineation of watersheds and stream channel networks from raster elevation models is based on the raster processing algorithms of O'Callaghan and Mark (1984), Jenson and Dominique (1988), and Garbrecht and Martz (1992). The raster processes involved in watershed and channel delineation will be summarized here.

The deterministic eight node (D8) method of O'Callaghan and Mark (1984) defines the drainage network of a DEM by identifying the steepest downslope flowpath between each cell of a raster DEM and its eight nearest neighbors. Flow travels downgradient until it reaches a relative minima or a boundary of the DEM. For effective stream channel delineation, relative minima, known as "sinks", should be eliminated from a DEM. Elimination of sinks ensures that all flow reaches the boundary of the DEM. The D-8 method has been criticized as it permits flow in one direction only from each cell and may not adequately represent divergent flow over complex slopes. A single flow direction algorithm is more appropriate if the primary objective is the delineation of the drainage network for large drainage areas with well developed channels (Garbrecht and Martz, 1992). The D-8 method is widely used as a raster processing method (DeBarry, et al., 1999) and is the basis of the algorithms used in this research.

To create an accurate drainage network using the D-8 method, a DEM must be free of relative minima or “sinks”. Sinks may result from natural terrain features or DEM sampling errors or discretization. Sinks are removed from a DEM by either a filling process, a breaching process, or a combination thereof. Filling sinks consists of raising the elevation of a sink until it is at least the elevation of its lowest neighbor, thereby permitting flow downgradient. In contrast, breaching sinks consists of lowering the lowest neighboring cell to the elevation of the sink, again permitting flow downgradient. For a sink free DEM, flow proceeds from any cell in the DEM until a boundary of the DEM is reached.

Garbrecht and Martz (2000) identify the two most prevalent methods to identify points of channel initiation as the constant threshold area method and the slope dependent critical support area method. The slope dependent method assumes that channel sources occur at the transition between the convex profile of the hillslope and the concave profile of the stream channel. Unfortunately, due to DEM resolution issues, accurate local slope measurements are difficult to obtain from a DEM. For a DEM with vertical resolution of 1m and horizontal resolution of 30m, local slopes can be only zero, 0.3 or increments thereof (Garbrecht and Martz, 2000). The constant threshold area method consists of comparing the number of cells upstream of each DEM cell with a user specified threshold and has found more widespread use. The constant threshold area method of channel initiation is used in this research.

Identification of flow direction and consequently channel networks is difficult in flat terrain and the process of DEM “burning” is often used. Flat areas typically result from inadequate DEM resolution and prevent accurate flow direction determination as drainage directions in these areas cannot be assigned directly from information in the DEM (Vieux, 2001). DEM burning consists of artificially lowering the raster elevation cells known to contain existing stream channels. Existing stream channels may be located from aerial photographs, be digitized from maps or be obtained through digital hydrography datasets. DEM burning is a raster algebra process and can be summarized in four general steps (Saunders, 2000):

- 1) rasterization of a vector stream network,
- 2) assignment of DEM elevation values to the cells of the raster stream network,
- 3) manipulation of the stream network raster cells to ensure that elevations descend toward the outlet points, and
- 4) introduction of a fixed elevation differential between the stream network raster cells and the land surface cells.

From a sink free or depressionless DEM, additional raster datasets are created describing the hydrologic response of the landscape. By identifying the steepest downslope direction from each cell, a grid of flow direction is created. For each cell in the DEM, the number of cells upstream or number of cells draining directly into the cell can be determined from the flow direction grid. Cells in the flow accumulation grid greater than the threshold area are assigned to the stream channel network. Cells with no upstream accumulation are potentially watershed boundaries. Watersheds are delineated by

specifying a series of outlet points. All cells upstream of an outlet point make up a watershed. Raster representations of the watershed boundaries and stream channels can be converted to vector formats for further use. The application of the watershed delineation algorithms of HEC-geoHMS to the Upper Roanoke Watershed is discussed in Chapter 3.

2.1.2 Calculation of Model Parameters

Hydrologic parameters that can be calculated from a paper map or field survey can be calculated from a GIS, assuming adequate data are available. From an elevation model, overland slopes, channel slopes and channel profiles may be calculated. Watershed area, centroid locations, and flow path and channel segment lengths can be determined from vector representations of watershed boundaries and channel networks. These parameters have typically been derived from paper maps or field surveys. The automated derivation of topographic watershed data from digital data sources however is faster, less subjective, and produces more reproducible measurements than traditional manual methods according to Garbrecht and Martz (2000).

2.1.3 Preparation of Hydrologic Model inputs

Many components of hydrologic runoff models depend strongly on spatial factors, therefore GIS can be an effective tool to generate hydrologic model inputs. The Center for Research in Water Resources Preprocessor (CRWR-PrePro) and the Geospatial Hydrologic Modeling Extension (HEC-GeoHMS) are both extensions for ESRI's ArcView and Spatial Analyst which aid the modeler in preparing inputs for HEC-HMS from digital datasets.

CRWR-PrePro is a system of ArcView GIS scripts and associated controls developed to extract topographic, topologic, and hydrologic information from digital spatial data, and to prepare ASCII files for the basin and precipitation components of HEC-HMS. These files, when opened by HEC-HMS, contain a topologically correct schematic network of subbasins and reaches attributed with hydrologic parameters and a protocol to relate gage and subbasin precipitation time series (Olivera and Maidment, 2000).

HEC-geoHMS is a software package for use within the ArcView GIS environment. GeoHMS uses ArcView and Spatial Analyst to develop a number of hydrologic modeling inputs including HEC-HMS basin models. Algorithms in GeoHMS may be used to quantify hydrologic characteristics such as: drainage area above a point, flow path length, land surface slope, and channel slope. From a digital elevation model, HEC-geoHMS delineates drainage paths and watershed boundaries and creates a hydrologic data structure that represents the watershed response to precipitation. Capabilities of HEC-GeoHMS include the development of grid-based data for a linear quasi-distributed runoff transformation (ModClark), the HEC-HMS basin model, physical watershed and stream characteristics, and a background map file (Doan, 2000).

2.1.4 Hydraulic Modeling of River Channels and Floodplains

The Triangulated Irregular Network (TIN) based terrain modeling capabilities of GIS are often used in hydraulic modeling and floodplain analysis. The TIN data structure has the ability to precisely represent linear features (banks, channel bottoms, ridges) and point features (hills and sinks) important in defining channel and floodplain geometry (Long, 2000).

HEC-GeoRAS is an ArcView GIS extension specifically designed to process geospatial data for use with the Hydrologic Engineering Center River Analysis System (HEC-RAS). The extension allows users with limited GIS experience to create an HEC-RAS import file containing river reach geometric data from an existing digital terrain model (DTM) and complementary data sets. Results exported from HEC-RAS may also be processed and displayed (Ackerman, 2000).

2.2 Radar Measurement of Precipitation

The measurement of precipitation by weather radar provides a critical data source to accurately describe the location and spatial distribution of precipitation. The spatial and temporal distribution of precipitation is typically quantified using ground based gage networks. Unfortunately, inadequate gage density as well as uncertainties in relative weighting of gage readings often prevent ground based gage networks from adequately defining the spatial variation of precipitation. Many engineering hydrologic modeling applications suffer due to a shortage of rainfall data. Traditionally, rainfall estimated from sparse rain gage networks has been considered a weak link in watershed modeling as precipitation varies on the scale of kilometers while rain gages in the U.S. are spaced 10's to 100's of kilometers apart (DeBarry, et al., 1999).

Spatially distributed, real time weather radar rainfall estimates are valuable for flood warning (DeBarry, et al., 1999). Though these real time, radar-only precipitation estimates may be quantitatively in error by as much as a factor of two or more in either direction, they allow forecasters to identify areas with locally intense rainfall and issue flash flood warnings accordingly. The accuracy of radar-derived precipitation estimates must be improved through calibration against satellite data or ground based gages in order for radar data to be used successfully in hydrologic modeling.

An understanding of the processes used in determining precipitation intensity or depth from radar reflectivity, as well as an understanding of the uncertainties involved, is necessary to appropriately use radar derived precipitation inputs in a hydrologic model. One of the most hydrologically significant radar systems in the US is the WSR-88D or NEXRAD radar (Vieux, 2001). The following discussion is most applicable to the WSR-88D radar network, however it is qualitatively applicable to other radar units as well.

2.2.1 Determination of Rainfall Intensity from Reflectivity

Radar derived precipitation depths are calculated from reflectivity. Reflectivity is the measurement by the radar of backscattered power. From this measurement of reflectivity, various empirical relations are used to calculate rainfall rate or intensity. Rainfall intensity is integrated over time to produce rainfall depth.

The equation that relates radar-measured power, P , to characteristics of the radar and characteristics of the precipitation targets is given by equation 2.1 (Vieux, 2001):

$$P = \frac{CLZ}{r^2} \quad 2.1$$

Where:

P = radar measured power (watts),

C = a constant dependent upon radar design parameters,

L = attenuation losses,

Z = reflectivity (mm^6/m^3), and

r = range in km.

The magnitude of error of the rainfall estimate is most sensitive to the Z-R relationship being used. The Z-R relationship relates reflectivity to rainfall rate based on an assumed drop size distribution. Utilizing the exponential drop-size distribution of Marshall and Palmer (1948), reflectivity, Z (mm^6/m^3), is related to rainfall rate, R (mm/hr), by equation 2.2 (Vieux, 2001):

$$Z = \alpha R^\beta \quad 2.2$$

Where α and β are empirically derived coefficients representing the drop size distribution.

The National Weather Service (2002) cites multiple Z-R relationships used in processing NEXRAD data. The parameters ($Z=200^{1.6}$) of Marshall and Palmer (1948) are used for general stratiform events. Other parameters used in NEXRAD processing include "convective" $Z=300R^{1.4}$, "tropical" $Z=250R^{1.2}$, "stratiform" for general stratiform events ($Z=200^{1.6}$) and for winter stratiform events at sites east ($Z=130R^{2.0}$) and west ($Z=75R^{2.0}$) of the continental divide.

The Z-R relationship used to convert reflectivity into rainfall rate is often in error, because this empirical relationship depends upon the drop size distribution. This distribution changes throughout the storm and depends upon the origin and evolution during the storm event of the precipitation-producing mechanism (Vieux 2001).

2.2.2 Uncertainties in Radar Measurement of Precipitation

Uncertainties in radar measurement of precipitation arise from two sources: first, errors in measuring of backscattered power, and second relating backscattered power and the corresponding reflectivity to rainfall rate.

Wilson and Brandes (1978) identify the following sources of measurement error: 1) beam blockage by obstacles close to the radar site, 2) anomalous propagation of the radar beam, 3) the buildup of precipitation films on the radome, and 4) attenuation by precipitation, cloud and atmospheric gasses. Error may also arise from hail contamination. Frozen precipitation has a significantly higher reflectivity than liquid precipitation. The presence of wet hail and snow can completely mask any useful information regarding liquid rain rates (DeBarry, et al., 1999).

An interesting example of beam blockage by terrain is evident in storm total precipitation shown by the Roanoke WSR-88D radar (KFCX). The storm total precipitation for September 27th, 2002 (figure 2.1 below) shows the effects of beam blockage by Poor Mountain and is typical for precipitation measured by the Roanoke radar (KFCX). A regularly shaped “slice” of decreased precipitation depths is noticeable to the NNE of the radar unit which is located at the center of the figure.

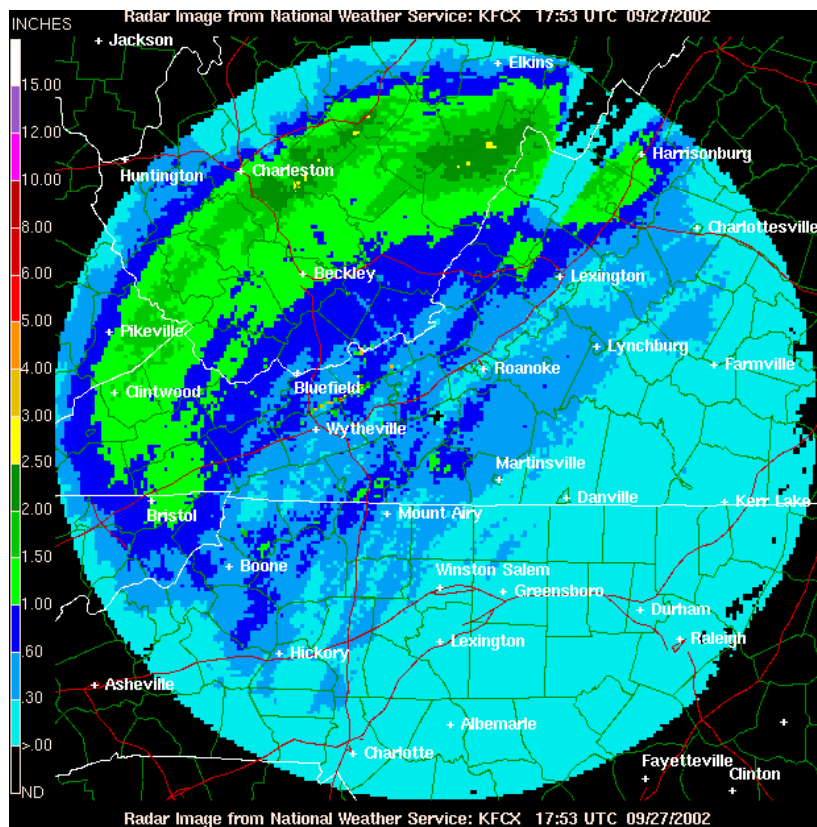


Figure 2.1: WSR-88D depiction of storm total precipitation for 9/27/2002.

Sources of uncertainty also exist in the computation of rainfall intensity from reflectivity. Wilson and Brandes (1978) summarize physical mechanisms that may alter drop size distributions as well as their probable influence on the Z-R relationship. These factors include evaporation, coalescence and breakup of drops and vertical air motions; updrafts and downdrafts.

Smith et al. (1996) examined systematic biases in WSR-88D hourly precipitation accumulation estimates using over 1 year of WSR-88D data and rain gage data from the southern plains. Biases were examined in three contexts:

- 1) biases that arose from range dependent sampling of the WSR-88D,
- 2) systematic differences in radar rainfall estimates from two radars observing the same area, and
- 3) systematic differences between radar and rain gage estimates of rainfall.

Radar-radar intercomparison studies suggested that radar calibration is a significant problem at some sites and radar-gage intercomparison analyses indicate systematic underestimation by the WSR-88D compared to rain gages. Analyses of spatial coverage of heavy rainfall, however, illustrate fundamental advantages of radar over rain gage networks for rainfall estimation especially in the context of flood hazard assessment (Smith et al. 1996). Much of the uncertainty in radar precipitation measurements can be removed by careful processing and calibration against other precipitation measurements such as ground based rain gages.

2.2.3 Calibration of Radar by Ground based Gages and Mosaicing

Calibration of radar against ground based gages can be performed in real time or in post storm analysis to improve the accuracy of radar derived precipitation estimates. This calibration is typically accomplished by comparing precipitation accumulations from radar and gage. The ratio of radar to gage is termed a bias (Vieux, 2001). A mean field bias is computed by averaging many pairs of radar and gage accumulations within a geographic area. Calibration of the radar to rain gage data, essentially an adjustment to the multiplicative constant of the Z-R relationship, is the most commonly used technique to calibrate radar rainfall estimates (Vieux, 2001).

Coverages from adjacent weather radars are often overlaid or mosaiced to improve estimates of precipitation depths. Unfortunately, calibration differences between radars can introduce uncertainty to this process.

2.2.4 NWS NEXRAD Processing

The product currently generated by the WSR-88D radar system most applicable to watershed modeling is the hourly digital precipitation array (DPA) (DeBarry, et al., 1999). Three levels, or stages, of processing occur in the production of the NEXRAD stage III precipitation estimates used in this research.

The DPA products, also known as stage I products, are radar only estimates of hourly rainfall accumulation on the approximately 4km x 4km rectilinear Hydrologic Rainfall

Analysis Project (HRAP) grid. Radar estimates of precipitation intensity are initially made relative to a radar-centered polar grid with 2km by 1° cells. Transfer of these estimates to the rectangular HRAP grid is made by averaging all rainfall estimates on the polar grid whose centers lie within the boundary of an HRAP grid box, regardless of how much of the polar grid box may lie outside of the given HRAP grid box. The average rainfall is then assigned to the HRAP grid box (Fulton, 1998).

The accuracy of the DPA products are affected mostly by: 1) how well the radar can see precipitation near the surface given the sampling geometry of the radar beams, 2) how accurately the microphysical parameters of the precipitation system are known, 3) the accuracy of radar calibration, and 4) sampling errors in the radar measurement of returned power (NWS, 2002). Stage I processing includes a significant amount of automated quality control including corrections for reflectivity outliers, beam blockages, and isolated reflectivity echos (DeBarry, et al., 1999).

Stage II processing occurs at the weather service forecast office (WFO) responsible for each particular radar. Stage II processing consists primarily of mean field bias adjustment. The mean field bias is the average of radar to gage precipitation ratios taken at a number of points over a geographic area. To adjust mean field bias, a multiplicative constant equal to the inverse of the mean field bias is applied to all precipitation depths. The mean field bias adjustment has the greatest quantitative impact on precipitation depths calculated in stage II products and can greatly impact the catchment wide volume of water being estimated (NWS, 2002).

Stage III processing is performed at the NWS River Forecast Center (RFC) associated with the particular radar. During stage III processing, data from a number of radar sites is merged together to form a mosaic of the area under the responsibility of the RFC. Data is then quality checked and adjusted by the Hydrometeorological Analysis and Service (HAS) forecasters at each RFC. Forecasters play a critical role in improving the quality and accuracy of the stage III data (NWS, 2002). The stage III gridded precipitation estimates are the Weather Service's best estimate of the magnitude and spatial distribution of liquid precipitation and involve radar and gage measurements and extensive processing and quality control. NEXRAD stage III precipitation products are available at a 4km spatial resolution and one hour temporal resolution.

2.3 Modeling Definitions and Classifications

Models are used by hydrologists to generate synthetic datasets when actual data is unavailable. In surface water hydrology, mathematical models are often used to estimate outputs, such as streamflow, given known inputs, such as precipitation. Computer models are implemented when the equations inherent in a mathematical model become too numerous or complex to be solved by hand. In the case of the models included in HEC-HMS for example, the known input is precipitation and the output is runoff or the known input is upstream flow and the output is downstream flow (Feldman, 2000).

Woolhiser and Brakensiek (1982) define a mathematical model as a symbolic, usually mathematical representation of an idealized situation that has the important structural properties of the real system. A theoretical model includes a set of general laws or theoretical principles and a set of statements of empirical circumstances. An empirical model omits the general laws and is in reality a representation of the data.

The accuracy of model results is a function of the accuracy of the input data and the degree to which the model structure correctly represents the hydrologic processes appropriate to the problem. Model structure is also referred to as model formulation or specification. As hydrology is inherently spatially varied, distributed models are of significant interest. Spatially-distributed modeling offers the capability of determining the value of any hydrologic variable at any grid-point in the watershed at the expense of requiring significantly more input than traditional approaches (Ogden, 1998).

There are a number of categorizations that can be applied to mathematical models. They are summarized in table 2.1 below (Ford and Hamilton, 1996).

Table 2.1: Hydrologic Model Classifications

event or continuous	An event model simulates a single storm with a typical duration of a few hours to a few days. A continuous model simulates a longer period and accounts for watershed response during and between precipitation events.
lumped or distributed	A distributed model accounts for the spatial variation of characteristics and hydrologic processes. Lumped models average or ignore the spatial variation of these characteristics.
empirical or conceptual	A conceptual model is based on knowledge of the pertinent physical, chemical, and biological processes that act on the input to produce the output. An empirical model is based upon observations of input and output without explicitly representing the conversion process.
deterministic or stochastic	If all input, parameters, and processes are considered free from random variation and known with certainty, a model is deterministic . A stochastic model describes these random variations and includes the effects of uncertainty in the output.
measured parameter or fitted parameter	In a measured parameter model, model parameters can be directly or indirectly measured from system properties. A fitted parameter model includes parameters that cannot be measured and instead must be found through empirical calibration or optimization techniques.

The models used in this research are deterministic and the user is forced to use sensitivity analysis along with knowledge of the uncertainties associated with the input data to determine the uncertainties in the model results.

2.4 Review and Comparison of potential distributed runoff models

The following models were reviewed and considered for this research. They are all grid based distributed parameter models. Model formulation, data requirements and model availability and ease of implementation are briefly discussed below.

2.4.1 CASC2D (Ogden, 1998)

CASC2D is a fully-unsteady, physically-based, distributed-parameter, raster (square-grid), two-dimensional, infiltration-excess (Hortonian) hydrologic model for simulating the hydrologic response of a watershed subject to an input rainfall field. Major components of the model include: continuous soil-moisture accounting, rainfall interception, infiltration, surface and channel runoff routing, soil erosion and sediment transport.

CASC2D takes advantage of recent advances in Geographic Information Systems (GIS), remote sensing, and low-cost computational power. CASC2D allows the user to select a grid size that appropriately describes the spatial variability in all watershed characteristics. Furthermore, CASC2D is physically-based; CASC2D solves the equations of conservation of mass, energy and momentum to determine the timing and path of runoff in the watershed. A high-quality input data set required for good model performance, and the quantity of input required is large.

The most recent version of CASC2D that is supported by the U.S. Army Corps of Engineers Waterways Experiment Station, can only be given to new users at this time with permission from the U.S. Army Corps of Engineers and the model author, Fred Ogden. The U.S. Army Corps of Engineers does not presently support non-Corps CASC2D users. Though the model formulation of CASC2D is appropriate for a study of the effects of grid resolution, data requirements and lack of availability and support prevented CASC2D from being used in this research.

2.4.2 Hydrotel (Fortin, et al. 2000)

Hydrotel is a grid based distributed hydrological model compatible with remote sensing and GIS. The HYDROTEL model is run on microcomputers with a user-friendly interface, and can be applied to a wide range of watersheds with due account for available data, as a choice of options is offered for the simulation of the various processes. Algorithms are derived as much as possible from physical processes, together with more conceptual or empirical algorithms. HYDROTEL's model grid based structure, physics, flexibility, and GIS-integrated design make it an effective tool to study the effects of grid scale. Unfortunately, the present model interface and manual are entirely in French effectively eliminating its use in this research.

2.4.3 MIKE-SHE

MIKE-SHE, developed by the Danish Hydrologic Institute (now DHI Water and Environment), is possibly the most comprehensive and physically based model available today (DHI Water and Environment, 2002 <http://www.dhisoftware.com/mikeshe/>). Unfortunately, MIKE-SHE is not in the public domain, is quite expensive, and requires

an inordinate amount of data for successful application. Though it is a gridded and primarily physically based model, MIKE-SHE is not commonly used in the United States, and its expense and data requirements prevent the use of MIKE-SHE in this research.

2.4.4 HEC-HMS (Scharffenberg, 2001)

The Hydrologic Modeling System (HMS) is designed to simulate the precipitation – runoff processes of dendritic watershed systems. It is designed to be applicable in a wide range of geographic areas for solving problems including large river basin water supply and flood hydrology, and small urban or natural watershed runoff. HMS models are traditionally lumped at the watershed level with the exception of the grid based modified Clark (ModClark) surface runoff model. The ModClark method is a linear quasi-distributed unit hydrograph method that can be used with gridded precipitation data. The ModClark runoff transformation is limited in that hydrographs may only be produced at a basin outlet and some model parameters require the use of observed streamflow for their calculation.

Preparation of the inputs required by the ModClark model is aided by the availability of HEC-geoHMS, an extension for ESRI ArcView and Spatial Analyst. HEC-geoHMS meets the needs of both traditional lumped and distributed basin approaches with the capability to develop HMS input files compatible with both approaches (Doan, 2000).

Though the model specification and capabilities of the distributed HMS model are limited, the availability and support for HEC-HMS and the capabilities of the processor HEC-geoHMS make it an effective tool for research concerning effects of grid scale and comparison of distributed and lumped modeling approaches.

2.5 Scale and Resolution in Distributed Hydrologic Modeling

To effectively account for the spatial variability inherent in a hydrologic system, an appropriate level of spatial discretization must be used for model parameters and inputs. Spatial discretization is accomplished in a distributed hydrologic model by breaking a watershed into a series of finite elements or cells having regular or irregular shape. In the case of a grid based model, grid cell size (quantified in this research by the length of a cell side) is directly related to the amount of deterministic variability (between cell) in a physical parameter or model input.

Raster data structures in GIS are a series of square grid cells each containing an attribute value. Raster attributes can describe any number of parameters such as: elevation, land use and land cover, or the depth of precipitation occurring during a certain time step. A single raster grid is deterministic in nature, meaning that any attribute variability within a cell is ignored. This approach is necessary for computational reasons and allows for the incorporation of a variety of data inputs via GIS. Grid size therefore must be small enough to describe important deterministic variability (Vieux, 2001).

Computational elements require parameter values that are representative throughout a grid cell. The choice of computational element size and the sampled resolution of the digital maps used to define parameters govern how a distributed model will represent the spatial variation of hydrologic properties and model parameters. There is great interest in determining the necessary grid scale to efficiently model hydrologic processes. Critical variability in space and time may be missed if a dataset is sampled at too coarse a resolution. A dataset sampled at too fine a resolution takes excessive storage space and computing resources. The ideal is to find the resolution that adequately samples the data for the purpose of the simulation, yet is not so fine that computational inefficiency results.

The literature contains very few specific recommendations concerning resolution requirements for grid based distributed modeling. In a study on a 7.27km² agricultural watershed in central Pennsylvania, Seybert (1996) concluded that discretization of a watershed into at least 100 cells provided reasonable results.

A primary barrier to successful application of physically based distributed models is the scaling problem. Field measurements are made at the point or local scale, while the application in the model is at the larger scale of the grid used to represent the hydrologic process (DeVries, Hromadka 1993). When applying point scale measurements to a gridded model, the grid scale chosen must be fine enough that the point measurement is representative of the entire grid cell.

Certain issues exist related to the rescaling and sampling of raster data structures. These issues are applicable to any raster dataset including: raster DEMs, gridded rainfall estimates, and remotely sensed images. Just as coarser DEM resolutions result in flatter calculated slopes, coarser rainfall resolution results in reduced rainfall gradients. Though the following discussion and the majority of this research is concerned with rainfall resolution, the issues discussed are applicable to a great deal of raster data.

2.5.1 Effects of Radar Rainfall Resolution

Ogden and Julien (1994) examined the sensitivity of a physically based distributed runoff model to resolution of radar rainfall data. They developed two dimensionless length parameters describing the effect of rainfall data aggregation: storm smearing and watershed smearing.

Storm smearing occurs as rainfall data length scale approaches or exceeds the rainfall correlation length. This reduces rainfall rates in high intensity regions and increases rainfall rates in low intensity regions, effectively reducing rainfall intensity gradients. This reduction in rainfall intensity is only a function of the rainfall input and is independent of basin size or physical parameters.

Watershed smearing is quantified by the ratio of rainfall resolution to the square root of watershed area. Watershed smearing increases the uncertainty concerning the location of

rainfall, which can result in the transfer of rainfall across basin boundaries. Watershed smearing is more likely to occur for smaller basins and coarser rainfall resolutions.

Ogden and Julien (1994) concluded for simulations including infiltration that excess rainfall volumes decrease as rainfall resolution becomes coarser relative to watershed area. This is analogous to spreading locally intense areas of rainfall over a larger area, therefore allowing greater infiltration. A reduction in peak discharge was also observed with coarser rainfall resolution.

The change in space required to store a raster dataset is proportional to the square of the inverse of the change in cell size. Concerning computational time in a gridded model, Kouwen and Garland (1988) stated that computational time tends to increase with the cube of inverse grid size due to increases in the number of elements and the reduction in routing time step. A very substantial decrease in data requirements, communication time, and computing time may be realized if, for example, a 10km rainfall resolution can be shown to give results comparable to a 2km resolution (Kouwen and Garland, 1988).

2.5.2 Conditions Governing the Dominance of Spatial or Temporal Variability

Ogden and Julien (1993) investigated the relative sensitivity of surface runoff to spatial and temporal variability of rainfall using a physically based distributed runoff model. They concluded that spatial variability of rainfall is dominant when rainfall duration is less than the time to equilibrium and temporal variability dominates when rainfall duration is greater than time to equilibrium. This work was done using CASC2D, a physically based distributed parameter hydrologic model, topography and physical characteristics of two western watersheds, and two dimensional rainfall fields generated by a numerical precipitation model.

2.6 Case Studies Utilizing Radar and GIS in Hydrology

The following case studies illustrate applications of GIS and weather radar to hydrologic modeling and flood forecasting and also illustrate the evolution of the Modified Clark, ModClark, method currently available in HEC-HMS.

2.6.1 Hydrologic Model of the Buffalo Bayou Using GIS (Doan, 2000)

Doan (2000) created a hydrologic model of the Buffalo Bayou (883km²) in Houston Texas using inputs derived from GIS. Watersheds and streams were delineated from USGS DEMs at 30m resolution, stream data from USGS digital line graphs (DLGs) and EPA river reach files. Physical parameters were extracted using the CRWR-PrePro (Olivera and Maidment, 2000) program. The model employed used gridded NEXRAD rainfall and the ModClark runoff transformation. All spatial data used in this study were projected to an Albers equal area projection known as the standard hydrologic grid.

GIS procedures were used to develop model inputs, including the basin, precipitation, and ModClark files with the conclusion that GIS methods were more consistent,

repeatable, and efficient than manual methods. The ARC/INFO, ArcView GIS, HEC-DSS, and other utilities used were time consuming however, and required significant effort and expertise to implement. HEC has since integrated the existing GIS tools used with the programs developed in this project into the comprehensive software package HEC-geoHMS (Doan, 2000).

Doan (2000) found that the existing 30 meter DEM resolution was too coarse for detailed subbasin and stream delineation, especially in areas of low relief. To alleviate this, vector stream data was used to impose selected streams and drainage structures on the DEM through the process of DEM burning.

2.6.2 Runoff Simulation using Radar Rainfall Data (Peters and Easton, 1996)

Peters and Easton (1996) discuss the development and application of a distributed adaptation of the conceptual Clark (1945) runoff model on the Illinois River Watershed above Tenkiller Lake (4160 km²) in Oklahoma and Arkansas. The methodology used was created to take advantage of the level of detail in rainfall data available from the WSR-88D radar network. In this adaptation of the Clark (1945) method, the watershed is subdivided into a series of grid cells, radar rainfall is applied, and rainfall and losses are tracked uniquely for each grid cell. Rainfall excess for each cell is lagged to the basin outlet by the cells travel time and then routed through a linear reservoir and summed to produce the total runoff hydrograph. Peters and Easton (1996) conclude that the ModClark method has data requirements similar to existing lumped models with the addition of GIS derived cell parameters and provides a relatively straightforward transition to the use of radar rainfall data.

2.6.3 Application of ModClark to the Salt River Basin, MO (Kull and Feldman, 1998)

Kull and Feldman (1998) applied the ModClark method to the 7304km² Salt River Watershed in northeastern Missouri. The intent of this study was simply to demonstrate the use of radar rainfall in the runoff modeling process. The calibration and application of the hydrologic models therefore was taken only as far as necessary to meet that objective. Stage I radar data was used as the model input. Kull and Feldman concluded that simulations using basin averaged radar rainfall were more accurate than simulations using basin averaged gage rainfall but not as accurate as simulations using spatially distributed radar rainfall. This was especially true in the case of a locally intense storm not picked up by the sparse gage network available in the study area. Kull and Feldman (1998) felt that radar rainfall data combined with rain gage data, as is the case in NEXRAD stage III products, would yield better results than Stage I data.

2.6.4 Resolution Considerations in Using Radar Rainfall Data for Flood Forecasting (Kouwen and Garland, 1988).

Kouwen and Garland (1988) investigated the effects of spatial resolution and discretization of rainfall intensities on modeled runoff hydrographs for the Grand River Watershed (3520 km²) in Ontario. Simulated hydrographs were compared for 2, 5, and

10km basin grid sizes. Spatial averaging of radar rainfall data was found to reduce the effect of erroneous radar readings and was found to give comparable results with simulations using finer resolutions. Hydrographs based on radar derived rainfall generally reproduced measured hydrographs better than those derived from rain gage data. Because the rainfall runoff process is highly non-linear, a heavy rainfall input to a small part of the watershed results in a high simulated runoff. Therefore, a smoothing of the rainfall results in computing lower runoff amounts and lower peak flows (Kouwen and Garland, 1988).

2.7 The Natural Resources Conservation Service Curve Number Method

The Natural Resources Conservation Service (NRCS), formerly Soil Conservation Service (SCS), Curve Number (CN) method is a mathematical model relating precipitation to runoff and will be referred to as the SCS CN method. Potential surface runoff is quantified by the curve number (CN), a value typically between 30 – 100 that accounts for soil properties and land use characteristics. CNs are determined, typically from tabulated values, based on a priori knowledge of soil characteristics and land use and land cover for a watershed or model element. In the case where CNs are available at a level of detail finer than a watershed or model element, CNs may be spatially averaged to determine a representative CN. The following section describes the history and development of the SCS CN method, the fundamental equations used, and describes deficiencies related to modeling of historical storm events.

2.7.1 History of the SCS CN Method

In 1954, the Soil Conservation Service (SCS) developed a procedure for estimating direct runoff from storm rainfall. This procedure was empirically developed from significant research on small rural watershed areas. The procedure, referred to as the curve number (SCS CN) technique, has proven to be a very useful tool for evaluating effects of changes in land use and treatment on direct runoff (Rallison and Miller, 1982).

The SCS CN method was initially used by the SCS in project planning for the small watershed program (Public Law 83-566) (Rallison and Miller, 1982). Since its inception, the simplicity of the SCS CN method has led to its application to many situations and in many areas not utilized in the initial empirical development of the method. The method's credibility and acceptance has suffered, however, due to its origin as agency methodology, which effectively isolated it from the rigors of peer review (Ponce and Hawkins, 1996).

Regardless of intended uses, the SCS CN method has become firmly entrenched in the field of hydrology and is commonly included as the method of rainfall excess generation in computer models. As the quantification of CN from existing digital data describing soil and land cover is a relatively straightforward process, the SCS CN method lends itself well to GIS based preparation of hydrologic model inputs.

2.7.2 Summary of SCS CN Method Runoff Equations

The Natural Resources Conservation Service (NRCS) Curve Number (CN) method is detailed in the National Engineering Handbook, section 4 – Hydrology (NRCS, 1972) and is summarized here.

Runoff is calculated by equation 2.3:

$$Q = \frac{(P - I_a)^2}{(P - I_a) + S} \quad 2.3$$

Where:

Q = direct runoff (mm)

P = rainfall (mm)

S = potential maximum retention after runoff begins (mm)

I_a = initial abstraction (mm)

Initial abstraction accounts for all losses before runoff begins such as ponding in surface depressions, interception by vegetation, evaporation, and infiltration. I_a is highly variable but for small agricultural watersheds can be approximated by equation 2.4:

$$I_a = 0.2S \quad 2.4$$

Combining equations 2.3 and 2.4 results in equation 2.5:

$$Q = \frac{(P - 0.2S)^2}{P + 0.8S} \quad 2.5$$

Potential maximum retention (S) is related to the physical characteristics of the landscape with the curve number (CN) as shown in equation 2.6.

$$S = \frac{25400 - 254CN}{CN} \quad 2.6$$

It is obvious from the above equations that the SCS CN method contains no provisions for varying rainfall intensity or duration. A storm of equal precipitation depth will produce equal surface runoff whether one hour or one day in duration. The CN method is commonly modified to account for varying storm intensity and duration for use in hydrologic computer models. This is done by calculating the total precipitation and the total runoff that have occurred by the end of each model time step. The difference between total runoff at the end of the time step and the beginning of the time step is the incremental runoff for that time step. This is the method of application in HEC-HMS (Feldman, 2000).

2.7.3 The Curve Number as Quantification of Soil and Land Use Characteristics

The quantification of watershed physical characteristics is a necessary step in the implementation of any distributed hydrologic model. The majority of watershed physical characteristics may be described by accounting for soil characteristics, land use and land cover (LULC) and terrain information. Soil characteristics and land use are often combined into a dimensionless parameter called the Soil Conservation Service Curve Number (SCS CN or CN). The CN is used to compute the volume of rainfall excess in the HEC-HMS gridded curve number distributed runoff model and is therefore used as the description of watershed soil and land use characteristics in this modeling study.

2.7.3.1 Hydrologic Soil Group (HSG)

The runoff CN is based on two classification of the landscape: the Hydrologic Soil Group (HSG) and the land use and land cover condition (LULC). HSG is a parameter that defines the propensity of drainage for a soil type and is tabulated for over 4000 soil series in the United States alone. Hydrologic Soil Group (A, B, C, or D) is assigned to soil series by the Natural Resources Conservation Service (NRCS) according to infiltration rate, which is obtained for bare soil after prolonged wetting (Rawls, et al. 1993).

Group A soils have low runoff potential and high infiltration rates even when thoroughly wetted. They consist chiefly of deep, well drained to excessively drained sands or gravels. The USDA soil textures normally included in this group are sand, loamy sand, and sandy loam. These soils have a transmission rate greater than 0.76 cm/hr.

Group B soils have moderate infiltration rates when thoroughly wetted and consist chiefly of moderately deep to deep, moderately well to well drained soils with moderately fine to moderately coarse textures. The USDA soil textures normally included in this group are silt loam and loam. These soils have a transmission rate of 0.38 to 0.76 cm/hr.

Group C soils have low infiltration rates when thoroughly wetted and consist chiefly of soils with a layer that impedes downward movement of water and soils with moderately fine to fine texture. The USDA soil texture normally included in this group is sandy clay loam. These soils have a transmission rate between 0.13 and 0.38 cm/hr.

Group D soils have high runoff potential. They have very low infiltration rates when thoroughly wetted and consist mainly of clay soils with a high swelling potential, soils with a permanent high water table, soils with a claypan or clay layer at or near the surface, and shallow soils over a nearly impervious material. The USDA soil textures normally included in this group are clay loam, silty clay loam, sandy clay, silty clay, and clay. These soils have a very low rate of water transmission (0-0.13cm/hr). Some soils

are classified in group D because of a high water table that creates a drainage problem.

Soil series may also be classified as complexes meaning that the variability in soil series is too fine to be displayed at the map resolution of the paper or digital soil survey. A complex of type B soils and type D soils that cannot be adequately separated is therefore assigned a HSG of B/D.

2.7.3.2 Land Use and Landcover (LULC)

Curve Numbers are calculated from HSG, described above, and Land Use and Land Cover (LULC). This is typically done through the use of tabulated values such as those of Technical Report 55 (TR-55) (SCS, 1986). Unfortunately, the land use categorizations of TR-55 do not directly correlate the attributes of available LULC datasets requiring judgment on the part of the modeler to determine an appropriate CN from digital data. CN tables from TR-55 are included in Appendix D.

Curve numbers were originally developed from gaged watershed data where soils, cover, and hydrologic conditions were known. Data were plotted as rainfall versus runoff, a grid of plotted curve numbers, assuming $I_a = 0.2S$, was superimposed on the plot and the median CN selected. The curve numbers represent the averages of median site values for hydrologic soil groups, cover, and hydrologic conditions (Rallison and Miller 1982). The CN associated with the soil cover complexes are median values, representing the average soil moisture condition of a watershed. Sample variability in CN occurs due to infiltration, evapotranspiration, soil moisture, lag time, rainfall intensity, and temperature. Antecedent Moisture Condition (AMC) is the variable used to explain this variability (Rallison and Miller, 1982).

2.7.4 CN Variability with Antecedent Moisture Condition

CNs vary with storm events. The SCS proposes accounting for this variability through the use of Antecedent Moisture Condition (AMC) (SCS, 1972). The index of watershed wetness used with the CN method is the Antecedent Moisture Condition (AMC). Three levels are used: AMC I, AMC II, and AMC III. AMC I corresponds to the lowest runoff potential and is defined by the watershed soils being dry enough for satisfactory plowing or cultivation. AMC II is the average or median condition. AMC III is the condition with the highest runoff potential meaning that the watershed is practically saturated from recent rains. The choice of AMC when modeling historical storm events can be the cause of significant uncertainty. When modeling historical storm events, the sensitivity to variation of CN and AMC should be examined.

Rainfalls in antecedent periods of 5 to 30 days prior to a storm are commonly used as indexes of watershed wetness. An increase in an index means an increase in the runoff potential. Such indexes are only rough approximations because they do not include the effects of evapotranspiration and infiltration on watershed wetness. It is not worthwhile

therefore, to try for great accuracy in computing the Antecedent Moisture Condition (NRCS, 1972).

Antecedent Moisture Conditions I and III are not limits on CN choice, the most appropriate CNs for a storm event can be outside limits given by AMC I and AMC III. By analyzing the potential retention (S) as random variables, Hjelmfelt and Kramer (1982) fit a lognormal distribution to observed values of S and found that the SCS conditions of AMC I, II, and III correspond to the values of S with exceedence probabilities of 10%, 50%, and 90% respectively.

AMC may be accounted for in the SCS CN method by first computing the median CN for a soil type and hydrologic treatment and then recalculating CN for the desired AMC. The NRCS (1972) provides a table of values used to reclassify CNs from the AMC II or median condition to AMC I and III. This technique was used to calculate gridded CN estimates for varied AMCs from CNs developed for the median, AMC II condition. The reclassification values are shown in figure 2.2 below.

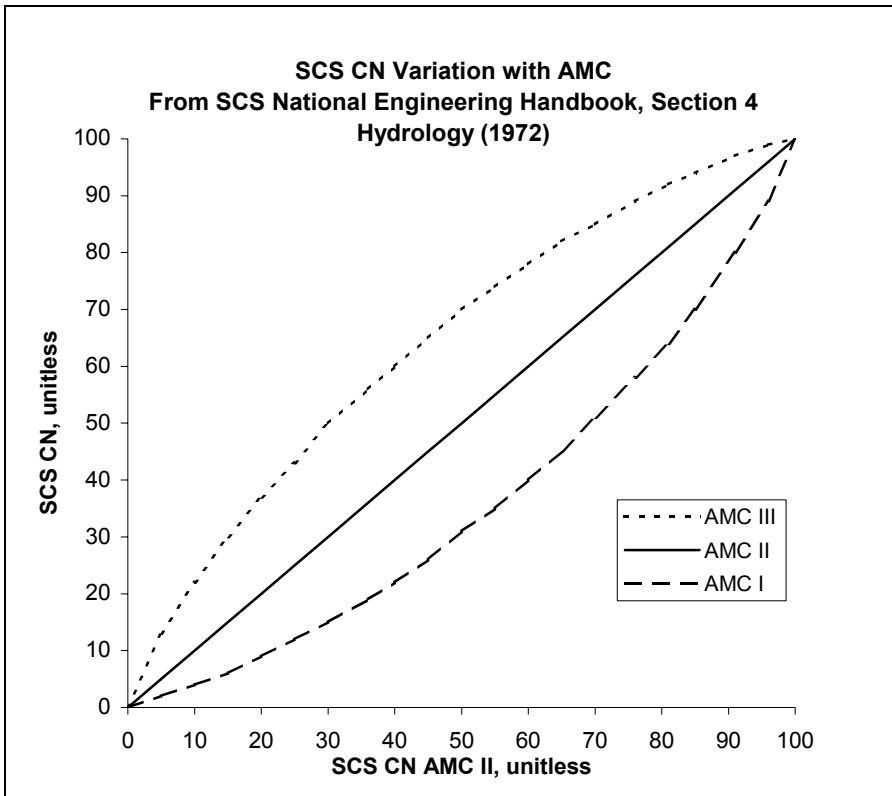


Figure 2.2: Variation of SCS CN with AMC (SCS, 1972).

2.7.5 Limitations of the SCS CN Method for Modeling Historical Events

As the SCS CN method was originally intended for use in evaluating design alternatives and is based on a variable (CN) representing average watershed conditions, it has limitations and uncertainties when applied to historical storm events. There is concern that the CN procedure does not always reproduce measured runoff from specific storm rainfall. In some instances lack of agreement occurs if an average condition CN is applied to a specific storm event. The CN for a storm event, however, can be anywhere within the enveloping CN range for the soil cover complex or even beyond this range (Rallison and Miler, 1982).

Choice of the appropriate CN and AMC for a certain watershed or model segment and storm event is critical for effective modeling. As the attributes of existing LULC datasets do not correlate directly with tabulated CN values, use of soil HSG and LULC to determine CN is subject to the modelers judgment. Storm to storm variation in CN can only be represented by choice of AMC and the most appropriate choice of AMC may vary across large watersheds such as the Upper Roanoke. It is critical therefore that the modeler examines sensitivity of model outputs to choice of CN and AMC.

3.0 Methodology: GIS and Modeling Techniques

Chapter 3 describes the methods used to address the research objectives stated in chapter

1. These objectives are, in summary, to:

- Implement a distributed hydrologic model using existing GIS datasets and tools.
- Utilize gridded precipitation estimates derived from NWS-88D NEXRAD stage III data as inputs to the distributed runoff model.
- Quantify the effects of precipitation resolution and physical parameter grid scale on a distributed hydrologic runoff model.
- Compare the performance of a distributed hydrologic runoff model to a similarly specified and parameterized lumped model.

The GIS processing techniques and modeling techniques used to examine the effects of rainfall resolution and grid scale on the HEC-HMS gridded SCS CN, ModClark runoff model are discussed. Section 3.1 discusses the architecture of the HMS model and the inputs required for a model run to show how grid scale and precipitation resolution may be isolated. Hydrologically significant GIS datasets are examined in section 3.2 for applicability to the modeling study. Required preprocessing of these datasets is discussed as well. Section 3.3 discusses the GIS and modeling software used in the modeling study. Map projections encountered in the modeling study are discussed in section 3.4. The study area, the Upper Roanoke River Watershed, VA, is described in section 3.5. GIS techniques to process the selected GIS datasets into model inputs are discussed in section 3.6. Issues related to data projection, spatial and temporal resolution and registration and data accuracy are examined. Model parameterization is discussed in section 3.7. The development of a similarly parameterized, lumped runoff model is discussed in section 3.8. Section 3.9 outlines the modeling techniques used to perform sensitivity analysis on precipitation resolution, grid scale, and CN and AMC.

The terms grid scale (or grid cell size) and resolution are often used interchangeably to describe the level of detail of a raster dataset. In this research, the terms grid scale and resolution are not synonymous however. Grid scale and grid cell size are terms used to describe the spacing of raster elements. Grid scale or grid cell size has units of length and quantifies the distance between the centers of any two adjacent cells or raster elements. Resolution describes the level of detail of a raster dataset and is also given in units of length. Figure 3.1 shows the difference between grid resolution and cell size. As the terms large scale and small scale can be confusing, grid cell size and dataset resolution are described in this document as coarse (less detail or larger element spacing) or fine (more detail or smaller element spacing). Converting a raster dataset to a coarser resolution or larger cell size is termed upscaling and converting to a smaller cell size is termed downscaling.

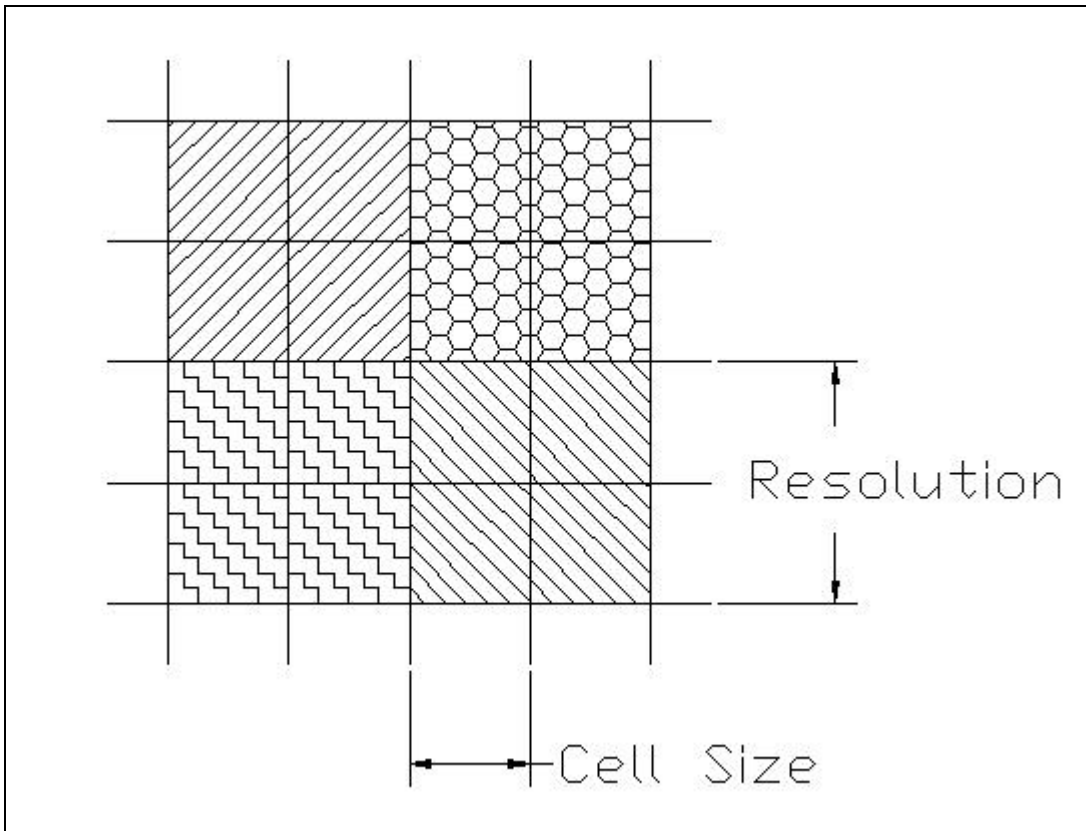


Figure 3.1: Resolution and Grid Cell Size.

It is possible to create a raster dataset with coarser resolution than grid cell size but it is not possible for resolution to be finer than cell size. Resolution may be upscaled, degraded, or made coarser by aggregating or averaging the values of neighboring grid cells. Detail cannot be added to a raster dataset during downscaling or resampling at a finer resolution. It is possible however, and probably appropriate for continuous data, to assume a continuous rate of change between raster cell centers. In this manner, a raster dataset may be smoothed during resampling to a smaller cell size. In order to isolate the effects of rainfall resolution while being constrained to a constant physical parameter grid cell size and registration, raster datasets of hourly precipitation depths with identical grid scale and varying resolutions were created.

As the goal of this study was an analysis of sensitivity to rainfall resolution, HEC-HMS parameterization was only taken far enough to produce reasonable results. In the case where such a model would be used in an operational or forecasting sense, parameterization would be improved as more storm events were observed and forecast.

Figure 3.2 shows a flowchart outlining the major processing steps and GIS datasets used in developing the inputs to the HEC-HMS runoff model.

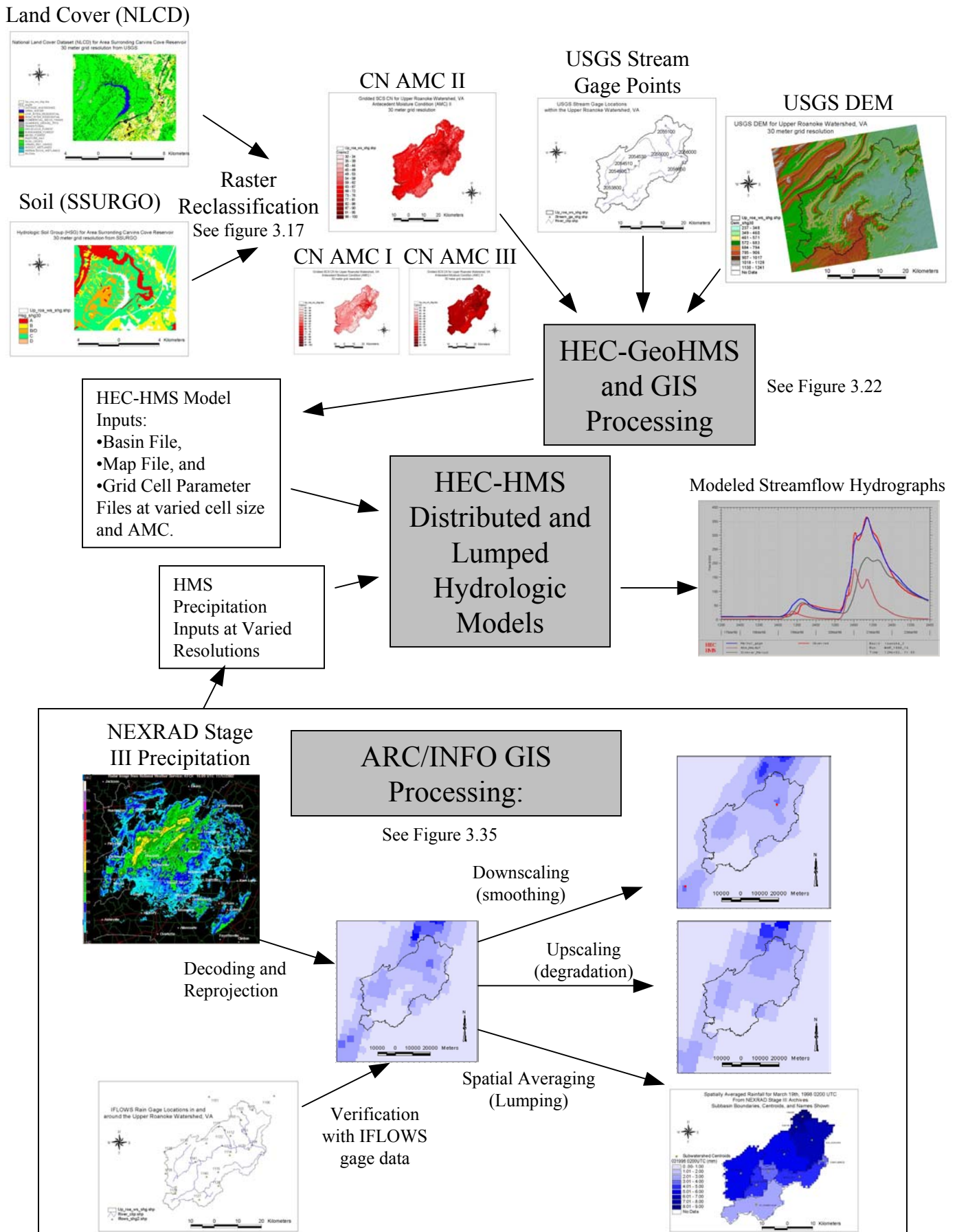


Figure 3.2: GIS Processing Flowchart

3.1 HEC-HMS Model Architecture and Required Inputs

The architecture of the HEC-HMS model is described to show how the effects on model results of precipitation resolution, grid scale, and CN and AMC may be isolated. A HEC-HMS model run is made up of three components: basin, meteorologic, and run control. All of these components are written in ASCII text and are therefore possible to generate with a number of different software tools including GIS software, spreadsheets, and text editors. Descriptions of these components are summarized below from Scharffenberg (2001) and Feldman (2000).

3.1.1 HEC-HMS Basin Model

A basin model in HEC-HMS describes the physical characteristics of watersheds or basins and river channels. The physical landscape is modeled by a series of hydrologic elements arranged in a dendritic, link – node manner. Hydrologic elements include subbasins (or subwatersheds), reaches (river or stream segments), junctions, reservoirs, diversions, sources and sinks. Computation proceeds from upstream elements downstream. In the case of the grid based, distributed basin model, a grid cell parameter file is used to describe the hydrologic characteristics of each grid cell. The grid cell parameter file contains location, area, travel length to the watershed outlet, and curve number or soil moisture accounting unit for each grid cell. The required grid cell parameter file may be created with GIS utilities such as HEC-GeoHMS and ESRI's Spatial Analyst.

A number of mathematical models are available in HEC-HMS to simulate subwatershed infiltration losses and runoff transformations. The infiltration method is specified for each subbasin in the basin model. Applicable loss methods for distributed runoff modeling include a gridded representation of the SCS CN and a gridded soil moisture accounting (SMA) method. Gridded SMA is more suited to continuous modeling than event modeling and requires significantly more data to implement and calibrate than gridded SCS CN. Only one runoff transformation, ModClark, is available for grid based distributed modeling.

Numerous hydrologic channel routing methods are available in HEC-HMS. Routing without attenuation may be accomplished with the lag method. The Muskingum, Muskingum – Cunge, and modified Puls routing methods may be used to simulate the effects of attenuation as well.

The modular arrangement of the HEC-HMS model components allows the user to create a series of grid cell parameter files and precipitation inputs at varied resolutions and antecedent moisture conditions. The components in the basin file describing hydrologic element connectivity, surface runoff transformation and channel routing are independent of the components describing the grid cells making up each subbasin.

3.1.2 HEC-HMS Meteorologic Model

The meteorologic model describes the spatial and temporal variation of precipitation inputs to the basin model. Various historic and synthetic precipitation methods are included in HEC-HMS. Historic precipitation events may be specified by point (typically rain gage) or gridded (typically radar derived) precipitation data. Various gage weighting techniques including Thiessen polygons, inverse distance weighting, and user specified weights are available. Gridded precipitation must be used with a grid based, distributed basin model. As no method exists to temporally interpolate gridded precipitation data, the time step of the HEC-HMS model is limited to the time step of the gridded precipitation data.

In order to use gridded precipitation and a gridded basin model, the cell size and registration of precipitation grid cells and watershed physical parameter grid cells must match exactly. This raises the question of how to vary precipitation resolution while holding grid scale constant. Gridded precipitation datasets were created with varied resolutions and identical cell size through the use of raster reprojection and resampling techniques described in section 3.6.

3.1.3 HEC-HMS Control Specifications and Model Runs

The control specifications of an HMS model run describe the start and end date and time as well as the temporal resolution or time step of the model. A model run is made up of a basin model, meteorologic model, and control specifications. By applying a series of meteorologic models with identical cell size and varied precipitation resolutions to the same basin model governed by the same set of control specifications, the effects of rainfall resolution may be isolated.

3.1.4 Gridded and Lumped SCS CN Rainfall Excess Calculation

The SCS CN method of rainfall excess determination is implemented both in a lumped and distributed manner in HEC-HMS. The mathematics of each are similar and based on equations 2.3 – 2.6 described in section 2.7. Incremental excess precipitation is computed for each subbasin or grid cell using cumulative precipitation and cumulative excess precipitation at the end of each model time step (Scharffenberg, 2001). Required parameters for the gridded SCS CN rainfall excess determination include the initial abstraction ratio (typically 0.2 as in equation 2.4), and the potential retention scale factor, a ratio applied to S in equation 2.3 or 2.5. The lumped representation of the SCS CN method uses constant values of 0.2 for initial abstraction ratio and 1.0 for potential retention scale factor. The lumped SCS rainfall excess calculation offers an option to specify percent imperviousness. As one of the goals of this study was to compare the performance of similarly specified and parameterized models, the initial abstraction ratio and potential retention scale factor were kept constant at 0.2 and 1.0 respectively for all distributed subbasins and simulations. As imperviousness is not explicitly accounted for in the gridded SCS CN method and is implied to be zero, percent imperviousness was kept at zero for all lumped subbasins and simulations.

3.1.5 ModClark / Clark UH surface runoff transformation

The Clark Unit Hydrograph (Clark UH) and modified Clark (ModClark) methods are based upon the work of Clark (1945). The Clark and ModClark methods account for the storage and attenuation properties of a watershed by lagging rainfall excess based on watershed travel time and routing rainfall excess through a linear reservoir. Required parameters for the Clark and ModClark methods are the time of concentration (t_c) and the reservoir coefficient (R), both with units of time. The fundamental equations of the Clark UH and ModClark methods as applied in HEC-HMS (Feldman, 2000) are described below.

Clark's model derives a watershed UH by explicitly representing two critical processes in the transformation of excess precipitation to runoff: translation and attenuation. Translation is the movement of excess from its origin throughout the drainage to the watershed outlet. Attenuation is the reduction of the magnitude of the discharge rate as excess is stored throughout the watershed.

The Clark model begins with the continuity equation (3.1):

$$\frac{dS}{dt} = I_t - O_t \quad 3.1$$

Where $\frac{dS}{dt}$ is the time rate of change of water in storage at time t ,

I_t is average inflow to storage at time t , and

O_t is outflow from storage at time t .

With the linear reservoir model, storage is related to outflow at time t by equation 3.2

$$S_t = RO_t \quad 3.2$$

Where S_t is the amount of water in storage at time t and

R is the constant linear reservoir parameter.

Combining and solving equations 3.1 and 3.2 with a finite difference approximation yields equation 3.3:

$$O_t = C_A I_t - C_B O_{t-1} \quad 3.3$$

Where C_A and C_B are routing coefficients calculated by equations 3.4 and 3.5.

$$C_A = \frac{\Delta t}{R + 0.5\Delta t} \quad 3.4$$

$$C_B = 1 - C_A \quad 3.5$$

The average outflow is calculated from equation 3.6.

$$\bar{O}_t = \frac{O_{t-1} + O_t}{2} \quad 3.6$$

The two required parameters for the Clark UH and ModClark runoff transformations, the time of concentration (t_c) and the reservoir coefficient(R), may be calculated by various methods, including optimization. Watershed time of concentration (t_c) is subject to varied definitions in the literature. Clark (1945) suggests that t_c may be graphically computed as the time interval between the end of runoff producing excess rainfall to the point of inflection of the recession limb of the hydrograph.

Though various definitions for the watershed reservoir coefficient exist in the literature, including graphical methods and regional analysis, the most effective way found to determine this parameter was through calibration. Clark (1945) suggests that R can be computed as the flow at the inflection point of the falling limb of the hydrograph divided by the time derivative of flow at that point. Kull and Feldman (1998) suggest computing R by regional analysis, by Clark's (1945) definition, or as the volume under the recession limb of the hydrograph after the point of inflection divided by the flow at that point. As observed streamflow data is necessary to calculate R, and the graphical definitions suggested above did not generally agree, the optimization methods of HEC-HMS and regional analysis to ungaged areas was determined to be the most effective method of subwatershed parameterization for t_c and R. These parameterization methods were found to produce results acceptable for the sensitivity analysis on rainfall resolution and grid scale. In an operational sense, these parameters would be improved with continued model use.

The ModClark method applies the equations of Clarks UH method in a spatially distributed manner. Rainfall excess for each grid cell is lagged based on cell travel time to the watershed outlet assuming a constant flow velocity (equation 3.7).

$$t_{\text{cell}} = t_c \frac{d_{\text{cell}}}{d_{\text{max}}} \quad 3.7$$

where t_{cell} = travel time from a cell to the watershed outlet, d_{cell} = travel distance from a cell to the watershed outlet, d_{max} = travel distance for the cell most distant from the watershed outlet.

The rainfall excess hyetograph for each cell is translated (lagged by t_{cell}) to the outlet where it is routed through a linear reservoir. All cells are routed through a linear reservoir with the same reservoir coefficient (R) and then summed to produce the subwatershed runoff hydrograph. In HEC-HMS, the reservoir coefficient (R) is specified for each subwatershed.

3.1.6 Spatial and Temporal Resolution Limitations and Requirements

For the distributed implementation of the HEC-HMS model when using gridded SCS CN, the ModClark runoff transformation and gridded precipitation are required (Scharffenberg, 2001). The grid cell size and registration for the precipitation data and the watershed grid cell parameter file must be identical. As HEC-HMS does not temporally interpolate between hourly precipitation grids, the model time step is constrained to the resolution of the precipitation data.

3.2 Discussion of Digital Datasets Used in Modeling Study

This section describes the digital and GIS datasets utilized in the modeling study of the Upper Roanoke River watershed. It contains data sources, qualitative descriptions of the information contained in each dataset, intended uses of each dataset, locational and attribute accuracy information, and native map projection and scale.

3.2.1 Surface Soil Characterization

The NRCS, formerly SCS, classifies soils based on predominant physical characteristics. Soils with similar physical characteristics are assigned to the same soil series. The spatial distribution of soil series and the attributes that describe these soil series are contained in NRCS soil surveys for much of the United States. To make soil survey data more easily available and usable, the NRCS is in the process of digitizing soil survey maps into the Soil Survey Geographic Database (SSURGO). A SSURGO data set consists of map data, attribute data, and metadata. SSURGO map data are available in modified Digital Line Graph (DLG-3) optional and Arc interchange file formats. Attribute data are distributed in ASCII format with DLG-3 map files and in Arc interchange format with Arc interchange map files (USDA, 1995).

The source of the attribute data is the Natural Resources Conservation Service Map Unit Interpretations Record database. The attribute data give the proportionate extent of the component soils and their properties. The data contain both estimated and measured physical and chemical soil properties and soil interpretations for engineering, water management, recreation, agronomic, woodland, range, and wildlife uses of the soil (USDA, 1995).

The attribute of interest for this modeling study was the Hydrologic Soil Group (HSG) classification. HSG is a parameter assigned to soil series by the NRCS to describe the potential of a soil series for infiltration and is described in section 2.7.3.

Coordinates for survey area wide coverages are in Geographic decimal degrees and referenced to the North American Datum of 1983. SSURGO data is mapped at a scale ranging from 1 : 12,000 to 1 : 63,360 and is defined as an order 2 or 3 survey (USDA, 1995). When rescaling soil data, as with all GIS data, native scale or original resolution of the dataset must be kept in mind. For example the common practice of enlarging soil maps does not result in more detailed or accurate maps. Soil survey maps enlarged to

1:12,000 scale from 1:20,000 scale are no more accurate or detailed than the original 1:20,000 map (USDA, 1995).

Not all areas are currently mapped or available at the county level of detail. Areas for which SSURGO data is not available may be mapped using State Soil Survey Geographic (STATSGO) data also from the NRCS. STATSGO data is mapped and distributed at the state level of detail meaning that larger areas are mapped at a coarser resolution.

SSURGO data is available for the majority of the upper Roanoke watershed. Montgomery, Botetourt, and Roanoke Counties are mapped and available. SSURGO data is not currently available for Floyd County, however provisional data for the Pilot and Check USGS quads (the portion of Floyd county within the Upper Roanoke Watershed) were obtained from Chris Fabian in the Bloomsburg, PA office of the NRCS.

Soil polygons from SSURGO were projected from geographic coordinates to the Standard Hydrologic Grid (SHG). Soil polygons are identified by a Map Unit Symbol ID (MUSYM). This is a unique ID relating each soil polygon to the attribute tables of the SSURGO database. This ID is unique only for the county being mapped and care should be taken that the appropriate counties MUSYM ids are used in joining and reclassification processes. Hydrologic Soil Group classification is contained in the "comp.dbf" table for each county. HSG was assigned by joining the "comp.dbf" table to the attribute table of the soil polygon shape file. A gridded representation of HSG for each soil survey area was created at a resolution and registration identical to the base elevation and land cover data. These grids were combined into a gridded representation of HSG for the entire watershed. Figure 3.3 shows a gridded representation of HSG for the Upper Roanoke Watershed, VA. Grid cell size is 30m.

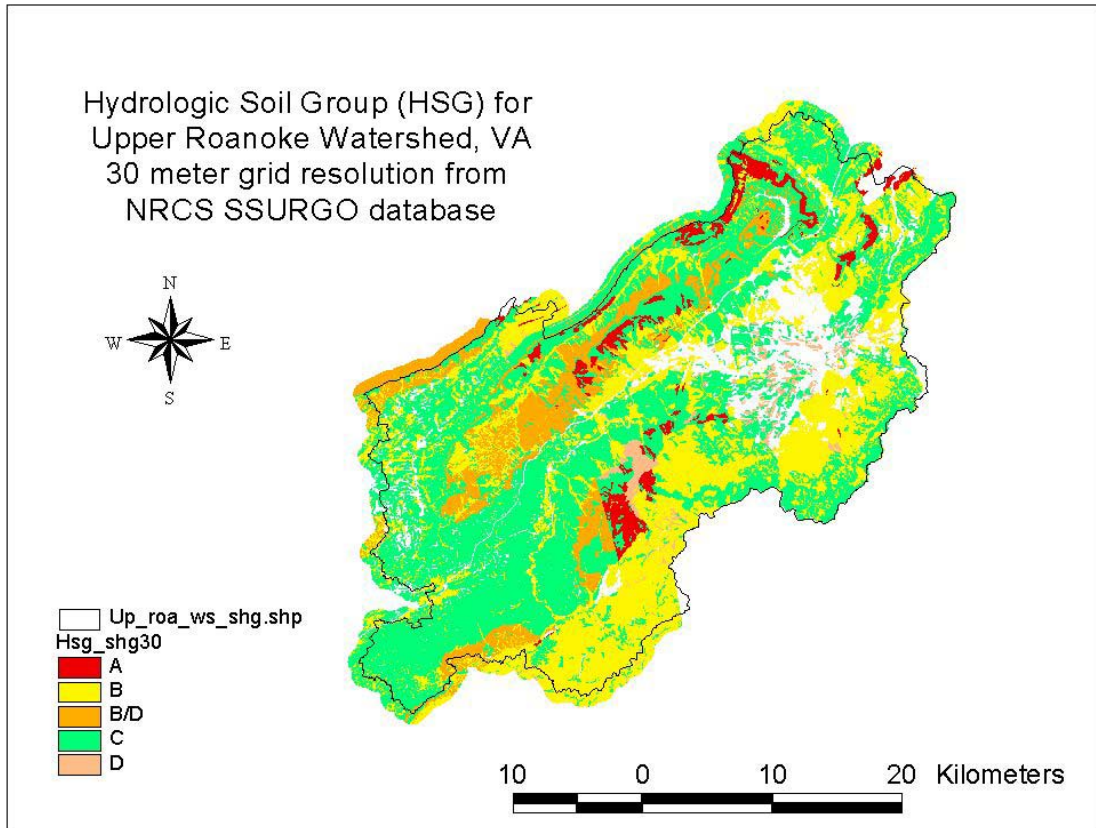


Figure 3.3 Hydrologic Soil Group Classification for Upper Roanoke Watershed from SSURGO database.

Soil polygons exist in the SSURGO database for which no HSG data is available. These polygons are usually urban or impervious areas for which there is little if any soil left on the land surface to survey. These areas are typically highly urbanized or developed making their infiltration characteristics more sensitive to land use and land cover than HSG.

Figure 3.4 shows a gridded representation of HSG for the area surrounding Carvins Cove reservoir. Note that no soil data is available for the area inundated by the reservoir or for the area paved over by Interstate 81 which runs from the northeast corner of the map south and west.

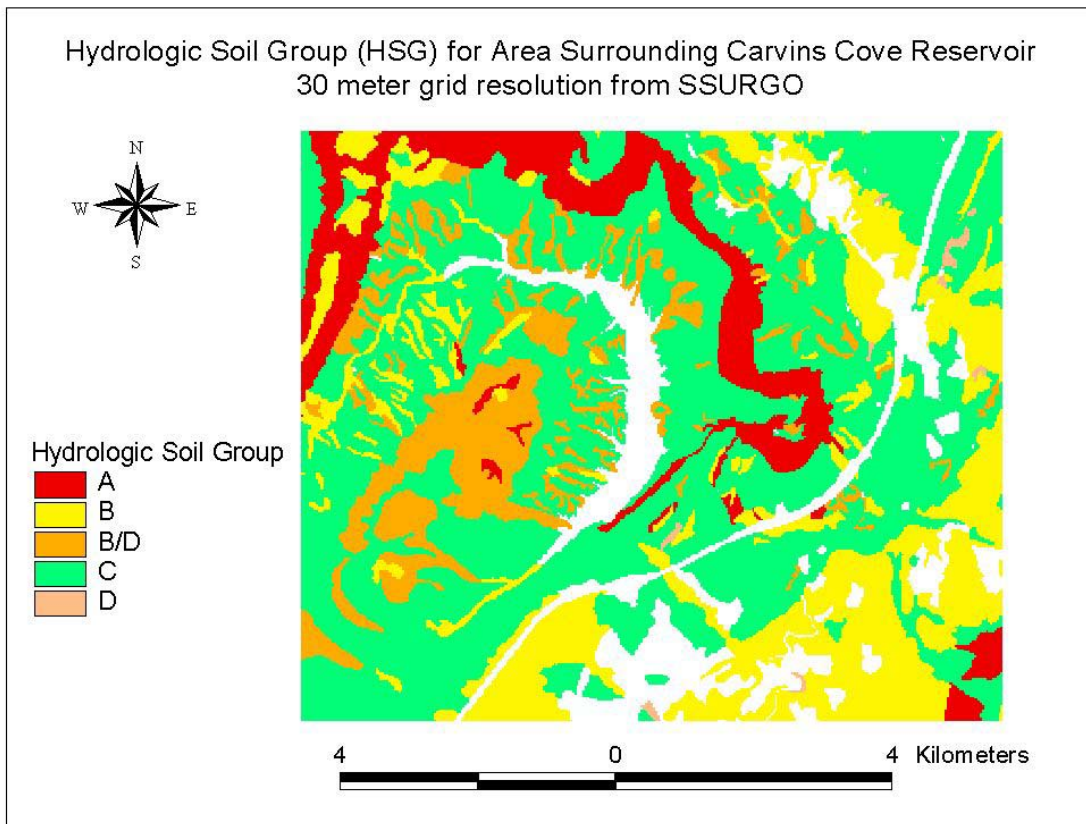


Figure 3.4 Hydrologic Soil Group Classification Carvins Cove Reservoir Area from SSURGO database.

The SSURGO Data Base Data Use Information document (USDA, 1995) describes the relative levels of detail and intended use of SSURGO and STATSGO data.

“The SSURGO data base provides the most detailed level of information and was designed primarily for farm and ranch, landowner/user, township, county, or parish natural resource planning and management. Using national mapping standards, soil maps in the SSURGO data base are made using field methods. Surveyors observe soils along delineation boundaries and determine map unit composition by field traverses and transects. Line segments (vectors) are digitized according to specifications and standards established by the Natural Resources Conservation Service for duplicating the original soil survey map.”

STATSGO data, though available over a larger geographic extent, does not contain the level of detail necessary for this modeling study. The following description is from the USDA (1995).

“The STATSGO data base was designed primarily for regional, multistate, river basin, state, and multicounty resource planning, management, and monitoring. STATSGO data are not detailed enough to make interpretations at a county level. Soil maps for STATSGO are compiled by generalizing more detailed (SSURGO) soil survey maps. Where more detailed soil survey maps are not available, data on geology, topography,

vegetation, and climate are assembled with Land Remote Sensing Satellite (LANDSAT) images. Soils of like areas are studied, and the probable classification and extent of the soils are determined.”

3.2.2 Land Use and Land Cover

Land Use and Land Cover for the Upper Roanoke watershed was described using the National Land Cover Dataset (NLCD) from the USGS. NLCD data is available from: <http://landcover.usgs.gov/nationallandcover.html>. The NLCD is a gridded representation of landcover for the United States at a 1 arc second (~30 meter) resolution. NLCD data was created to provide a source of current, consistent, seamless, and accurate land cover data for the conterminous United States. The NLCD has many potential uses including ecosystem assessment, land use planning and hydrologic assessment.

Land uses are classified by a modified Anderson level II classification scheme shown in table 3.1 below. The NLCD uses this classification scheme as the Anderson classification scheme is best suited for Aerial photography. Additionally, some Anderson Level II classes were consolidated into a single NLCD class (USGS, 1999 (2)).

Table 3.1: NLCD Classifications and Descriptions

Category	Classification	Description
Water	11	Open Water
	12	Perennial Ice/Snow
Developed	21	Low Intensity Residential
	22	High Intensity Residential
	23	Commercial/Industrial/Transportation
Barren	31	Bare Rock/Sand/Clay
	32	Quarries/Strip Mines/Gravel Pits
	33	Transitional
Forested Upland	41	Deciduous Forest
	42	Evergreen Forest
	43	Mixed Forest
Shrubland	51	Shrubland
Non-natural Woody	61	Orchards/Vineyards/Other
Herbaceous Upland	71	Grasslands/Herbaceous
Herbaceous Planted/Cultivated	81	Pasture/Hay
	82	Row Crops
	83	Small Grains
	84	Fallow
Wetlands	85	Urban/Recreational Grasses
	91	Woody Wetlands
	92	Emergent Herbaceous Wetlands

Unfortunately, the land cover classifications above are not currently directly correlated with hydrologic characteristics. Vieux (2000) states that:

There is usually no land use cover classification scheme extant in map form that has direct applicability to hydrology. Maps derived from remote sensing could be used to develop hydrologic parameters but they require extensive training and/or calibration to derive model parameters from surrogate measures. Some judgment is always required to assign meaningful parameters to generalized classification schemes based on characteristics that may relate to hydrology only peripherally.

The NLCD is referenced to an Albers equal area conical projection identical to the Standard Hydrologic Grid (SHG). NLCD data is available for the continental United States at a 30 meter grid resolution. The data source is:

<http://landcover.usgs.gov/nationallandcover.html>.

The NLCD grid for the state of Virginia was obtained for this modeling study. This grid was clipped by a 1km buffer around the Upper Roanoke Watershed to reduce data storage and processing requirements. The resolution and registration of this grid was checked against the elevation and soil data used to ensure accurate spatial placement.

Figure 3.5 shows the NLCD for the Upper Roanoke Watershed. Grid resolution is 30 meters. Figure 3.6 shows the NLCD for the area surrounding the Carvins Cove reservoir also with 30 meter grid resolution.

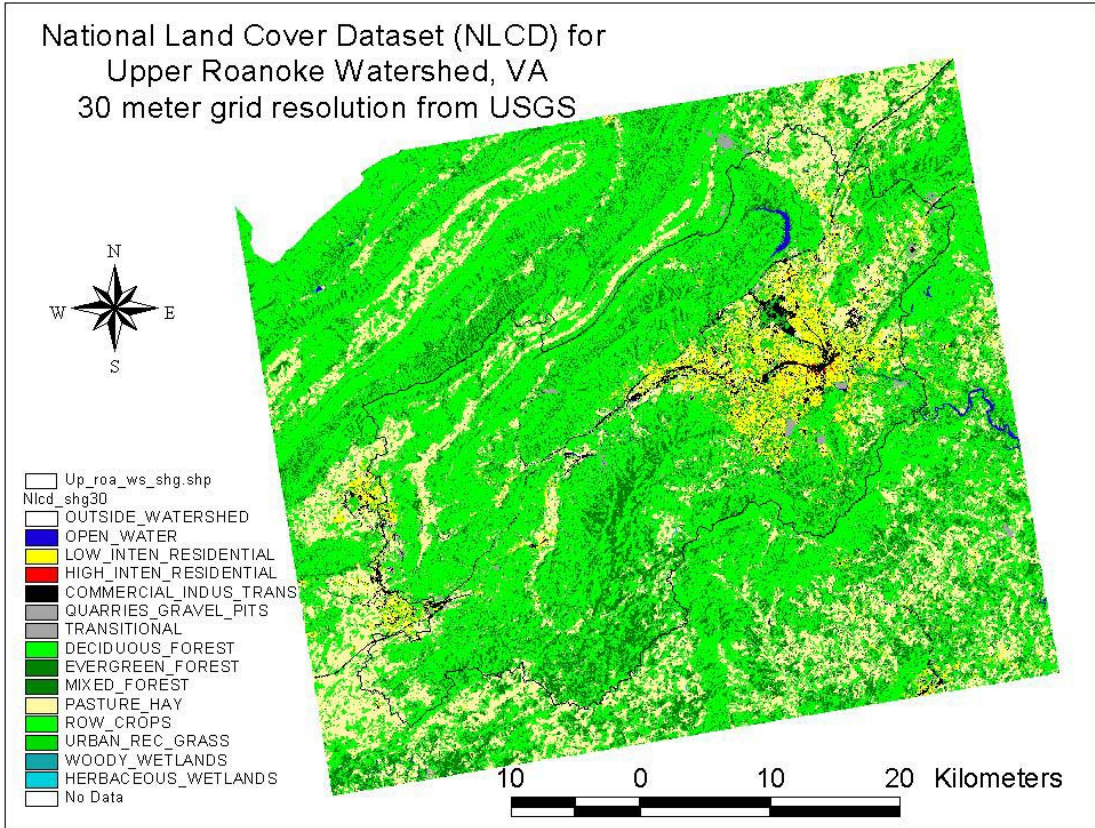


Figure 3.5: National Land Cover Dataset for Upper Roanoke River Watershed

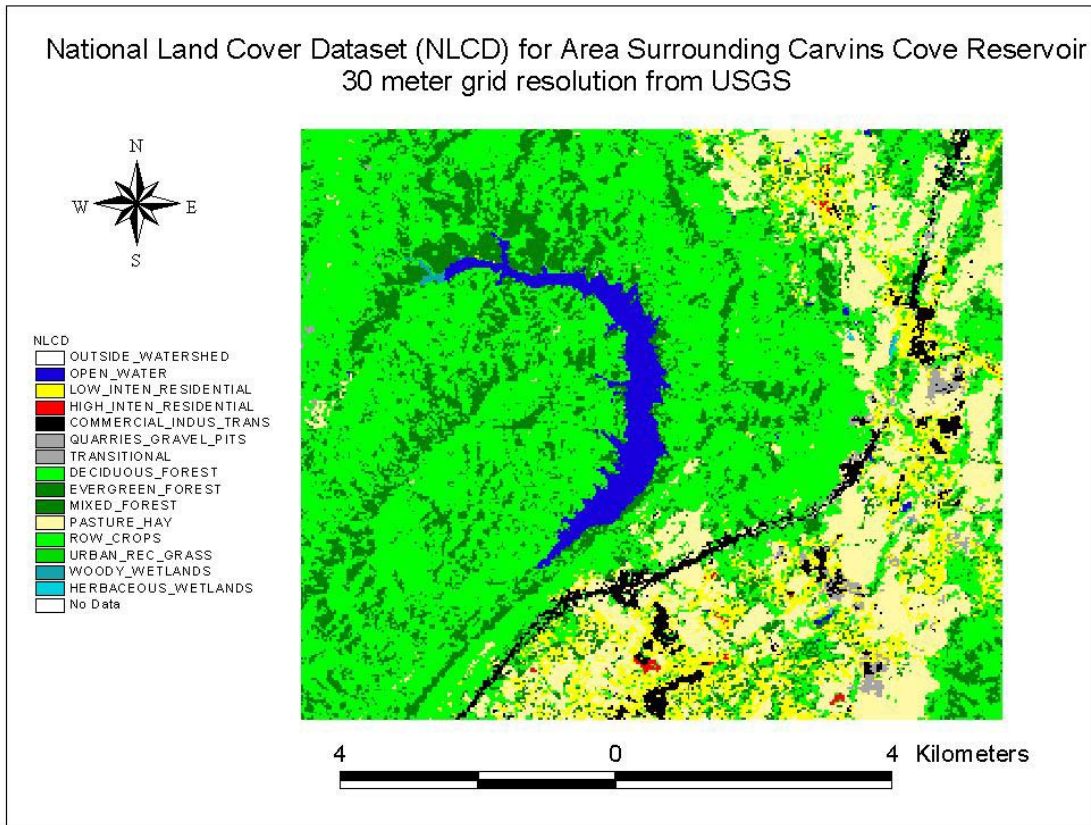


Figure 3.6: National Land Cover Dataset for Area surrounding Carvins Cove Reservoir

3.2.3 Elevation Data

Elevation data referenced to a 30 meter grid was obtained from USGS digital elevation models (DEMs) for the Upper Roanoke Watershed. Digital elevation data for the United States is available for no cost from the USGS at: <http://gisdata.usgs.net/NED/default.asp>. The USGS has developed a seamless gridded representation of elevation at a 30m resolution for the United States. This product is known as the National Elevation Dataset and was developed from the highest quality and resolution elevation data available for the United States. Data corrections were made in the NED assembly process to minimize artifacts, perform edge matching, and fill sliver areas of missing data. NED has a resolution of one arc second (approximately 30 meters), horizontal location in geographic coordinates referenced to NAD 83 and elevations in decimal meters. (USGS, 2002).

NED data is referenced to geographic coordinates to NAD 83. Vertical units (elevations) are given in decimal meters. NED data are available from the following website: <http://gisdata.usgs.net/NED/default.asp>

Elevation data for an area containing the Upper Roanoke Watershed was obtained from USGS DEMs. This elevation data was reprojected to the Standard Hydrologic Grid with

a 30 meter cell size. Resolution and registration were checked to ensure that elevation data matched with soil and land cover datasets.

Figure 3.7 shows the elevation data for the Upper Roanoke Watershed. A hillshade is applied for visualization purposes. Grid resolution is 30 meters.

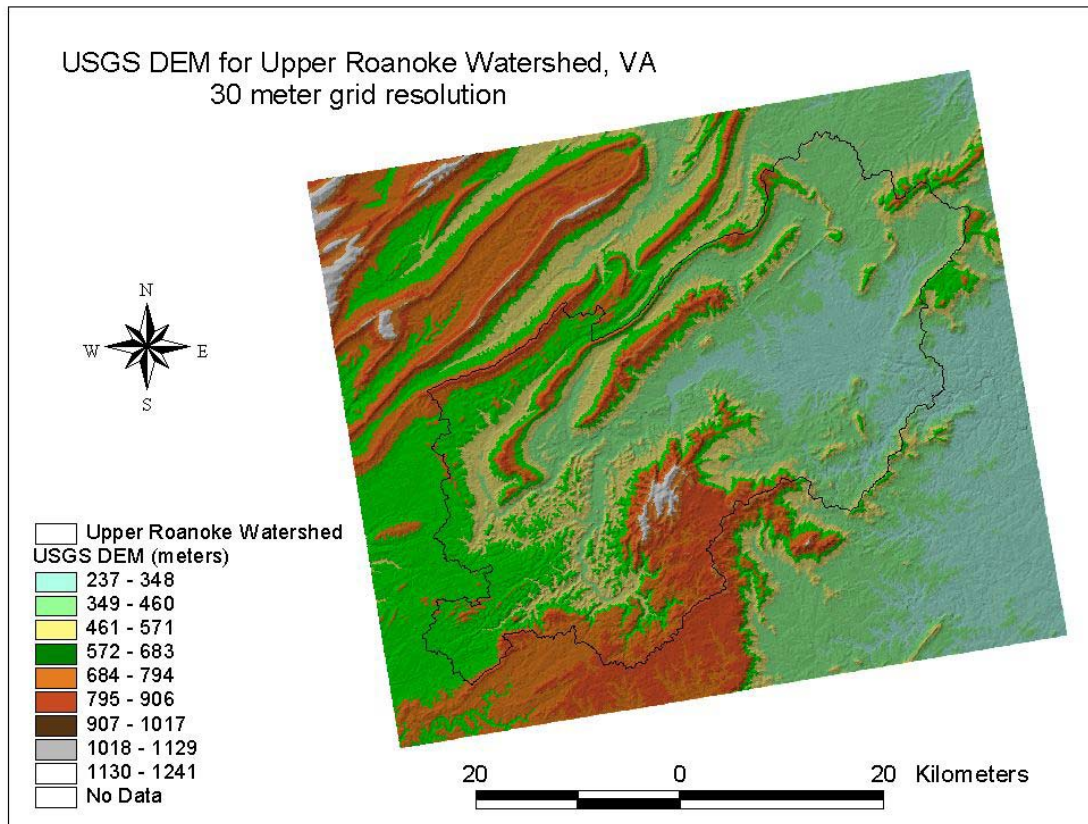


Figure 3.7: Digital Elevation Model for Upper Roanoke River Watershed, VA from USGS

3.2.4 NEXRAD Rainfall Data

In order to model spatially variable hydrologic processes, the spatial and temporal variation of precipitation inputs must be known. Precipitation inputs for the Upper Roanoke Watershed were developed from archives of NEXRAD stage III precipitation data. One of the most important sources of spatially distributed rainfall is radar. Spatial and temporal distribution of rainfall is the driving force for both infiltration and saturation excess. One of the most hydrologically significant radar systems in the US is the WSR-88D (popularly known as NEXRAD) radar (Vieux, 2001).

The NEXRAD stage III product is the weather services best estimate of spatially variable liquid precipitation depths for a region. Processing of the stage III product is the result of inputs from multiple radar units, ground based gages and human quality control and is described in section 2.2.4.

The stage III archives used in modeling the Upper Roanoke Watershed are hourly precipitation depths in integer hundredths of millimeters on the 4km by 4km HRAP grid in the NWS XMRG file format. A C program is available (xmrctoasc.c) from the weather service to decode these archives into hourly ASCII grids of precipitation depths in cm. Xmrctoasc.c is intended for use on Big Endian UNIX machines and is included in Appendix E. The VTAIX machine at the Virginia Tech Computing Center was used to decode archived XMRG files to ASCII grids. Processing, reprojection, changes of resolution and verification of gridded precipitation data are described in section 3.6.3-3.6.5.

NEXRAD stage III archives are referenced to the Hydrologic Rainfall Analysis Project (HRAP) grid. HRAP is a polar stereographic projection with nominal 4km x 4km cell size. Details on the projection parameters defining the HRAP projection may be found in section 3.4 and Appendix C.

The NEXRAD data archives are referenced to coordinated universal time (UTC). The IFLOWS data and streamflow data were temporally shifted to UTC to simplify the modeling study.

Archives of hourly, 4km stage III precipitation depths were made available to the public as part of the National Weather Services Distributed Model Intercomparison Project (DMIP). <http://weather.gov/oh/hrl/dmip/nexrad.html>. These archives are available as far back as 1993 with at least a few years of data available for each NWS river forecast center (RFC). Three storm events:

- October 24th to 28th 1997,
- March 17th to 22nd 1998, and
- April 16th to 21st 1998

were selected for this study as these storms exhibited spatially varied precipitation depths. Examination of gridded storm total precipitation for each of these storm events provides evidence of spatial variability. Additionally, radar derived precipitation hyetographs were created at various points throughout the watershed for each storm event. These hyetographs, included in Appendix I, also provide evidence of spatial variability of precipitation.

The following table (3.2) shows summary statistics for storm total precipitation depths. These statistics are for the 4000m precipitation resolution. Precipitation depths are shown in mm. Figures 3.8, 3.9, and 3.10 show storm total precipitation for the October 1997, March 1998, and April 1998 storm events respectively. Precipitation resolution is 4km, grid cell size is 1km.

Table 3.2: Storm total precipitation summary statistics for Upper Roanoke Watershed. 4000m resolution, depths in mm.

Storm	Mean	Min	Max	Standard Deviation
Oct_97	19.81	0.32	62.56	9.59
Mar_98	78.11	27.31	132.04	22.30
Apr_98	64.43	13.43	119.33	14.20

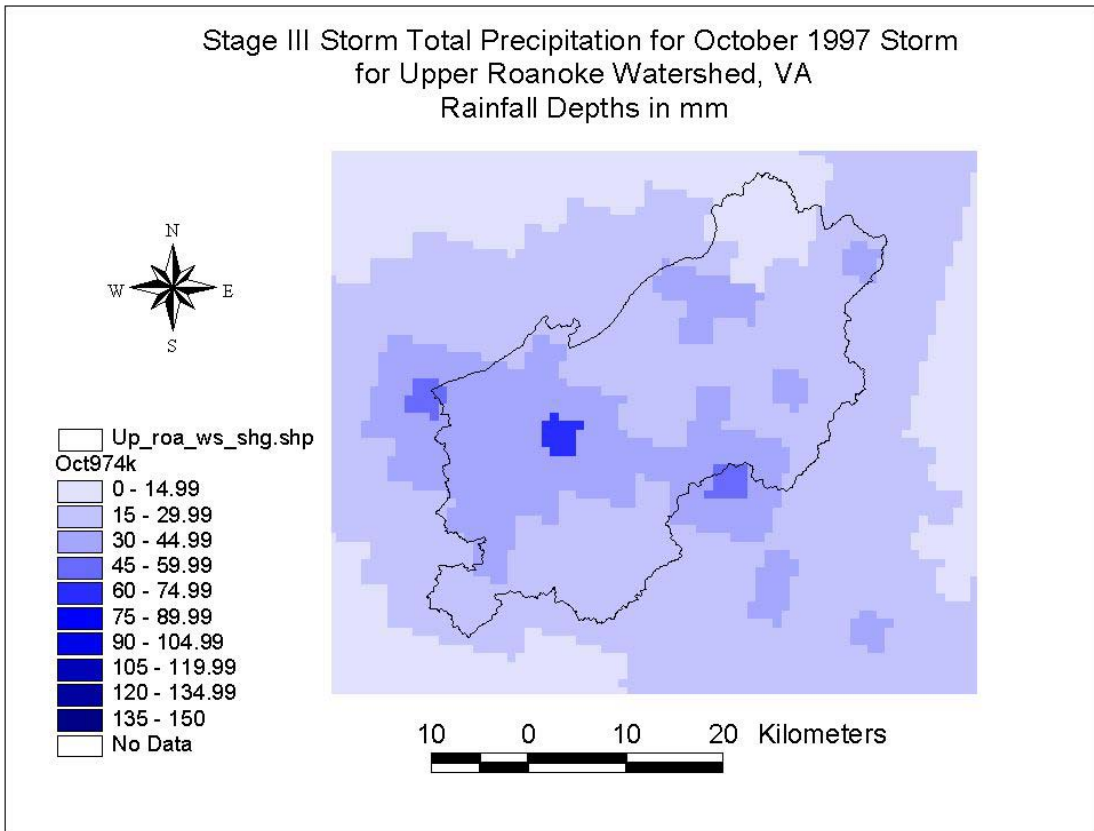


Figure 3.8: Storm total precipitation for the October 1997 storm event.

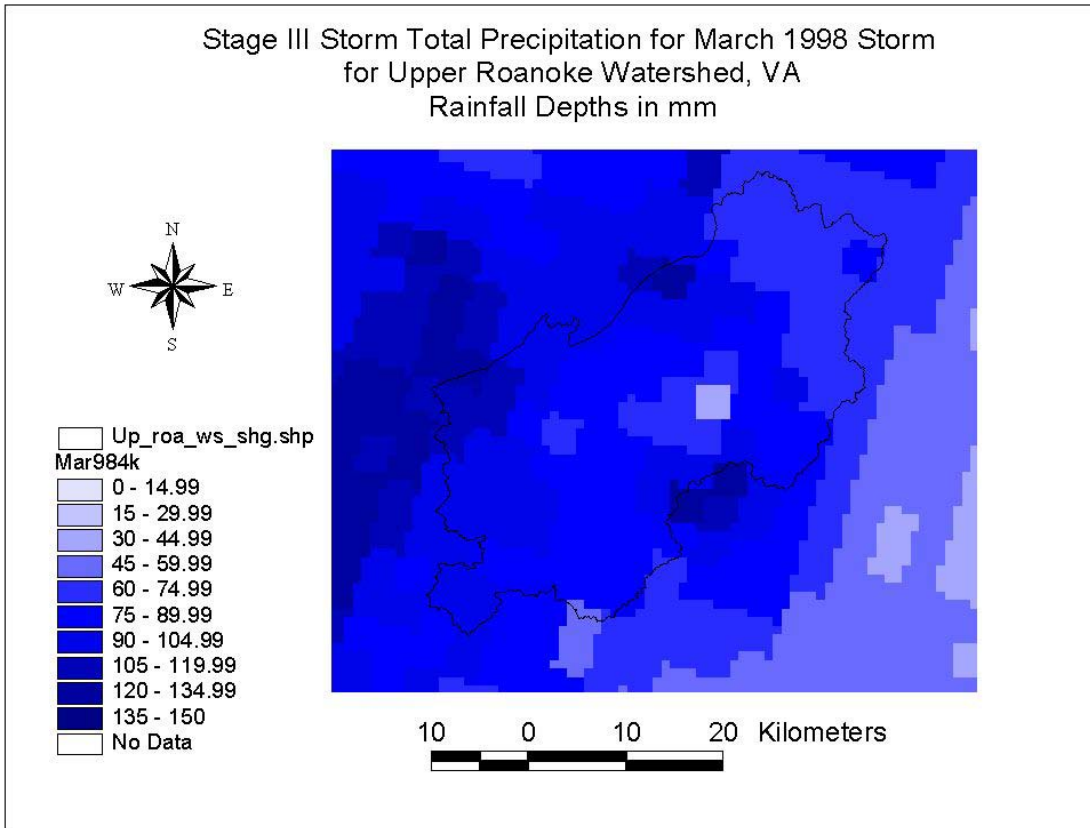


Figure 3.9: Storm total precipitation for the March 1998 storm event.

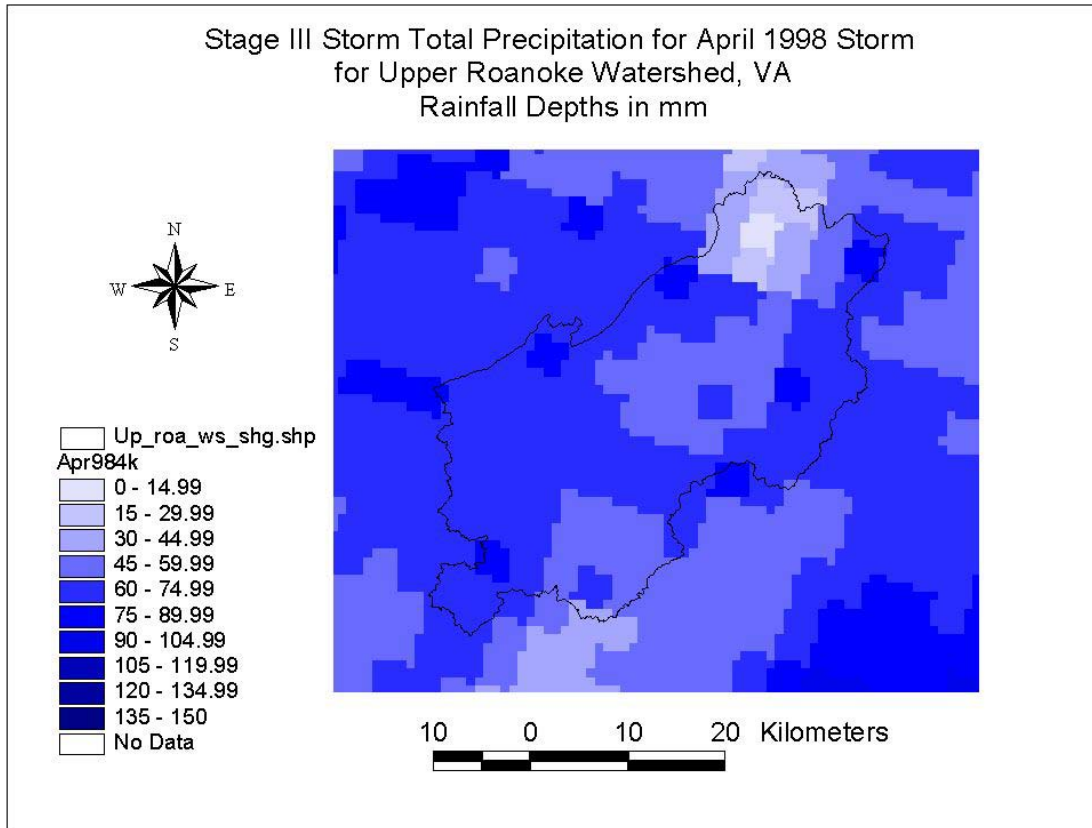


Figure 3.10: Storm total precipitation for the April 1998 storm event.

3.2.5 IFLOWS Rainfall Data

The Interactive Flood Level Observation and Warning System (IFLOWS) of the NWS is a network of telemetered rain gages and stream gages designed for use in flood forecasting. Approximately 23 IFLOWS rain gages are located in and around the Upper Roanoke watershed. Thiessen polygons delineated from these gages show areas of influence ranging from 50km² to 150km² for each gage. IFLOWS rain gages are typically tipping bucket gages with 1 mm (0.04in) resolution and report rainfall depths every 15min. Archives of rainfall depths for these gages were obtained from the National Weather Service for the storm periods being studied.

Gage locations were provided in geographic coordinates (latitude and longitude) referenced to NAD 27. Gage locations were reprojected to the SHG projection and NAD 83. The elevation attribute associated with each gage was checked with the ground elevation at that location from the DEM to ensure accurate reprojection.

Table 3.3: Rain gage locations and names for the Upper Roanoke Watershed.

LID	State	Gage_Name	County	Latitude, DDMSS	Longitude, DDMSS	Elev, ft MSL
1102	VA	Daleville	Botetourt	372503	795608	1218
1103	VA	Carvin Creek	Botetourt	372300	795648	1180
1105	VA	Troutville	Botetourt	372507	795225	1510
1106	VA	Lithia	Botetourt	372749	794427	1250
1111	VA	Mason Cove	Roanoke	372218	800435	1280
1112	VA	Peters Creek	Roanoke	371922	800112	1210
1114	VA	Sugarloaf Mtn.	Roanoke	371419	800231	1520
1115	VA	Witt's Orchard	Roanoke	371026	800720	2740
1117	VA	Fort Lewis Mtn	Roanoke	371831	800939	3260
1119	VA	Crawfords Ridge	Roanoke	371915	801623	2200
1120	VA	Mill Mountain	Roanoke	371502	795556	1720
1121	VA	Tinker Creek S.	Roanoke	371910	795548	984
1122	VA	Mason Creek	Roanoke	372108	800249	1195
1123	VA	Salem Pump Sta.	Roanoke	371712	800431	1000
1124	VA	Roa Sewer Plant	Roanoke	371601	795439	902
1126	VA	Copper Hill	Floyd	370652	800802	2600
1127	VA	Mountain View Ch	Floyd	370406	801509	2620
1128	VA	Montclair	Roanoke	371930	800110	1091
1133	VA	Rose Hill	Montgomery	370642	802243	2100
1135	VA	Blacksburg	Montgomery	371222	802454	2090
1136	VA	Brush Mtn	Montgomery	371805	802357	2730
1140	VA	Poor Mountain	Montgomery	370943	801128	3760
1141	VA	Ironto	Montgomery	371410	801421	1230

Figure 3.11 shows the locations of IFLOWS rain and stream gages in and around the Upper Roanoke Watershed.

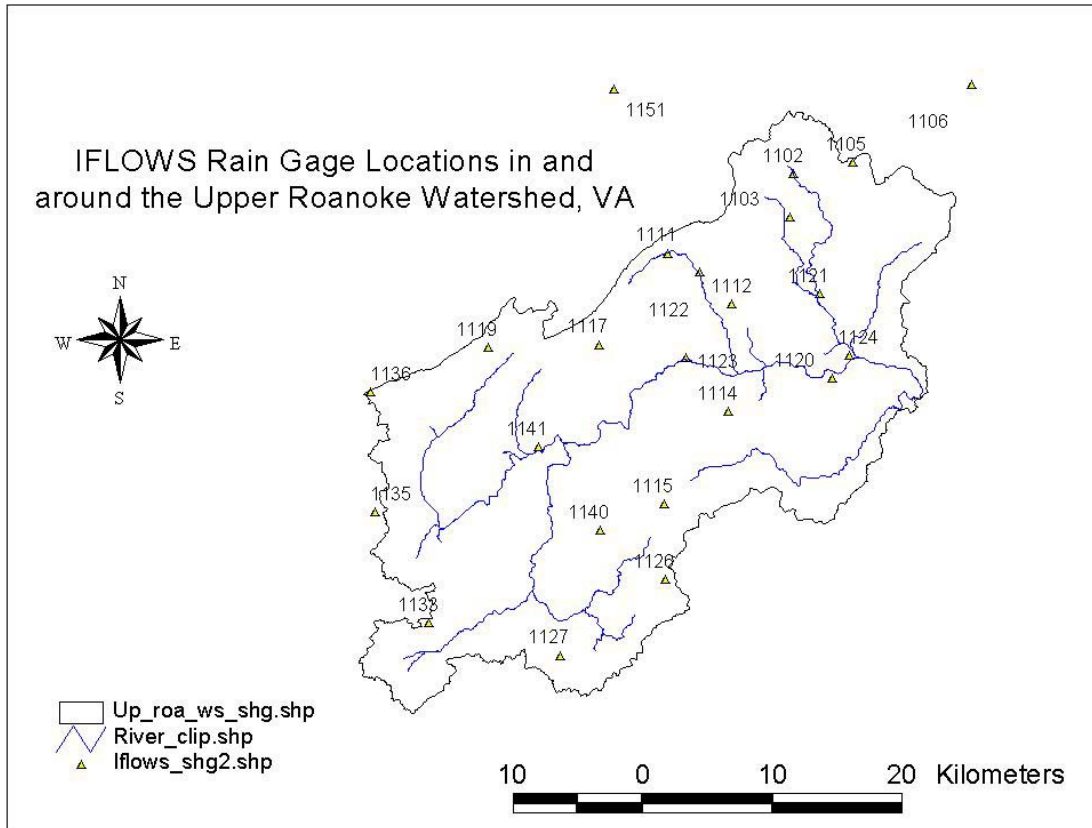


Figure 3.11: IFLOWS rain gage locations in and around the Upper Roanoke River Watershed

Data for the gages of interest was exported from the IFLOWS archives in a fixed width text format. This data was imported into a spreadsheet for further analysis. Hourly precipitation time series for each gage in and around the Upper Roanoke Watershed were generated in this manner.

IFLOWS data are meant to provide local communities warning about locally intense rainfall or flash flooding. The low resolution of the gages and their reactionary placement (after a devastating flood, communities can appropriate funding to improve the gage network) evidence that the intent of the IFLOWS network is not to develop a high resolution precipitation measurement. However, these gage records provide a good data source to check the spatial and temporal registration of the gridded precipitation datasets derived from NEXRAD products.

Figure 3.12 shows the IFLOWS rain gage locations along with storm total precipitation for the March 1998 storm event.

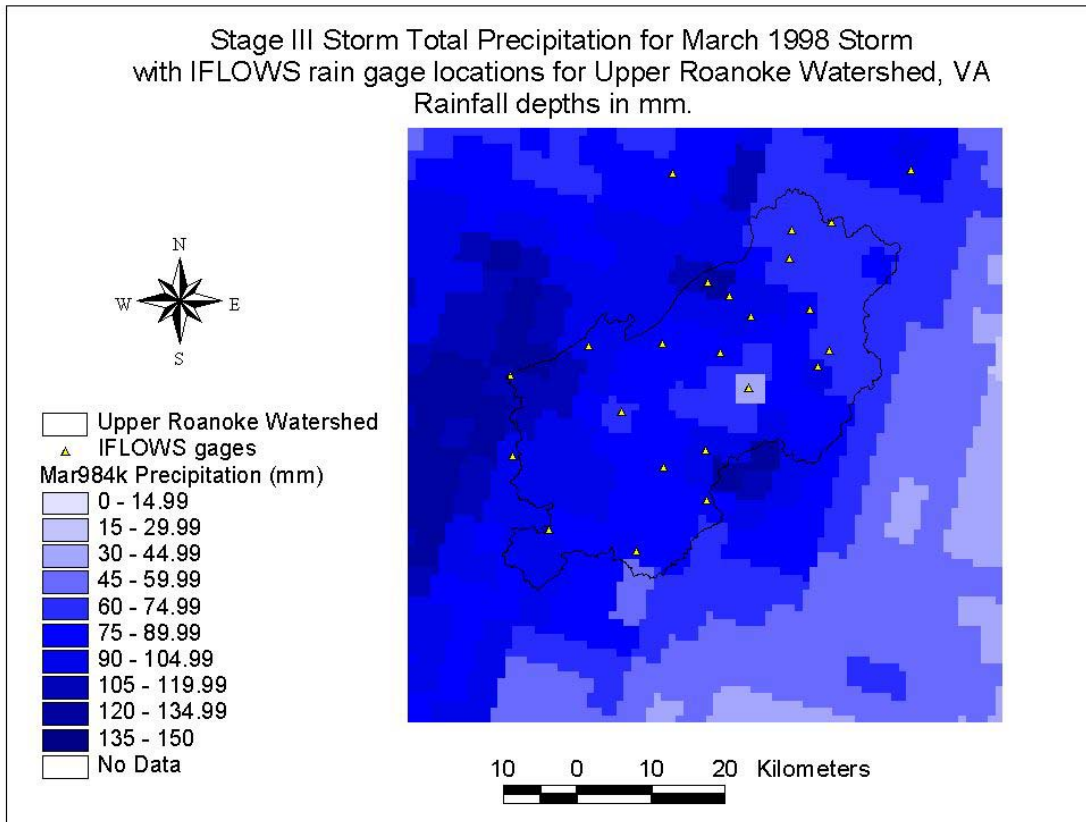


Figure 3.12: IFLOWS rain gage locations and storm total precipitation depths for March 1998.

3.2.6 USGS Streamflow Data

The USGS and the Virginia Department of Environmental Quality (VADEQ), maintain 8 stream gaging stations throughout the Upper Roanoke Watershed. Records from these gages are maintained by the USGS at 15min or 30min resolution and were obtained from Roger White at the USGS for this modeling study. These records contain time series of instantaneous stream flow in cubic feet per second.

Table 3.4: USGS Stream Gage locations for the Upper Roanoke River Watershed.

SITE_NUM	SITE_NAME	LATDMS	LONGDMS	LAT_DAT	ELEV_FT
2053800	S F ROANOKE RIVER NEAR SHAWSVILLE, VA	37°08'24"	80°16'00"	NAD27	1361.9
2054500	ROANOKE RIVER AT LAFAYETTE, VA	37°14'11"	80°12'34"	NAD27	1174.5
2054510	ROANOKE RIVER NEAR WABUN, VA	37°14'48"	80°09'55"	NAD27	
2054530	ROANOKE RIVER AT GLENVAR, VA	37°16'04"	80°08'23"	NAD27	
2055000	ROANOKE RIVER AT ROANOKE, VA	37°15'30"	79°56'20"	NAD27	906.8
2055100	TINKER CREEK NEAR DALEVILLE, VA	37°25'03"	79°56'08"	NAD27	1217.5
2056000	ROANOKE RIVER AT NIAGARA, VA	37°15'18"	79°52'18"	NAD27	820.2
2056650	BACK CREEK NEAR DUNDEE, VA	37°13'39"	79°52'06"	NAD27	822.7

Stream gage locations are available in geographic coordinates referenced to NAD27. These locations were reprojected to SHG, NAD83. The locations of these gages were adjusted to match the point on the modeled stream channel network with a contributing area closest to the contributing area to each gage published by the USGS. Figure 3.13 shows stream gage locations within the Upper Roanoke Watershed along with the stream channel network delineated from the DEM.

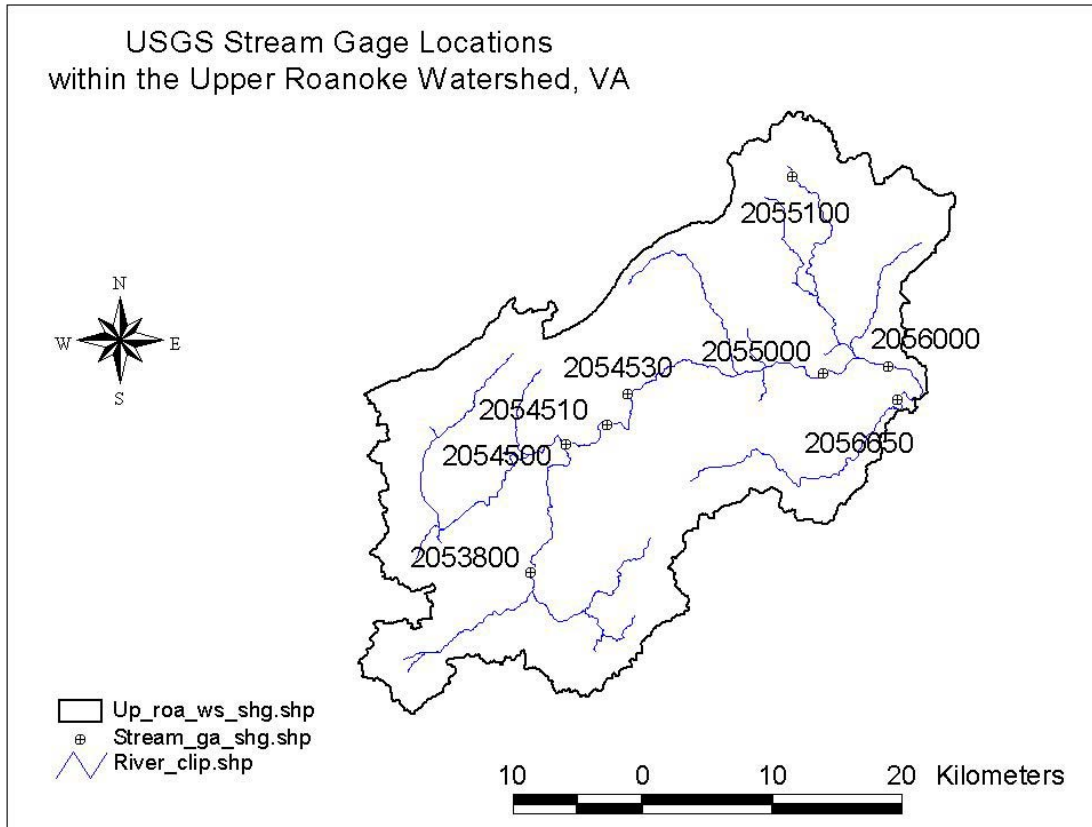


Figure 3.13: USGS Stream Gage Locations in Upper Roanoke River Watershed, VA

Time series of instantaneous stream flow rates were shifted to UTC and the anomalies in some of the gage records caused by daylight savings time changes were removed. These time series of flow rates were imported into the HEC database using the DSSTS (DSS Time Series) program (HEC, 1995) for use in the modeling study.

Table 3.5: Summary of datasets used.

Data Type	Description	Source
Digital elevation model (DEM) data	Available as 7.5 min quads from USGS of authorized distributor or from seamless data distribution system.	USGS at gisdata.usgs.net/NED/default.asp
Land use and land cover (LULC) data	USGS National Land Cover Dataset (NLCD). Modified Anderson Level II classification of land use for the conterminous United States at 30m resolution.	USGS at landcover.usgs.gov/nationallandcover.html
Soil characteristics	Soil Survey Geographic (SSURGO) Database from NRCS. County level vector database of soil series with attributed describing physical properties, engineering and agronomic classifications. Limited geographic availability.	NRCS at ftw.nrcs.usda.gov/ssurgo_ftp3.html
Radar rainfall. NEXRAD stage III archives	Hourly 4km gridded precipitation estimates referenced to the HRAP coordinate system.	NWS Hydrology Lab weather.gov/oh/hrl/dmip/nexrad.html
Gage Rainfall. IFLAWS archives	23 telemetered rain gages in and around the Upper Roanoke Watershed at 15 min temporal resolution.	National Weather Service Blacksburg Forecast Office.
Historical Streamflow	8 USGS and VADEQ stream gages in the Upper Roanoke Watershed. 15 to 30 minute temporal resolution.	Roger K. White Chief, Hydrologic Data Program, USGS.

3.3 Software and Programs Utilized

This section describes the GIS software, modeling software, and other programs used in the distributed hydrologic modeling study of the Upper Roanoke Watershed. All software used is available in the public domain, or in the case of ESRI software, available for purchase and widely used in academia and engineering practice. In keeping with the theme that two thirds of GIS is IS (information systems) multiple computing platforms and operating systems were necessary to perform this modeling study. Interchangeability of data between programs and computing platforms was most effectively accomplished using ASCII file formats rather than proprietary file formats.

3.3.1 GIS Software: ARC/INFO, GRID, ArcView

The GIS software used for the modeling study of the Upper Roanoke Watershed consisted of products produced by the Environmental Systems Research Institute (ESRI). Though these products are not in the public domain, they are widely used and supported in academia, government, and in engineering practice. ARC/INFO and its raster environment GRID were used as the primary platform for reprojecting, rescaling and

evaluating spatially distributed watershed physical parameters and precipitation data. Though ARC/INFO workstation's command line interface has a slight learning curve, its raster processing abilities, ease of scripting with Arc Macro Language (AML), and numerical efficiency made it a very effective tool in this research. ArcView and the Spatial Analyst extension were also used along with software from HEC, HEC-GeoHMS, to develop model inputs from digital data.

ARC/INFO is composed of ARC/INFO Desktop and ARC/INFO Workstation. ARC/INFO Desktop consists of a set of data management, analysis and conversion tools to perform data conversion, generalization, aggregation, overlays, buffer creation, and statistical calculations. Each of the desktop tools has a menu-driven interface with wizards where appropriate. ARC/INFO Workstation provides geoprocessing via a command line interface and allows customization through Arc Macro Language (AML). ARC/INFO Workstation operates on Windows NT, Windows 2000, and several UNIX platforms (ESRI, 2002).

GRID is a raster based analysis environment within ARC/INFO Workstation. GRID, through the map-algebra language, equips the user with tools to perform local, focal, zonal, global, surface, hydrologic, groundwater and multivariate spatial functions. For specialized requirements, the GRID algebra provides facilities to control processing at the level of an individual cell or neighborhood. Since GRID is integrated with ARC/INFO, all of the functionality associated with AML can be used in conjunction with GRID tools to develop complex models (ESRI, 2002).

Arc Macro Language (AML) is a scripting language available in ARC/INFO workstation that greatly improves the efficiency of repetitive GIS operations. AML allows the user to automate frequently performed actions, create commands, and develop menu-driven user interfaces to meet the needs of end users. Through AML, programs, menus, and forms can be shared between operating systems with little or no modification (ESRI, 2002).

ArcView is graphically interfaced providing the power to visualize, explore, query and analyze data spatially. ArcView Spatial Analyst provides a broad range of powerful spatial modeling and analysis features, and allows the user to create, query, map, and analyze cell-based raster data and perform integrated vector-raster analysis.

3.3.2 Programs to Decode NEXRAD Stage III Archives

The archived stage III NEXRAD precipitation data used in this study required significant processing prior to its use in the HEC-HMS model. Archived data is stored in a NWS proprietary, binary file format known as XMRG. For details on the XMRG file format, the reader is referred to Appendix E.

The National Weather Service Hydrology Lab has written various C programs for a UNIX platform to decode their archives of NEXRAD data. `xmrgtoasc.c` was used to translate hourly precipitation records into ASCII grids for use in ARC/INFO. As each

hourly segment of data is its own binary file, scripting was used to iteratively decode xmrgr files to ASCII files. Xmrgrtoasc.c and the UNIX, Bourne shell, script used to decode xmrgr archives are included in Appendix E.

3.3.3 GIS Based Model Preprocessor: HEC-GeoHMS

A preprocessor is available from HEC, HEC-geoHMS, to aid the modeler in preparing HEC-HMS model inputs. HEC-geoHMS is an extension for ArcView 3.x and Spatial Analyst 1.x. HEC-GeoHMS, by analyzing digital terrain information, transforms drainage paths and watershed boundaries into a hydrologic data structure that represents the watershed response to precipitation. Capabilities also include development of grid-based data for linear quasi-distributed runoff transform (ModClark) (Doan, 2000). HEC-geoHMS is a versatile tool in watershed and stream channel delineation and quantification of watershed physical properties, even if the intent is not to create HEC model inputs.

3.3.4 Modeling Software: HEC-HMS

HEC distributes software known as the Hydrologic Modeling System or HEC-HMS.

The Hydrologic Modeling System (HMS) is designed to simulate the precipitation – runoff processes of dendritic watershed systems. HEC-HMS is a comprehensive software package developed for use by the US Army Corps of Engineers, but available without cost to the general public. HEC does not support users in the general public, but outside agencies and vendors provide support for a fee. The HEC-HMS program is a completely integrated work environment including a database, data entry utilities, computation engine, and results reporting tools. A graphical user interface allows the user seamless movement between the different parts of the program (Scharffenberg, 2001).

3.4 Map Projections and Coordinate Systems Used

One of the powerful capabilities of a GIS is the ability to compare the spatial locations of various data. Unfortunately, in the process of modeling a round earth with a flat map or a two dimensional GIS, locations are referenced to many varied coordinate systems and datums. For accurate modeling, it is necessary to ensure that all data are correctly projected to the same coordinate system and datum. Following are descriptions of the map projections encountered in this study along with the ARC/INFO projection parameters used to define or approximate each projection. Sample ARC/INFO projection (*.prj) files are included in Appendix C.

3.4.1 Hydrologic Rainfall Analysis Project (HRAP)

The Hydrologic Resource Analysis Project Grid (HRAP) is a nested grid within the National Weather Service Limited Fine Mesh (LFM) grid. The LFM is the name of an early atmospheric numerical model used by the NWS, and the name of the grid it used was the LFM grid. A finer mesh version of the LFM grid (with grid cell length 1/40th of

the LFM grid) was adopted for the use of radar precipitation processing and is called the HRAP grid (Fulton, 1998). The HRAP grid is a quasi-rectangular grid with a nominal grid size of 4km x 4km but ranges from about 3.5km in southern contiguous U.S. latitudes to about 4.5km in northern contiguous US latitudes (Fulton, 1998). The HRAP projection is a polar stereographic map projection using a spherical earth datum.

The use of a spherical earth datum with HRAP precipitation estimates is the result of the developers experience with general circulation models (GCMs) in numerical weather prediction (Reed and Maidment, 1999). GCMs solve typically solve their numerical equations in spherical coordinates.

Precipitation records referenced to the HRAP grid are defined in the plane of a polar stereographic map projection with the following parameters:

HRAP Projection Parameters:

Longitude of Projection Center: -105 degrees or 105 degrees west,
Standard (true) latitude: 60 degrees north, and
Spherical Earth Radius: 6371.2km.

ARC/INFO does not support customizing both the sphere radius and the true latitude in a polar stereographic projection. Therefore, the HRAP polar stereographic projection may be approximated using the default sphere radius of 6,370,997m and a true latitude of 60 degrees 0 min 24.5304792 seconds. Differences between using this approximate projection and the exact equations are negligible at 33 degrees north as approximately 0.4 meter differences were found when comparing these results to the exact transformation for single points (NWS, 1998).

Approximate HRAP Projection Parameters:

Longitude of Projection Center: -105 degrees or 105 degrees west,
Standard (true) latitude: 60 degrees 0 min 24. 5304792 sec,
Spherical Earth radius: 6,370,997 meters.

The archived stage III radar rainfall data used in this modeling study was referenced to the HRAP grid. These precipitation records were reprojected to the Standard Hydrologic Grid (SHG) described in the following section.

3.4.2 Standard Hydrologic Grid (SHG)

The Standard Hydrologic Grid (SHG) is an Albers equal area conical projection. SHG is a convention proposed by the Corps of Engineer's Hydrologic Engineering Center (HEC) to simplify data transfer in GIS based hydrologic modeling. The characteristics of SHG that make it suitable for hydrologic modeling include:

- the Albers equal area conical projection is well supported by the majority of GIS software,
- many datasets (NLCD and STATSGO for example) are already projected to this coordinate system, and

- an equal area projection leads to equal volume of runoff. In other words, a 1km square grid cell with 1mm of rainfall excess will produce 1000m³ of runoff regardless of grid cell location.

The standard Hydrologic Grid is based on the Albers Equal Area map projection with the following parameters (Doan, 2000).

Datum: North American Datum, 1983 (NAD83)
 1st standard parallel: 29 degrees 30 min 0 sec north
 2nd standard parallel: 45 degrees 30 min 0 sec north
 Central Meridian: 96 degrees 0 min 0 sec West
 Latitude of Origin: 23 degrees 0 min 0 sec North
 False Easting: 0
 False Northing: 0

Cell locations in the standard hydrologic grid are either given by x and y coordinates (in m) or by cell address. Cell address is a pair of integer indices indicating position, by cell count, of the cells southwest or lower left corner relative to the grids origin at 96W 23N (Doan, 2000). Cell address may be computed by dividing northing and easting (in the Albers equal area projection defined above) by cell size and choosing the largest integer less than or equal to the result.

Due to the high level of support by GIS packages and the equal area property, the Standard Hydrologic Grid projection was chosen for the model study.

3.4.3 Geographic Coordinates (Latitude and Longitude)

Geographic coordinates of latitude and longitude are commonly used in geographic information systems as geographic coordinates may be projected to any coordinate system of interest. For this reason, projection of geographic data from one projection to another is often a two step process, specifically by projecting from the first coordinate system to latitude and longitude, and then to the second coordinate system. Geographic coordinates are not without idiosyncrasies however as the map datum and ellipsoid used in developing the latitude and longitude must be considered.

The North American Datum of 1927, or NAD27, was developed from a least squares adjustment of all horizontal geodetic surveys which had been completed to date. The adjustment was based on the Clarke Ellipsoid of 1866. The National Geodetic Survey performed another general adjustment of the North American horizontal datum with a targeted completion date of 1983. The North American Datum of 1983, or NAD 83, is referenced to the GRS 80 ellipsoid and is adjusted based on the earth's mass center rather than an arbitrarily chosen point.

3.5 Study Area: The Upper Roanoke River Watershed, VA

The Upper Roanoke watershed is defined as the area that drains through an outlet point at the confluence of Back Creek and the Roanoke River. This confluence is located in

Roanoke County, VA. The Upper Roanoke watershed is extremely variable in topography, soil characteristics, and land use and land cover. Precipitation is spatially variable in precipitation as well due to orographic effects.

The Upper Roanoke watershed drains an area of 1480km² and contains portions of Botetourt, Floyd, Montgomery, and Roanoke counties and the cities of Salem and Roanoke. The Watershed contains portions of the Blue Ridge and Valley and Ridge physiographic provinces. Elevations vary from 246m (810ft MSL) at the outlet point to 1198m (3930ft MSL) at the summit of Poor Mountain. Land use is as widely varied from the heavily forested slopes of the Jefferson National Forest to the highly impervious downtown areas of Roanoke and Salem.

The Upper Roanoke basin is typical of many Appalachian headwater basins for which flood forecasts are produced. It is currently modeled using a three hour unit hydrograph and a three hour mean areal precipitation amount. This method, with its assumption of uniform rainfall over the entire basin is not well suited for producing the best forecasts of peak flows and times to peak because precipitation events in the area are non-uniform and may be highly localized due to terrain influences (Kibler, et al. 1999).

Following significant flooding along the Roanoke River in 1985, the Interactive Flood Observation and Warning System (IFLOWS) gage network in the area was expanded with the installation of several stream and rain gages throughout the watershed (Kibler, et al. 1999). There are currently 23 IFLOWS rain gages in and around the Upper Roanoke watershed. IFLOWS rain gage locations are described in section 3.2.5. Thiessen polygons delineated from these gages show areas of influence ranging from 50km² to 150km² for each gage. Long term archives of 15 minute rainfall depths exist for these gages.

Long term stream flow records are available from the US Geological Survey for 8 locations throughout the upper Roanoke watershed. USGS Stream gage locations are shown in section 3.2.6. Observed streamflow is necessary for model calibration, verification, and evaluation of accuracy.

The Upper Roanoke Watershed has a history of damaging flooding including the infamous “election day” flood of 1985. The peak streamflow during this event of 32,300 cfs at the Roanoke River gage at Roanoke, VA is the maximum peak streamflow recorded by this gage in over 100 years of service. The USGS (2000) describes the flooding and associated damage from the 1985 flood as follows:

Heavy rainfall from October 31 through November 6, 1985, caused record breaking floods over a large region, including western and northern Virginia. Most of the rain fell on November 4 and 5 and was indirectly related to Hurricane Juan. New maximum peak discharges were recorded at 63 stream gaging stations during this flood. In the Roanoke area, 10 people died as a result of the flood, 22 died in the Commonwealth of Virginia. The cost of this flood for the Roanoke – Salem area was estimated to be \$440 million.

Figure 3.14 below shows the Upper Roanoke River Watershed location in the Commonwealth of Virginia. Figure 3.15 shows the Upper Roanoke River Watershed location relative to the county boundaries of Southwest Virginia.

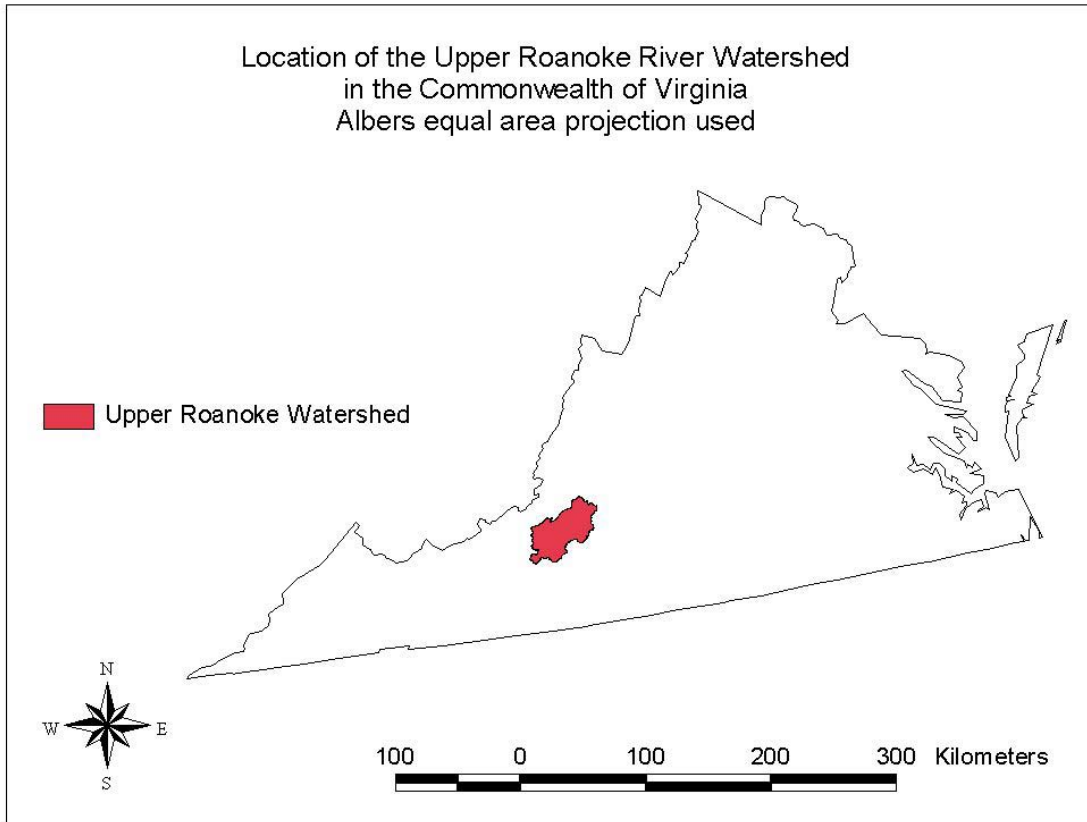


Figure 3.14: Location of Upper Roanoke River Watershed in Virginia

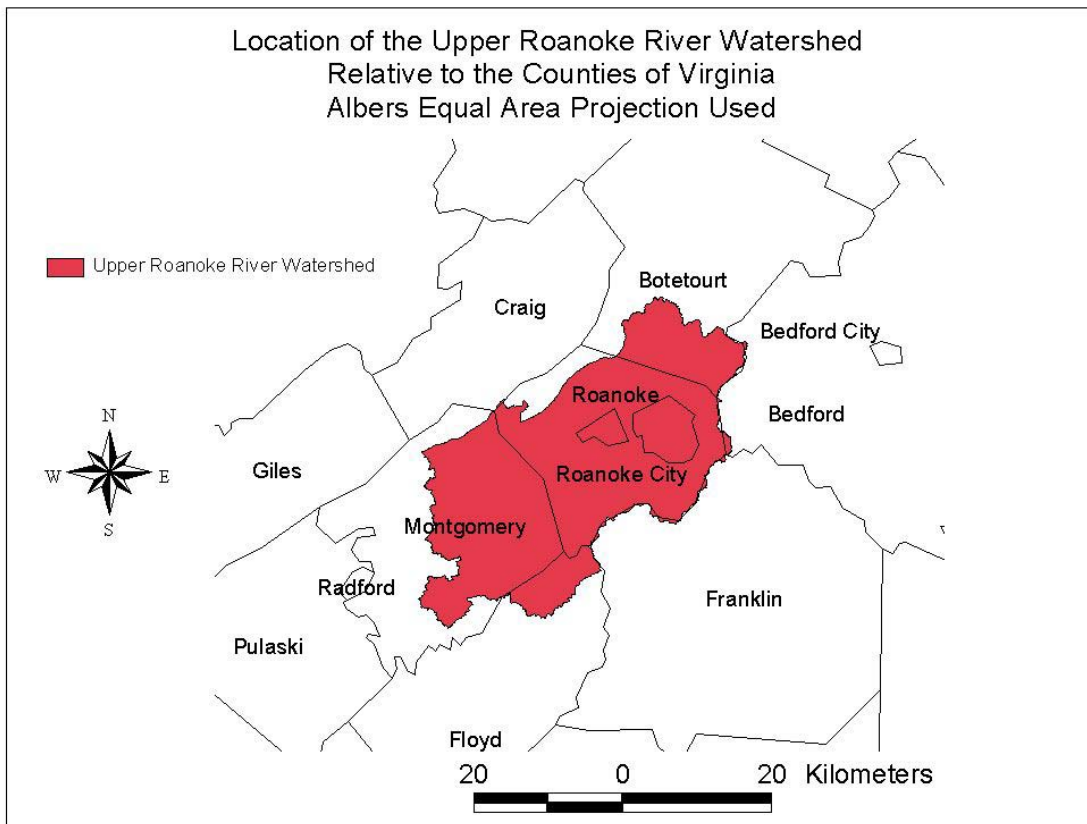


Figure 3.15: Location of Upper Roanoke Watershed in Southwest Virginia

Figure 3.16 shows the Upper Roanoke watershed along with hydrography derived from USGS Digital Line Graph (DLG) files.

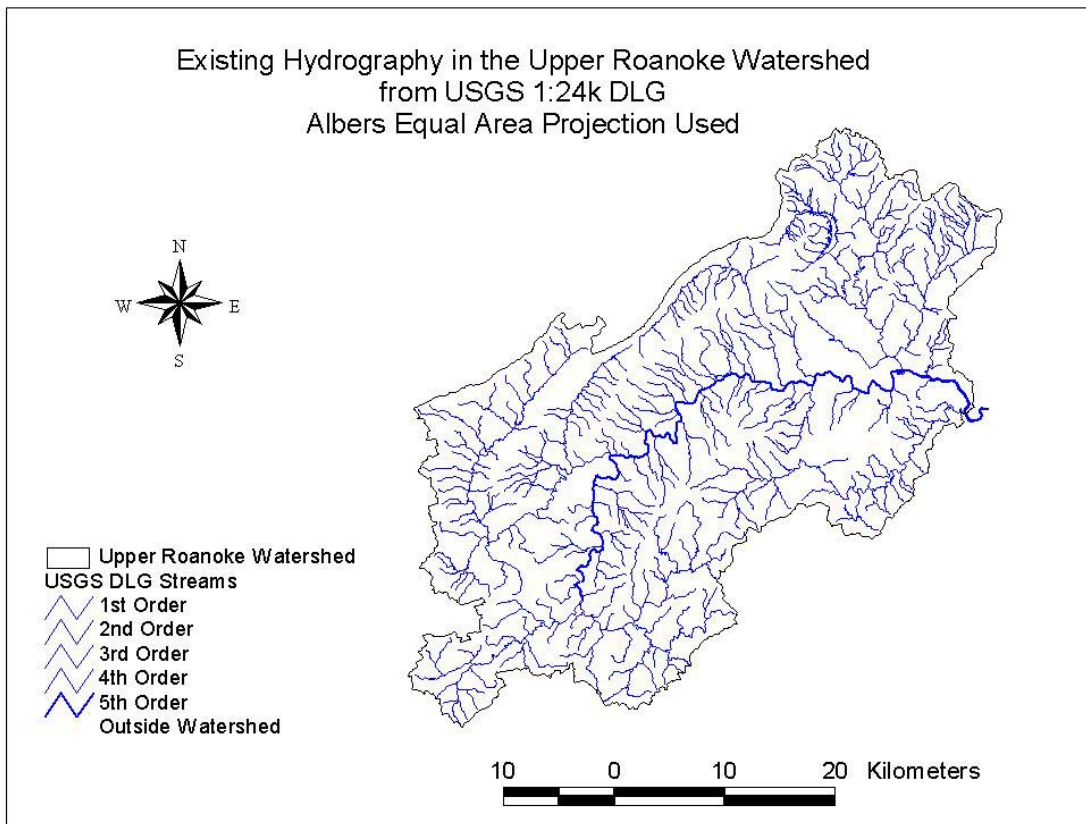


Figure 3.16: USGS Digital Line Graph Data for Upper Roanoke River Watershed

3.6 Data Processing and Preparation of Model Inputs

This section describes the GIS based processing of digital datasets into hydrologic model inputs for the Upper Roanoke Watershed. The raster based reclassification of SSURGO and NLCD data into a gridded representation of CN in ARC/INFO GRID is discussed. Watershed and stream channel delineation from the DEM using HEC-GeoHMS is outlined. Creation of necessary HMS model inputs including the basin file, map file and grid cell parameter file by HEC-GeoHMS are explained. Finally, the processing techniques used to create precipitation inputs at varied resolutions and grid scales are discussed.

3.6.1 Creation of Gridded SCS CN Estimate

A raster based reclassification in ARC/INFO GRID was used to calculate spatially distributed curve numbers from SSURGO and NLCD data. The AML scripts and reclassification tables used in this process are included in Appendix D. A flowchart, graphically illustrating this process, is shown in figure 3.17.

The method most often used to generate spatially varied input maps for distributed parameter hydrologic models is to make inferences of parameter values from available maps. For example, both the soil survey and LULC maps can be used to construct soil

infiltration characteristic input maps using rules based reclassification in a GIS. Hydrologic model calibration is therefore dependent on the rules developed for reclassifying base maps (DeBarry et al., 1999).

Following is a matrix of the reclassification values used to develop the gridded CN estimate along with their sources and the underlying assumptions. Table 3.6 below shows CN values for each combination of HSG and LULC. As the NLCD does not directly correlate with the curve number classifications in the literature, it is necessary for the modeler to apply judgment and make assumptions concerning the most appropriate CN to assign to each soil and land cover combination.

The SSURGO database contains a large number of areas with a hydrologic soil group complex of B/D. This means that the spatial variability of soil HSG was too small to be differentiated in the SSURGO database. Curve numbers in complex soil series (B/D) were assumed to be the average of curve numbers for HSG B and HSG D.

SSURGO datasets contain areas for which no soil series information is available. These areas are typically classified as urban and therefore are not relevant to an agricultural survey. As these areas are primarily urbanized (~50% by area in the watershed are commercial or residential), CN determination is more sensitive to LULC than HSG. Curve numbers for areas where no soil data were available were assumed to be between the average CN for the NLCD classification and the CN for HSG classification C.

Table 3.6 Curve Numbers for SSURGO and NLCD attributes

Value	Classification	A	B	C	D	B/D	URB*	Source
11	Open Water	100	100	100	100	100	100	(1)
21	Low Intensity Residential	54	70	80	85	77	80	(1) Average of Residential 1/4, 1/3, 1/2, 1 acre lots.
22	High Intensity Residential	77	85	90	92	88	90	(1) 1/8 acre lots
23	Commercial/Industrial/Transportation	85	90	93	94	92	93	(1) Average of Commercial/Business and Industrial
32	Quarries/Strip Mines/Gravel Pits	76	85	89	91	88	89	(1) Gravel Road
33	Transitional	49	69	79	84	77	75	(1) Pasture/Grassland/Range Fair Condition
41	Deciduous Forest	30	55	70	77	66	60	(1) Woods – Good Condition
42	Evergreen Forest	30	55	70	77	66	60	(1) Woods – Good Condition
43	Mixed Forest	30	55	70	77	66	60	(1) Woods – Good Condition
81	Pasture/Hay	39	61	74	80	71	70	(1) Pasture – Good Condition
82	Row Crops	68	77	83	87	82	80	(1) Average of Poor and Good condition contoured row crops.
85	Urban/Recreational Grasses	39	61	74	80	71	70	(1) Open space – good condition
91	Woody Wetlands	45	66	77	83	75	70	(1) Woods – Poor Condition.
92	Emergent Herbaceous Wetlands	45	66	77	83	75	70	(1) Woods – Poor Condition.

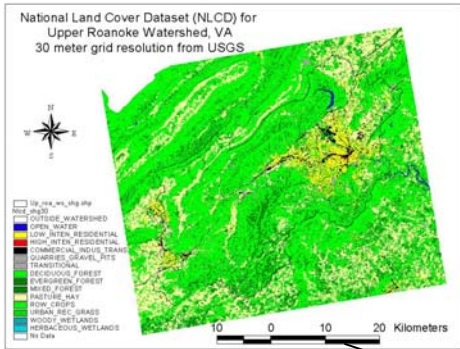
* URB = No SSURGO data available, primarily urban land

Sources:

(1) SCS TR-55

The comments in the Source column of the above table reflect which classification or combination of classifications in TR-55 was used to generate the CN for each NLCD attribute.

NLCD Land Cover Data

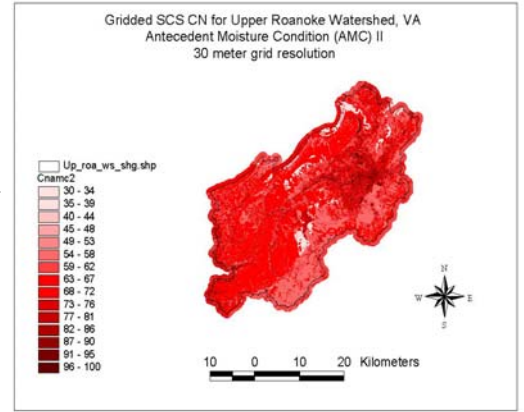


Raster Overlay and
Reclassification in
ARC/INFO GRID

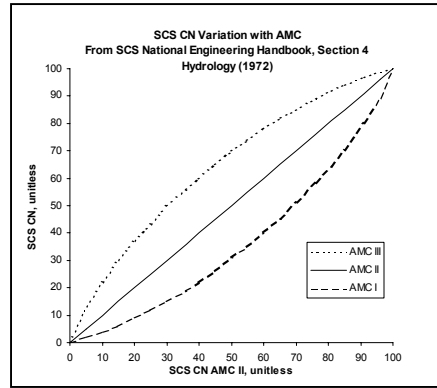
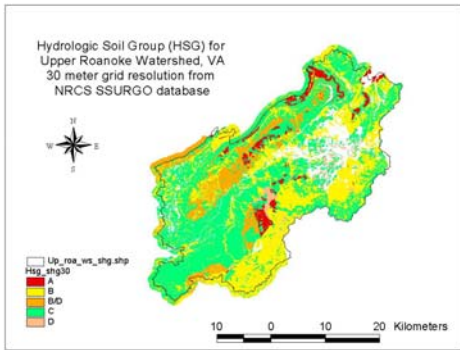
Table 3.1. Data Tables for 200200 and 100 200 1988

Table Name	Table Path	Table Description
100	100	100
200	200	200
1988	1988	1988

SCS CN, AMC II

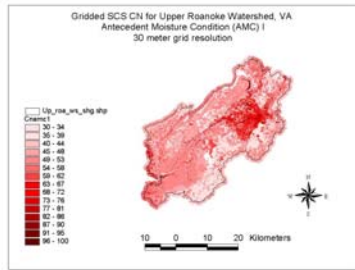


SSURGO Soil Data



Reclassification in
ARC/INFO GRID
based on SCS NEH-
section 4.

SCS CN, AMC I



SCS CN, AMC III

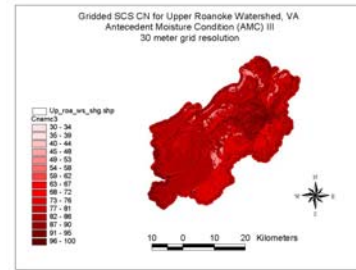


Figure 3.17: Flowchart for CN Processing

Figure 3.18 below shows the spatial distribution of SCS CN for the Upper Roanoke watershed as determined from the above reclassification matrix. The values calculated above represent the median watershed condition or AMC II. Grid resolution is 30 meters.

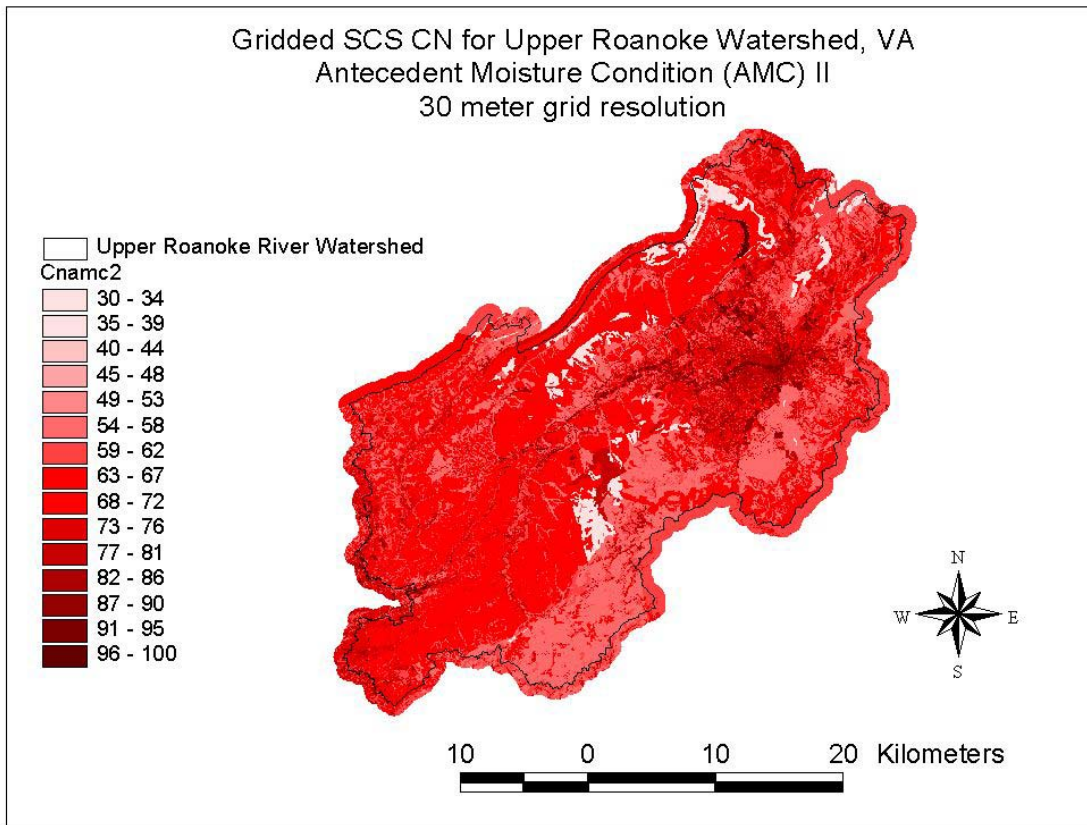


Figure 3.18: Gridded SCS CN, AMC II, for Upper Roanoke River Watershed

Figure 3.19 below shows curve numbers for the area surrounding Carvins Cove Reservoir. Grid resolution is 30 meters.

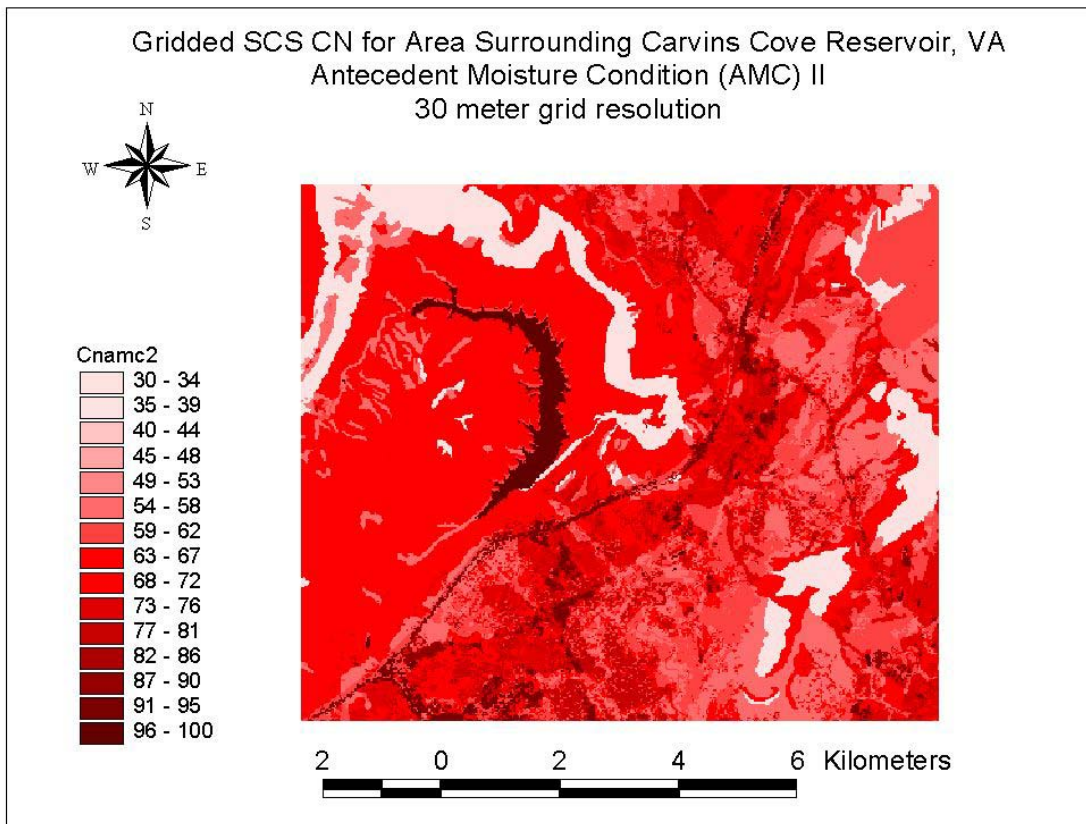


Figure 3.19: Gridded SCS CN, AMC II, for Carvins Cove Reservoir.

To account for storm to storm variation of curve number, spatially distributed curve number grids at varied antecedent moisture conditions were created. These grids were created by reclassifying the CN grid for AMC II based on the values provided by SCS (1972). The variation of CN with AMC is discussed in section 2.7. A sample reclassification table used to convert AMC II to AMC III is included in Appendix D. Figure 3.20 and 3.21 show curve numbers for the Upper Roanoke Watershed at AMC I and AMC III conditions respectively. Grid resolution is 30 meters.

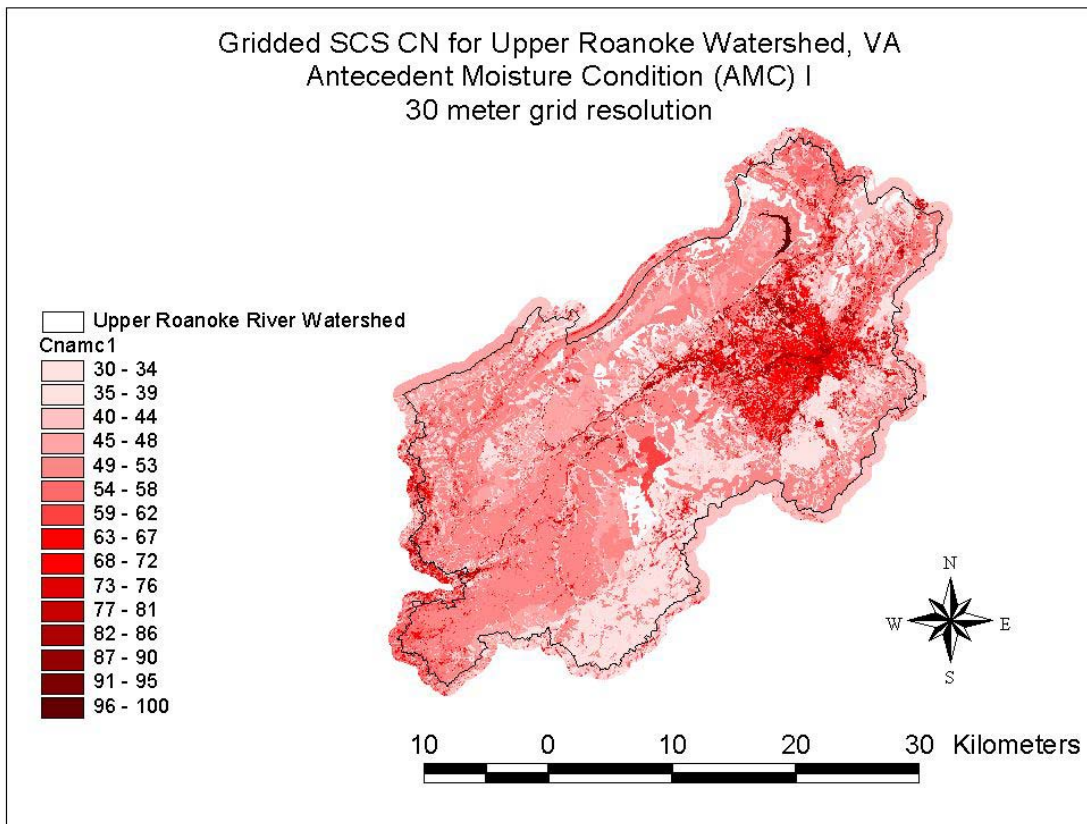


Figure 3.20: Gridded CN, AMC I, for Upper Roanoke River Watershed

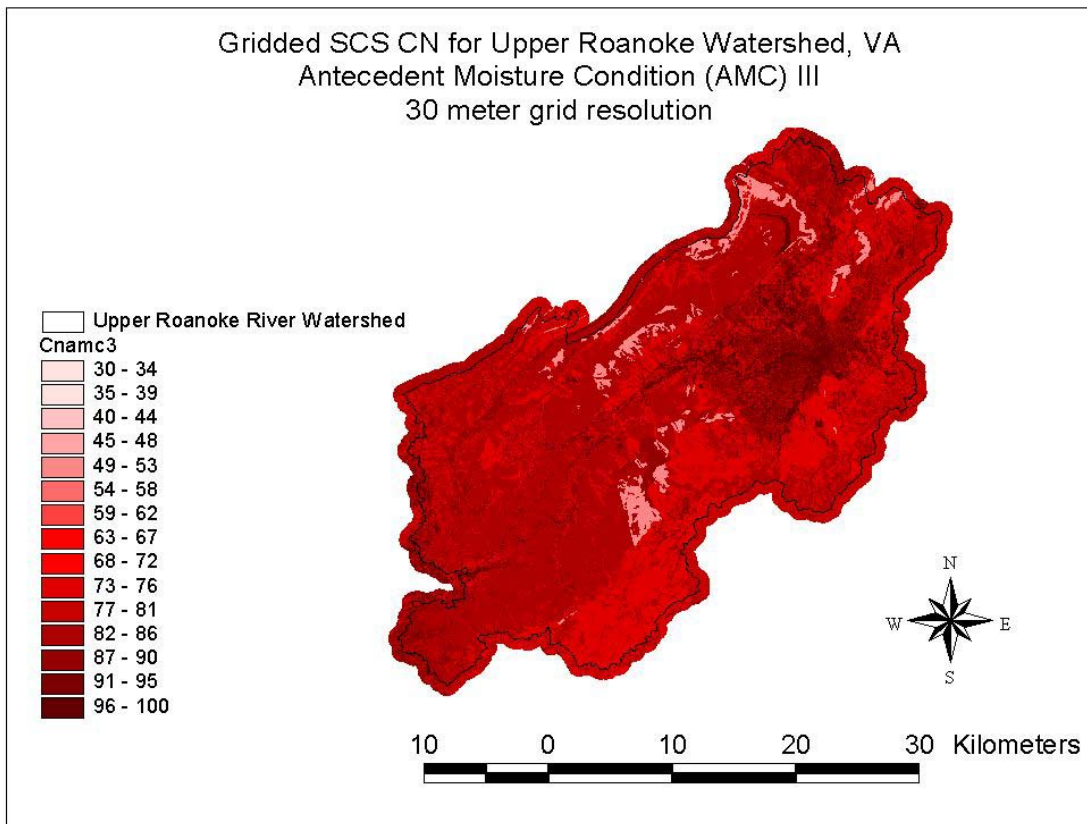


Figure 3.21: Gridded CN, AMC III, for Upper Roanoke River Watershed

3.6.2 HEC-GeoHMS Processing

This section describes the steps taken in HEC-GeoHMS to create the HMS model inputs required for the Upper Roanoke Watershed. For detailed instructions on processing GIS data with HEC-GeoHMS, the reader is referred to Doan (2000). Processing steps are shown here applied to the Upper Roanoke Watershed. Elevation data preprocessing, subwatershed and stream channel delineation, and creation of HEC-HMS input files are discussed. Figure 3.22 shows a flowchart describing HEC-GeoHMS processing from GIS datasets to HEC model inputs.

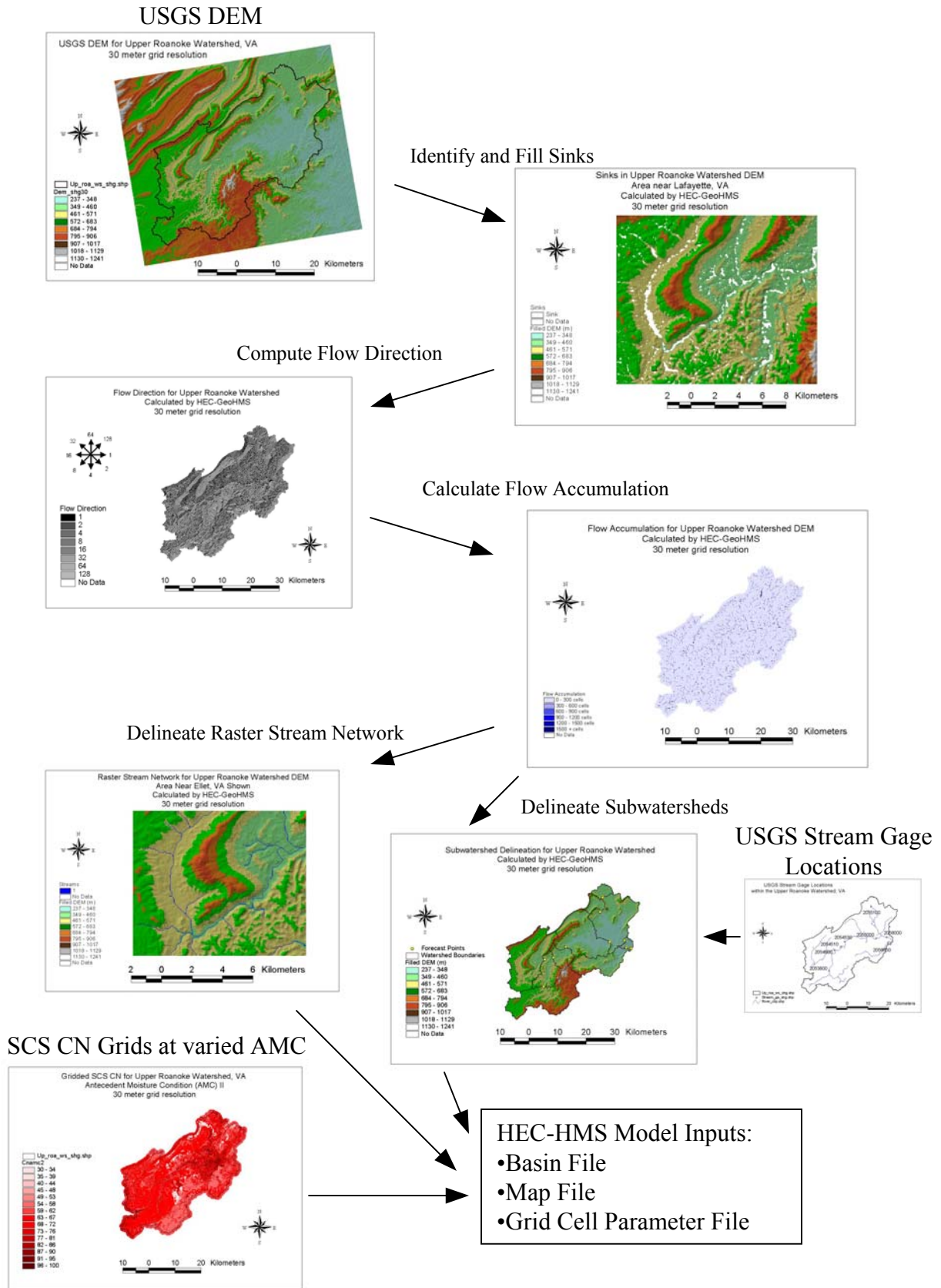


Figure 3.22: Flowchart for HEC-GeoHMS Processing

3.6.2.1 Watershed and Stream Channel Delineation

Subwatersheds and stream channels were delineated from a “hydrologically correct” raster elevation model. In a hydrologically correct raster elevation model, relative minima in the interior of the DEM are eliminated causing all flow to proceed downgradient until the DEM boundary is reached. The elimination of relative minima, or sinks, is necessary for application of the 8 point pour method used in HEC-geoHMS. The eight point pour method is based on the algorithms, or D8 method, of O’Callaghan and Mark (1984), later expanded by Jenson and Dominique (1988).

The depressionless DEM is created by increasing the elevation of the pit cells to the level of the surrounding terrain in order to fill the depressions or pits (Doan, 2000). Flow directions can then be assigned. Figure 3.23 shows the Upper Roanoke River watershed DEM with sinks shown in white. Sinks occur primarily in areas of low relief such as valley bottoms.

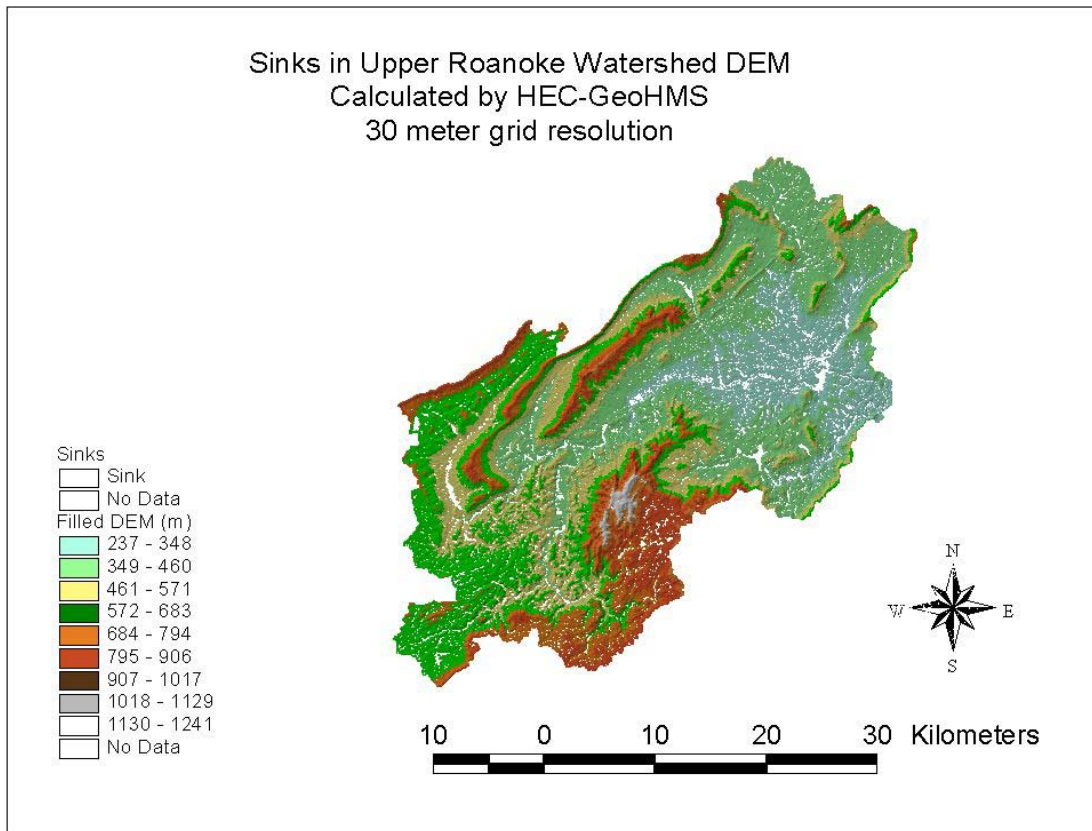


Figure 3.23: Sinks in Upper Roanoke River Watershed DEM

From the depressionless DEM, flow direction is calculated using the eight point pour algorithm and defines the direction of steepest descent for each terrain cell. The following directions are possible and are powers of 2:

Table 3.7: Eight point pour flow directions.

east	2^0	1
southeast	2^1	2
south	2^2	4
southwest	2^3	8
west	2^4	16
northwest	2^5	32
north	2^6	64
northeast	2^7	128

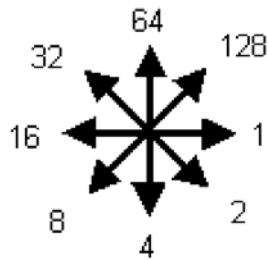


Figure 3.24: Eight point pour flow directions.

Figure 3.25 below shows flow directions computed for the Upper Roanoke Watershed from the depressionless DEM by the eight point pour method.

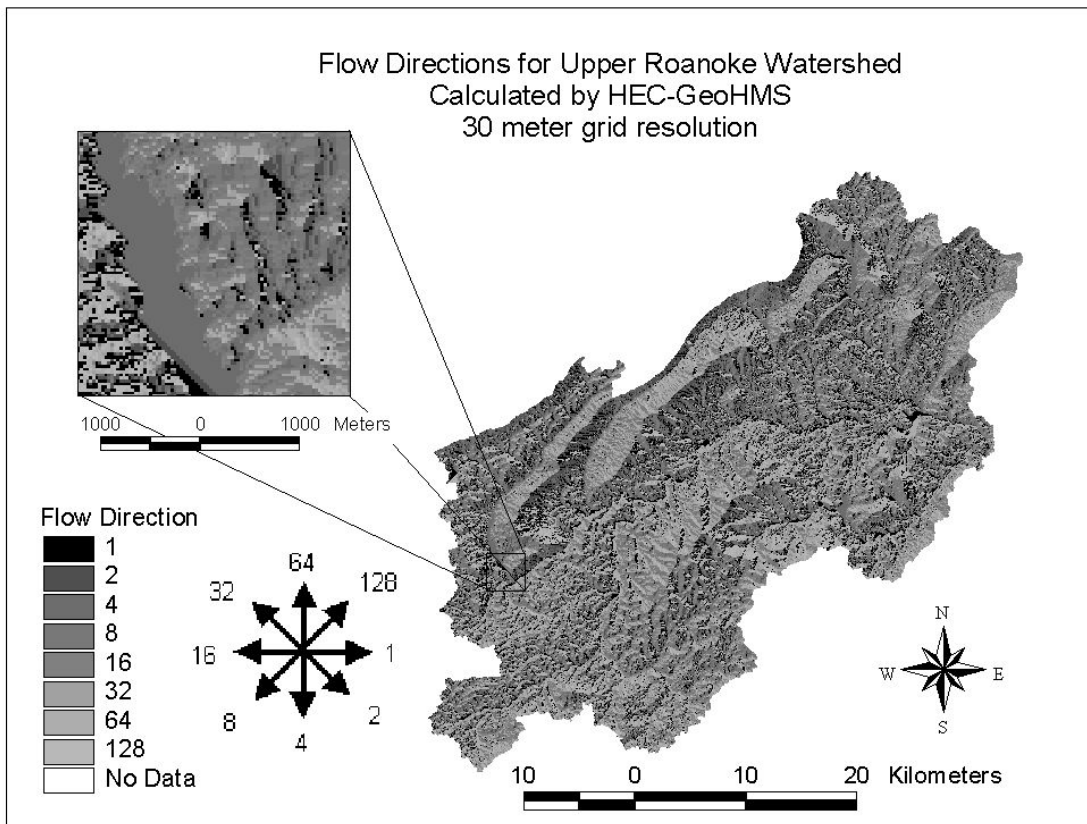


Figure 3.25: Flow Directions for Upper Roanoke River Watershed

A grid of flow accumulation is created by determining the number of upstream cells draining to a given cell. Upstream drainage area can be calculated by multiplying the flow accumulation value by the cell area (Doan, 2000). Figure 3.26 shows flow accumulation for the Upper Roanoke watershed. Flow accumulation values are in number of 30m (900m²) cells.

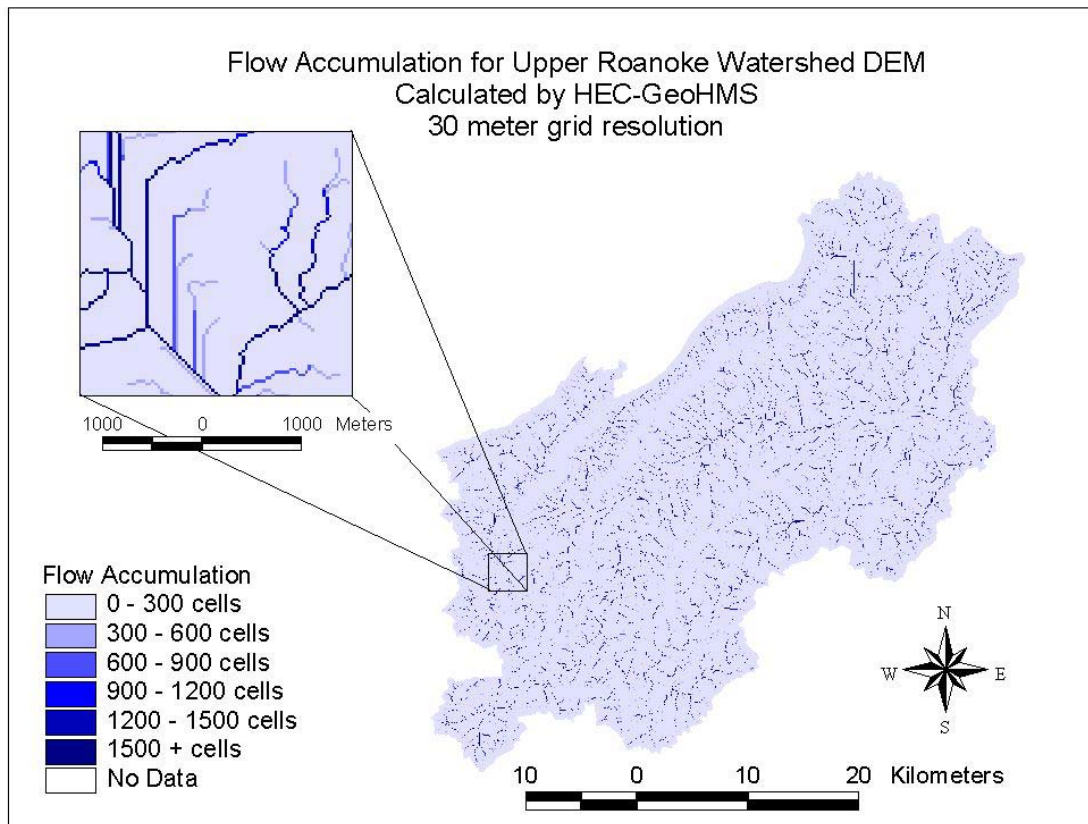


Figure 3.26: Flow Accumulation for Upper Roanoke River Watershed

Stream channel definition is defined by a user specified threshold for channel initiation. Typically cells with high flow accumulation, greater than a user defined threshold value, are considered part of a stream network (Doan, 2000). As the threshold area for channel formation becomes smaller, the number of subwatersheds and number of channel segments becomes larger. Selection of the threshold was not a critical step in this research as subwatersheds were defined above stream gage points and channel segments finer than those between subwatersheds were not modeled. Figure 3.27 below shows the delineated stream channel network for the Upper Roanoke River Watershed. A more detailed view of the stream network near Ellet, VA on the North Fork of the Roanoke River is shown in Figure 3.28. Threshold value used in these figures was 3km^2 (~3300 cells).

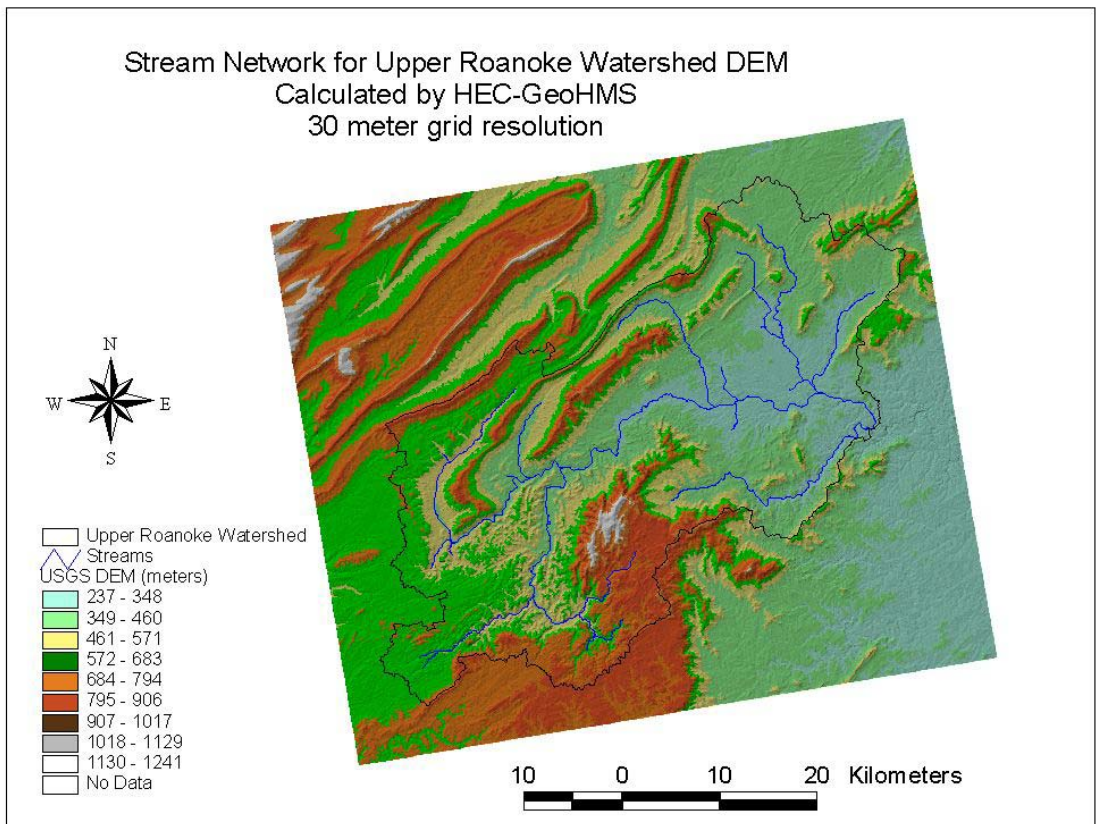


Figure 3.27: Stream Network for Upper Roanoke River Watershed.

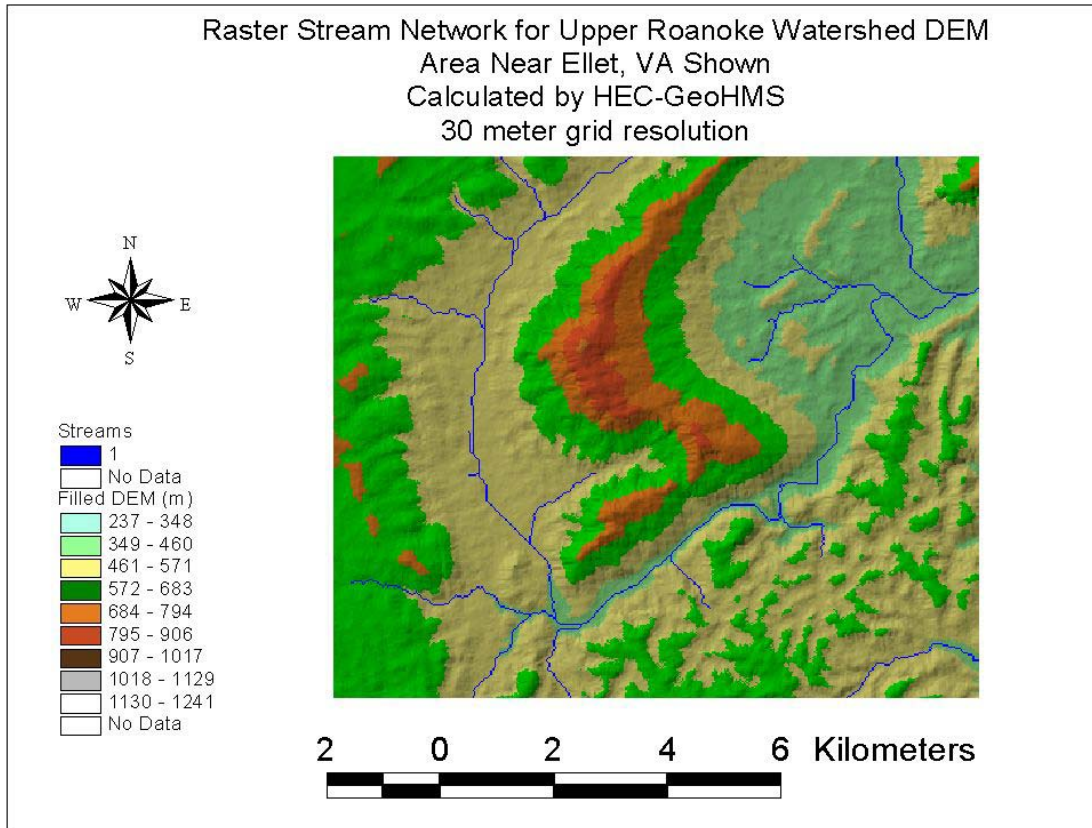


Figure 3.28: Raster Stream Network for Area Near Ellet, VA on North Form of Roanoke River.

Subwatershed delineation is accomplished by default for each stream segment in the raster channel network. Subwatersheds may be aggregated or split and new subwatersheds may be delineated at user specified points by tools available in HEC-GeoHMS. As the desired outlet points for this modeling study coincided with USGS stream gage locations, stream gage locations, along with other points of interest were aggregated into a point file. These points were used as subwatershed delineation points. Subwatersheds were aggregated as necessary to produce the desired watershed discretization and connectivity. Forecast points include seven of the eight USGS stream gages, one IFLAWS stream gage (Ironto), the outlet of Carvins Cove Reservoir, and the confluence of Back Creek and the Upper Roanoke River. The USGS stream gage at Wabun, VA was not used because travel time between the upstream gage (Lafayette, VA) and Wabun, VA is much shorter than travel times in other river reaches. Travel time from Wabun, VA to the next gage downstream (Glenvar, VA) is also significantly shorter than travel time in other segments. The outlet of Carvins Cove reservoir was chosen as a forecast point in case additional control of the reservoirs effects was needed to produce reasonable results. Due to the small catchment area above the reservoir, reservoir effects were not explicitly modeled. For accuracy, forecast point locations were adjusted to the closest cells in the raster stream network with contributing area closest to the value tabulated for each USGS stream gage. Figure 3.29 shows subwatershed boundaries, forecast points, and the DEM for reference.

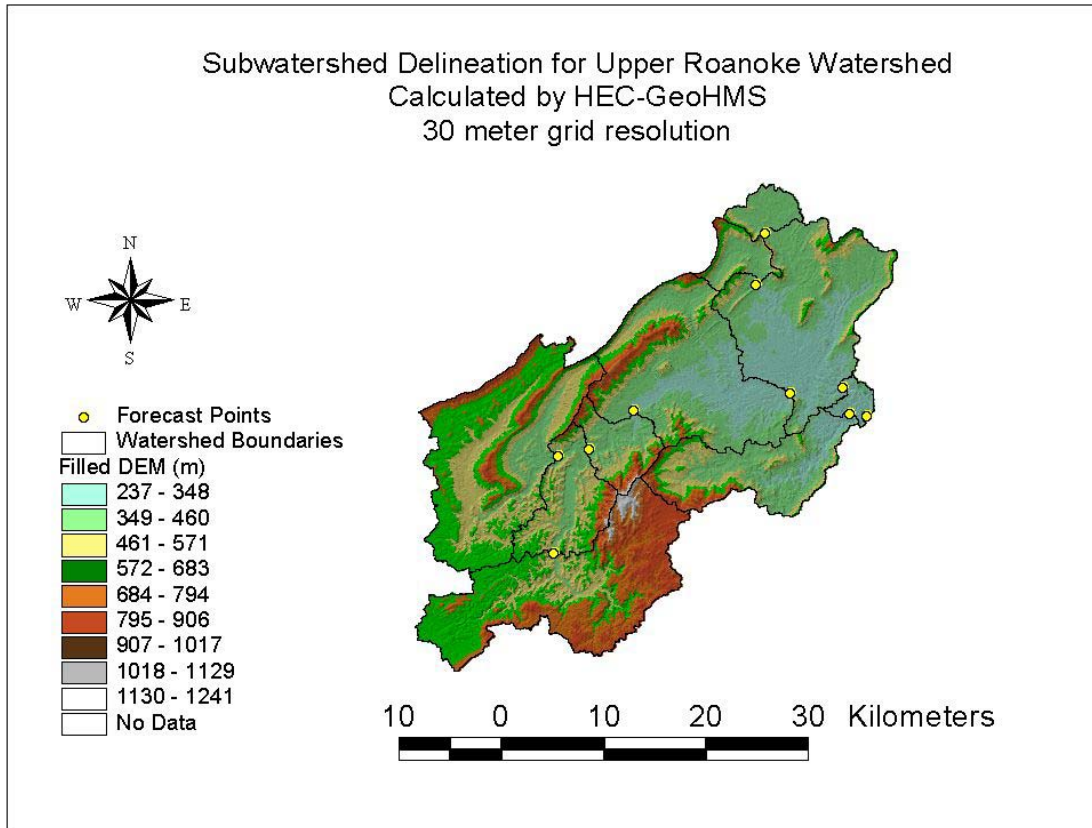


Figure 3.29: Subwatershed Delineation for Upper Roanoke River Watershed.

3.6.2.2 HEC-HMS Basin File and Map File Creation

HEC-GeoHMS creates a number of hydrologic inputs for HEC-HMS including the background map file, lumped – basin schematic model file, grid cell parameter file, and distributed – basin schematic model file (Doan, 2000).

The background map file captures the geographic information of the subbasin boundaries and stream alignments in an ASCII text file that can be read by HMS (Doan, 2000). The background map file provides a locational reference when working in the basin model editor within HEC-HMS.

The basin file contains the hydrologic elements and their model parameters, their connectivity, and related geographic information in an ASCII text file that can be read by HEC-HMS (Doan, 2000). The basin model may then be parameterized using traditional techniques in HEC-HMS. Figure 3.30 shows the subwatershed discretization and connectivity as modeled by HEC-HMS. Appendix G includes a sample basin file for the Upper Roanoke Watershed.

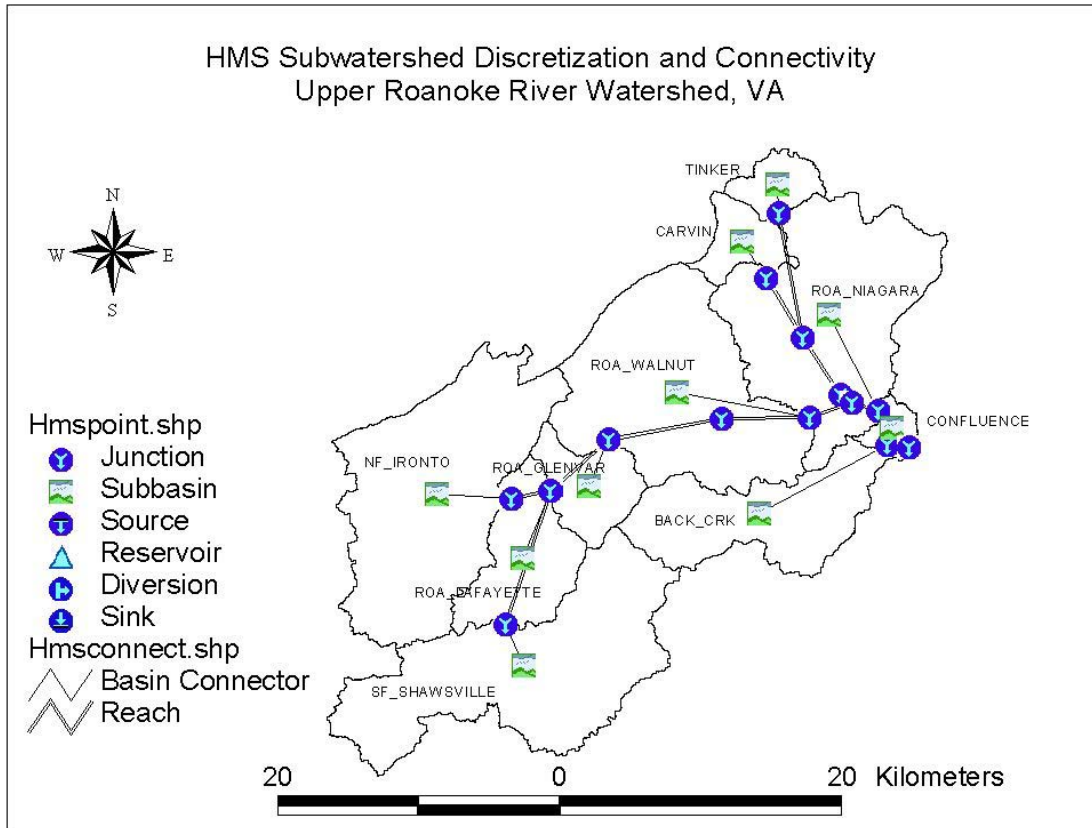


Figure 3.30: Subwatershed Discretization and Connectivity for Upper Roanoke River Watershed.

3.6.2.3 HEC-HMS Grid Cell Parameter File Creation

The grid cell parameter file is the key component of the distributed runoff model. The grid cell parameter file provides the information necessary to model each sub basin as a series of grid cells. The grid cell parameter file contains cell locations, travel length to the watershed outlet, and infiltration parameters, such as the SCS CN, for each grid cell in the model. Multiple grid cell parameter files were created for the modeling scale study with various grid resolutions and antecedent moisture conditions. Grid cell parameter files at 400m, 500m, 1km, 2km, and 5km were created with curve numbers corresponding to AMC I, II, and III.

HEC-GeoHMS creates the grid cell parameter file by intersecting a vector lattice of regularly shaped square grid cells with the vector representation of the watershed boundaries delineated above. Each cell in each subwatershed is either a square cell or a portion of a square cell in the case of a watershed boundary passing through a cell. Cell location for the lower left corner of each cell is referenced to the origin of the coordinate system by an integer number of cells. Cell location, cell area, and travel length (based on the resolution of the original DEM) are computed for each grid cell. The registration of the subwatershed grid cells was checked to ensure that it matched with the registration of the gridded precipitation inputs developed for this modeling study. Figure 3.31 shows a 1 kilometer gridded representation of the Upper Roanoke watershed. Figure 3.32 and 3.33

show gridded representations of the Upper Roanoke Watershed at 500 meter and 4 kilometer resolutions respectively.

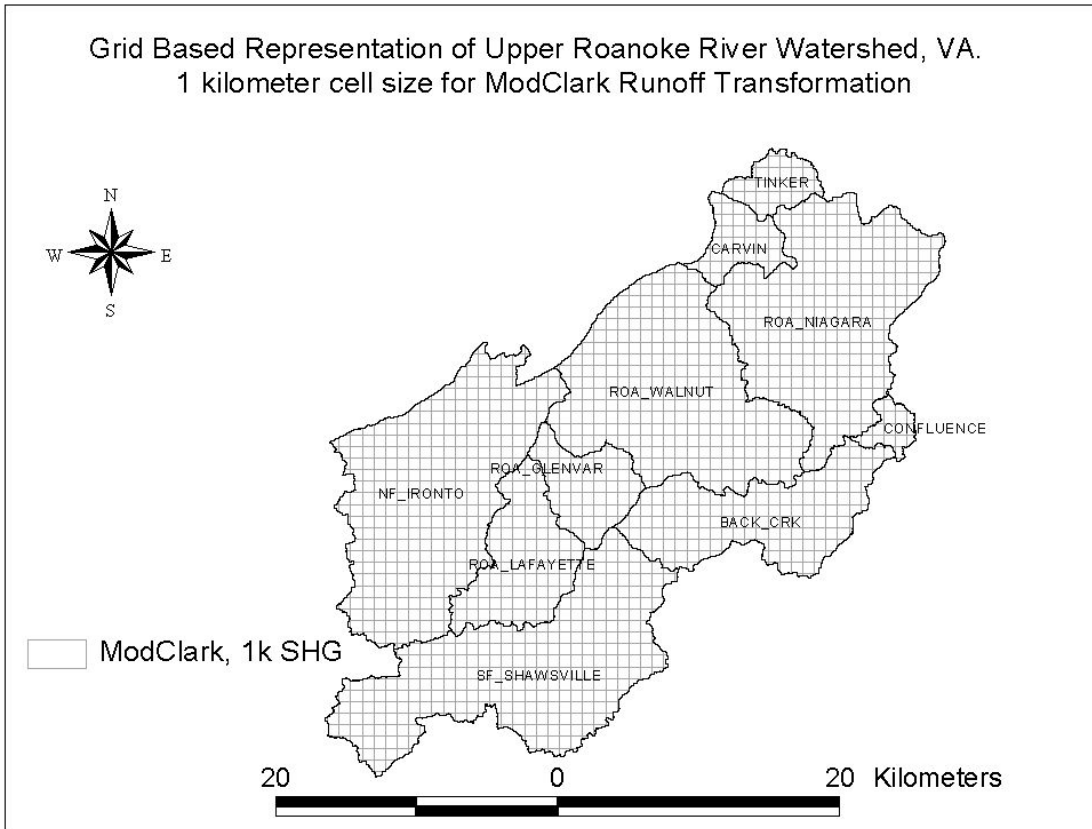


Figure 3.31: Gridded Representation of Upper Roanoke River Watershed, 1 kilometer grid resolution.

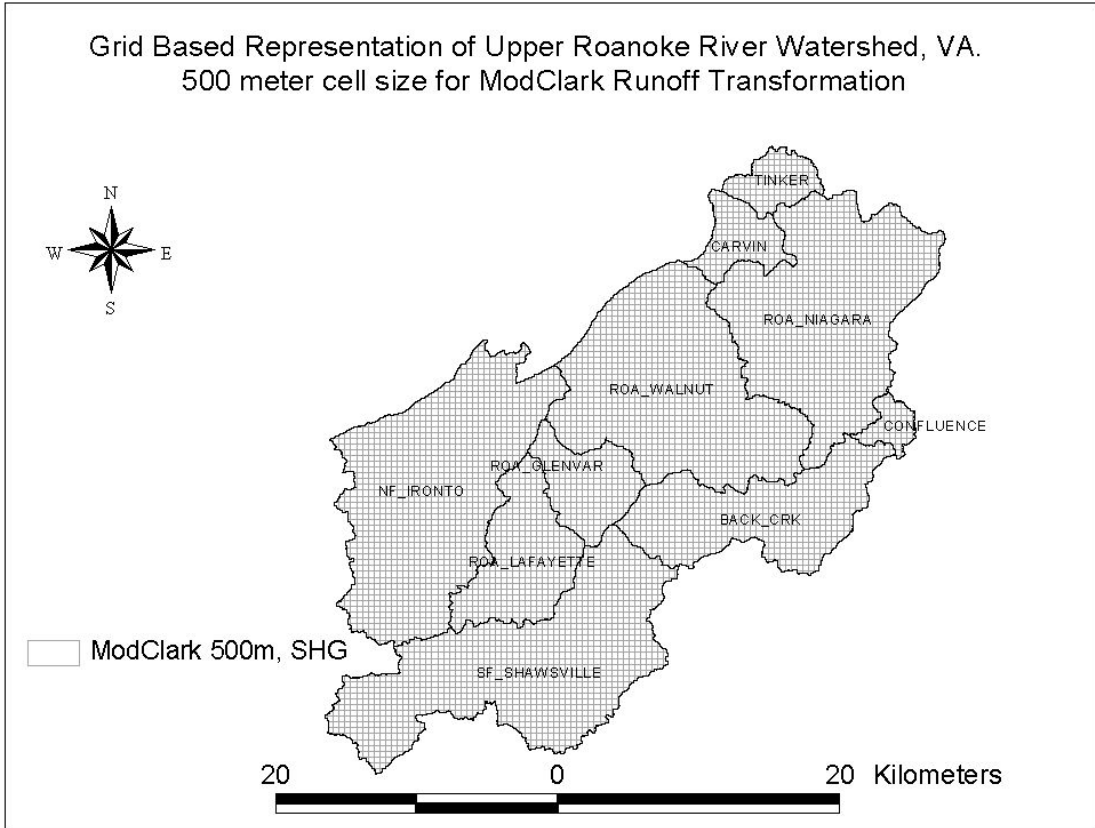


Figure 3.32: Gridded Representation of Upper Roanoke River Watershed, 500 meter grid resolution.

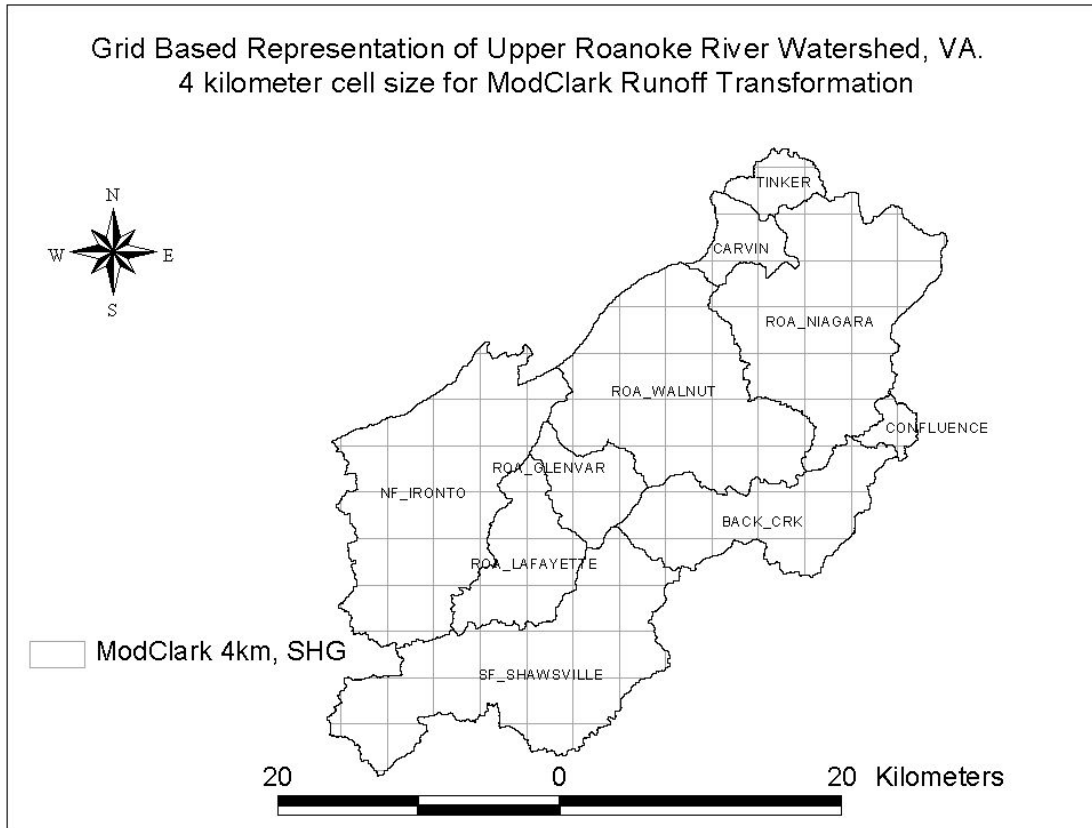


Figure 3.33: Gridded Representation of Upper Roanoke River Watershed, 4 kilometer grid resolution.

Because HEC-GeoHMS currently does not currently include a method to calculate SCS CN for grid cells, the “summarize zones” function of Spatial Analyst was used to determine curve numbers for the grid cell parameter file. “Summarize zones” determines summary statistics for the attribute of a raster dataset within the polygons of a vector theme. The curve number grids created above were used along with the vector grid cell parameter file created by HEC-GeoHMS to determine mean CNs for each subwatershed grid cell. Figure 3.34 shows the mean CN for 1km grid cells for a representative area near Roanoke, VA.

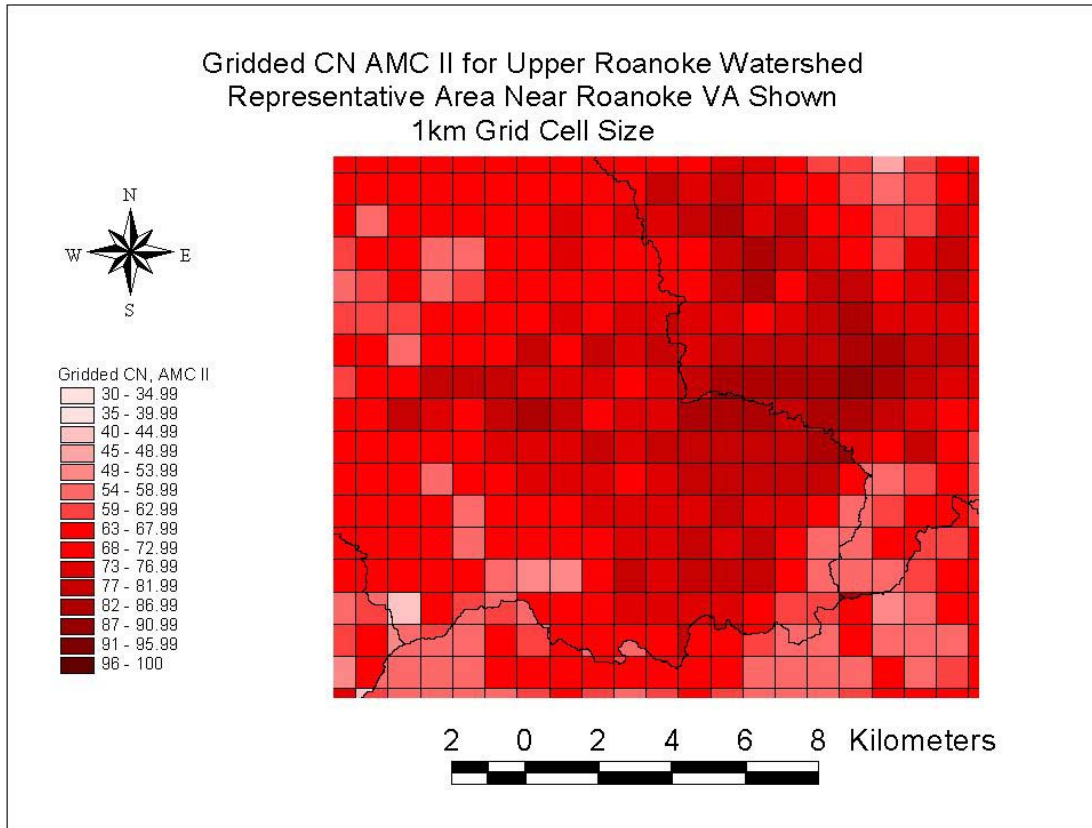


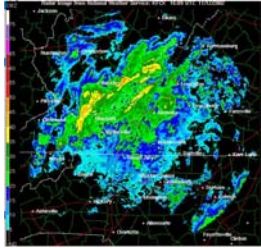
Figure 3.34: Gridded CN for area near Roanoke VA, 1km cell size.

The grid cell parameter file in the format required by the HEC-HMS model was created from the attribute table of the gridded subbasin shapefile using a spreadsheet program and text editor. Grid cell parameter file specifications are detailed by Doan (2000). An example grid cell parameter file is included in Appendix G.

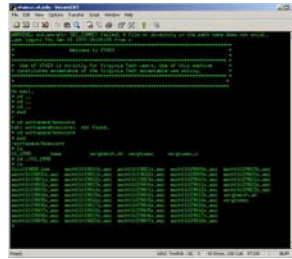
3.6.3 Processing of archived NEXRAD Stage III Data

This section describes the steps taken to decode, resample, and reproject the archived NEXRAD stage III precipitation data used in the modeling study. To evaluate the effects of rainfall resolution on model results, a series of gridded precipitation input sets were created at varied resolutions using the raster interpolation techniques of bilinear interpolation and nearest neighbor reassignment. Figure 3.35 shows a flowchart of the steps used to decode and process the precipitation data.

NEXRAD Stage III Precipitation

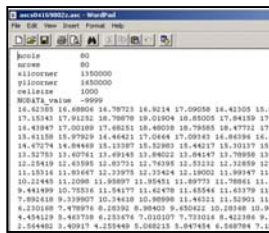


Decoding and Reprojection with xmrgrtoasc.c on UNIX platform.

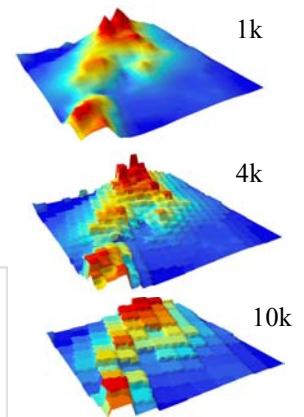


UNIX Decoding of Archived Data

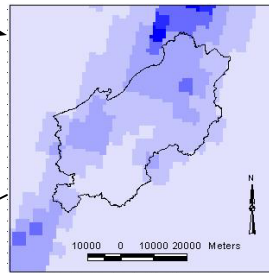
Sample ASCII Precipitation Grid



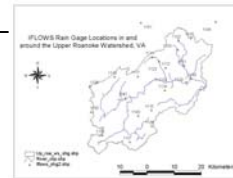
3D Visualization of varied Precipitation Resolutions



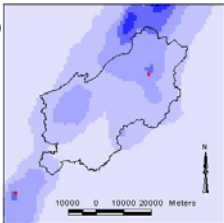
Conversion to ESRI Grid and Reprojection



Verification with IFLOWS gage data

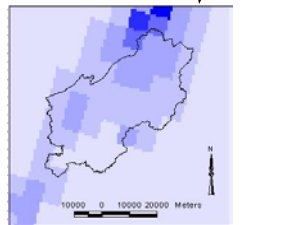


Downscaling (smoothing)

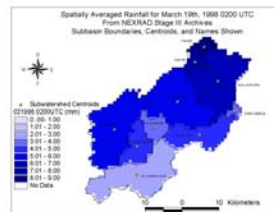


ARC/INFO GRID Processing

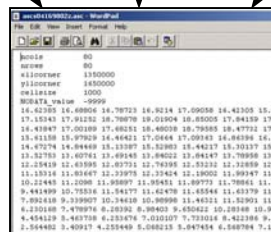
Upscaling (degradation)



Spatial Averaging (Lumping)



ASCII Precipitation Grids



Encoding to HEC DSS Database with grid2dss.exe

Figure 3.35: Gridded Precipitation Data Processing

NEXRAD stage III archives are stored in the xmrgr file format referenced to the HRAP coordinate system. Details on the xmrgr file format are in Appendix E. Details on the HRAP coordinate system are available in section 3.4.1. Archives were decoded into ASCII grids referenced to the HRAP polar stereographic coordinate system using the xmrgrtoasc.c program. Details and code for xmrgrtoasc.c are available in Appendix E. Performance of the compiled xmrgrtoasc program was checked successfully against a sample dataset provided by the NWS.

Hourly precipitation grids referenced to the HRAP coordinate system for three storm events: October 24th to 28th 1997, March 17th to 22nd 1998, and April 16th to 21st 1998, were created in ASCII grid format. For details on the ASCII grid format, the reader is referred to Appendix E. ASCII grids were converted to ESRI grids such that the reprojection and resampling tools of ARC/INFO GRID could be used.

To perform a sensitivity analysis on rainfall data resolution, the NEXRAD stage III archived precipitation data for the October 1997, March 1998 and April 1998 storms were upscaled and downscaled to a series of spatial resolutions. Temporal resolution was kept constant at one hour time steps. Spatial scaling was accomplished in the ARC/INFO GRID environment using the PROJECT() and RESAMPLE() functions. Gridded hourly precipitation depths for each storm event were scaled to 6 resolutions ranging from 10km to 1km.

As the original data archives are at a 4km resolution referenced to the HRAP coordinate system, and the desired outputs must be a 1km grid in the SHG Projection (see section 3.4.2), there will be slight locational uncertainties associated with reprojection of archived data. These uncertainties are similar however to those encountered in the creation of the stage III radar products. See Fulton (1998) for a discussion of the WSR-88D Polar to HRAP mapping. In the process of creating the stage III precipitation estimates, precipitation estimates from each radar cell (polar 2km by 1°) are remapped to the 4km HRAP grid by simply averaging the values of all cell centers which fall within an HRAP cell. This is a simple and efficient manner to reassign the radar data (Fulton 1998) and also prevents any double counting of radar cells.

When downscaling the radar data, the assumption of a continuous rainfall surface, or a smooth transition from grid cell to grid cell, may be made. No detail is added in downscaling, however the radar data is treated as a continuous surface in downscaled grids, ideally leading to a more accurate approximation of reality. In upscaling, detail is removed by spatial averaging. Consequently, peak precipitation depths are reduced and the overall range of rainfall values is reduced.

In order to isolate the effects of rainfall resolution, precipitation volumes for each hourly time step should remain equal regardless of spatial resolution. A quantitative check made on the precipitation grids revealed that overall storm volume changes of less than 1% resulted from the upscaling and downscaling techniques applied to the historical precipitation data. The comparison of rainfall volumes under different resolutions is discussed in section 4.2.

Resampling of gridded precipitation within one coordinate system was accomplished with the ARC/INFO GRID, RESAMPLE function. RESAMPLE changes the cell size of a grid and may use a nearest neighbor assignment (nearest), a bilinear interpolation (bilinear), or a cubic convolution (cubic), as the resampling method (ESRI, 2002). Details concerning the bilinear interpolation and nearest neighbor resampling methods are included in Appendix F.

A nearest neighbor assignment is the most computationally efficient method of grid resampling. In this method a new grid cell is assigned the value of the old cell center closest to the new grid cell center. This causes no smoothing of the data and is more appropriate for categorical data sources rather than continuous surfaces. A nearest neighbor assignment is useful for a continuous surface such as rainfall depth or intensity when utilizing a precipitation resolution coarser than the grid cell size required by the hydrologic model. In this way, a 4km precipitation resolution may be used in a 1km basin model without any smoothing of the input data.

A bilinear interpolation determines the value of a new cell as a distance weighted average from the four nearest old cell centers. A bilinear interpolation is useful for continuous data and will cause some smoothing of the input data. Bilinear interpolation is computationally efficient and useful for aggregating or upscaling and smoothing or downscaling continuous surfaces. Using bilinear interpolation in upscaling better preserves overall precipitation volume than a nearest neighbor assignment.

A cubic convolution assigns a new cell value based on a surface fit through the nearest 16 cell centers. It is computationally intensive and may result in new values outside the range of the input grid. Cubic convolution was not used in this study to adjust precipitation resolution.

Precipitation data is archived as 4km x 4km hourly grids of precipitation depth referenced to the HRAP coordinate system. Reprojection must be employed to reference the archived radar data to the SHG coordinate system. The ARC/INFO GRID, PROJECT function was used to transfer radar archives from HRAP to SHG. PROJECT converts a grid between two coordinate systems and can resample and resize by nearest neighbor assignment, bilinear interpolation, or cubic convolution (ESRI, 2002).

Precipitation databases were created in the SHG projection for the distributed hydrologic model of the upper Roanoke watershed at a 1k cell size and at resolutions of 10k, 8k, 6k, 4k, 2k, and 1k. A computational cell size of 1k was chosen as a compromise between spatial discretization and computational and data storage requirements based on the recommendations of Seybert (1996). A 1k cell size splits the Upper Roanoke Watershed into approximately 1500 cells with between 30-300 cells per subwatershed. In order to isolate the effects of precipitation resolution while holding physical characteristics constant, various interpolation and degradation schemes were applied and are discussed below.

To create precipitation databases at a 10k resolution and 1k cell size, 4km HRAP data was bilinearly interpolated to 10k with the RESAMPLE() command and then reprojected by nearest neighbor assignment to the 1k SHG. 8k and 6k resolution data sets were created by the same method. The precipitation database at the 4k resolution was created by performing a nearest neighbor based reprojection from the 4km HRAP grid to the 1k SHG. This is the closest this research comes to using the resolution of the original data archives. This will be the resolution against which the downscaling (smoothing) and the upscaling (degradation) techniques are evaluated. 2k and 1k resolutions were created by reprojecting the 4km HRAP data to the SHG projection at 1km and 2km resolutions using a bilinear interpolation. The 2km data were then resampled by a nearest neighbor assignment to a 1km grid cell size.

Additional gridded precipitation datasets referenced to the SHG projection with grid cell sizes and resolution of 400m, 500m, 1km, 2km, and 5km were created by bilinear interpolation from the original 4km HRAP precipitation grids. These precipitation datasets are intended for use in a sensitivity analysis on physical parameter resolution and computational grid cell size.

Figure 3.36 below qualitatively shows the smoothing and degradation that were performed by the above techniques. The “jagged” edges appearing in the 4k and 8k resolutions are the result of using the SHG projection and 1k cell size to represent 4k or 8k cells referenced to the HRAP coordinate system.

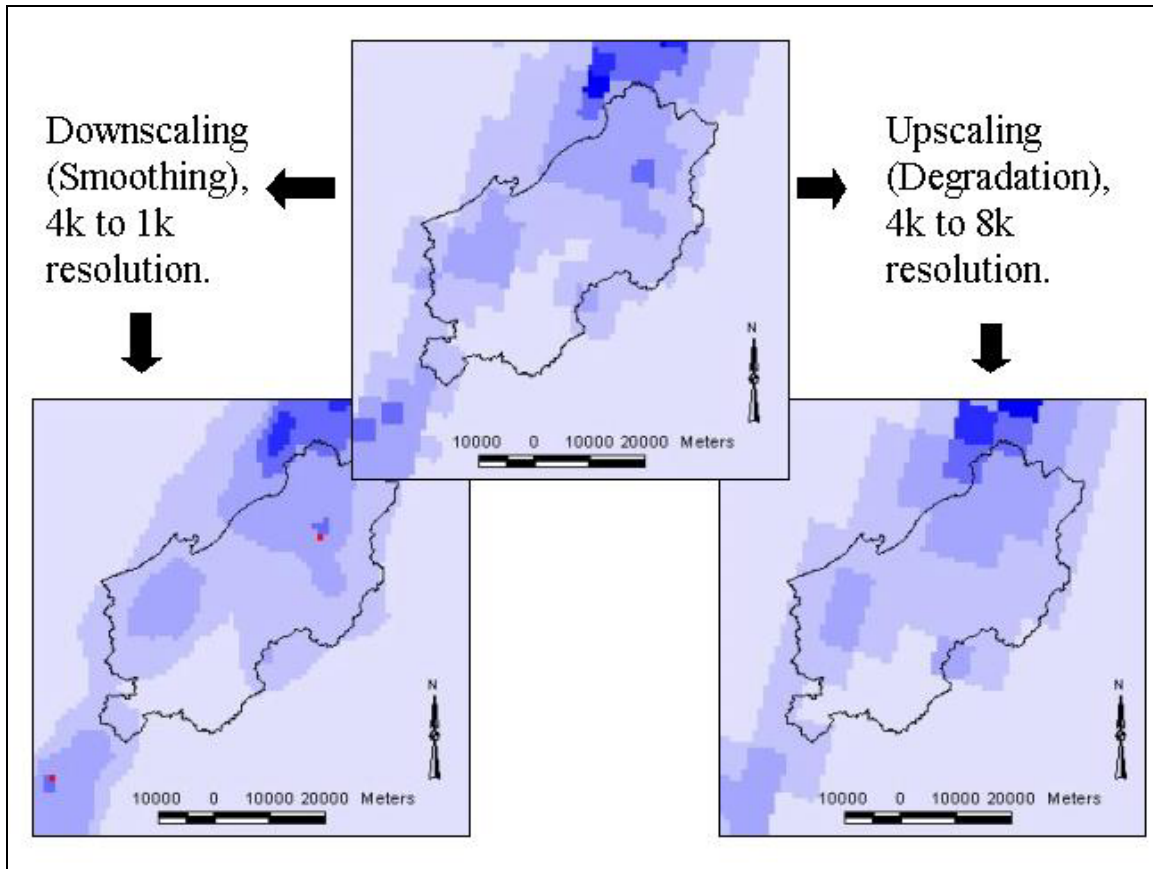


Figure 3.36: Upscaling and Downscaling of NEXRAD data for March 19th, 1998, 0200 UTC.

The resulting reprojected and resampled ESRI grids were converted back to ASCII grids using the ARC/INFO GRID) GRIDASCII() function. GRIDASCII converts an ESRI grid to an ASCII grid (ESRI, 2002). ASCII grids describing hourly precipitation depths at varied resolutions and referenced to the SHG were encoded into the HEC modeling database with the use of the ai2dssgrid.exe program obtained from HEC. For details on the ai2dssgrid.exe program and the DOS batch files used to efficiently utilize this program, the reader is referred to Appendix E.

3.6.4 Comparison of Radar to Gage Precipitation

To check the spatial and temporal accuracy of the decoding and coordinate reprojection process, a comparison was made between gridded precipitation records and gage records for each of the three storm events. Precipitation hyetographs were extracted from the gridded precipitation records for each rain gage location. These hyetographs were correlated with the hyetographs available from the IFLOWS gage archives. Because the stage III data undergoes significant processing (including adjustment to ground based gages), the intent of this comparison was to verify that precipitation grids were appropriately located in space and time and not to adjust the radar data.

Radar derived precipitation hyetographs for the gage points were created using the LATTICESPOT() function in ARC/INFO. LATTICESPOT() computes surface values

for each point in a point coverage by interpolating from a lattice. The surface value of each point in the coverage is interpolated from the lattice surface using bilinear interpolation (ESRI, 2002). Appendix E includes the AML script used to iteratively query hourly rainfall grids and create the necessary hyetographs. The results of the radar and gage comparison is detailed in section 4.1.

3.6.5 Comparison of Varied Precipitation Resolutions

To ensure that the effects of rainfall resolution would be isolated, the author verified that the reprojection and resampling techniques used would not significantly affect overall volume of rainfall input into the Upper Roanoke Watershed. This was accomplished by comparing the storm total precipitation grids for each of the three storm events at all of the various grid resolutions. For equal area grids, the mean grid value is proportional to the overall precipitation volume. For this reason, the mean grid value for storm total precipitation for each storm event and resolution was tabulated and is evaluated in section 4.2.

3.6.6 Creation of streamflow database from USGS records (DSSTS)

Time series of instantaneous streamflow for the eight USGS stream gage locations in the Upper Roanoke Watershed at 15min to 30min resolution were obtained from the USGS. These records were converted in time to UTC and the effects of time changes from daylight savings time were removed. Once accurate time series were obtained, these files were input to the HEC DSS database via the DSSTS (DSS Time Series) program. DSSTS is a program for entering regular interval time series data into a HEC-DSS database file. Regular interval time series data has an implicit data/time associated with each data value (HEC, 1995).

3.7 Basin Model Parameterization

This section discusses the selection of hydrologic model parameters for the HEC-HMS runoff model including: times of concentration (t_c), reservoir coefficients (R), antecedent moisture condition (AMC), and Muskingum channel routing parameters: travel time (k) and attenuation (x). Development of these parameters using both traditional methods and optimization are discussed. As the intent of this modeling study was to evaluate the effects of precipitation resolution and grid scale on model results, model parameterization was only taken far enough to meet this objective. In operational or forecast use, model parameterization could be improved with time as more storm events were observed.

3.7.1 Subwatershed Baseflow Calculation

HEC-HMS offers multiple methods to model baseflow (Feldman, 2000):

- constant, monthly varying value,
- exponential recession model, and
- linear reservoir volume accounting model.

As baseflow is seasonably variable between fall low flow and spring runoff periods, a monthly average is a more effective specification than an exponential recession model. The current coding of HMS will only allow one set of exponential baseflow parameters per basin model. Thus an exponential recession baseflow model would require multiple basin models, or changes to the basin model, for changes in storm event or time specifications.

Monthly constant baseflow for each subwatershed were calculated from gage records for each storm event. For stream gages in series, local baseflow was calculated as the difference in baseflow between the upstream gage and downstream gage. For ungaged areas, baseflow from the next downstream gage was split between subwatersheds based on the ratio of subwatershed area to gage contributing area. Baseflow was set for subwatersheds and storm events as shown in table 3.8 below.

Table 3.8: Subwatershed Baseflow for Upper Roanoke River Subwatersheds.

Subwatershed	Baseflow (m ³ /s)		
	OCT 97	MAR 98	APR 98
NF IRONTO	0.300	3.650	5.370
SF SHAWSVILLE	0.878	3.115	2.832
ROA LAFAYETTE	0.100	1.190	1.760
ROA GLENVAR	0.142	0.283	0.283
ROA WALNUT	0.425	1.699	2.549
ROA NIAGARA	0.646	4.321	4.272
CARVIN	0.091	0.606	0.599
TINKER	0.085	0.736	0.510
BACK CRK	0.283	2.379	2.322
CONFLUENCE	0	0	0

3.7.2 Subwatershed Parameterization: AMC, t_c , R

3.7.2.1 Antecedent Moisture Condition (AMC)

Because runoff volume in the SCS CN method is most sensitive to choice of CN or AMC, selection of appropriate AMC is the first priority in model parameterization. Parameters for t_c , R, k, and x were assigned a priori and model runs were made for each storm event at AMC I, AMC II, and AMC III. The AMC producing the modeled storm total runoff volume closest to the observed storm total runoff volume was selected as the AMC for that storm event. AMC II was found to best model the October 1997 storm event, while AMC III was found to best model the March 1998 and April 1998 storm events.

3.7.2.2 Time of Concentration (t_c)

Various definitions of time of concentration and Clark's Reservoir coefficient exist in the literature. Unfortunately, many of these methods are graphical or empirical and require an observed hydrograph for implementation. Once runoff volume most accurately matches observed runoff volume, optimization techniques may effectively be used to calculate time of concentration and reservoir coefficient.

Clark (1945) suggests that t_c may be graphically computed as the time interval between the end of runoff producing excess rainfall to the point of inflection of the recession limb of the hydrograph. For the scale of the watersheds used in this study, channel flow and channel flow velocity is the most important factor affecting time of concentration. Time of concentration, even conceptually, is defined in multiple ways in the literature: as the time for a parcel of water to travel from the watershed boundary to the outlet, as the wave travel time from the watershed boundary to the outlet, and graphically as the time between the end of rainfall excess and the point of inflection (POI) of the outflow hydrograph, or the time between the centroid of the rainfall excess and the centroid of the runoff hydrograph.

As gage records existed for the majority of subwatershed forecast points, time of concentration was found to be best calculated by optimization techniques within HEC-HMS.

3.7.2.3 Clark's Reservoir Coefficient (R)

Clark's reservoir coefficient is the parameter that describes the storage and attenuation characteristics of the landscape. The reservoir coefficient, with units of time, is a qualitative measure only, and may be estimated by multiple methods. Clark (1945) recommends the negative of the flow at the POI of the hydrograph divided by the time derivative of flow at the POI. This relationship is shown by equation 3.8 below.

At the point of inflection of the observed runoff hydrograph:

$$R = \frac{-Q}{dQ/dt} \quad 3.8$$

Where Q is the observed flow at the point of inflection (POI) on the recession limb of the measured hydrograph, and

R is the reservoir coefficient.

R will have units of time and be positive assuming the point of inflection is chosen on the recession limb of the hydrograph.

Kull and Feldman (1998) cite an internal HEC training document defining reservoir coefficient as the “Volume under the recession limb after the POI divided by the flow at the POI” This is shown in equation 3.9 below.

$$R = \frac{\int_{t_{POI}}^{\infty} Q \cdot dt}{Q_{POI}} \quad 3.9$$

Where Q is the observed flow at the POI (occurring at time t_{poi}).

Unfortunately, for gage records in the Upper Roanoke watershed, reservoir coefficients calculated by equations 3.8 and 3.9 were in disagreement by up to a factor of two. Initial reservoir coefficients were calculated by equation 3.8 above and improved by optimization techniques within HEC-HMS. The optimization methods of HEC-HMS and regional analysis to ungaged areas was determined to be the most effective method of subwatershed parameterization for t_c and R. These parameterization methods were found to produce results acceptable for the sensitivity analysis on rainfall resolution and grid scale.

3.7.3 Channel Network Parameterization: k, x

Channel flow times between stream gages were calculated from observed streamflow hydrographs for the 8 USGS stream gages in the Upper Roanoke watershed. By observing the times associated with similar points on the hydrographs at the upstream and downstream ends of a channel segment, travel time may be estimated.

Of the multiple methods to model channel routing in HEC-HMS, the Muskingum method was selected for this modeling study. Two parameters are required to describe the routing for each channel section: the travel time (k) and a weighting factor (x) describing the effects of storage and attenuation.

Travel time (k) may be estimated by examining hydrographs between upstream and downstream gaging stations. The weighting factor (x) defines the relative weighting of upstream and downstream influences on storage and attenuation. (x) ranges between 0.5 (pure attenuation, with upstream influences only) to 0.0 (reservoir, with downstream influences only). Natural streams typically have an x of approximately 0.2. Muskingum

x values of 0.2 were used as the initial parameterization and were improved through optimization techniques in HEC-HMS.

Optimized parameters for each subbasin are shown in table 3.9 below. Again, parameterization was taken only far enough to produce reasonable results and is by no means optimal.

Table 3.9: Model Parameters for Upper Roanoke River Subwatersheds

Subbasin	Area (km ²)	Time of Concentration (t _c), hours	Reservoir Coefficient (R), hours	Spatially Averaged SCS CN
ROA_NIAGARA	263.791	12.0	8.35	68.15
ROA_WALNUT	269.124	5.1	6.4	67.21
CONFLUENCE	15.691	6.0	1.0	64.79
ROA_LAFAYETTE	95.093	8.0	1.6	68.50
SF_SHAWSVILLE	279.808	4.0	25.0	63.26
ROA_GLENVAR	58.046	6.0	2.41	66.90
TINKER	30.123	3.0	0.2	66.23
BACK_CRK	144.964	2.6	20.0	62.18
CARVIN	37.039	2.0	0.2	59.74
NF_IRONTO	288.804	4.5	26.0	66.72

Table 3.10 shows optimized parameters for each stream reach. Parameterization was taken only far enough to produce reasonable results and is by no means optimal. Travel times in the channel segments between the Niagara gage and the outlet and the Dundee gage and the outlet were too small to be modeled with the Muskingum method at a 1 hour time step. These channel segments were modeled as lag only with no attenuation.

Table 3.10: Model Parameters for Upper Roanoke River Channel Segments

Reach	Muskingum (k), hours	Muskingum (x), unitless
Ironto_Lafayette	0.8	0.3
Shawsville_Lafayette	0.8	0.3
Lafayette_Glenvar	2.0	0.2
Glenvar_Walnut	4.0	0.2
Walnut_Niagara	2.0	0.2
Carvin_JR330	2.0	0.2
Tinker_JR330	3.0	0.2
JR330_Niagara	3.0	0.2
Niagara_Outlet	Lag time = 20min	
Back_Crk_Outlet	Lag time = 20min	

3.8 Development of Similarly Parameterized, Spatially Lumped Model

In order to evaluate potential improvements in model performance under spatially distributed hydrologic characteristics, a similarly parameterized, spatially lumped model of the Upper Roanoke River Watershed was developed in HEC-HMS. The

lumped model uses the SCS CN method to calculate infiltration and rainfall excess, and uses the Clark Unit Hydrograph to route rainfall excess to the watershed outlet. SCS CN for each subwatershed is the areal mean CN calculated from the CN grid developed in section 3.6. Precipitation inputs are areally averaged at the subwatershed level from NEXRAD stage III archives.

3.8.1 Lumped SCS CN Rainfall Excess Calculation

The SCS CN method of rainfall excess determination in HEC HMS was used in the lumped runoff model of the Upper Roanoke River Watershed. The application of the SCS CN method in HEC-HMS, both in a distributed and lumped sense, is discussed in section 3.1.4 and is summarized here. The mathematics of the gridded and lumped SCS CN methods are similar and based on equations 2.3-2.6 described in section 2.7. The lumped representation of the SCS CN method uses constant values of 0.2 for initial abstraction ratio and 1.0 for potential retention scale factor. The lumped SCS rainfall excess calculation offers an option to specify percent imperviousness. The initial abstraction ratio and potential retention scale factor were kept constant at 0.2 and 1.0 respectively for all distributed subbasins and simulations. Because imperviousness is not explicitly accounted for in the gridded SCS CN method and is implied to be zero, percent imperviousness was kept at zero for all lumped subbasins and simulations. The only parameter that needed to be explicitly specified was the areal average curve number for each subbasin.

Areal average curve numbers for each subwatershed were calculated using the summarize zones function of Spatial Analyst. The 30 meter resolution grid of curve numbers created in section 3.6 was used along with a vector representation of the subwatershed discretization to calculate average CN for each subwatershed.

3.8.2 Clark Unit Hydrograph Surface Runoff Transformation

The surface runoff transformation used in the lumped representation of the Upper Roanoke River Watershed model was the Clark Unit Hydrograph. Application of the Clark UH method and the ModClark version in HEC-HMS are discussed in section 3.1.5 and are summarized here.

The Clark and ModClark methods account for the storage and attenuation properties of a watershed by lagging rainfall excess based on watershed travel time and routing rainfall excess through a linear reservoir. Required parameters for the Clark and ModClark methods are the time of concentration (t_c) and the reservoir coefficient (R), both with units of time. The times of concentration (t_c) and reservoir coefficients (R) developed by optimization for the distributed basin model were applied to the lumped basin model.

The lumped basin model used in HEC HMS is included in Appendix G.

3.8.3 Spatially Averaged Precipitation Inputs

Spatially averaged precipitation inputs were calculated for each subwatershed from the NEXRAD stage III archives. Averaging was done at the subwatershed level using a ZONALMEAN function in ARC/INFO GRID. ZONALMEAN records in each output cell the mean of the values of all cells in the value grid that belongs to the same zone as the output cell. Zones are identified by the values of the cells in the input zone grid. The zone grid is an integer grid that identifies the zone for each cell. The value grid is an integer or floating-point grid that defines the values of the cells in which the mean is to be calculated. The mean of the values of the value grid in each zone will be assigned to every cell in that zone on the output grid (ESRI, 2002). Figure 3.37 shows subwatershed averaged precipitation for March 19th 1998, 0200 UTC.

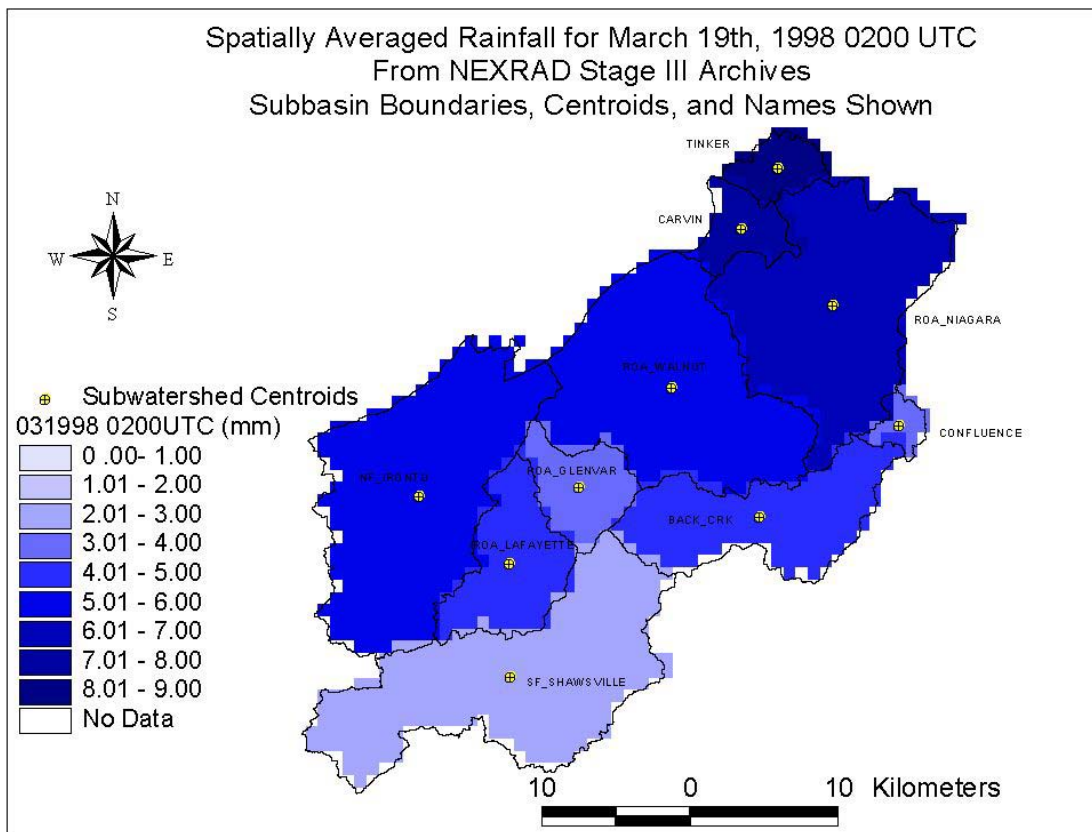


Figure 3.37: Subwatershed Average Precipitation for March 19th, 1998, 0200UTC.

Hyetographs of average subwatershed precipitation calculated by the ZONALMEAN function were created for each subwatershed by using the LATTICESPOT command and the point dataset of subwatershed centroids shown above. These hyetographs of average subwatershed precipitation were input as gages to HEC-HMS for use in the lumped modeling study.

3.9 Data Collection and Analysis Plans

This section describes the data collection and analysis plans to address the objectives of this research. A series of model runs were made at varied rainfall resolutions, grid scales, and antecedent moisture conditions to evaluate the sensitivity of the HEC-HMS runoff model to spatial variability, precipitation resolution, grid scale, and antecedent moisture condition. For each of the three storm events, at each subwatershed outlet, stream gage location, and at the overall watershed outlet, data was collected from the runoff model. For each storm event, data for all model runs were compared and evaluated against observed streamflow.

To analyze precipitation resolution, model runs were made with a 1km computational grid cell size and precipitation resolutions of 1km, 2km, 4km (original), 6km, 8km, and 10km.

For each subbasin, storm event and model run, the following data were collected and are shown in Appendix H:

- Modeled peak flow and time of peak,
- Observed peak flow and time of peak (where applicable),
- Modeled total precipitation,
- Modeled precipitation loss,
- Modeled precipitation excess,
- Modeled direct runoff volume,
- Modeled baseflow volume,
- Modeled discharge volume, and
- Observed discharge volume (where applicable).

For each stream gage with more than one contributing subwatershed, the following data were recorded:

- Modeled peak flow and time of peak,
- Modeled volume,
- Observed peak flow and time of peak, and
- Observed volume.

3.9.1 Sensitivity to Rainfall Resolution and Grid Scale

To investigate the sensitivity of the runoff model to precipitation resolution, a series of model runs were made in which all parameters and inputs were held constant excepting the precipitation input. Gridded precipitation input datasets at varied resolutions (1k, 2k, 4k, 6k, 8k, and 10k) and 1k grid cell size were created (as discussed in section 3.6.3) and used as model inputs. For each storm event, basin model, grid cell parameter file, and control specifications were held constant and the meteorological model varied. Model runs were made with a 1k gridded basin model and precipitation resolutions of 1k, 2k, 4k, 6k, 8k, and 10k for each of the three storm events (October 1997, March 1998, and April 1998).

To investigate model sensitivity to physical parameter resolution and computational grid scale, grid cell parameter files and precipitation inputs were varied for the March 1998 storm event. Grid cell parameter files developed at 400m, 500m, 1km, 2km, 4km, and 5km resolutions and computational cell sizes were used along with their corresponding bilinearly interpolated precipitation inputs.

3.9.2 Sensitivity to CN and AMC

To evaluate model sensitivity to Antecedent Moisture Condition (AMC) a series of model runs were made for the March 1998 and April 1998 storm events. A constant precipitation resolution of 4km and basin grid scale of 1km were used. Grid cell parameter files containing CNs calculated at AMC I, AMC II, and AMC III, were used for rainfall excess calculation.

3.9.3 Comparison of Lumped and Distributed Runoff Models

To compare the performance of the lumped and distributed runoff models, the same data described in section 3.9 above were collected for lumped model runs for each of the three storm events. These lumped model runs utilized the lumped basin model and precipitation inputs described in section 3.8.

4.0 Results

The overall objective of this research is to investigate the effects of precipitation resolution on model results. To accomplish this objective, the spatial and temporal registration of the gridded precipitation data is first verified against ground based gage data and a comparison is made of volume contained in precipitation datasets at varied resolutions. This comparison is made to quantify the variability that may be expected in model results due to variations in the input datasets. Observed streamflow hydrographs are compared with modeled runoff hydrographs at the base (4km) resolution to ensure that model parameterization is reasonable for an evaluation of grid scale and resolution effects. The effects of precipitation resolution and physical parameter grid scale on distributed model results are quantified. Finally, results from similarly parameterized lumped and distributed HEC-HMS models of the Upper Roanoke Watershed are compared.

4.1 Correlation of NEXRAD and IFLOWS Precipitation Data

A comparison was made between gridded precipitation records and precipitation gage records for each of the three storm events to check the spatial and temporal accuracy of the decoding and coordinate reprojection process. Precipitation hyetographs were extracted from the gridded precipitation records for each rain gage location by methods discussed in section 3.6.4. Hyetographs derived from the gridded precipitation records were correlated with the hyetographs available from the IFLOWS gage archives. As NEXRAD stage III data undergoes significant processing, including adjustment to ground based gages, the intent of this comparison was only to verify that precipitation grids were appropriately registered spatially and temporally. Spatial reprojection of the NEXRAD stage III archives from HRAP to SHG is discussed in section 3.6.3.

NEXRAD products are referenced to coordinated universal time (UTC). Radar records show the hourly precipitation depth accumulated in the hour prior to the time stamp. For example, rainfall occurring between 0000 UTC and 0100 UTC would be shown in the 0100 UTC grid. IFLOWS gage records are recorded in local time, either eastern standard time (EST) or eastern daylight time (EDT) depending upon the time of year. IFLOWS records also show the precipitation accumulated at a point in the hour previous to the time stamp on the record. Again, rainfall occurring between 0000 and 0100 would be contained in the 0100 record.

Daylight savings time is used in the study area between the first Sunday in April and the last Sunday in October. During daylight savings time, IFLOWS gage records are referenced to EDT. The remainder of the year, IFLOWS records are referenced to EST. Conversions between local time and universal time are:

$$\text{EST} = \text{UTC} - 500$$

$$\text{EDT} = \text{UTC} - 400$$

The above relations were used to temporally shift the IFLOWS gage data to UTC.

Plots and regression analysis were used to evaluate and quantify the correlation between radar and gage derived precipitation hyetographs. Plots containing radar and gage derived hyetographs for varied gages and storm events were created to visually evaluate the correlation between radar and gage data.

Figures 4.1 and 4.2 show sample hyetographs created for the March 1998 storm event for the Masons Cove (LID 1111) and Peters Creek (LID 1112) IFLOWS gages. Precipitation depths are in inches.

Hyetographs at various points throughout the watershed were developed from the Stage III data for each storm event. These hyetographs, included in appendix I, support the assumptions of spatially variable precipitation depths.

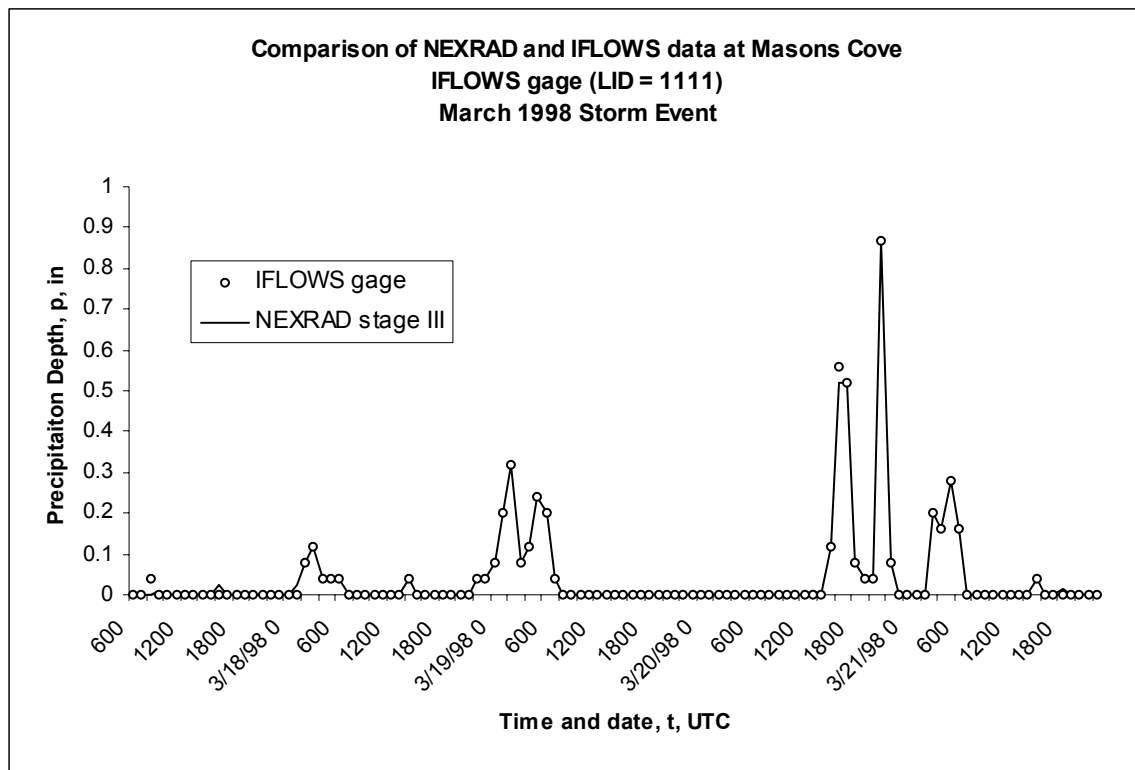


Figure 4.1: Comparison of NEXRAD and IFLOWS Data at Masons Cove IFLOWS gage (LID 1111)

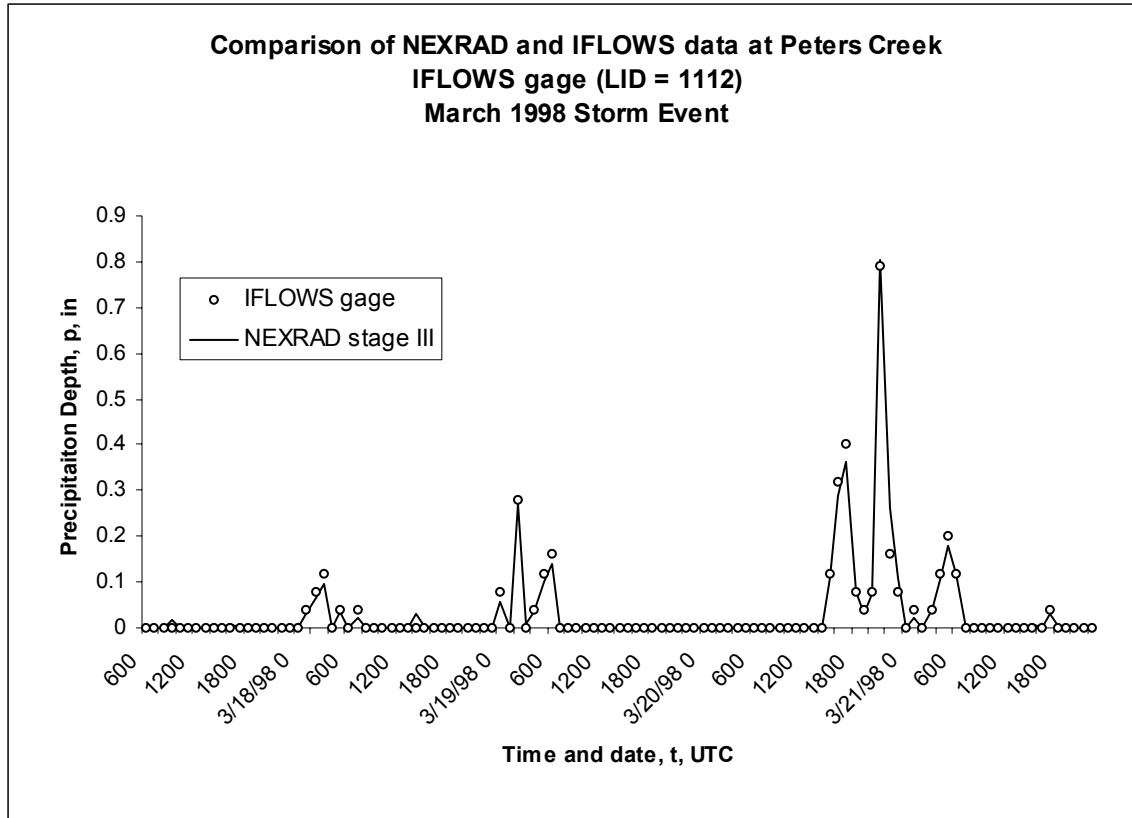


Figure 4.2: Comparison of NEXRAD and IFLOWS Data at Peters Creek IFLOWS gage (LID 1112)

A linear regression between gage and radar data was performed on the hyetographs for the 23 gages in and around the Upper Roanoke Watershed. This regression was performed for each storm event on records from all gage locations. Correlation coefficients, and the regression equation for each storm event is shown in table 4.1 below.

Table 4.1: Regression results on gage and radar data.

Storm Event	Correlation coefficient between radar and gage hyetographs	Linear regression results on radar vs. gage depths
October 1997	0.8705	Gage=0.949Radar+0.356mm
March 1998	0.9094	Gage=0.883Radar+0.102mm
April 1998	0.8974	Gage=1.062Radar+0.381mm

Offsetting the radar and gage hyetographs by one hour caused significant degradation of the correlation coefficient (from ~0.9 to ~0.3) implying accurate temporal registration of the precipitation grids used in the modeling study.

A comparison of radar and gage derived storm total precipitation for each of the three storm events quantifies the differences between radar and gage derived precipitation estimates. Table 4.2, 4.3, and 4.4 show radar and gage derived storm total precipitation for the October 1997, March 1998, and April 1998 storm events respectively. The locations exhibiting the largest residuals are: Lithia(1106), New Castle (1151), Daleville (1102), and Carvin Creek (1103). Lithia and New Castle are located near the edge of the gridded precipitation records and well outside of the Upper Roanoke Watershed boundary. The Daleville and Carvin Creek gages are located in an area in which terrain shielding by Poor Mountain causes significant systematic underestimation of precipitation by the Roanoke (KFCX) radar unit (see Figure 2.1).

Tables 4.2, 4.3, and 4.4 also provide evidence to support the assumption of spatial variable precipitation depths.

Table 4.2: Storm Total Precipitation for Radar – Gage Pairs, October 1997

Gage LID	Gage Name	IFLOWS (mm)	NEXRAD (mm)	Residual(mm)=(NEXRAD-IFLOWS)
1102	Daleville	28.4	10.6	-17.9
1103	Carvin Creek	18.3	9.1	-9.2
1105	Troutville	28.4	8.7	-19.8
1106	Lithia	56.9	23.1	-33.8
1111	Mason Cove	40.6	42.5	1.9
1112	Peters Creek	29.5	26.7	-2.8
1114	Sugarloaf Mtn.	30.5	31.9	1.4
1115	Witt's Orchard	28.4	30.7	2.3
1117	Fort Lewis Mtn	20.3	22.0	1.7
1119	Crawfords Ridge	35.6	33.1	-2.5
1120	Mill Mountain	30.5	32.0	1.5
1121	Tinker Creek S.	25.4	27.6	2.2
1122	Mason Creek	29.5	34.2	4.8
1123	Salem Pump Sta.	25.4	26.7	1.3
1124	Roa Sewer Plant	25.4	26.1	0.7
1126	Copper Hill	23.4	25.4	2.0
1127	Mountain View Ch	24.4	26.4	2.0
1133	Rose Hill	38.6	36.6	-2.0
1135	Blacksburg	44.7	41.7	-3.0
1136	Brush Mtn	58.9	52.0	-6.9
1140	Poor Mountain	33.5	34.7	1.2
1141	Ironto	63.0	62.6	-0.4
1151	New Castle	50.8	13.0	-37.8

Mean Residual = -4.93mm

Mean residual excluding Lithia (1106) and New Castle (1151) = -1.80mm

Table 4.3: Storm Total Precipitation for Radar – Gage Pairs, March 1998

Gage LID	Gage Name	IFLOWS (mm)	NEXRAD (mm)	Residual(mm)=(NEXRAD-IFLOWS)
1102	Daleville	55.9	61.2	5.3
1103	Carvin Creek	42.7	65.9	23.2
1105	Troutville	41.7	62.0	20.4
1106	Lithia	109.5	86.5	-23.0
1111	Mason Cove	124.7	124.8	0.0
1112	Peters Creek	93.2	90.8	-2.5
1114	Sugarloaf Mtn.	38.6	41.1	2.5
1115	Witt's Orchard	96.3	95.6	-0.6
1117	Fort Lewis Mtn	77.0	82.5	5.5
1119	Crawfords Ridge	102.4	102.5	0.2
1120	Mill Mountain	97.5	99.1	1.6
1121	Tinker Creek S.	80.3	81.6	1.3
1122	Mason Creek	100.3	108.2	7.9
1123	Salem Pump Sta.	87.1	91.2	4.1
1124	Roa Sewer Plant	78.2	80.3	2.1
1126	Copper Hill	90.2	88.3	-1.9
1127	Mountain View Ch	78.2	80.0	1.7
1133	Rose Hill	86.4	89.0	2.6
1135	Blacksburg	100.6	103.4	2.9
1136	Brush Mtn	120.7	122.0	1.3
1140	Poor Mountain	89.2	90.4	1.3
1141	Ironto	62.0	67.2	5.3
1151	New Castle	102.6	85.8	-16.8

Mean residual = 1.93mm

Mean residual excluding Lithia (1106) and New Castle (1151) = 3.66mm

Table 4.4: Storm Total Precipitation for Radar – Gage Pairs, April 1998

Gage LID	Gage Name	IFLOWS (mm)	NEXRAD (mm)	Residual(mm)=(NEXRAD-IFLOWS)
1102	Daleville	72.1	12.4	-59.7
1103	Carvin Creek	73.2	12.0	-61.2
1105	Troutville	47.8	22.5	-25.2
1106	Lithia	141.2	65.9	-75.3
1111	Mason Cove	80.3	73.4	-6.8
1112	Peters Creek	65.0	61.0	-4.0
1114	Sugarloaf Mtn.	57.9	59.9	2.0
1115	Witt's Orchard	70.1	67.4	-2.7
1117	Fort Lewis Mtn	64.0	62.1	-1.9
1119	Crawfords Ridge	82.3	76.0	-6.3
1120	Mill Mountain	77.2	75.3	-1.9
1121	Tinker Creek S.	59.9	57.1	-2.8
1122	Mason Creek	75.2	72.4	-2.8
1123	Salem Pump Sta.	15.2	52.3	37.1
1124	Roa Sewer Plant	67.1	68.4	1.3
1126	Copper Hill	62.0	60.2	-1.8
1127	Mountain View Ch	62.0	62.4	0.5
1133	Rose Hill	91.4	87.0	-4.4
1135	Blacksburg	73.2	73.0	-0.2
1136	Brush Mtn	89.4	87.4	-2.0
1140	Poor Mountain	68.1	67.6	-0.4
1141	Ironto	71.1	71.5	0.4
1151	New Castle	106.7	48.2	-58.4

Mean residual = -12.04mm

Mean Residual excluding Lithia (1106), New Castle (1151), Daleville (1102) or Carvin Creek (1103) = -0.97mm

4.2 Comparison of Precipitation Resolutions

When the resolution of precipitation data is made coarser by upscaling, peak rainfall intensities are typically reduced, minimum intensities are typically increased, and the range of values is consequently reduced. After upscaling, precipitation is also located less precisely with respect to basin boundaries. To ensure that the effects of these changes are isolated, one must ensure that the overall volume of rainfall contained in each grid is not significantly changed by the rescaling process. This section shows the results of a comparison of precipitation datasets at varied resolutions. This comparison was made to quantify the variability that may be expected in model results due to variations in overall volume contained in the input precipitation datasets.

4.2.1 Storm Total Statistics for 1km to 10km Precipitation Resolution at 1km Cell Size

For a gridded precipitation estimate, the mean value of the grid is proportional to the volume of precipitation contained in the grid. A comparison of mean grid value is analogous to a comparison of precipitation volume for precipitation grids of equal extents. Gridded storm total precipitation depths for each of the three storm events and six resolutions were created in ARC/INFO GRID by raster algebra. Summary statistics for each storm total grid were calculated including maximum, minimum, mean, and standard deviation. Table 4.5, 4.6, and 4.7 show the summary statistics for the storm total grids for the October 1997, March 1998, and April 1998 storm events respectively. In review, the 4km resolution is the original resolution of the NEXRAD stage III archives. Precipitation grids were upscaled or aggregated to 6km, 8km, and 10km resolutions and downscaled or smoothed to 2km and 1km resolutions.

The summary statistics indicate that during upscaling, the minimum grid value is increased, the maximum grid value is decreased, and consequently the range of grid values is reduced as well. During downscaling (smoothing) the same effects occur, but to a much smaller extent.

Table 4.5: Storm total summary statistics for October 1997 Event

October 1997 all values in mm				
Resolution (m)	Mean	Min	Max	σ
1000	19.79	0.95	60.18	9.18
2000	19.80	1.14	56.32	9.17
Original data 4000	19.81	0.32	62.56	9.59
6000	19.76	1.23	45.90	9.06
8000	19.72	2.19	39.23	8.96
10000	19.84	3.06	45.98	9.38

σ = standard deviation

Table 4.6: Storm total summary statistics for March 1998 Event

March 1998 all values in mm				
Resolution (m)	Mean	Min	Max	σ
1000	78.06	33.44	131.36	21.57
2000	78.07	35.66	129.81	21.57
Original data 4000	78.11	27.31	132.04	22.30
6000	77.97	26.33	126.61	21.63
8000	77.81	27.45	125.70	21.99
10000	77.27	29.99	125.69	21.57

σ = standard deviation

Table 4.7: Storm total summary statistics for April 1998 Event

April 1998 all values in mm				
Resolution (m)	Mean	Min	Max	σ
1000	64.43	14.52	117.10	13.30
2000	64.44	15.25	116.58	13.30
Original data 4000	64.43	13.43	119.33	14.20
6000	64.36	18.73	108.80	13.44
8000	64.33	15.50	105.25	13.43
10000	64.45	25.58	108.72	13.66

σ = standard deviation

Table 4.8 quantifies the changes in precipitation volume that occur with changes in precipitation resolution. The largest change that occurred was for the March 1998 storm event when upscaling from 4km to 10km resolution.

The percent changes in volume occurring during smoothing of the precipitation grids to finer resolutions is less than one tenth of one percent for all storm events studied. This implies that smoothing of gridded precipitation data by bilinear interpolation is appropriate for distributed modeling where precipitation resolution is greater than computational cell size. Percent changes encountered during upscaling (aggregation) are less than one half of one percent excepting the case of the March 1998 storm event at 10km resolution. Bilinear interpolation calculates the new cell value based on the cell values in the four nearest cells of the input grid. As more than four 4km cells fit into each 10km cell, it is likely that the values from some of the 4km cells are not used in the upscaling process. Upscaling of gridded precipitation data by bilinear interpolation to a resolution greater than 2x the original resolution is therefore not recommended.

Table 4.8: Percent Changes in Storm Total Precipitation Volume with Changes in Resolution

	Oct_97		Mar_98		Apr_98	
Resolution (m)	Mean (mm)	$\Delta\%$ from 4k	Mean (mm)	$\Delta\%$ from 4k	Mean (mm)	$\Delta\%$ from 4k
1000	19.79	-0.08	78.06	-0.06	64.43	0.01
2000	19.80	-0.07	78.07	-0.05	64.44	0.02
4000	19.81	0.00	78.11	0.00	64.43	0.00
6000	19.76	-0.28	77.97	-0.17	64.36	-0.11
8000	19.72	-0.44	77.81	-0.38	64.33	-0.15
10000	19.84	0.15	77.27	-1.07	64.45	0.04
Maximum % change	0.59		1.07		0.19	
Maximum % greater than 4k	0.15		0.00		0.04	
Maximum % less than 4k	-0.44		-1.07		-0.15	

4.2.2 Visualization of Varied Precipitation Resolutions

To help visualize the effects of changing precipitation resolution, three dimensional renderings of gridded precipitation depths for March 19th, 1998 0200UTC were created at the base (4km), 1km, and 10km resolutions. These renderings are shown in figures 4.3, 4.4, and 4.5. The area shown is a bounding box around the Upper Roanoke Watershed 80km by 80km. The view is looking northeast. As precipitation depths are in mm and grid size is on the order of km, a vertical exaggeration of 1000 is used for these figures.

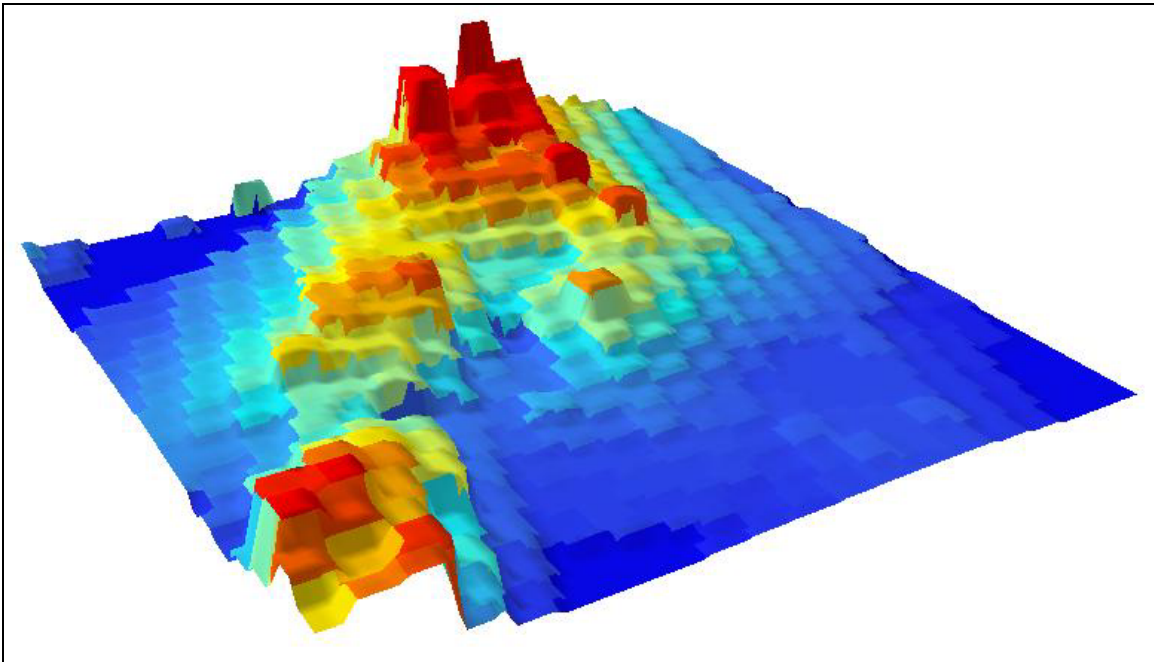


Figure 4.3: Rendering of Gridded Precipitation Depth for March 19th, 1998 0200UTC 4km (base) Resolution.

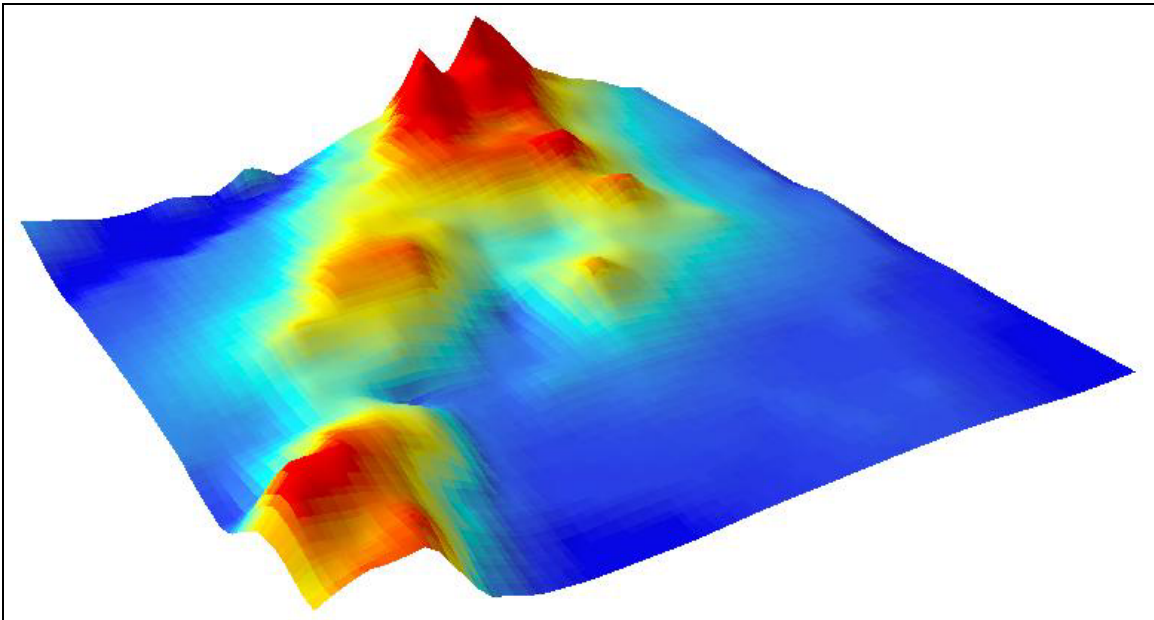


Figure 4.4: Rendering of Gridded Precipitation Depth for March 19th, 1998 0200UTC 1km (smoothed) Resolution.

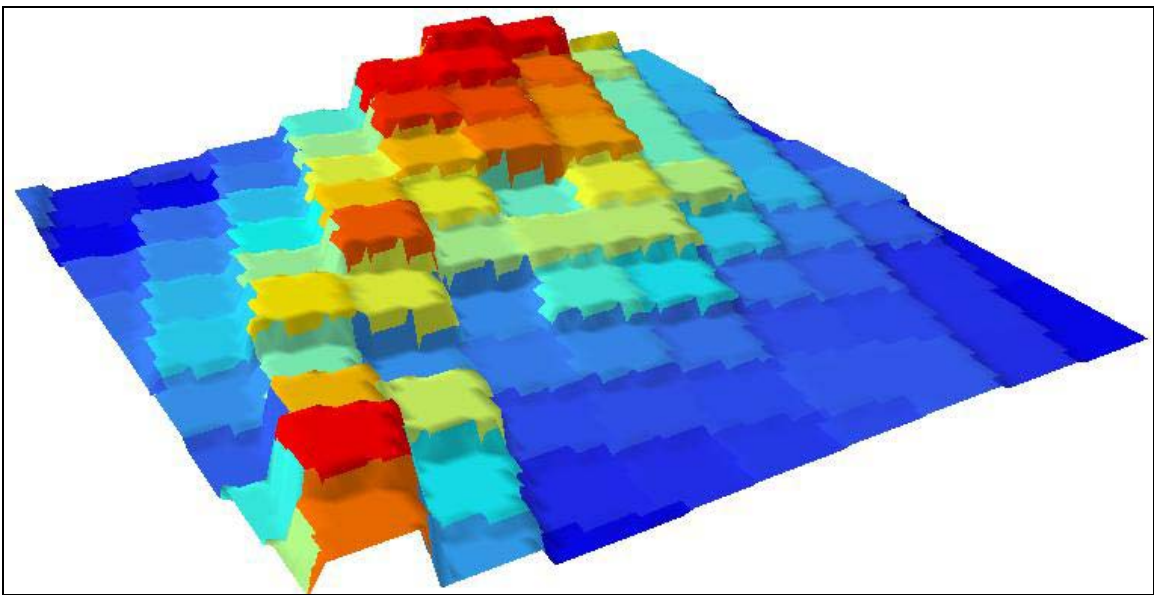


Figure 4.5: Rendering of Gridded Precipitation Depth for March 19th, 1998 0200UTC 10km (degraded) Resolution.

4.2.3 Storm Total Statistics for 400m to 5km Precipitation Resolution and Cell Size

Table 4.9 shows the mean grid value for storm total precipitation grids created by bilinear interpolation from the original 4km HRAP data to SHG at cell sizes and resolution of 400m – 5km. These datasets were created for the sensitivity analysis on computational grid cell size. When bilinearly interpolating to a grid cell size and resolution smaller than the resolution of the original dataset, mean grid value and precipitation volume do not significantly change. When bilinearly interpolating to coarser resolution, especially when final resolution is greater than 2x the original resolution, more significant changes in precipitation volume occur.

Table 4.9: Storm Total Summary Statistics for Bilinearly Interpolated Precipitation Data

Bilinear Interpolation Resolution and cell size (m)	Oct_97 Mean	Mar_98 Mean	Apr_98 Mean
400	19.79	84.27	64.43
500	19.79	84.27	64.43
1000	19.79	84.28	64.43
2000	19.80	84.29	64.44
4000	19.90	85.21	64.74
5000	19.86	84.47	64.49

4.3 Model Results at Base (4km) Precipitation Resolution

This section shows a comparison between observed and modeled streamflow for each storm event at the most downstream stream gage point with observed data. Modeled results are driven by gridded precipitation at the original, 4km, resolution. A distributed basin model with the 10 subwatershed discretization discussed in section 3.6.2.1 and a 1km computational cell size as shown in figure 3.31 were used. Modeled hydrographs are compared with observed streamflow to ensure that model specification and parameterization are reasonable for the proposed sensitivity analysis on precipitation resolution and grid scale. Hydrograph shapes are evaluated visually, and summary values of modeled peak flow, time to peak, and overall runoff volume are quantitatively compared with observed values. Model results and observed data are included in Appendix H.

Subwatershed times of concentration and linear reservoir coefficients were improved beyond the initial a priori estimates using parameter optimization techniques in HEC-HMS. The key parameters which govern hydrograph shape, time to peak, and peak flow are the time of concentration and the reservoir coefficient. To effectively optimize these parameters, the volume of the observed hydrograph and the modeled hydrograph should be approximately equal. For the gridded SCS CN method, choice of CN and AMC govern modeled runoff volume. The March 1998 storm event, modeled at an AMC III, exhibited modeled streamflow closest to observed results and was used for the majority of the optimization runs. Modeled hydrograph accuracy is best for the March 1998 event. Though accuracy could be improved through further refinement of model parameters,

parameterization was found to be reasonable for the sensitivity analysis to gridded precipitation resolution and computational cell size.

4.3.1 Evaluation of October 1997 Storm Event

The October 1997 storm event was modeled at an AMC II (see section 3.7.2.1 for storm event AMC selection). Overall runoff volume at the Walnut street gage (the most downstream gage with available data) was $1.40 \times 10^6 \text{ m}^3$ modeled and $1.20 \times 10^6 \text{ m}^3$ observed. Overall modeled total runoff volume (including baseflow) was $2.00 \times 10^6 \text{ m}^3$ at the confluence of Back Creek and the Roanoke River. Gage data for the Niagara gage was not available for the October 1997 storm event. The October 1997 storm event caused a very small amount of runoff. Subbasin storm total precipitation ranged between 9mm – 35mm and modeled subbasin precipitation excess depths were between 0mm-2mm. A peak flowrate of 12.25 cms was modeled at the watershed outlet. Peak flowrates of 9.2cms (modeled) and 5.6cms (observed) occurred at the Walnut street gage. Time to peak was in disagreement by 17 hours.

As can be observed from Figure 4.6 hydrograph fit could be improved. Inaccuracy in modeled data is primarily a result of the small amount of rainfall excess occurring during this storm event.

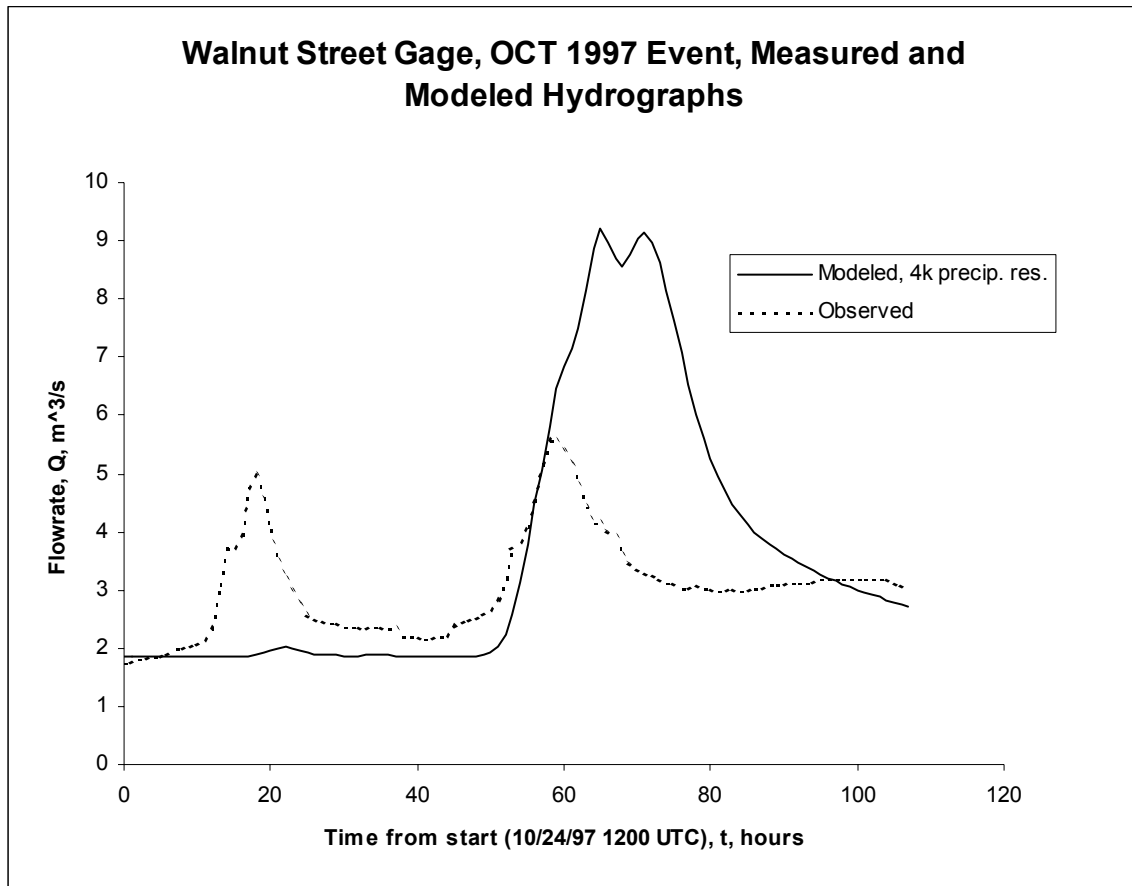


Figure 4.6: Measured and Modeled Hydrographs at Walnut Street Gage, October 1997

4.3.2 Evaluation of March 1998 Storm Event

The March 1998 storm event was modeled at an AMC III. Observed and modeled runoff volume were in good agreement. Overall runoff volume at the Niagara gage (the most downstream gage with available data) was $57.2 \times 10^6 \text{ m}^3$ modeled and $61.7 \times 10^6 \text{ m}^3$ observed. Overall total modeled runoff volume (including baseflow) was $63.6 \times 10^6 \text{ m}^3$ at the watershed outlet. The March 1998 storm event caused a moderate amount of runoff. Subbasin storm total precipitation ranged between 62mm – 97mm and modeled subwatershed precipitation excess depths were between 24mm - 54mm. A peak flowrate of 529cms was modeled at the watershed outlet. Peak flowrates of 483cms (modeled) and 521cms (observed) occurred at the Niagara gage. Time to peak at the Niagara gage was in disagreement by 4 hours. This value is somewhat misleading considering the double peaked shape of the hydrographs shown in figure 4.7. Figure 4.7 shows that the gridded SCS CN method and ModClark runoff transformation produce reasonable results when adequate data is available to define model parameters.

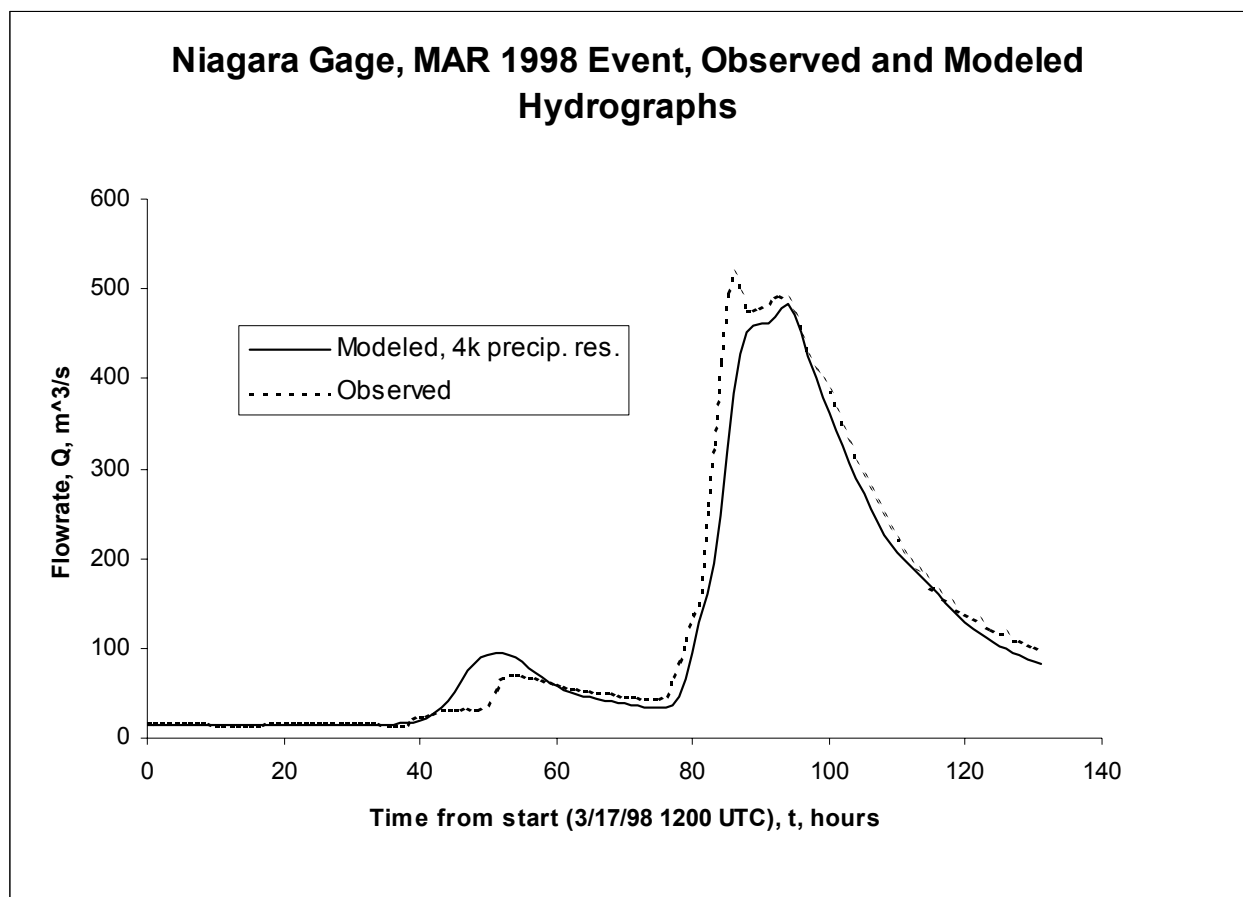


Figure 4.7: Measured and Modeled Hydrographs at Niagara Gage, March 1998

4.3.3 Evaluation of April 1998 Storm Event

The April 1998 storm event was modeled at an AMC III. Overall runoff volume at the Niagara gage (the most downstream gage with available data) was $37.9 \times 10^6 \text{ m}^3$ modeled

and $36.9 \times 10^6 \text{ m}^3$ observed. Overall total modeled runoff volume (including baseflow) was $42.0 \times 10^6 \text{ m}^3$ at the watershed outlet. The April 1998 storm event caused a moderate amount of runoff. Subbasin storm total precipitation ranged between 20mm – 69mm and modeled subwatershed precipitation excess values were between 3mm-31mm. A peak flowrate of 349cms was modeled at the watershed outlet. Peak flowrates of 326cms (modeled) and 222cms (observed) occurred at the Niagara gage. Time to peak was in agreement within the precision offered by the model time step. Figure 4.8 shows observed and modeled hydrographs for the April 1998 storm event at the Niagara gage. Accuracy of peak flow could be improved by further refinement of model parameters.

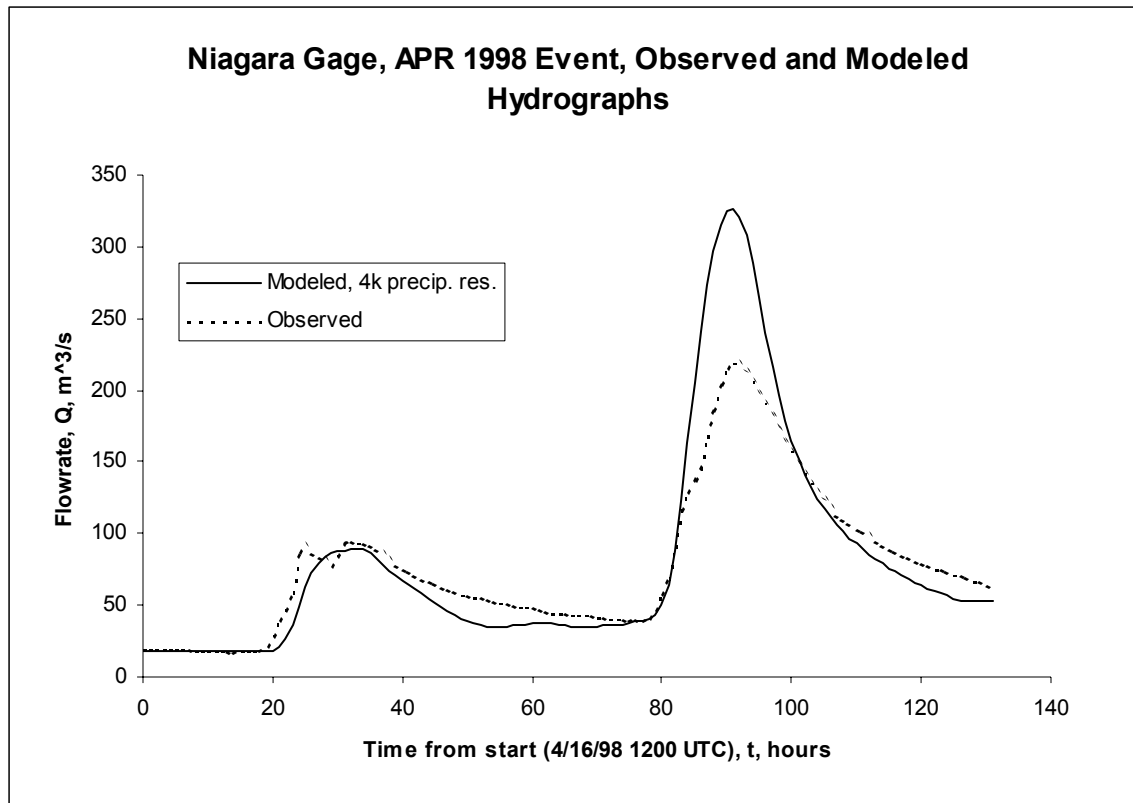


Figure 4.8: Observed and Modeled Hydrographs at Niagara Gage, April 1998

4.4 Model sensitivity to CN / AMC

This section discusses sensitivity of modeled peak flow, modeled time to peak, and most importantly, modeled runoff volume to the choice of CN and AMC values. The HEC-HMS gridded SCS CN rainfall excess calculation was found to be extremely sensitive to the choice of curve number and antecedent moisture condition. Optimal CNs and AMC were found to vary between storms and between subwatersheds during individual storms. The between-watershed variation may be due to fundamental differences in soil and landcover and may be improved by refining CN estimates based on NLCD and SSURGO. Between-watershed variation may also be due to spatial variability in antecedent conditions. Antecedent moisture condition is lumped at the watershed level in

this model. Storm to storm variation of rainfall excess is expected, but cannot necessarily be optimized when the modeler is limited to curve numbers at AMC I, AMC II, or AMC III. AMC conditions between I and II and II and III of 1.5 and 2.5 were created to better evaluate the effects of AMC on modeled runoff volume. CNs at AMC 1.5, 2.5 for each soil and land use combination were calculated by averaging the appropriate CN at AMC I and AMC II and AMC II and AMC III respectively.

Figure 4.9 shows the variation in modeled runoff hydrographs with changes in AMC at the Walnut street gage for the October 1997 storm event. The disagreement between the modeled hydrograph at AMC II (the optimum AMC for the October 1997 storm event) and the observed hydrograph is seen to be small relative to the differences in hydrographs at varied AMC.

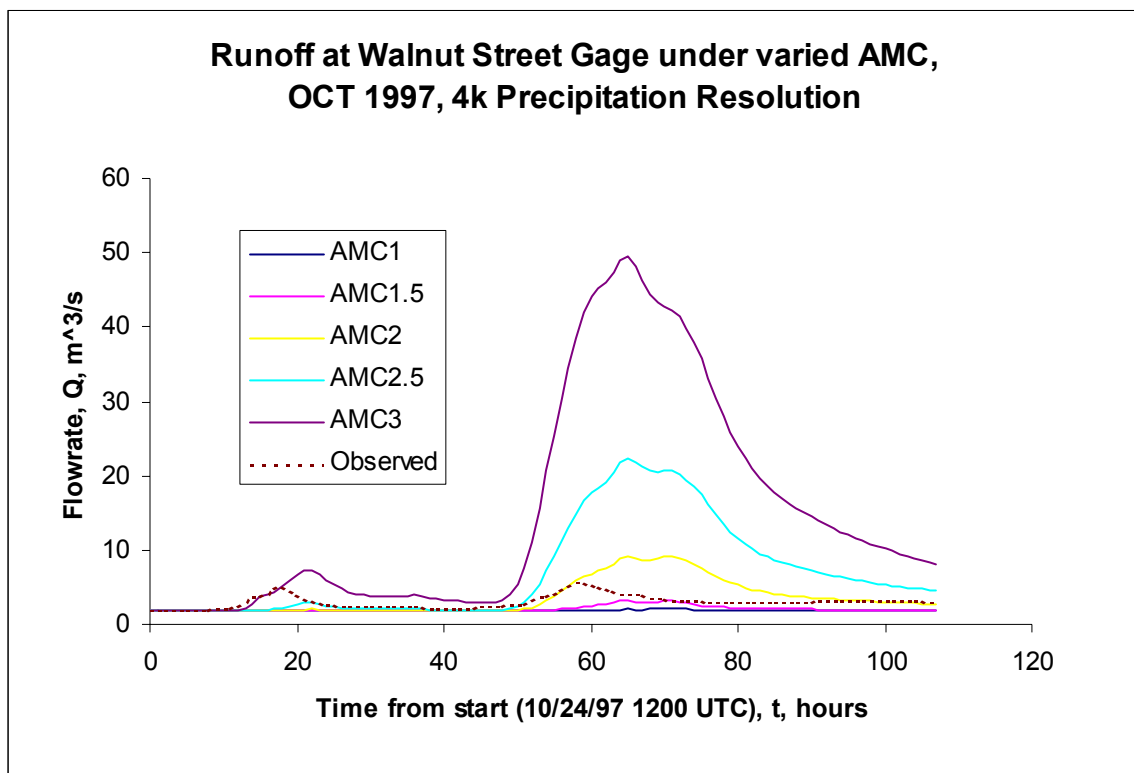


Figure 4.9: Hydrographs at the Walnut Street Gage under varied AMC, October 1997

Figures 4.10 and 4.11 below show modeled hydrograph sensitivity to AMC for the March 1998 storm event at the Walnut Street and Niagara gages respectively.

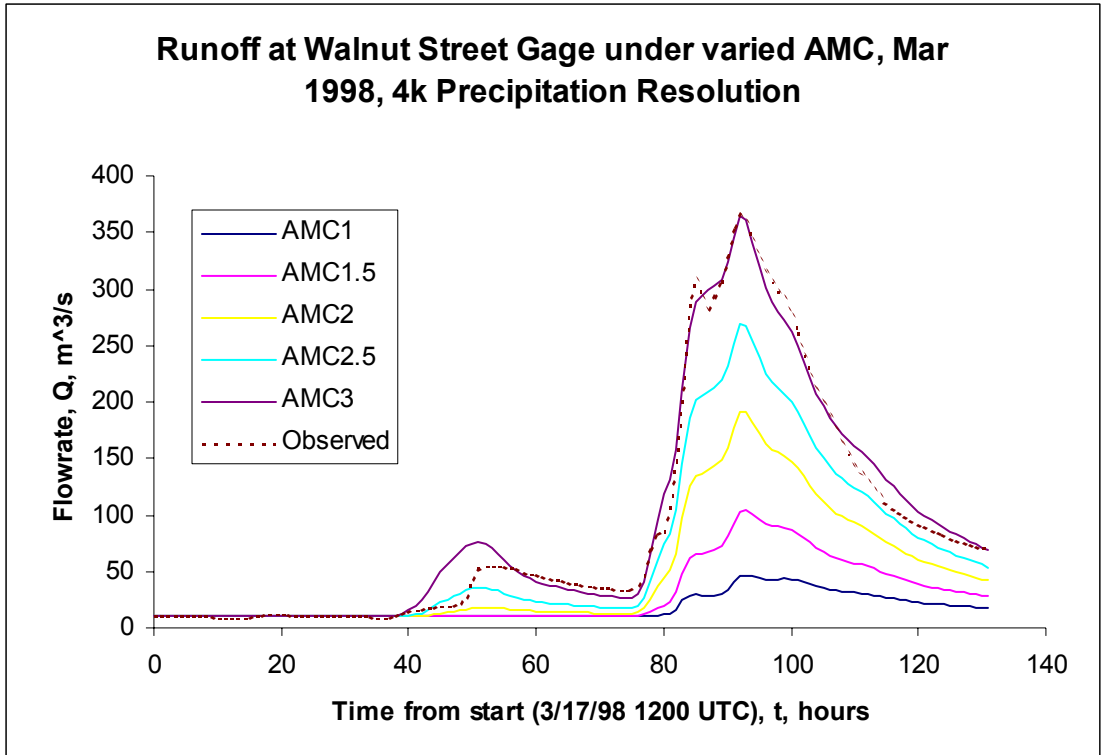


Figure 4.10: Hydrographs at the Walnut Street Gage under varied AMC, March 1998

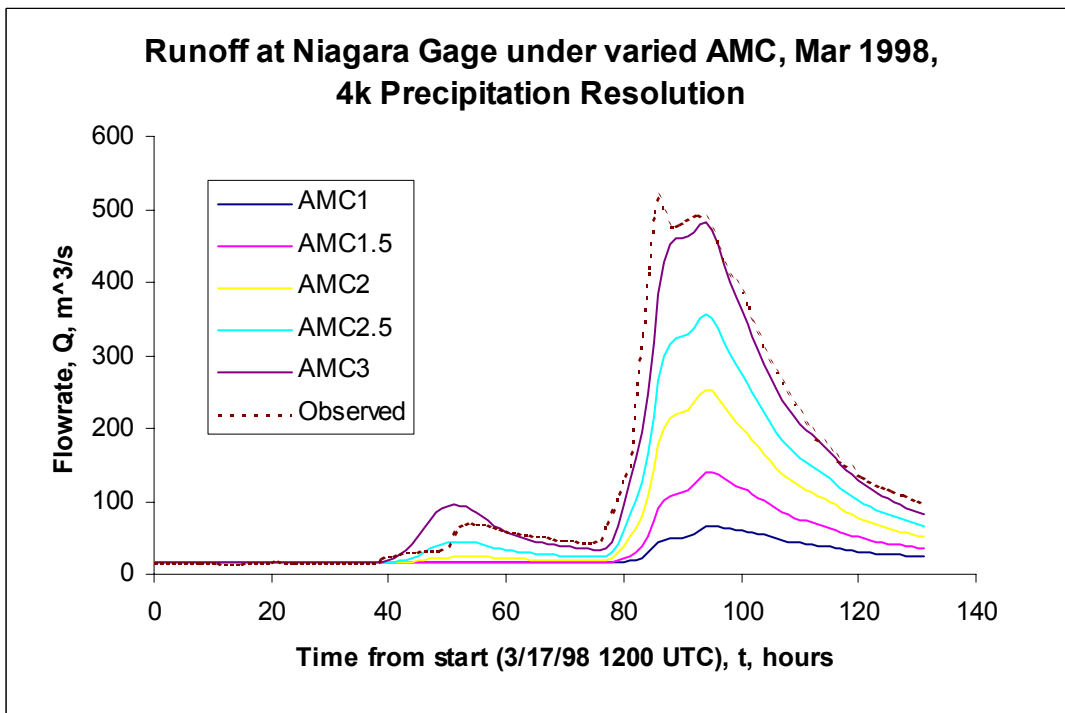


Figure 4.11: Hydrographs at the Niagara Gage under varied AMC, March 1998

Figure 4.12 and 4.13 below show modeled hydrograph sensitivity to AMC for the April 1998 storm event at the Walnut Street and Niagara gages respectively. Though accuracy of peak flowrate is improved through changes in AMC, overall runoff volume is best modeled at an AMC III for the April 1998 event.

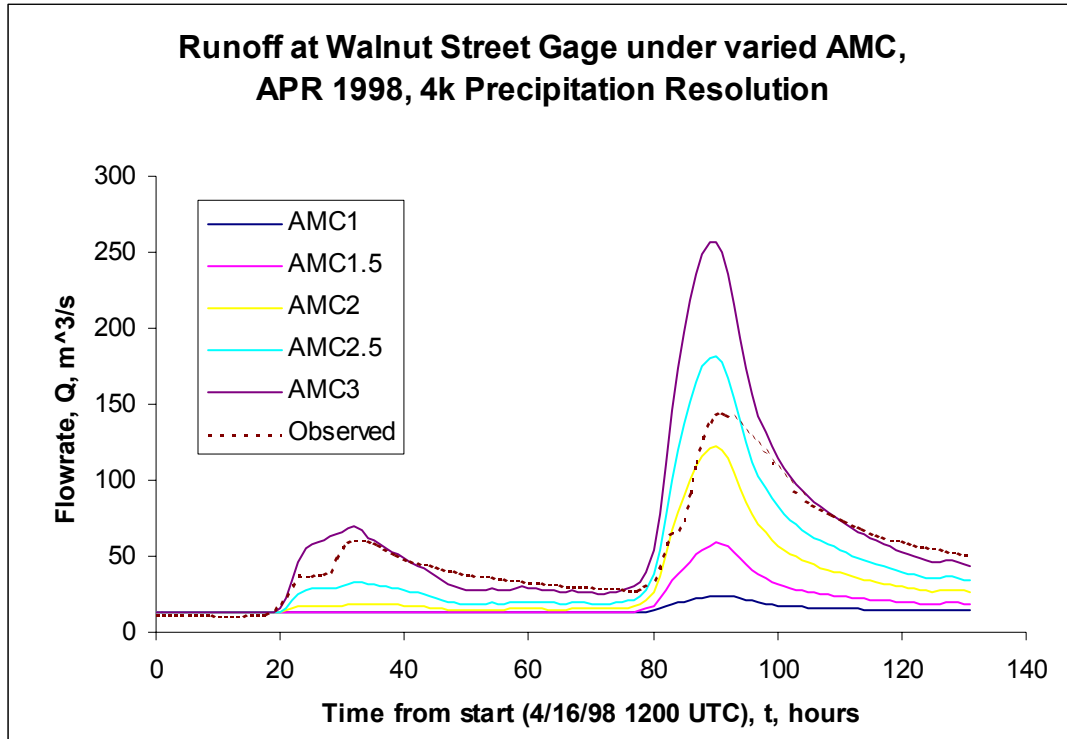


Figure 4.12: Hydrographs at the Walnut Street Gage under varied AMC, April 1998

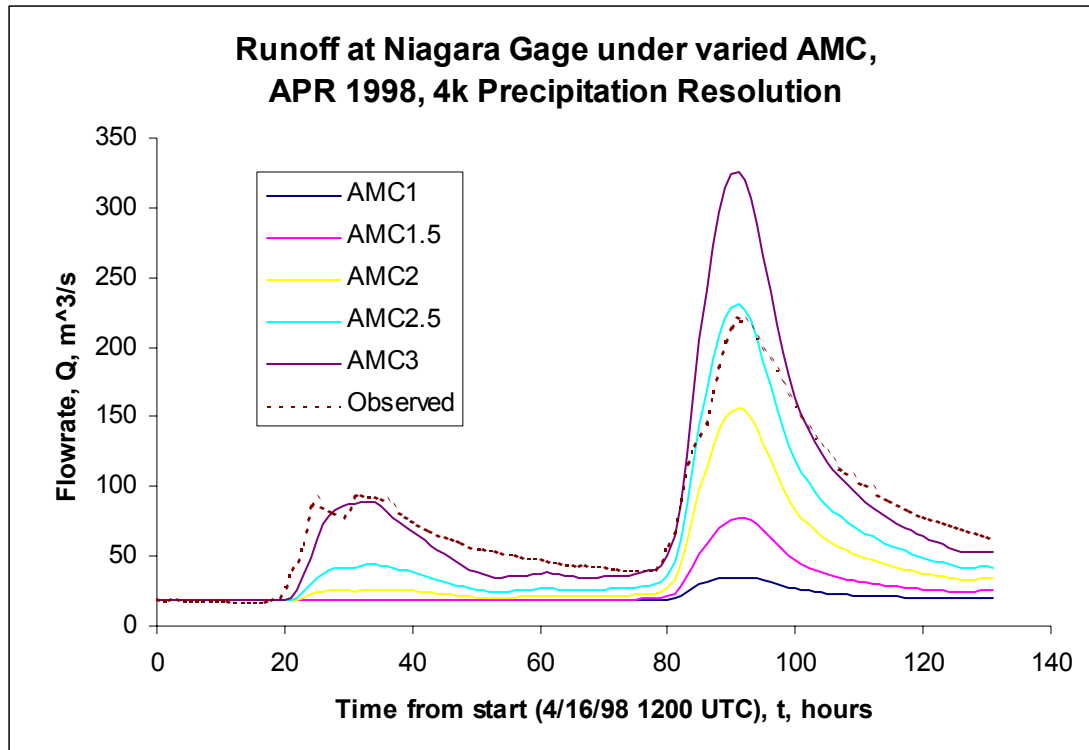


Figure 4.13: Hydrographs at the Niagara Gage under varied AMC, April 1998

Rainfall excess calculated by the HEC-HMS gridded SCS CN method was found to be extremely sensitive to choice of antecedent moisture condition. Changes in AMC are represented in this model by changes in CN for each land use and soil type combination. The model is extremely sensitive, therefore, to the CN values selected for each combination of NLCD and SSURGO data shown in table 3.6. Differences between hydrographs of observed and modeled streamflow at optimum AMC were found to be small relative to differences between modeled streamflow hydrographs at varied AMC.

Tables 4.10, 4.11, and 4.12 show peak flow, time to peak, and runoff volume at the confluence of Back Creek and the Roanoke River for each AMC and storm event combination.

Table 4.10: Hydrograph characteristics at watershed outlet, October 1997 event

Location: Watershed Outlet			
Event: October 1997			
AMC	Peak Flow	Time of Peak	Volume
	cms	mm/dd/yy hhhh	10^3 m^3
1	3.2	10/27/97 1300	1153
1.5	4.6	10/27/97 700	1261
2	12.2	10/27/97 800	2003
2.5	28.2	10/27/97 700	3663
3	65.0	10/27/97 700	7678

Table 4.11: Hydrograph characteristics at watershed outlet, March 1998 event

Location: Watershed Outlet			
Event: March 1998			
AMC	Peak Flow	Time of Peak	Volume
	cms	mm/dd/yy hhhh	10 ³ m ³
1	70.0	03/21/98 1100	13519
1.5	149	03/21/98 1100	20985
2	272	03/21/98 1000	33403
2.5	386	03/21/98 1000	45930
3	529	03/21/98 1000	63550

Table 4.12: Hydrograph characteristics at watershed outlet, April 1998 event

Location: Watershed Outlet			
Event: April 1998			
AMC	Peak Flow	Time of Peak	Volume
	cms	mm/dd/yy hhhh	10 ³ m ³
1	37.5	4/20/98 700	10951
1.5	81.6	4/20/98 800	14238
2	165	4/20/98 700	21278
2.5	245	4/20/98 700	29360
3	349	4/20/98 700	41998

4.5 Effects of Precipitation Resolution on Model Results

A sensitivity analysis was performed on the HEC-HMS distributed runoff model of the Upper Roanoke Watershed to quantify the effects of gridded precipitation resolution on model outputs. This section shows results from model runs made for each of the three storm events driven by precipitation resolutions of 1km, 2km, 4km, 6km, 8km, and 10km. The expected effects of varied precipitation resolution on peak flow, time to peak, and runoff volume were observed. No significant changes in hydrograph shape were observed with changes in precipitation resolution. Model sensitivity to precipitation resolution was found to be small compared to sensitivity to curve number and antecedent moisture condition.

As precipitation resolution was made coarser from the 4km (base) resolution, peak flowrates decreased, times to peak increased, and runoff volumes decreased. The effects of watershed smearing, or less precise location of precipitation with respect to basin boundaries, was observed as precipitation resolution was degraded. The effects of watershed smearing are more significant for smaller subwatersheds.

As precipitation grids were smoothed to a smaller cell size by bilinear interpolation, peak flowrates and runoff volumes decreased. These decreases in peak flowrate were smaller than the decreases caused by upscaling or degradation of precipitation resolution especially when changes in input volume of precipitation are accounted for. Changes in precipitation volume input and runoff volume output between 1km and 2km resolutions were insignificant.

As discussed in section 4.2, the decreases in precipitation input volume with changes in resolution are on the order of 0.50% during upscaling and on the order of 0.10% during smoothing (see table 4.8). Percent changes in runoff volume with changes in precipitation resolution are larger in magnitude than changes in precipitation volume input but follow the same patterns.

4.5.1 Effects of Precipitation Resolution on Runoff Volume

As precipitation resolution was made coarser from the 4km (base) resolution, runoff volumes typically decreased. As precipitation grids were smoothed to a smaller cell size by bilinear interpolation, runoff volumes also decreased, but by a smaller amount. Changes in runoff volume resulting from changes in precipitation resolution were small compared to changes in runoff volume resulting from choice of CN or AMC and compared to the differences between modeled and observed streamflow. Changes in runoff volume between the 1km and 2km precipitation resolutions were insignificant compared to the change in runoff volume caused by smoothing precipitation resolution from 4km to 2km or 4km to 1km. Table 4.13 shows runoff volumes and the percent changes above or below the base resolution (4km) for all three storm events modeled. Percent changes in runoff volume are on the order of 0.5% when using downscaled (smoothed) precipitation and on the order of 1% when using upscaled (degraded) precipitation for the March and April 1998 storm events. Percent changes are on the order of 5-10% for the October 1997 storm event. Percent changes of runoff volume with resolution were found to decrease as overall runoff volume increased.

Table 4.13: Effects of Precipitation Resolution on Runoff Volume

Resolution (m)	Oct_97		Mar_98		Apr_98	
	Volume (10 ³ m ³)	Δ% from 4k	Volume (10 ³ m ³)	Δ% from 4k	Volume (10 ³ m ³)	Δ% from 4k
1000	1895	-5.38	63297	-0.40	41689	-0.74
2000	1893	-5.46	63312	-0.37	41683	-0.75
4000	2003	0.00	63550	0.00	41998	0.00
6000	1846	-7.81	63325	-0.35	41552	-1.06
8000	1795	-10.37	62984	-0.89	41374	-1.49
10000	1929	-3.69	62489	-1.67	41717	-0.67
Maximum % greater than 4k	0.00		0.00		0.00	
Maximum % less than 4k	-10.37		-1.67		-1.49	

4.5.2 Effects of Precipitation Resolution on the Runoff to Rainfall Ratio

A portion of the variation in runoff volume with changes in precipitation resolution may be explained by variation in precipitation input volume. As discussed in section 4.2 the changes in precipitation input volume with changes in resolution are typically on the order of 0.50% during upscaling and on the order of 0.10% during smoothing (see table 4.8). Percent changes in runoff volume with changes in precipitation resolution are larger in magnitude than changes in precipitation input volume but are qualitatively similar. Figures 4.14-4.17 show mean storm total precipitation depths from the gridded records at varying resolutions. Figure 4.14 shows the mean storm total precipitation for each storm event at all resolutions. Figures 4.15, 4.16, and 4.17 show variation in mean storm total precipitation with precipitation resolution for the October 1997, March 1998 and April 1998 storm events respectively. A significantly enlarged scale is used on the ordinate axis of figures 4.15, 4.16, and 4.17 to show that, though small in magnitude, the anticipated trends in model results with precipitation resolution exist. These plots are shown so that trends in runoff volume with precipitation resolution may be compared to trends in precipitation volume and rainfall runoff ratio with precipitation resolution.

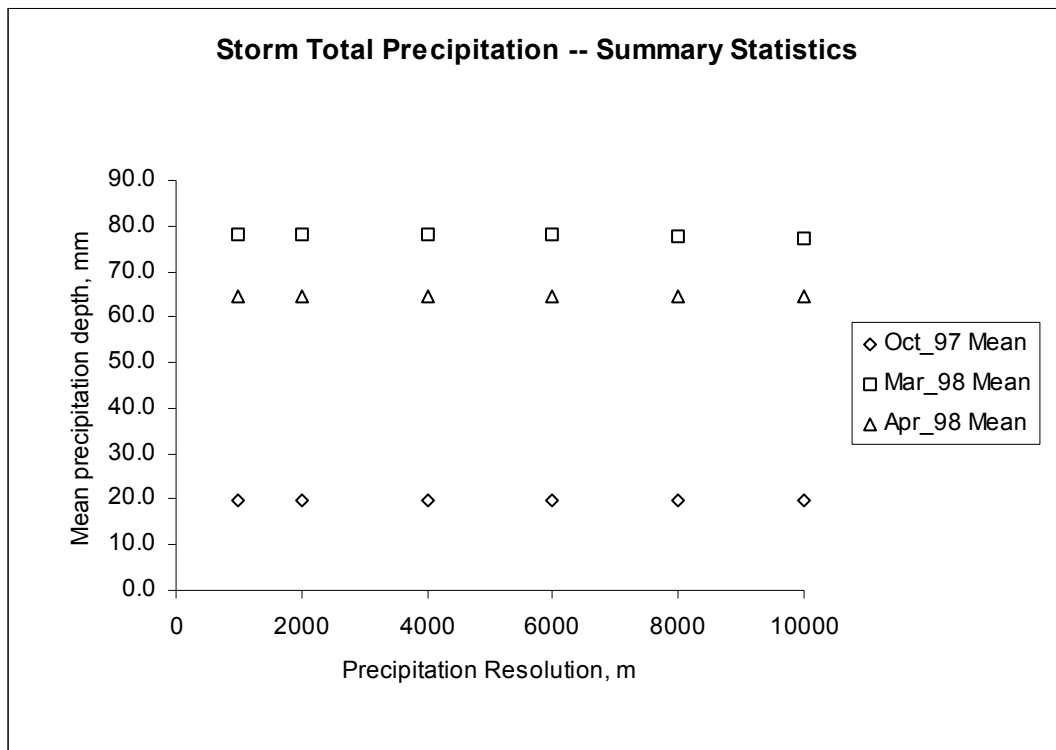


Figure 4.14: Storm Total Precipitation Depths at Varied Precipitation Resolutions

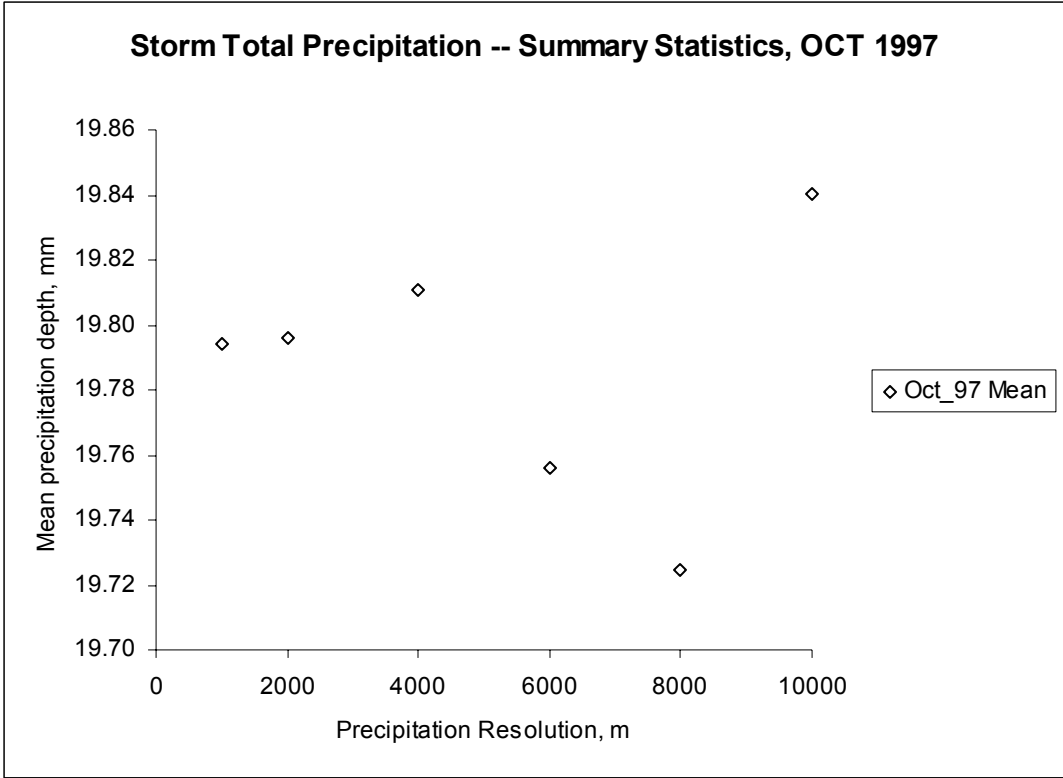


Figure 4.15: Mean Storm Total Precipitation, October 1997

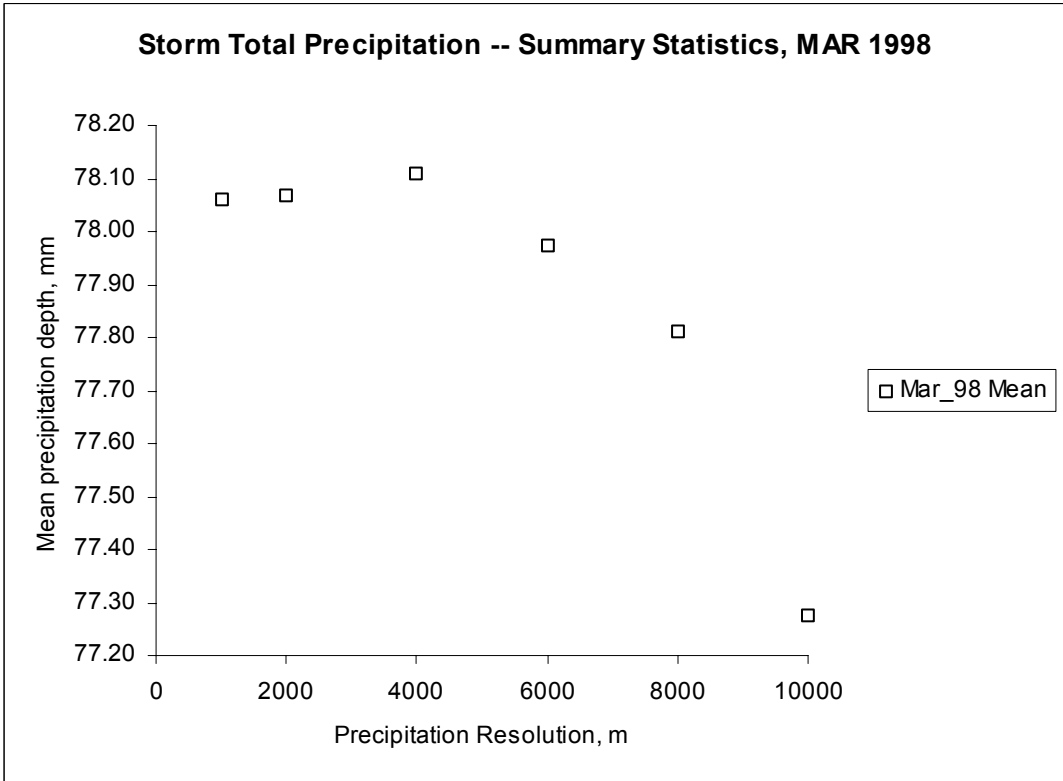


Figure 4.16: Mean Storm Total Precipitation, March 1998.

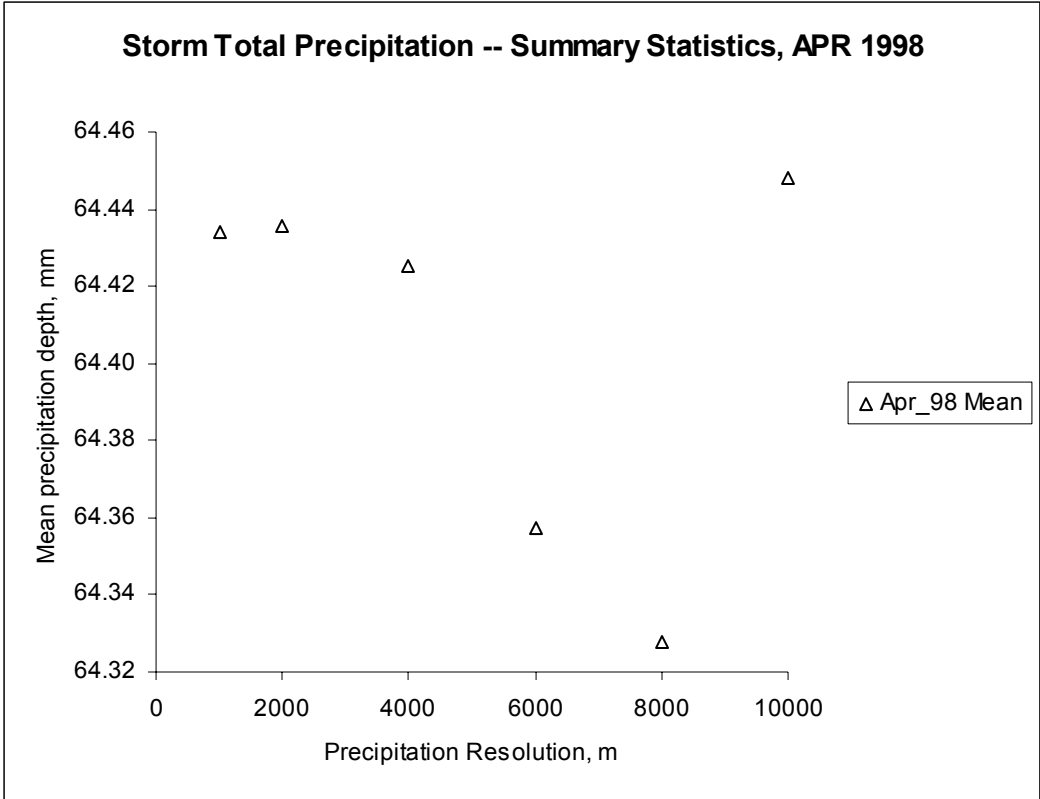


Figure 4.17: Mean Storm Total Precipitation, April 1998.

Figure 4.18 shows the runoff to rainfall ratio for each storm event at all resolutions. Runoff to rainfall ratio is calculated as runoff volume (in mm of depth) divided by mean storm total precipitation depth. Figures 4.19, 4.20, and 4.21 show variation in the runoff to rainfall ratio with precipitation resolution for the October 1997, March 1998 and April 1998 storm events respectively. A significantly enlarged scale is used on the ordinate axis of figures 4.19, 20, and 21 to show that, though small in magnitude, the anticipated trends in model results with precipitation resolution exist.

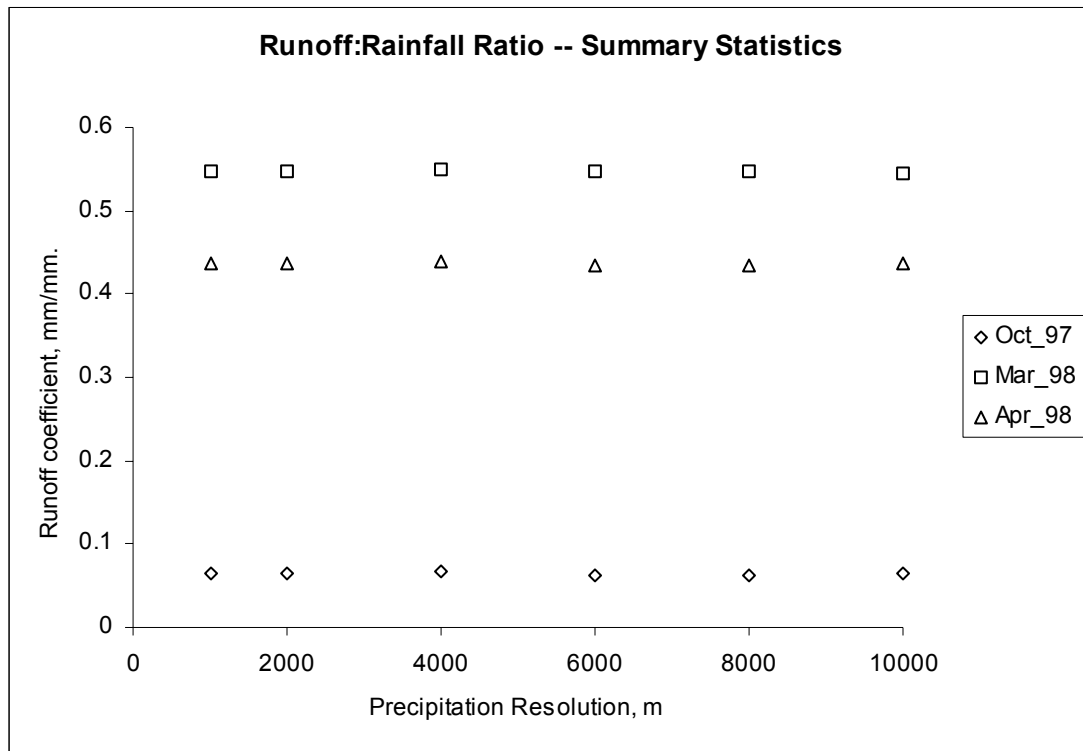


Figure 4.18: Runoff to Rainfall Ratio at varied Precipitation Resolutions

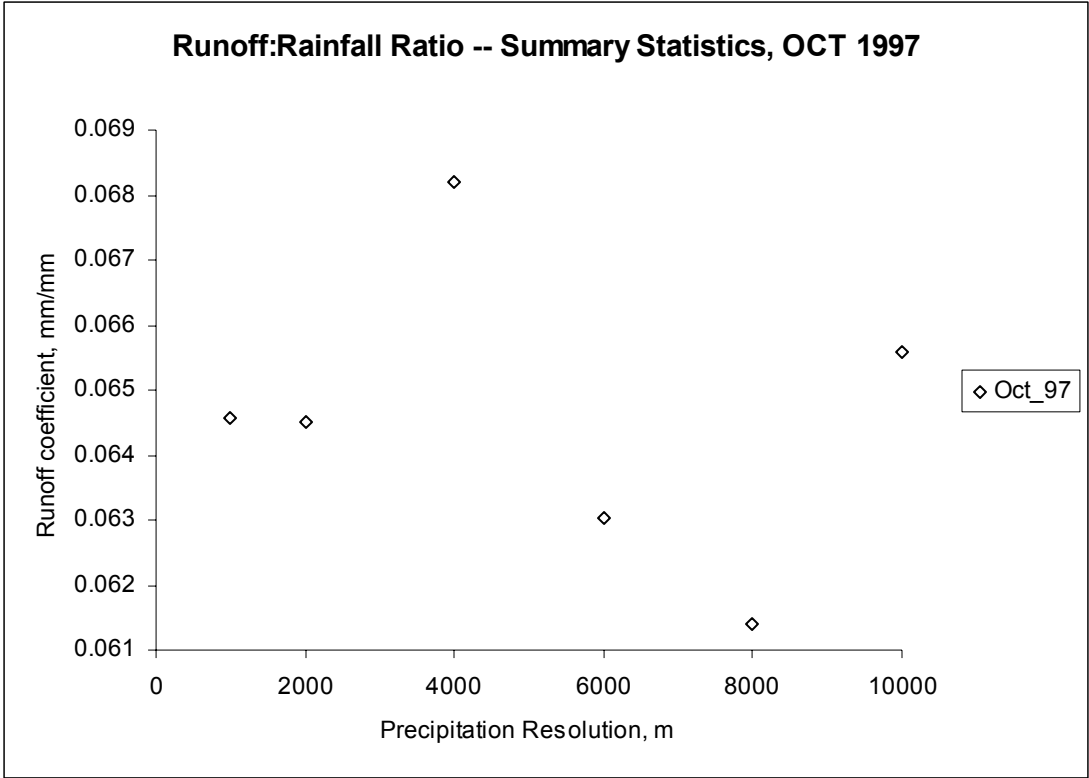


Figure 4.19: Runoff to Rainfall Ratio, October 1997

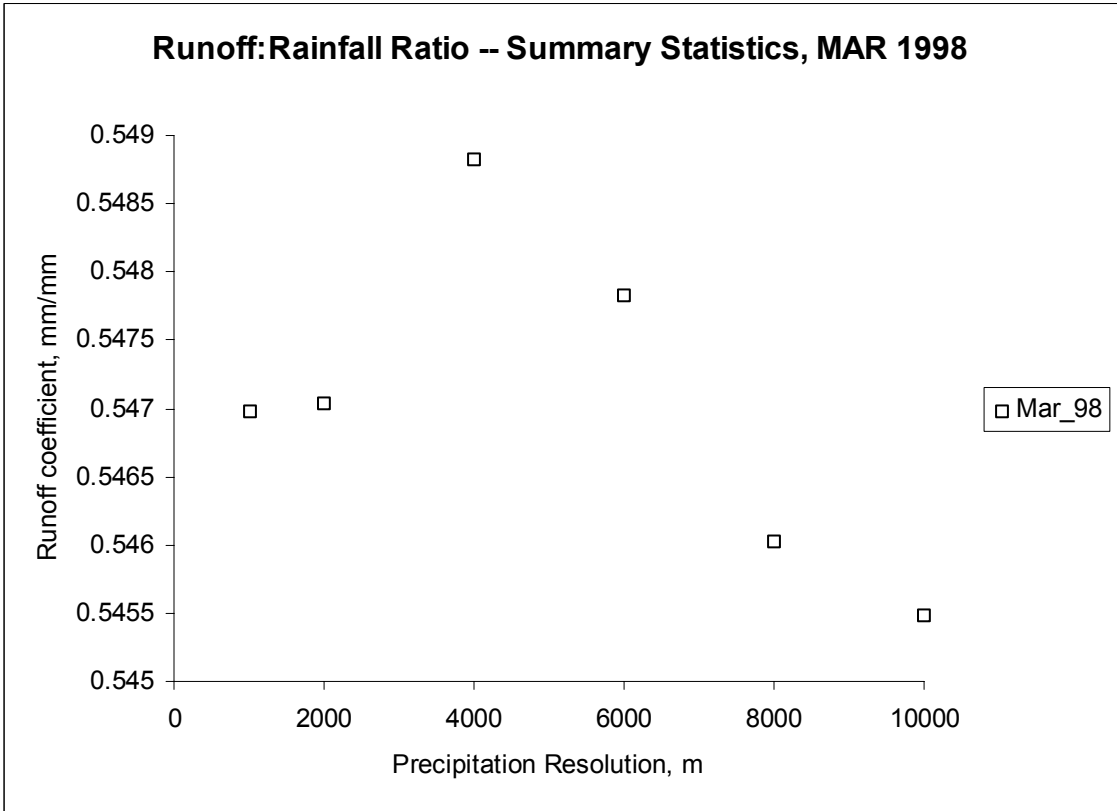


Figure 4.20: Runoff to Rainfall Ratio, March 1998

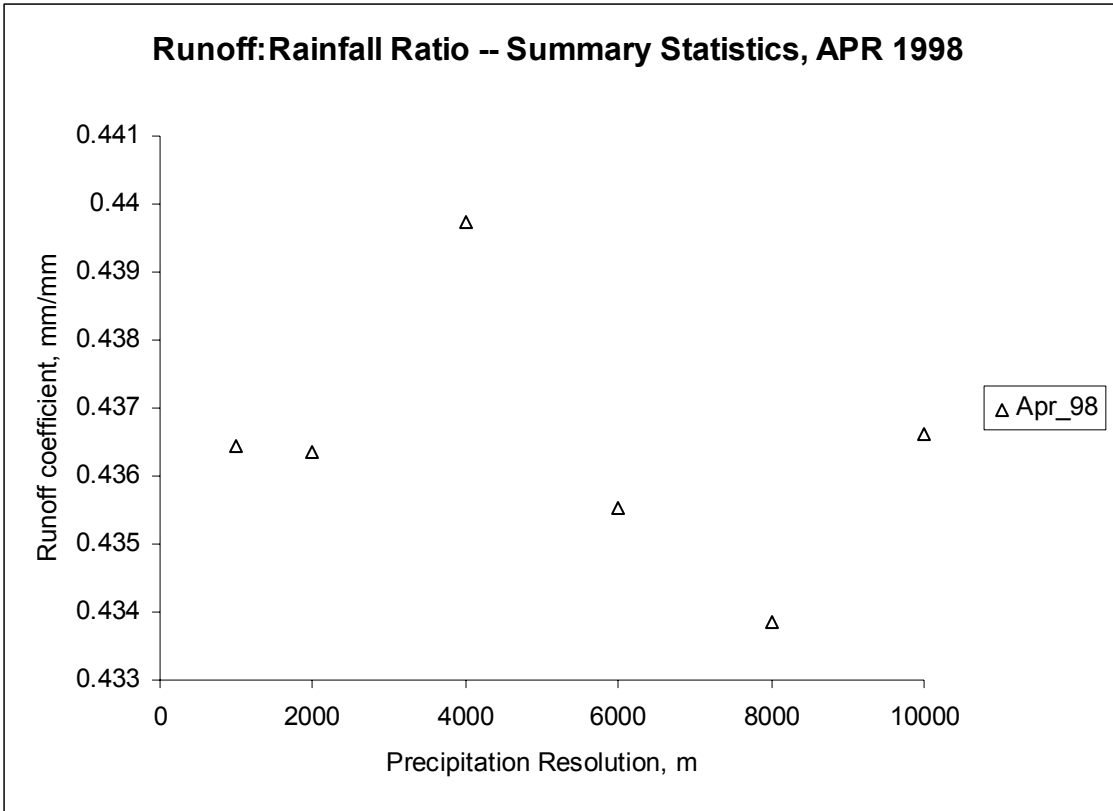


Figure 4.21: Runoff to Rainfall Ratio, April 1998

Figures 4.22 to 4.27 show observed and modeled runoff volumes at varied resolutions at six points in the system moving from upstream to downstream: Shawsville (4.22), Lafayette (4.23), Glenvar (4.24), Walnut (4.25), Niagara (4.26), and at the confluence of Back Creek and the Roanoke River (4.27). Changes in runoff volume with resolution are seen to be small compared to disagreement between observed and modeled runoff volumes. The model is found to over-predict or under-predict runoff volume at different points in the system implying that CN or AMC values need refinement or that spatial variability exists in AMC.

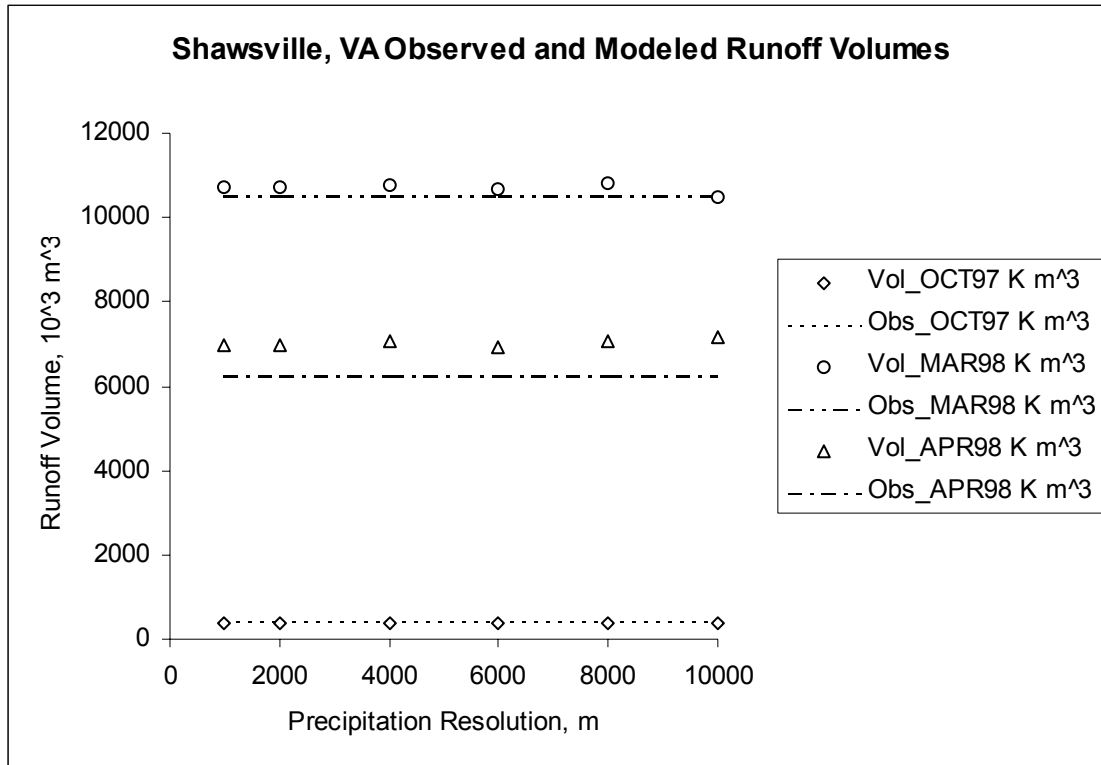


Figure 4.22: Observed and Modeled Runoff Volume, Shawsville, VA

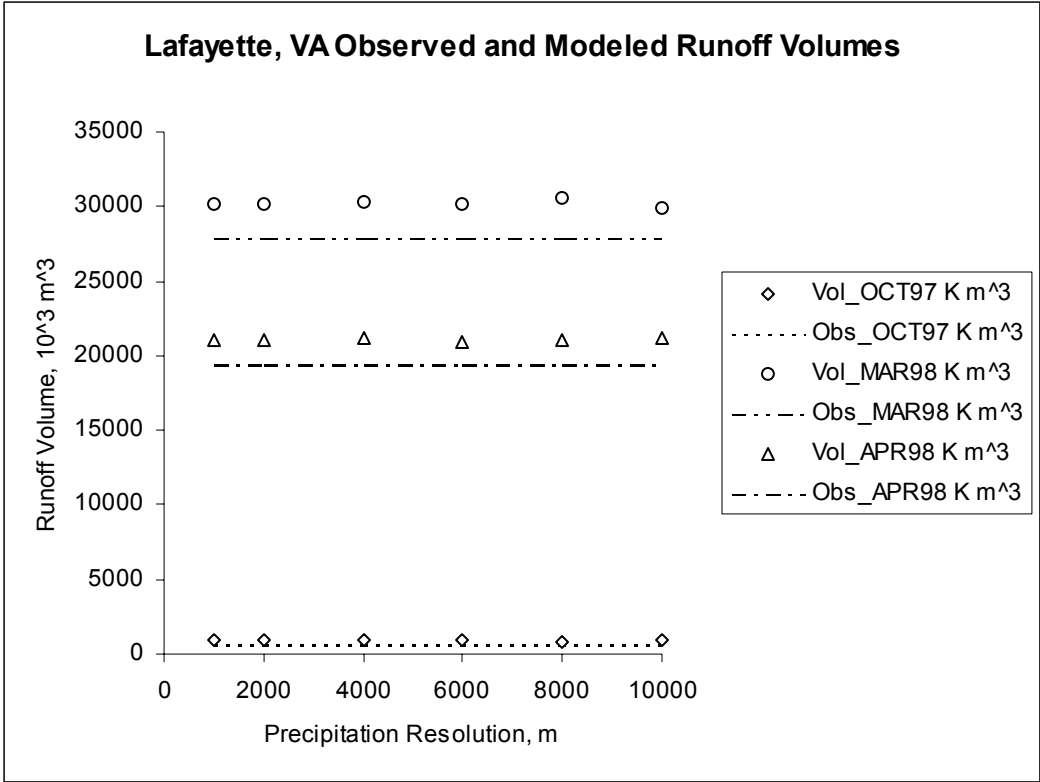


Figure 4.23: Observed and Modeled Runoff Volume, Lafayette, VA

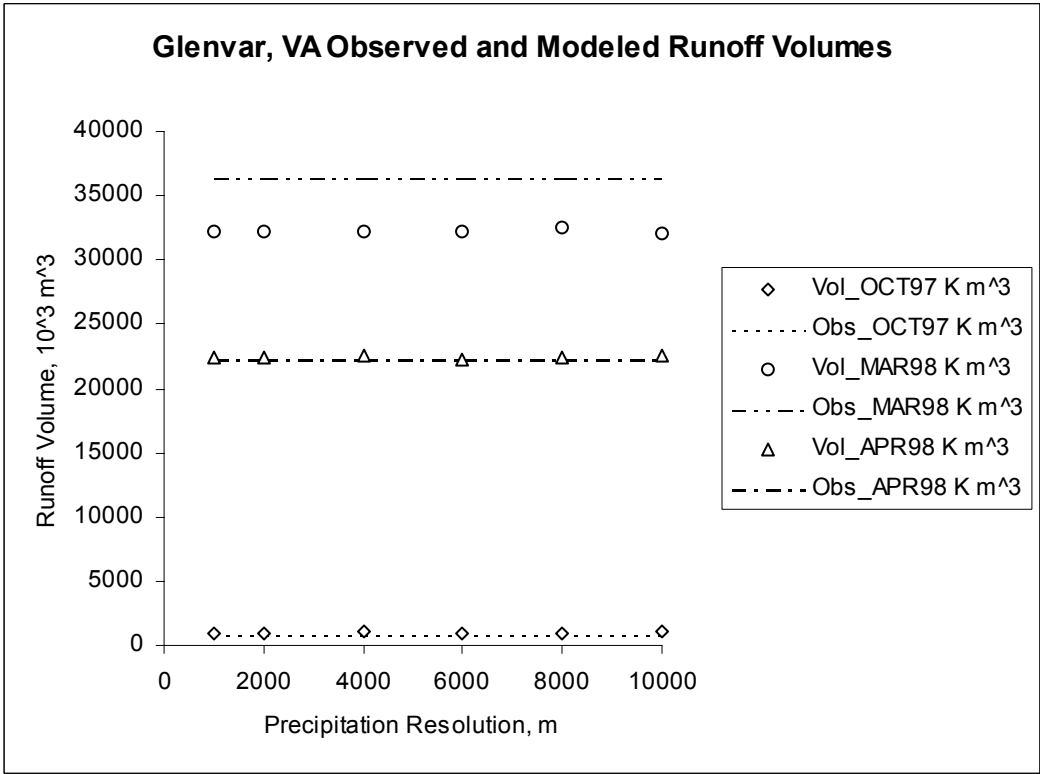


Figure 4.24: Observed and Modeled Runoff Volume, Glenvar, VA

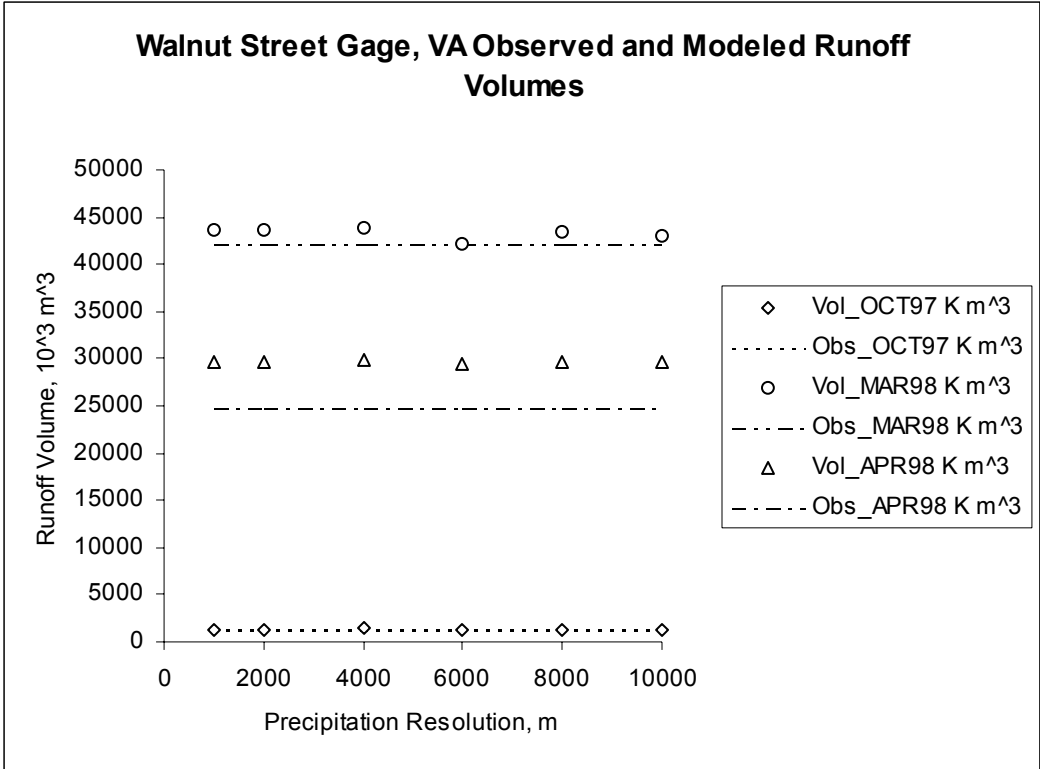


Figure 4.25: Observed and Modeled Runoff Volume, Walnut Street Gage

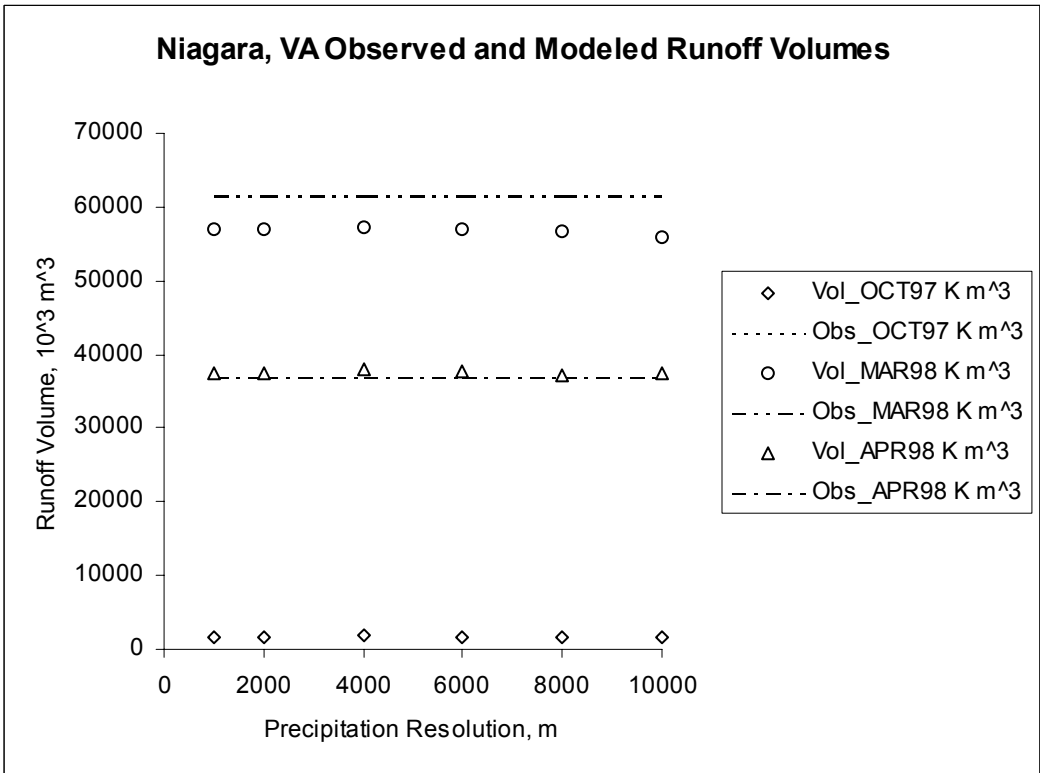


Figure 4.26: Observed and Modeled Runoff Volume, Niagara, VA

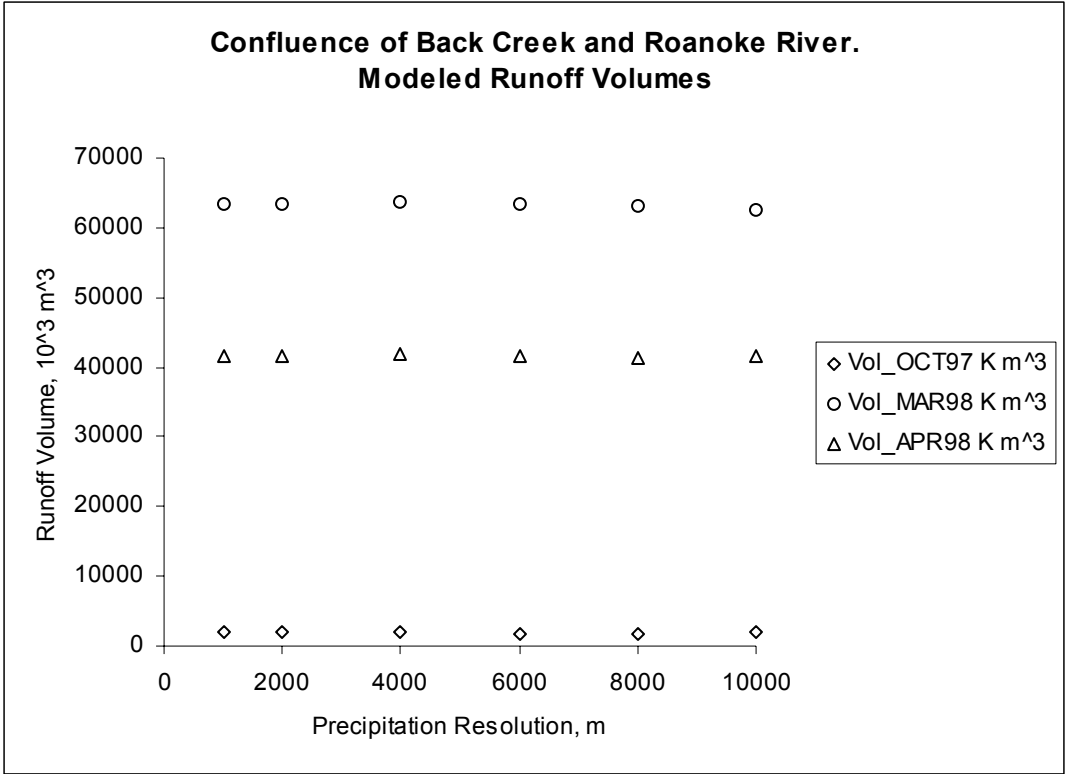


Figure 4.27: Observed and Modeled Runoff Volume, Confluence of Back Creek and Roanoke River

Figures 4.28 to 4.30 show observed and modeled runoff volume at the most downstream gage point with available data for the October 1997, March 1998, and April 1998 storm events respectively. A significantly enlarged scale is used on the ordinate axis of figures 4.28, 4.29, and 4.30 to show the small, but discernible, trends in model results with precipitation resolution. These plots are shown so that trends in runoff volume with may be compared to trends in precipitation volume.

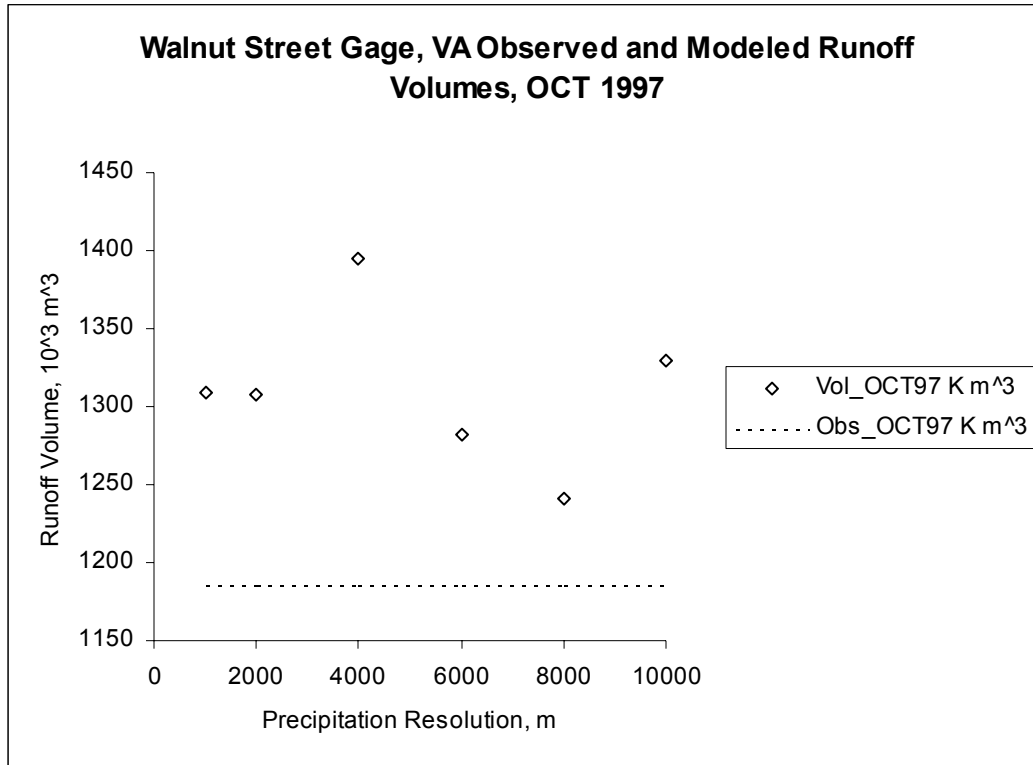


Figure 4.28: Observed and Modeled Runoff Volume at Walnut Street Gage, October 1997

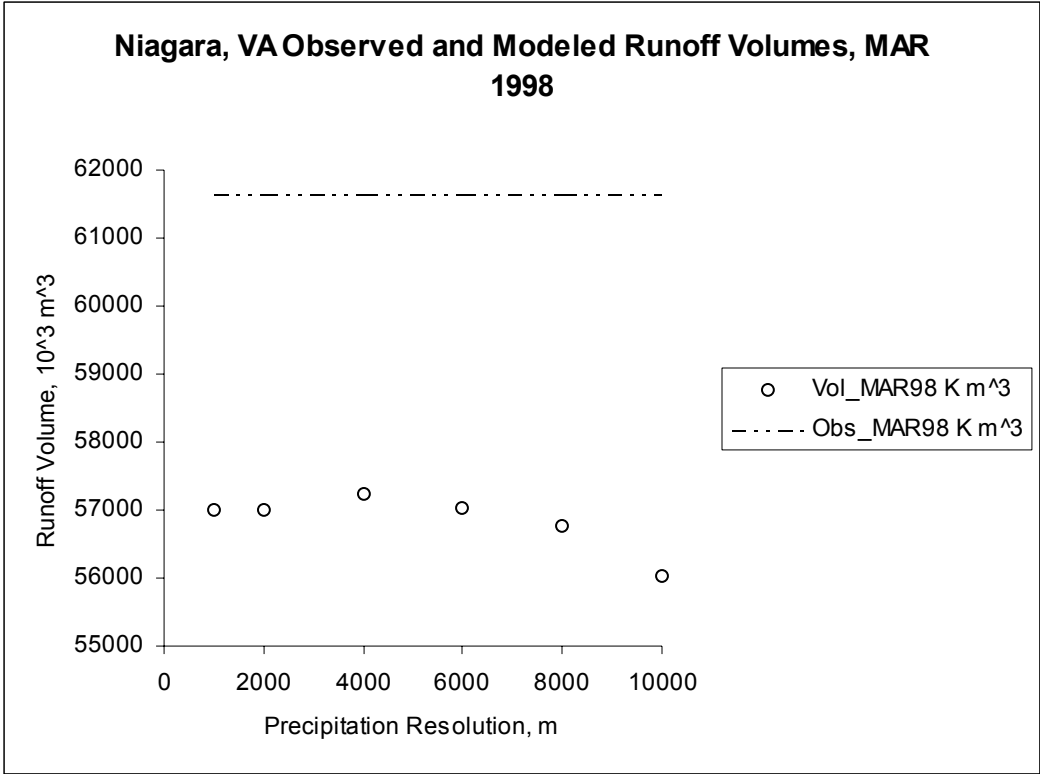


Figure 4.29: Observed and Modeled Runoff Volume at Niagara Gage, March 1998

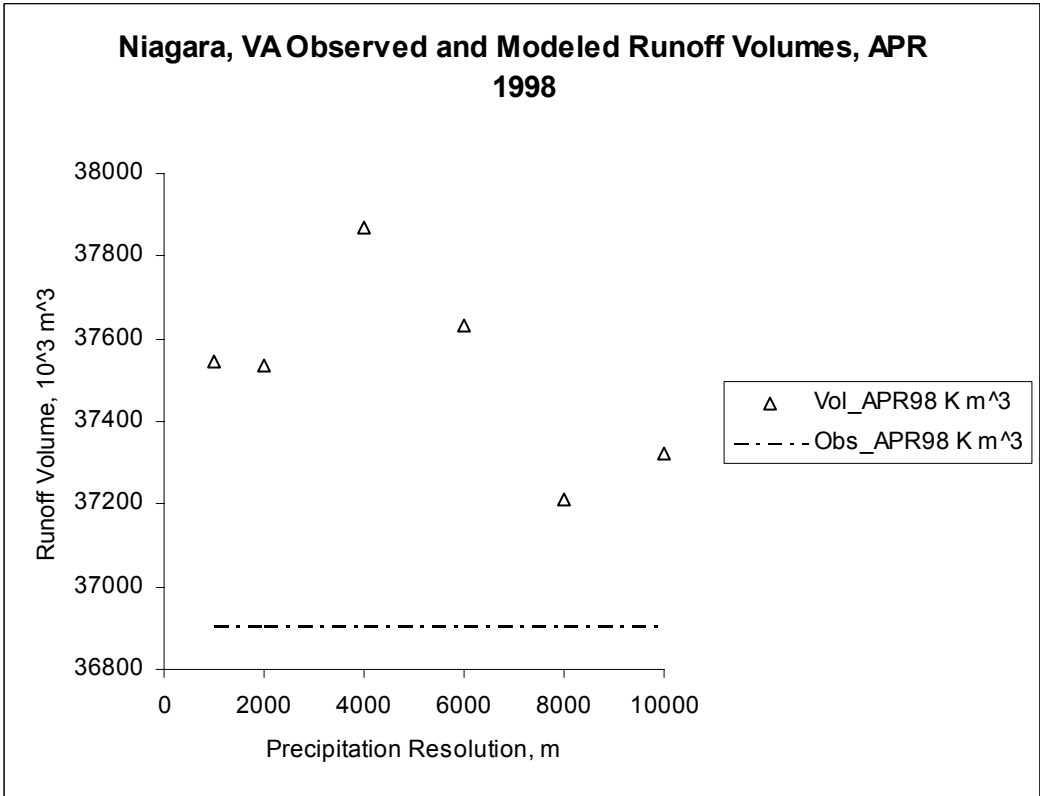


Figure 4.30: Observed and Modeled Runoff Volume at Niagara Gage, April 1998

4.5.3 Effects of Precipitation Resolution on Hydrographs, Peak Flow, and Time to Peak

Figures 4.31 through 4.34 show runoff hydrographs under varied precipitation resolutions. These plots are presented to evaluate the changes in peak flowrate, time to peak, and hydrograph shape resulting from changes in input precipitation resolution. The greatest changes in runoff hydrographs are seen for the October 1997 storm event for which a very small amount of rainfall excess occurred. Figure 4.31 shows hydrographs at the Walnut Street gage for the October 1997 storm event. The largest peak flowrate results from the 4km (base) resolution. Hydrographs are virtually identical for the 1km and 2km precipitation resolutions. Hydrographs for the 6k, 8k, and 10k storm events exhibit the trend of decreasing peak flow with increasing rainfall resolution. Changes in time to peak are not seen most likely due to the relatively long (hourly) time step of the model.

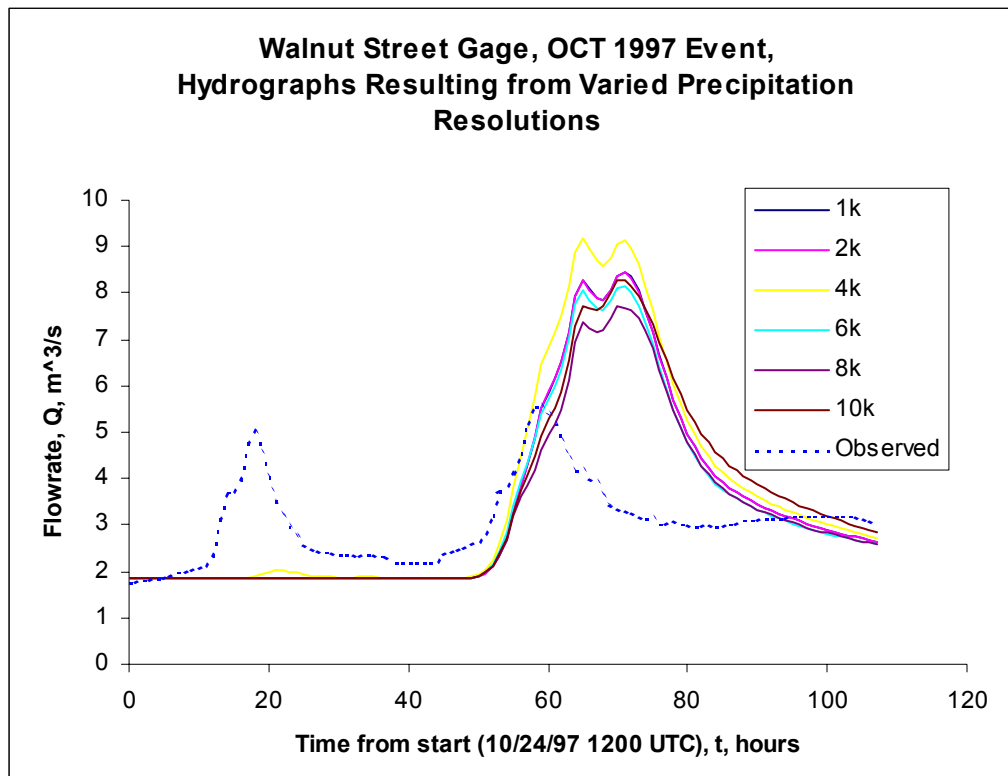


Figure 4.31 Hydrographs at the Walnut Street Gage, October 1997

Figures 4.32 and 4.33 show runoff hydrographs and hydrograph peaks for the Niagara gage during the March 1998 storm event. The changes in the runoff hydrographs that result from changes in precipitation resolution are small compared to the disagreement between observed and modeled data. As precipitation resolution was made coarser from the 4km (base) resolution, peak flowrates decreased and times to peak increased. As precipitation grids were smoothed to a smaller cell size by bilinear interpolation, peak flowrates also decreased, but by a lesser amount. These decreases in peak flowrate were smaller than the decreases caused by upscaling or degradation of precipitation resolution. Figure 4.34 shows similar trends for the April 1998 storm event.

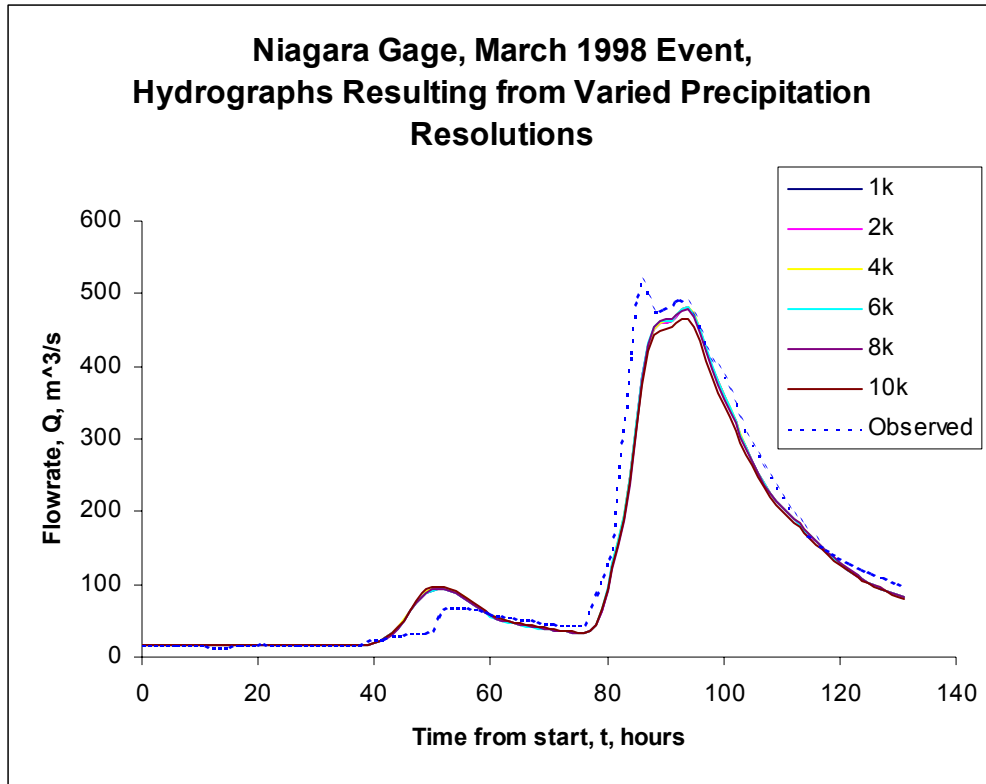


Figure 4.32: Hydrographs at the Niagara Gage, March 1998

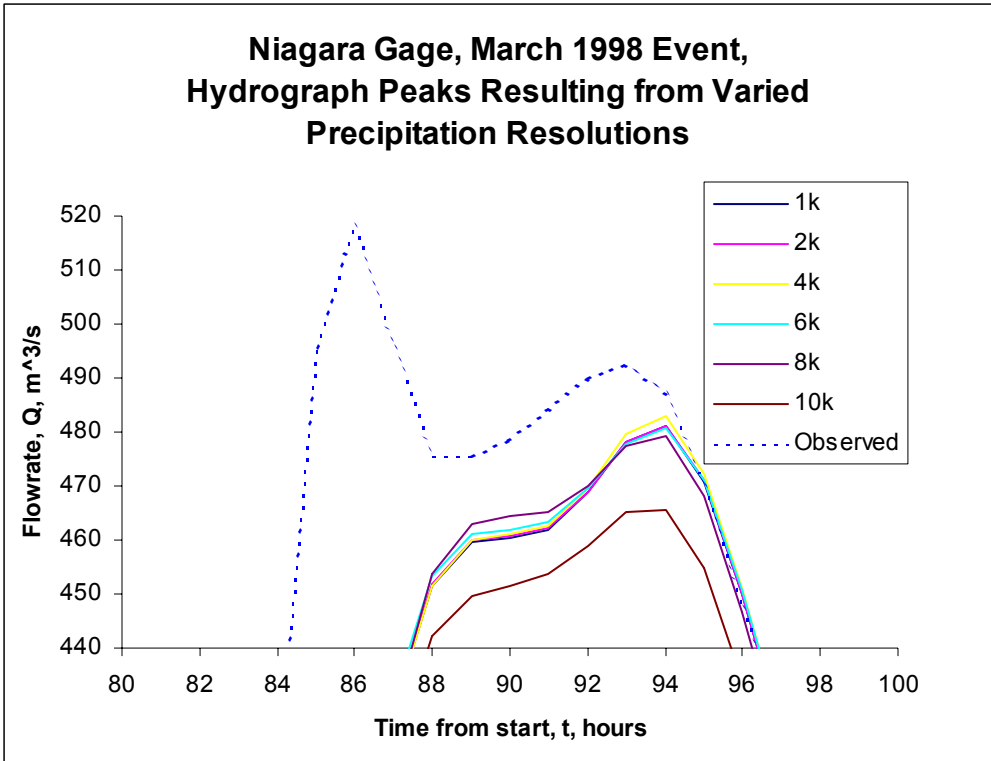


Figure 4.33: Hydrographs Peaks at the Niagara Gage, March 1998

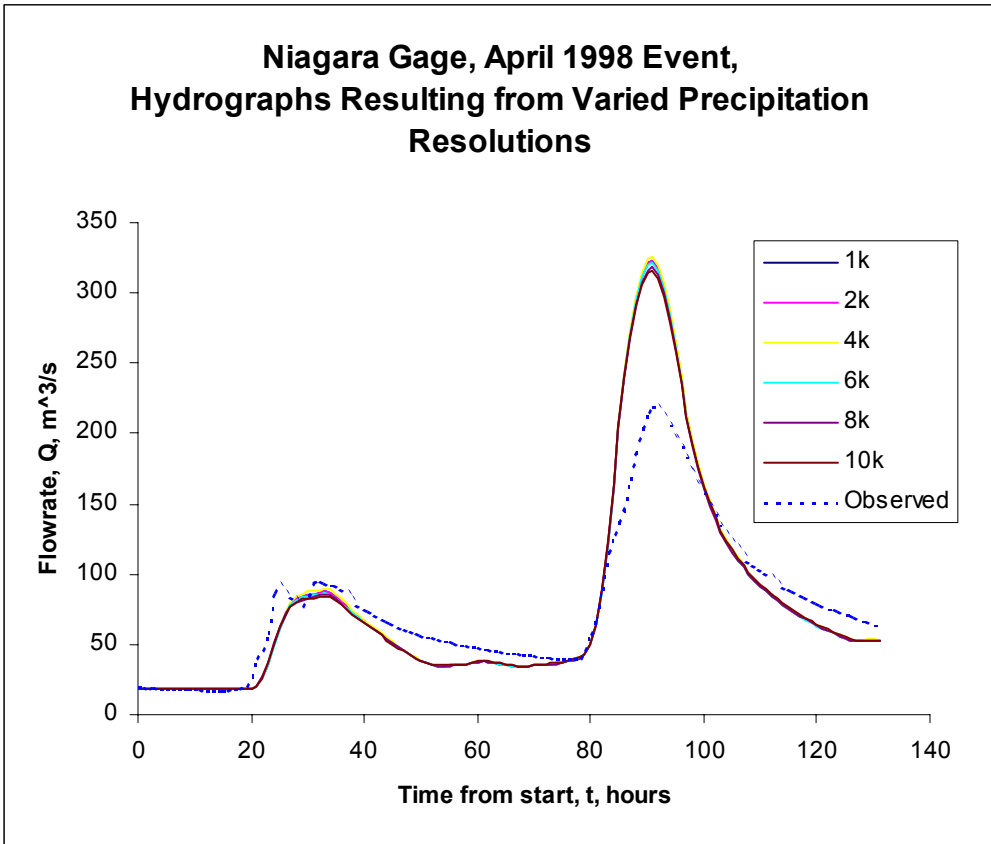


Figure 4.34: Hydrographs at the Niagara Gage, April 1998

4.6 Effects of Physical Parameter Resolution on Model Results

The effects of physical parameter and precipitation resolution and computational grid cell size on model results were examined for the March 1998 storm event. Model runs were made at computational cell sizes and precipitation and physical parameter resolutions of 400m, 500m, 1km, 2km, 4km, and 5km. 400m was the lower limit of watershed discretization in this research due to computing constraints. At the 400m discretization, the larger subwatersheds are divided into approximately 1700 grid cells and the smallest subwatersheds divided into at least 200 grid cells. This discretization is finer than the threshold given by Seybert (1996) to produce reasonable results. The main focus of the following analysis will be on model runs with resolution less than 4km as precipitation input volume (see section 4.2.3 and table 4.9) changes very little between these resolutions. Changes in precipitation input volume are on the order of 0.01% between 400m and 2km precipitation resolutions. Compared to the magnitude of change in runoff volume, these changes in precipitation input volume are insignificant.

Runoff volumes at subwatershed outlets and stream gage points increased as computational cell size, precipitation resolution, and physical parameter grid resolution became finer. These changes are on the order of 1-2% compared to the base (4km) resolution. Trends of decreasing runoff volume with larger computational grid cell size were clearly observed at all points in the system. Greater uncertainty in runoff volume was observed in smaller subwatersheds most likely due to the effects of watershed smearing, the imprecise location of precipitation with respect to basin boundaries.

Table 4.14 and 4.15 show runoff volumes and percent changes from 4km resolution for subwatersheds and gage points respectively. Note that percent changes in runoff volume are typically greater for smaller subwatersheds due to the effects of watershed smearing. The trends of decreasing runoff volume with larger computational grid cell size are clearly seen.

Table 4.14: Subwatershed Runoff Volumes for Varied Physical Parameter and Precipitation Resolution

Subwatershed Runoff Volumes for March 1998 Storm Event (1 of 2)										
Cell Size	Ironto (288km ²)		Shawsville (280km ²)		Lafayette (95km ²)		Glenvar (58km ²)		Walnut (269km ²)	
M	10 ³ m ³	Δ% from 4k	10 ³ m ³	Δ% from 4k	10 ³ m ³	Δ% from 4k	10 ³ m ³	Δ% from 4k	10 ³ m ³	Δ% from 4k
400	14817	0.50	10774	1.48	4784	-0.25	2375	2.44	12397	2.07
500	14807	0.43	10761	1.36	4784	-0.26	2372	2.29	12378	1.92
1000	14783	0.27	10705	0.83	4777	-0.40	2353	1.48	12293	1.22
2000	14759	0.11	10675	0.55	4774	-0.45	2342	1.00	12250	0.86
4000	14743	0.00	10617	0.00	4796	0.00	2319	0.00	12145	0.00
5000	14698	-0.31	10674	0.54	4819	0.48	2358	1.68	12321	1.45

Subwatershed Runoff Volumes for March 1998 Storm Event (2 of 2)										
Cell Size	Carvin (37km ²)		Tinker (30km ²)		Niagara (264km ²)		Back_Crk (145km ²)		Confluence (16km ²)	
M	10 ³ m ³	Δ% from 4k	10 ³ m ³	Δ% from 4k	10 ³ m ³	Δ% from 4k	10 ³ m ³	Δ% from 4k	10 ³ m ³	Δ% from 4k
400	1274	2.80	1228	4.57	11405	2.20	5962	0.67	464	2.02
500	1271	2.62	1211	3.12	11379	1.96	5955	0.55	463	1.80
1000	1253	1.18	1203	2.41	11321	1.44	5935	0.22	461	1.30
2000	1219	-1.64	1261	7.34	11257	0.87	5918	-0.06	461	1.25
4000	1239	0.00	1174	0.00	11160	0.00	5922	0.00	455	0.00
5000	1166	-5.90	1207	2.80	11194	0.30	5892	-0.50	469	2.99

Table 4.15: Gage Runoff Volumes for Varied Physical Parameter and Precipitation Resolution

Runoff Volumes at Gage Points for March 1998 Storm Event										
Grid Scale	Lafayette_Gage		Glenvar_Gage		Walnut_Gage		Niagara_Gage		Outlet	
M	10 ³ m ³	Δ% from 4k	10 ³ m ³	Δ% from 4k	10 ³ m ³	Δ% from 4k	10 ³ m ³	Δ% from 4k	10 ³ m ³	Δ% from 4k
400	30246	0.73	32278	0.87	43901	1.23	57365	1.54	63701	1.46
500	30222	0.65	32250	0.78	43855	1.12	57274	1.38	63602	1.30
1000	30135	0.36	32143	0.44	43659	0.67	56992	0.88	63297	0.82
2000	30078	0.17	32075	0.23	43547	0.41	56838	0.60	63127	0.55
4000	30027	0.00	32001	0.00	43369	0.00	56497	0.00	62783	0.00
5000	30061	0.11	32072	0.22	43612	0.56	56731	0.41	63001	0.35

Figures 4.35 and 4.36 show plots of runoff volume versus physical parameter and precipitation resolution for the March 1998 storm event. Compared to variation in runoff volume between subwatersheds and gages, variations in runoff volume due to resolution changes are small.

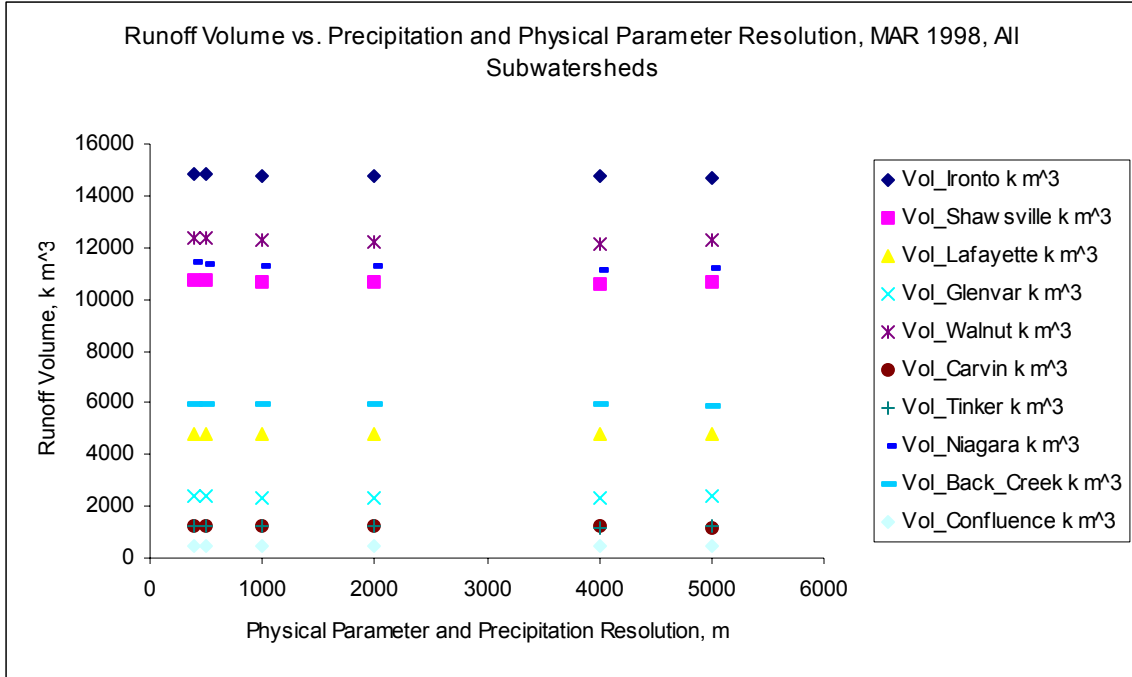


Figure 4.35: Subwatershed Runoff Volumes For Varied Physical Parameter and Precipitation Resolution

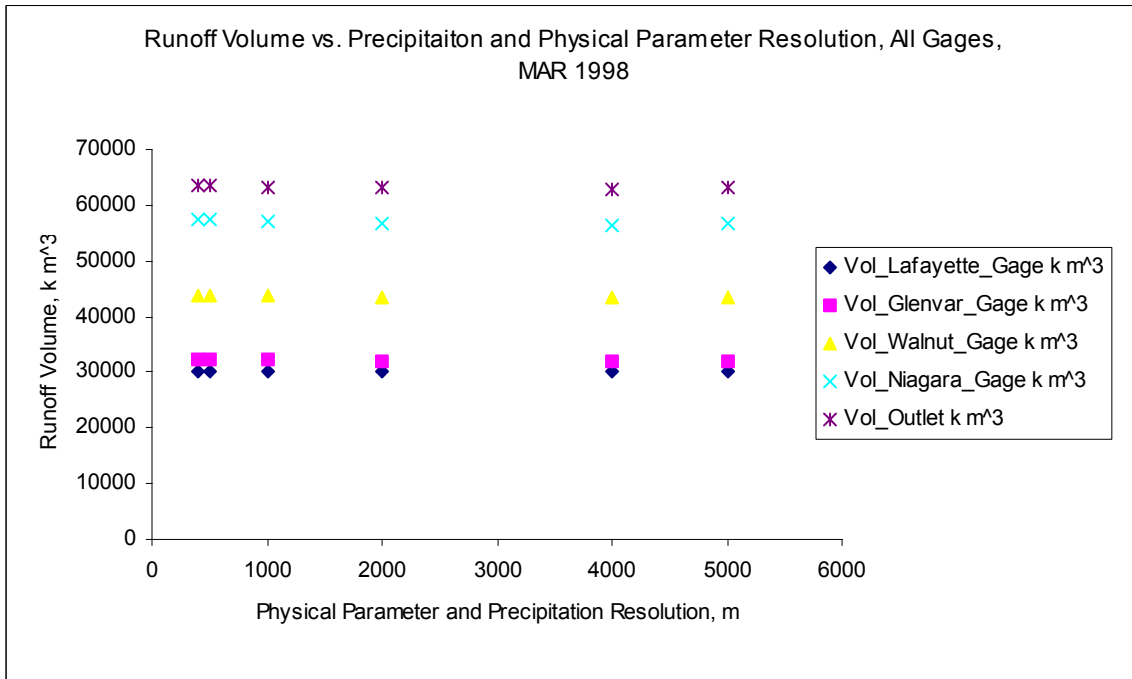


Figure 4.36: Runoff Volumes at Stream Gage Points For Varied Physical Parameter and Precipitation Resolution

Figures 4.37 and 4.38 show typical trends in runoff volume with changes in precipitation and physical parameter resolution. A significantly enlarged scale is used on the ordinate axis of these figures. Figure 4.37 shows runoff volumes for the Ironto subwatershed during the March 1998 storm event. Figure 4.38 shows runoff volumes at the confluence of Back Creek and the Upper Roanoke River.

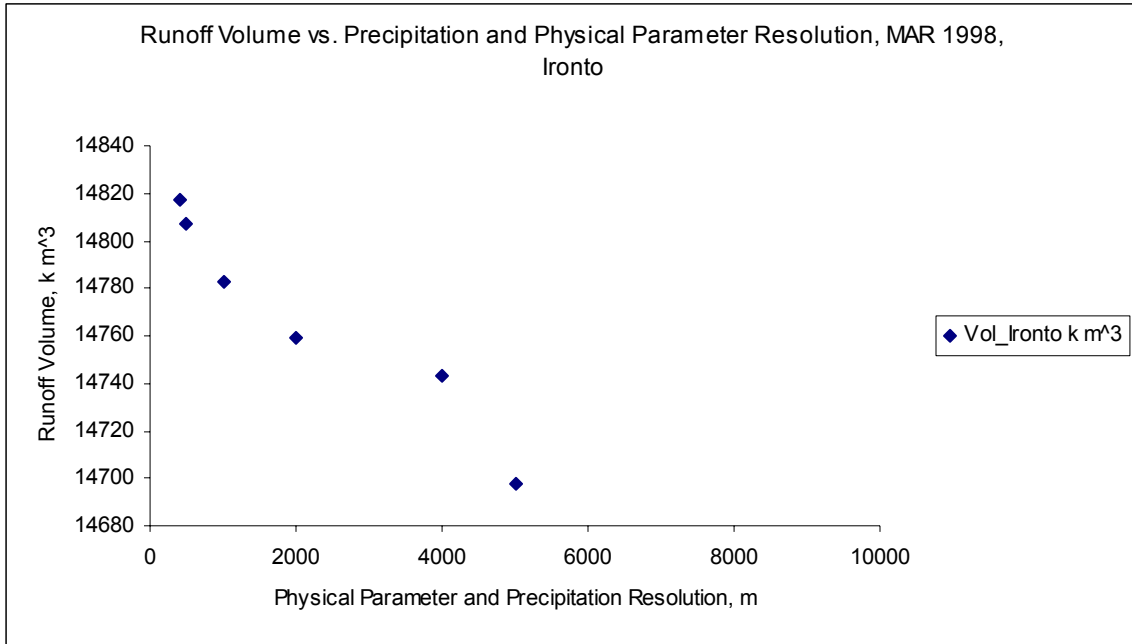


Figure 4.37: Runoff Volumes For Varied Physical Parameter and Precipitation Resolution, Ironto Subbasin

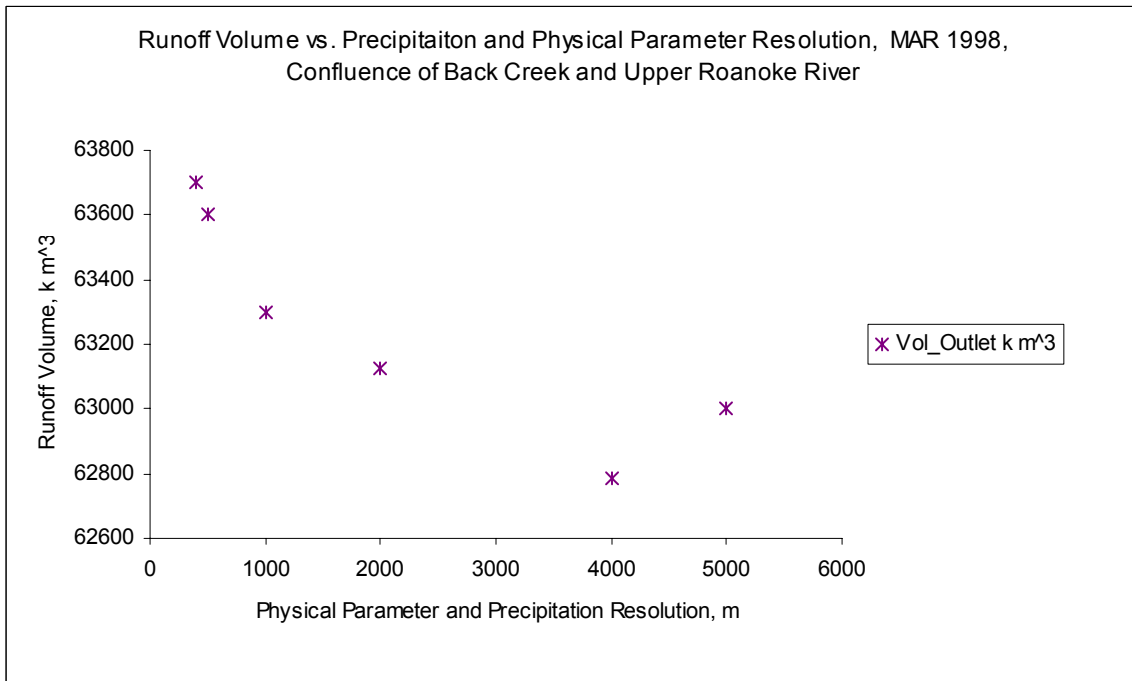


Figure 4.38: Subwatershed Runoff Volumes For Varied Physical Parameter and Precipitation Resolution, Confluence of Back Creek and Upper Roanoke River

4.7 Comparison of Lumped and Distributed Model Results

This section compares model results for the lumped and distributed HEC-HMS runoff models for the Upper Roanoke River Watershed, VA. Development of the spatially lumped HEC-HMS runoff model is discussed in section 3.8. Curve numbers and hourly precipitation grids were spatially averaged at the subwatershed level to create the lumped model. The lumped model results can be thought of as a limit that the distributed model results will approach as computational cell size approaches subwatershed size.

The results from the lumped model show slightly longer times to peak and decreased peak flows. A slight loss of detail in hydrograph shape occurs in the lumped model as compared to the distributed model results. These variations are relatively insignificant compared to uncertainties due to CN and AMC, model parameterization, and when compared to the differences between modeled and observed streamflow. Overall runoff volumes from the lumped model are typically less than from the distributed model.

Though slight losses of hydrograph detail occur and peak flowrates and runoff volumes are slightly decreased, lumped modeling in HEC-HMS does offer some advantages over distributed modeling. A lumped SCS CN model would allow empirical optimization of CN along with the parameters Tc and R optimized in the distributed model. Lumped modeling also offers other methods of infiltration computation. NEXRAD stage III precipitation data provides an effective input to lumped models when appropriately reprocessed. To utilize NEXRAD stage III data in a lumped model, a watershed average precipitation hyetograph should be calculated rather than sampling a hyetograph at the watershed centroid or at an arbitrary network of gages.

4.7.1 Effects of Spatial Lumping on Runoff Volume

Figure 4.39 shows overall runoff volume generated by the lumped and distributed HEC-HMS runoff models for all of the storm events. The change in runoff volume between lumped and distributed models is small compared to variation in runoff volume between storms and between measured and observed runoff volumes. Figures 4.40, 4.41, and 4.42 show lumped and distributed runoff volumes for the October 1997, March 1998, and April 1998 storm events respectively. A significantly enlarged scale is used on the ordinate axis of figures 4.40 and 4.41 to show that, though small in magnitude, the anticipated trends in model results with spatial lumping exist. Overall runoff volumes from the lumped model are typically less than from the distributed model.

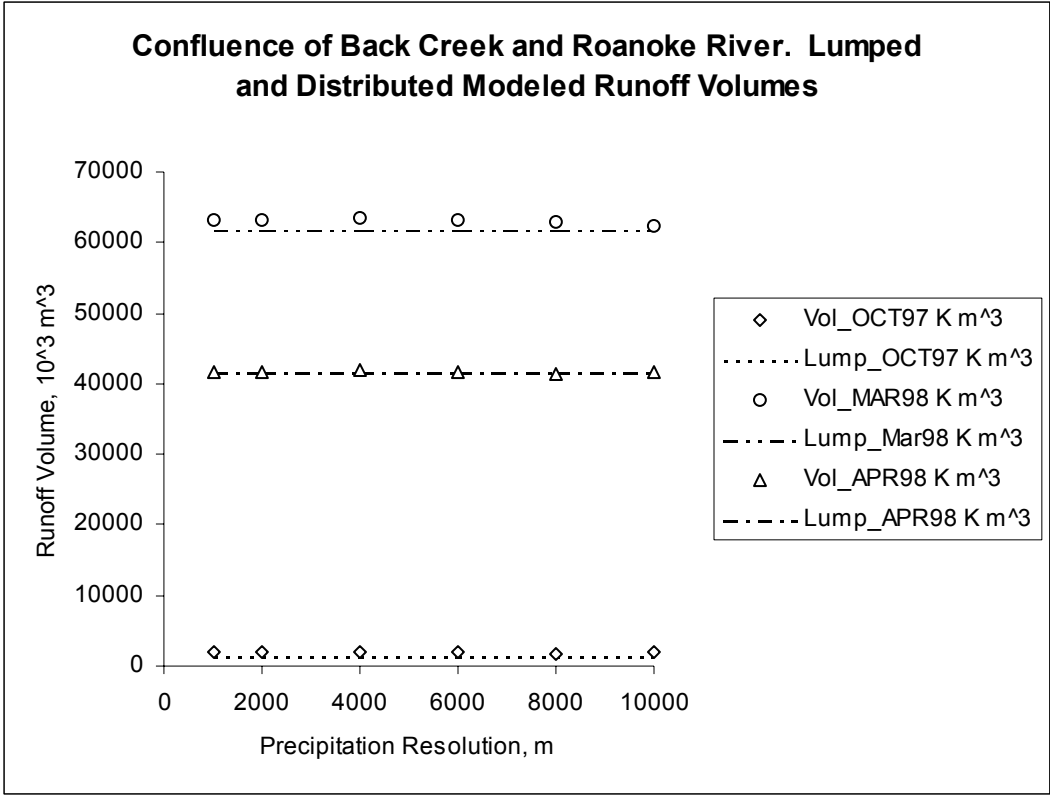


Figure 4.39: Runoff Volumes from Lumped and Distributed Models

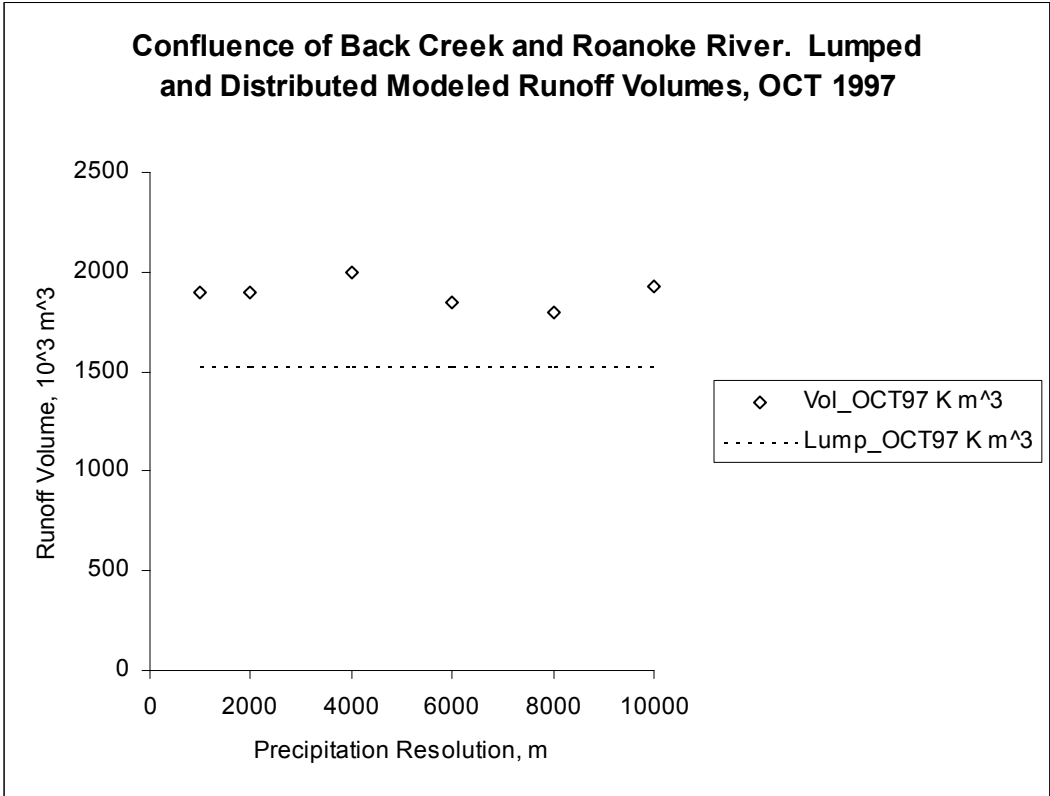


Figure 4.40: Runoff Volumes from Lumped and Distributed Models, October 1997

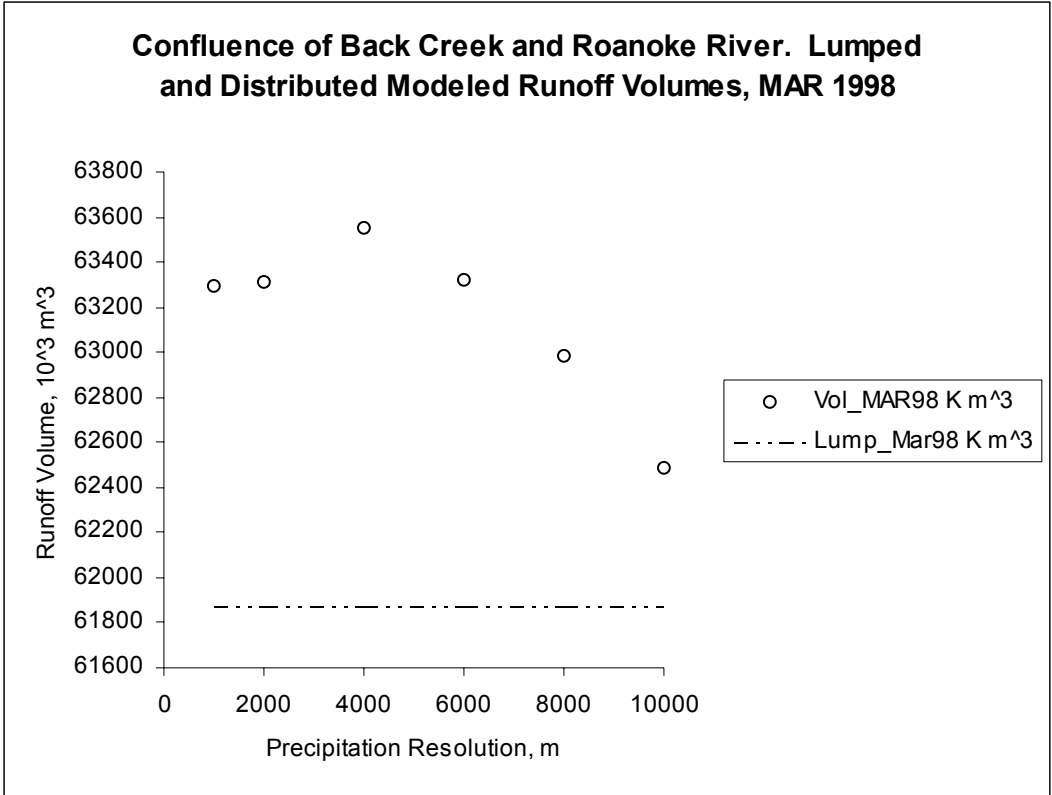


Figure 4.41: Runoff Volumes from Lumped and Distributed Models, March 1998

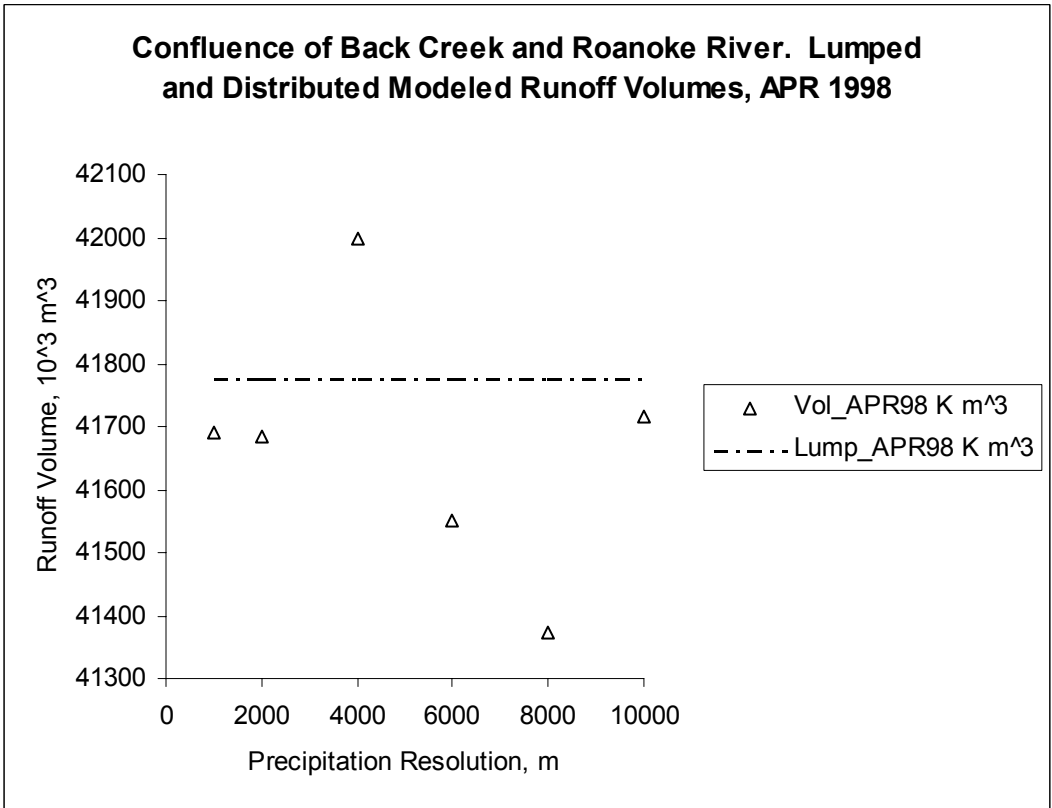


Figure 4.42: Runoff Volumes from Lumped and Distributed Models, April 1998

4.7.2 Effects of Spatial Lumping on Hydrographs, Peak Flows, Times to Peak

Figures 4.43 through 4.46 show runoff hydrographs from the lumped and distributed HEC-HMS runoff models. These plots are presented to evaluate the changes in peak flowrate, time to peak, and hydrograph shape resulting from spatial averaging of model parameters and precipitation inputs.

Figure 4.43 shows modeled and observed runoff hydrographs for the Walnut Street gage during the October 1997 storm event. A relatively significant change in hydrograph shape was noted between distributed and lumped model results for the October 1997 storm event. The percent changes in peak flow, time to peak, and runoff volume are greatest for this storm event most likely due to the relatively small amount of rainfall excess occurring during the October 1997 storm event.

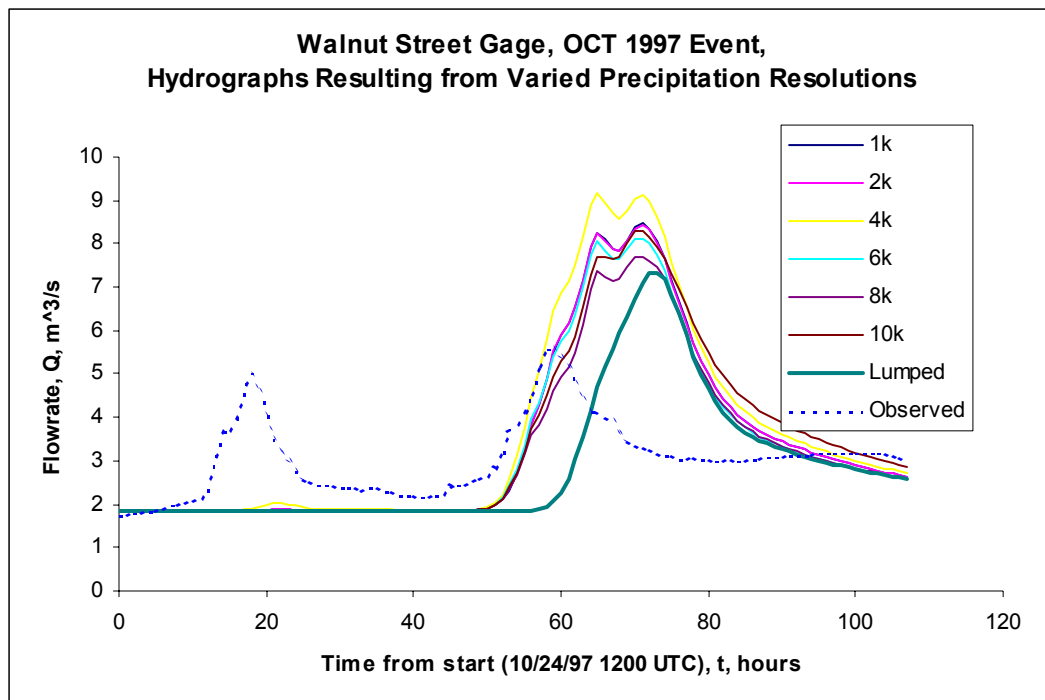


Figure 4.43: Hydrographs at Walnut Street Gage, October 1997

Figures 4.44 and 4.45 show runoff hydrographs and hydrograph peaks respectively at the Niagara gage during the March 1998 storm event. The changes in hydrograph qualities caused by spatial averaging are small compared to the differences between observed and modeled data. The hydrograph peaks in figure 4.45 show that spatial averaging causes small losses of hydrograph detail.

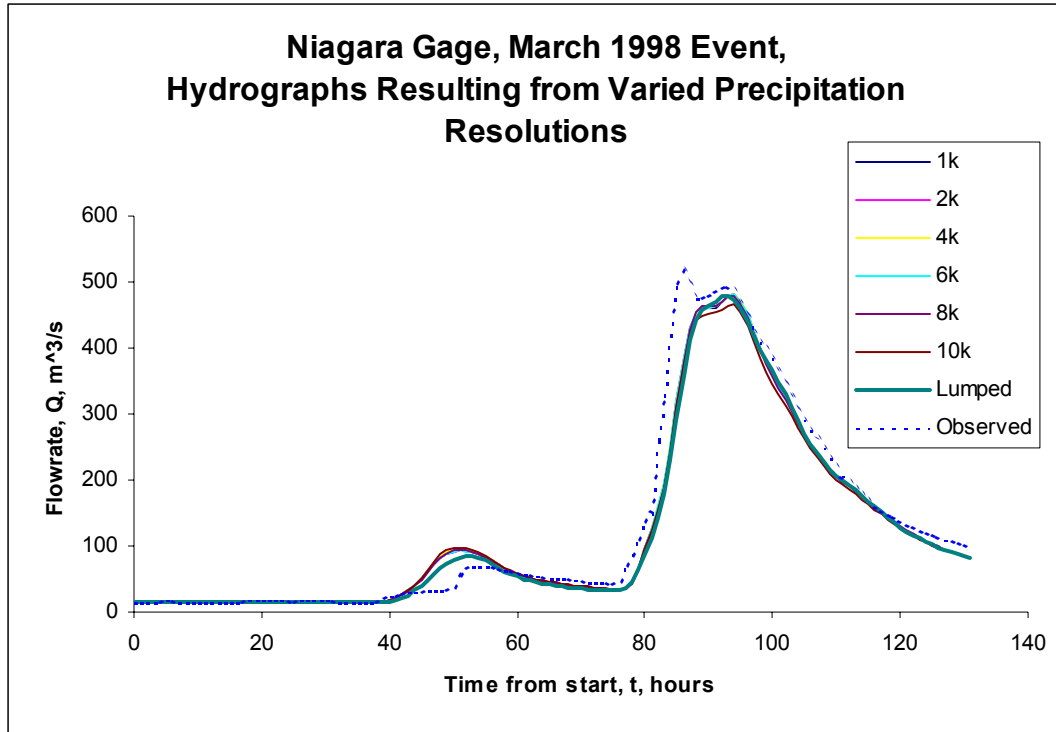


Figure 4.44: Hydrographs at Niagara Gage, March 1998

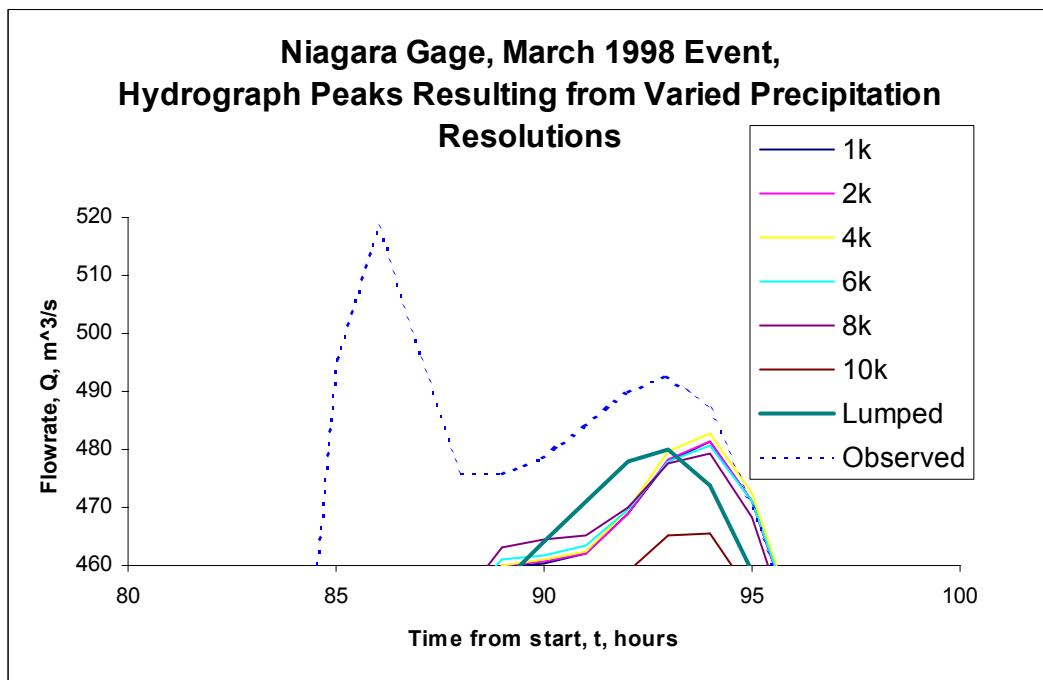


Figure 4.45: Hydrograph peaks at Niagara Gage, March 1998

Figure 4.46 shows the modeled and observed runoff hydrographs at the Niagara gage during the April 1998 storm event. The peak flowrate resulting from the lumped model is less than one percent greater than the peak flowrate from the distributed model.

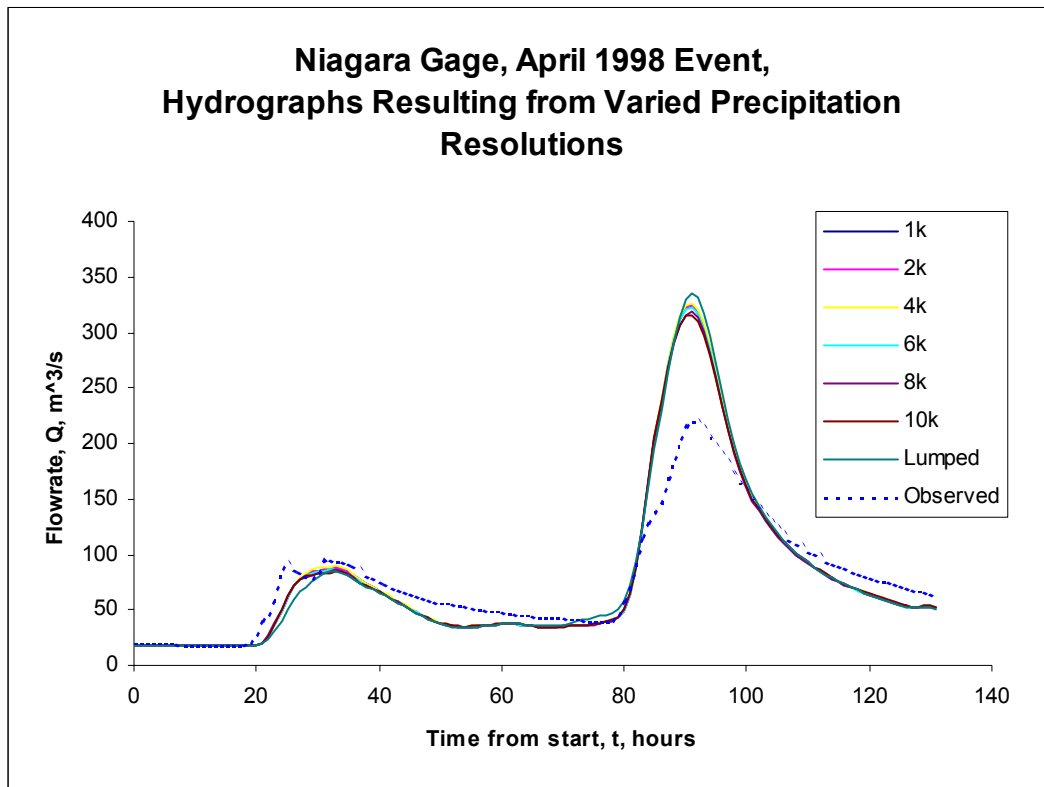


Figure 4.46: Hydrographs at Niagara Gage, April 1998

5.0 Discussion and Conclusions

NEXRAD stage III gridded precipitation data is an effective and accurate data source for distributed and lumped hydrologic modeling. The HEC-HMS model parameters chosen for the Upper Roanoke Watershed produced reasonable results for a sensitivity analysis on precipitation resolution and grid scale. The HEC-HMS gridded SCS CN rainfall excess calculation and ModClark runoff transformation does not exhibit significant sensitivity to precipitation resolution, grid scale, or spatial distribution of parameters and inputs as applied to the Upper Roanoke Watershed *during the storm events used in this study*. Expected trends in peak flowrate, time to peak, and overall runoff volume are observed with changes in precipitation resolution, however these changes are small compared with their magnitudes and compared to the discrepancies between modeled and observed values. Significant sensitivity of runoff volume to the choice of CN and AMC was observed. Changes in model outputs between the distributed and lumped versions of the model were also small compared to the magnitudes of model outputs.

5.1 Achievement of Objectives

This research achieved the objectives specified in chapter 1. These objectives are summarized below.

- **Implement a distributed hydrologic runoff model using existing GIS datasets and tools.**

A HEC-HMS distributed runoff model was created using data from the NRCS, USGS, and NWS. Datasets utilized include: SSURGO, NLCD, NED, USGS stream gage records, NEXRAD stage III gridded precipitation estimates, and IFLOWS precipitation gage records. Model development from GIS data and model parameterization are discussed extensively in chapter 3.

- **Utilize gridded precipitation estimates derived from NWS-88D NEXRAD stage III data as inputs to the distributed runoff model.**

NEXRAD stage III data was successfully decoded, reprojected, checked against gage data, and encoded into the database required by the HEC-HMS runoff model. The processes developed to reproject and rescale archived NEXRAD stage III precipitation data are extensively documented in chapter 3 and Appendix E for use in future research.

- **Quantify the effects of precipitation resolution and physical parameter grid scale on a distributed hydrologic runoff model.**

Model sensitivity to precipitation resolution, physical parameter grid scale and computational cell size was quantified by a series of model runs. Chapter 4 details the results of these model runs. The HEC-HMS gridded SCS CN, ModClark model, as applied to the Upper Roanoke River Watershed in this research exhibited small, but predictable, changes in model outputs due to changes in resolution and computational grid cell size.

- **Compare the performance of a distributed hydrologic runoff model to a similarly specified and parameterized lumped model.**
The creation of a similarly parameterized spatially averaged model is described in chapter 3. Lumped model results are compared to distributed model results in chapter 4. For the watershed and storm events used in this research, the spatially distributed HEC-HMS model was seen to offer little improvement in accuracy over the similarly parameterized lumped HEC-HMS model.

5.2 Use of NEXRAD Stage III products in Hydrologic Modeling.

Archived NEXRAD stage III precipitation data is an accurate and effective data source for hydrologic modeling when appropriately reprojected and processed. The amount and complexity of reprocessing required to use this data in hydrologic modeling can be formidable, however. Care must be taken to appropriately specify coordinate systems and earth datums if spatial reprojection of gridded precipitation data is required. The processing techniques developed for using archived NEXRAD stage III data have achieved the desired spatial and temporal accuracy. Though these techniques and tools may easily be applied to other areas for which archived stage III data is available, the modeler is advised to check the spatial and temporal registration of gridded precipitation data against gage data if possible. For use of NEXRAD stage III data in a spatially lumped hydrologic model, watershed or subwatershed average precipitation should be calculated rather than point sampling gridded records at watershed centroids or at arbitrary gage locations.

Rescaling of gridded precipitation data will often be necessary in distributed hydrologic modeling as the physical parameter grid scale or computational cell size of a model may not match the native resolution or projection of the precipitation data. When downscaling precipitation data, the raster interpolation techniques of bilinear interpolation and nearest neighbor reassignment were found to both produce acceptable results. Downscaling by bilinear interpolation produces a more intuitive representation of a continuous surface such as the spatial variation of precipitation depth. Downscaling by bilinear interpolation, as opposed to nearest neighbor reassignment, results in slightly reduced precipitation input volumes. Less than a 0.10% change was observed following downscaling by bilinear interpolation for the storm events used in this research. When comparing precipitation datasets downscaled from the 4km (base) resolution, changes in precipitation input volume are on the order of 0.01% between 400m and 2km precipitation resolutions. The small magnitude of change in precipitation input volume within this range makes it possible to isolate the effects of physical parameter grid scale and computational cell size from changes in input precipitation volume.

When upscaling or degrading a continuous raster dataset, the limits of bilinear interpolation must be considered. Bilinear interpolation calculates each cell value in the output dataset based on the cell values in the four nearest cells of the input dataset. If output resolution is greater than twice the input resolution, values from some cells in the input raster will not be used in the interpolation process. Figure 5.1 shows that data from some cells in the input raster will not be used if output resolution is significantly larger than input resolution. Upscaling of gridded precipitation data by bilinear interpolation to a resolution greater than twice the original resolution is not recommended. The use of a spatial averaging technique that accounts for the values of all input cell centers lying within the output cell is recommended when upscaling by a factor greater than two.

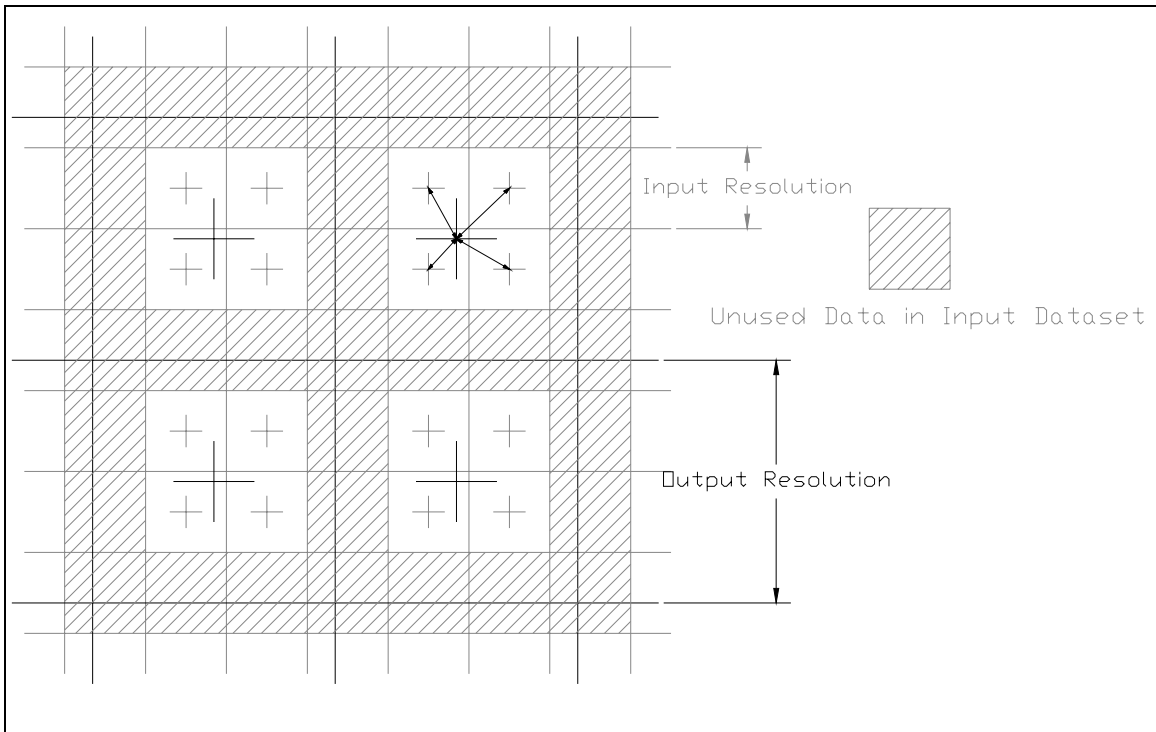


Figure 5.1: Unused Cells in Bilinear Interpolation

5.3 Effects of Precipitation Resolution on Model Results

When gridded precipitation data is upscaled, local minima are increased, local maxima are decreased, and consequently the range of precipitation depths is reduced. After upscaling, precipitation is also located less precisely with respect to basin boundaries. During downscaling (smoothing) by bilinear interpolation, the range of precipitation depths is also reduced, but by a much smaller amount. For the storm events and study area used in this research, decreases in precipitation input volume with changes in resolution on the order of 0.5% during upscaling and on the order of 0.1% during smoothing were observed. Percent changes in runoff volume with changes in precipitation resolution were larger in magnitude than changes in precipitation input volume, but followed the same trends.

Percent changes in runoff volume were on the order of 0.5% when using downscaled (smoothed) precipitation data and on the order of 1% when using upscaled (degraded) precipitation for the March and April 1998 storm events. Percent changes in runoff volume were on the order of 5-10% for the October 1997 storm event. This percent change was large, most likely due to the small amount of rainfall excess occurring during this storm. Changes in runoff volume with resolution were seen to be small compared to disagreement between observed and modeled runoff volumes.

5.4 Effects of Physical Parameter and Computational Cell Size on Model Results

When applying a grid based distributed hydrologic runoff model to a watershed, the grid scale chosen must be fine enough to represent critical spatial variability in hydrologic processes. The most efficient grid scale will vary with the watershed, the model chosen, and assuming the spatial distribution of physical characteristics is held constant, the spatial variability inherent in the rainfall inputs. The modeler should perform a sensitivity analysis to quantify the effects of computational cell size and physical parameter resolution on model results. For the HEC-HMS gridded SCS CN rainfall excess calculation and the ModClark runoff transformation applied to the Upper Roanoke Watershed, computational grid cell size and physical parameter resolution were seen to have predictable, but very small, effects on modeled results.

Precipitation input volume changed very little between 400m and 2km precipitation resolutions. For model runs made at computational cell sizes and physical parameter resolutions within this range, changes in precipitation input volume were on the order of 0.01%. Compared to the magnitude of change in runoff volume, these changes in precipitation input volume are insignificant, effectively isolating the effects of computational grid cell size and physical parameter resolution on model results.

Runoff volumes at subwatershed outlets and stream gage points increased as computational cell size, and consequently precipitation resolution and physical parameter resolution, became finer. These changes were on the order of 1-2% compared to the base (4km) resolution. Trends of increasing runoff volume with finer computational grid cell size were clearly observed at all points in the system. As computational cell size

increased, greater uncertainty in runoff volume was observed in smaller subwatersheds due to the effects of watershed smearing; the imprecise location of precipitation with respect to basin boundaries.

5.5 Effects of Spatial Distribution on Model Results

The results from the similarly parameterized lumped HEC-HMS model of the Upper Roanoke Watershed indicate slightly longer times to peak and decreased peak flowrates compared to the distributed model. A slight loss of detail in hydrograph shape compared to the distributed model occurs in the lumped model. These variations are relatively small compared to uncertainties due to CN and AMC, model parameterization, and when compared to the differences between modeled and observed streamflow. Overall runoff volumes from the lumped model are typically less than from the distributed model.

Though slight losses of hydrograph detail occur and peak flowrates and runoff volumes are slightly decreased, lumped modeling in HEC-HMS does offer advantages over distributed modeling. The lumped SCS CN model allows empirical optimization of CN leading to more accurate runoff volumes. Lumped modeling also offers other methods of rainfall excess calculation. NEXRAD stage III precipitation data provides an effective input to lumped models when appropriately reprocessed. The modeler should first evaluate the performance of a lumped model and then decide if additional investment in data, parameterization, and computational resources is necessary to produce the results required by the modeling study.

5.6 Evaluation of HEC-GeoHMS Processing Capabilities

HEC-geoHMS was found to be an effective GIS utility for watershed and stream channel delineation and computation of watershed geometric properties. HEC-geoHMS is a very useful GIS utility for hydrologists even if the intent is not to create HEC-HMS model inputs. The capabilities of HEC-geoHMS are limited however, and traditional hydrologic methods are still required to estimate hydrologic model parameters such as time of concentration. Observed streamflow data was necessary to adequately define watershed time of concentration and the linear reservoir coefficient required by the recommended HEC-HMS ModClark runoff transformation.

Substantial GIS processing was necessary to add curve numbers to the HEC-HMS grid cell parameter file. Computationally, this step would not be difficult to automate in a future version of HEC-geoHMS.

The greatest challenge to the modeler is the creation of spatially distributed precipitation inputs from NEXRAD stage III data, a process not supported by HEC-geoHMS. Gridded precipitation is required for the distributed HEC-HMS runoff model. Until spatially distributed precipitation inputs become easier to process and create, the distributed HEC-HMS runoff model will likely see limited use in industry.

As the GIS community is rapidly upgrading from ArcView 3.x to ArcGIS desktop version 8.x, there will likely be some disappointment that HEC-geoHMS is limited to use with ArcView3.x. Additionally, neither ArcView 3.x nor the ArcGIS desktop products are capable of efficiently dealing with large volumes of gridded precipitation data. The computing capabilities of ARC/INFO workstation were necessary to efficiently reproject and resample archived NEXRAD data.

5.7 Evaluation of HEC-HMS Gridded SCS CN, ModClark Model

The gridded SCS CN rainfall excess calculation in HEC-HMS was found to be extremely sensitive to the choice of CN and AMC. As one of the current weaknesses in GIS based hydrologic modeling is the estimation of model parameters from existing digital datasets, the uncertainty in CN selection from NLCD and SSURGO was found to be a significant source of uncertainty in this modeling study.

Optimal choice of CN and AMC was found to vary between storms and between subwatersheds during individual storms. The model was found to over-predict or under-predict runoff volume at different points within the watershed, implying that CN or AMC values need refinement, or that spatial variability exists in AMC. The between-watershed variation may be due to fundamental differences in soil and landcover and may be improved by refining CN estimates based on NLCD and SSURGO. Between-watershed variation may also be due to spatial variability in antecedent moisture condition. AMC is lumped at the watershed level in this model. Storm to storm variation of CN is expected, but cannot necessarily be optimized when the modeler is limited to curve numbers at AMC I, AMC II, or AMC III.

Concerning the ModClark transformation, no significant improvement in model performance was seen over the spatially averaged Clark unit hydrograph. The ModClark transformation does not currently account for spatial variability of flow velocity or the reservoir coefficient. Unfortunately, even if the model had the capability of spatially varying these parameters, parameterization and model calibration would be intractable. As evidenced by the close agreement of modeled and observed hydrographs during the March 1998 storm event, the HEC-HMS gridded SCS CN, ModClark model and the lumped SCS CN, Clark unit hydrograph model, produce reasonable results when adequate data is available to define model parameters.

5.8 Future Research

The HEC-HMS gridded SCS CN, ModClark model did not show significant sensitivity to precipitation resolution, physical parameter grid scale, or spatial distribution of precipitation and physical characteristics. This may be due to spatial uniformity of precipitation inputs (a product of the storm events chosen), or spatial uniformity of watershed runoff producing characteristics (a product of the study area chosen). Limited sensitivity to spatial distribution of model parameters and inputs may also be caused by limitations in model specification and parameterization. Future research should examine the assumptions of spatially variable precipitation and physical characteristics inherent in

this research and should focus on the limitations encountered. Investigation of some of these topics will require capabilities beyond those of the current HEC-HMS modeling package or will require higher resolution data than is currently available.

5.8.1 Investigation of Spatial Variability in Precipitation Events

The three storm events chosen for this modeling study were chosen for their spatial variability. Spatial and temporal variability of precipitation is evidenced by examination of precipitation hyetographs and storm total precipitation depths at points throughout the watershed as shown in Appendix I. To ensure that the limited sensitivity seen in this modeling study is not a result of the storm events chosen, more storm events should be modeled. The model results exhibited predictable trends with changes in precipitation resolution within the limits of bilinear interpolation. If NEXRAD stage III data is used to model other storm events, spatially lumped precipitation and spatially distributed precipitation resolutions of 4km (base), 1km (smoothed), and 8km (degraded) will be sufficient to show the effects of precipitation resolution and spatial averaging on model results.

The spatial (4 km) and temporal (1 hour) resolution of the spatially distributed precipitation data may also be a limitation on model accuracy. Unfortunately, NEXRAD stage III precipitation estimates are not available at finer spatial or temporal resolutions. Higher resolution radar derived precipitation estimates are available, however these datasets do not undergo the processing against ground based gages and quality control inherent in the NEXRAD stage III processing algorithms.

5.8.2 Investigation of Spatial Variability in Watershed Characteristics

To ensure that limited sensitivity to watershed physical parameter grid scale was not the result of spatial uniformity of hydrologic characteristics, the GIS based hydrologic modeling techniques utilized should be applied to other watersheds. Data from the NEXRAD stage III archives, the NED, NLCD, and SSURGO or STATSGO databases may be used to generate spatially distributed HEC-HMS model inputs for watersheds all across the continental United States. Investigation of model sensitivity to spatial distribution as applied to other watersheds may help determine if the limited sensitivity found in this modeling study was a result of the study area chosen.

5.8.3 Improvements in Model Specification and Parameterization

The limited sensitivity to precipitation resolution, physical parameter grid scale and spatial distribution exhibited by the HEC-HMS model of the Upper Roanoke watershed may be a result of limitations in model specification and parameterization. Parameterization was established primarily by optimization techniques and regional analysis to unengaged areas. That model parameterization could be improved is evidenced by the differences in accuracy between modeled storm events. Precipitation and runoff data developed for more storm events, as discussed in section 5.8.1, may be used to improve model parameterization by optimization techniques. As the GIS based modeling

techniques are applied to other watersheds as discussed in section 5.8.2, a larger database relating GIS attributes and optimized model parameters may be generated. This data may be used to correlate GIS derived attributes with model parameters, especially important if the model is to be applied to ungaged areas.

Improvements in parameterization may be effected by the application of precipitation and observed streamflow from more storm events or by better utilization of existing watershed geometric data. HEC-geoHMS calculates a number of hydrologically relevant values describing each subwatershed and stream channel segment that were not explicitly used in this research. Again, better correlation of these values with hydrologic model parameters would likely improve model accuracy.

One of the current weaknesses in GIS based hydrologic modeling is the correlation of hydrologic model parameters with available GIS dataset attributes. Parameters such as SCS CN, Manning's coefficient, overland flow velocity, and soil infiltrative capacity require assumptions and judgment on the part of the modeler to be defined from GIS data.

One of the limitations of the HEC-HMS model used in this research was the gridded SCS CN rainfall excess calculation. The SCS CN method has limitations when applied to historical storm events as discussed in section 2.7.5. These limitations degraded the accuracy of the rainfall excess volume calculation. The use of a constant linear reservoir coefficient and assumption of constant flow velocity at the subwatershed level in the ModClark transformation may have limited model sensitivity to spatial distribution. Other rainfall excess calculations and surface runoff transformations should be investigated prior to making overall conclusions concerning optimal grid resolution and distributed versus lumped modeling.